

NUREG/CR-4401

SAND85-0469

R7

Printed September 1985

Behavior of Control Rods During Core Degradation: Pressurization of Silver-Indium-Cadmium Control Rods

D. A. Powers

Prepared by
Sandia National Laboratories
Albuquerque, New Mexico 87185 and Livermore, California 94550
for the United States Department of Energy
under Contract DE-AC04-76DP00789

Prepared for
U. S. NUCLEAR REGULATORY COMMISSION

SF2900Q(8-81)

8512270269 851130
PDR NUREG
CR-4401 R PDR

NOTICE

This report was prepared as an account of work sponsored by an agency of the United States Government. Neither the United States Government nor any agency thereof, or any of their employees, makes any warranty, expressed or implied, or assumes any legal liability or responsibility for any third party's use, or the results of such use, of any information, apparatus product or process disclosed in this report, or represents that its use by such third party would not infringe privately owned rights.

Available from
Superintendent of Documents
U.S. Government Printing Office
Post Office Box 37082
Washington, D.C. 20013-7982
and
National Technical Information Service
Springfield, VA 22161

NUREG/CR-4401
SAND85-0469
R7

BEHAVIOR OF CONTROL RODS DURING CORE DEGRADATION:
PRESSURIZATION OF SILVER-INDIUM-CADMIUM CONTROL RODS

D. A. Powers

September 1985

Sandia National Laboratories
Albuquerque, NM 87185
Operated by
Sandia Corporation
for the
U.S. Department of Energy

Prepared for
Division of Accident Evaluation
Office of Nuclear Regulatory Research
U.S. Nuclear Regulatory Commission
Washington, DC 20555
Under Memorandum of Understanding DOE 40-550-75
NRC FIN No. A1227

ABSTRACT

Activity data for the liquid binary systems Ag-Cd, Ag-In, and In-Cd are correlated in terms of the Wilson equation. These correlations are used to construct a model of the ternary system Ag-In-Cd. Spectroscopic data for the vapor species Ag(g) , $\text{Ag}_2\text{(g)}$, $\text{Ag}_3\text{(g)}$, $\text{Ag}^+\text{(g)}$, In(g) , $\text{In}_2\text{(g)}$, $\text{In}^+\text{(g)}$, Cd(g) , $\text{Cd}_2\text{(g)}$, $\text{Cd}^+\text{(g)}$, AgIn(g) , and CdIn(g) are reviewed and are used to define thermodynamic functions for these species for temperatures between 298 and 3500 K. Vapor pressures for the liquid phase pure elements, liquid binary alloys, and the liquid ternary alloy are calculated using the Wilson equation model and using the assumption that the condensed phase is an ideal mixture. An azeotrope is predicted for the Ag-In system. Predictions are made of the vaporization of alloys of 80 percent Ag, 15 percent In, and 5 percent Cd used as control materials in some pressurized water reactors.

CONTENTS

	<u>Page</u>
List of Illustrations	vii
List of Tables	xii
I. The Nature of the Problem	1
II. Models of the Thermochemistry of Silver- Indium-Cadmium Liquid Alloys	4
A. Nonideal Solution Models	6
B. Fitting Procedure	9
C. Pressure Dependence of Activity Coefficients	11
D. Critical Properties of the Elements and Alloys	13
E. Activity Coefficients for Binary Constituent Alloys	22
1. The Cadmium/Silver System	23
2. The Cadmium/Indium System	23
3. The Indium/Silver System	34
4. Summary of Activity Coefficient Models for the Binary Constituent Alloys	40
F. Results for Ternary Alloys	40
III. Vapor Species in the Ag-In-Cd System	59
A. Monomeric Species	59
B. Polymeric Gaseous Species	63
1. Silver Dimer- Ag_2	67
2. Silver Trimer- Ag_3	70
3. Cadmium Dimer- Cd_2	74
4. Cadmium Trimer- Cd_3	77
5. Indium Dimer- In_2	77
C. Mixed Metal Species.	77
1. CdIn	80
2. AgIn	82
3. AgCd	82
D. Summary of Free Energy of Formation Data	82

CONTENTS (Continued)

	<u>Page</u>
IV. Vapor Pressures	88
A. Vapor Pressures Over Pure Elements	88
B. Vapor Pressures Over Binary Alloys	96
B-1. Vapor Pressures Over Silver/ Indium Alloy	97
B-2. Vapor Pressures Over Silver/ Cadmium Alloys	104
B-3. Vapor Pressures Over Indium/ Cadmium Alloys	104
C. Vapor Pressures Over Ternary Alloys.	108
V. Application to Control Rod Behavior in a Reactor Accident	121
A. Internal Pressurization.	121
B. Vaporization of the Control Rod Alloy From a Breached Rod	123
VI. Conclusions.	125
References	127
Appendix A Activity Coefficient Data for Liquid Binary Alloys	A-1
References	A-9
Appendix B Thermodynamic Data for Species in the Ag-In-Cd System	B-1
References	B-27

LIST OF ILLUSTRATIONS

<u>Figure</u>	<u>Page</u>
1 Correlation of Critical Temperatures of Metals With Their Boiling Points	17
2 Correlation of Critical Temperatures of Metals Having Unpaired s Electrons With Their Boiling Points	20
3 Correlation of Critical Temperatures of Metals Having Paired s Electrons With Their Boiling Points	21
4 Experimental Data for the Activity Coefficients of Cadmium in Liquid Cadmium/Silver Alloys Plotted Against the Mole Fraction of Cadmium	25
5 Plot of Cadmium Activity Coefficients Calculated With the Two-Parameter Wilson Equation Against Observed Cadmium Activity Coefficients in Liquid Cadmium/Silver Alloys.	26
6 Plot of Cadmium Activity Coefficients Calculated With the Two-Parameter Subregular Solution Model Against Observed Cadmium Activity Coefficients in Liquid Cadmium/Silver Alloys	27
7 Experimental Data for the Activity Coefficients of Cadmium in Liquid Cadmium/Indium Alloys Plotted Against the Mole Fraction of Cadmium	28
8 Comparison of Cadmium Activity Coefficients Calculated With the Two-Parameter Wilson Equation Model to Those Observed by Predel and Berka	31
9 Comparison of Cadmium Activity Coefficients Calculated With the Two-Parameter Wilson Equation to Cadmium Activity Coefficients Measured in Studies by Predel and Berka, Servis and Munir, and Heumann and Predel	32
10 Comparison of Cadmium Activity Coefficients Calculated With the Four-Parameter Wilson Equation to Cadmium Activity Coefficients Measured by Predel and Berka, Servis and Munir, and Heumann and Predel	33
11 Comparison of Cadmium Activity Coefficients Calculated With the Four-Parameter Wilson Equation to Cadmium Activity Coefficients Measured by Predel and Berka and by Servis and Munir	35

LIST OF ILLUSTRATIONS (Continued)

<u>Figure</u>	<u>Page</u>
12 Indium Activity Coefficients Observed in Various Studies of Liquid Indium/Silver Alloys Plotted Against the Mole Fraction of Indium	36
13 Comparison of the Activity Coefficients of Indium Calculated Using the Two-Parameter Wilson Equation With Activity Coefficients Observed by Alcock et al. and Activity Coefficients Observed by Mycielska et al. for Alloys With $x_{In} > 0.4$	39
14 Calculated Activity Coefficient of Cadmium in a Cadmium/Silver Alloy at 1076 K as a Function of the Mole Fraction of Cadmium	41
15 Calculated Activity Coefficient of Cadmium in a Cadmium/Indium Alloy at 821 K as a Function of the Mole Fraction of Cadmium	42
16 Calculated Activity Coefficient of Indium in an Indium/Silver Alloy at 1300 K as a Function of the Mole Fraction of Indium	43
17 Activity Coefficient of Cadmium in a Cadmium/Silver Alloy With a Cadmium Mole Fraction of 0.06 as a Function of Temperature	44
18 Activity Coefficient of Cadmium in a Cadmium/Indium Alloy With a Cadmium Mole Fraction of 0.25 as a Function of Temperature	45
19 Activity Coefficient of Indium in an Indium/Silver Alloy With an Indium Mole Fraction of 0.19 as a Function of Temperature	46
20 Activity of Cadmium in Ag-In-Cd Alloys at 1000 K . .	47
21 Activity of Indium in Ag-In-Cd Alloys at 1000 K . .	48
22 Activity of Silver in Ag-In-Cd Alloys at 1000 K . .	49
23 Activity of Cadmium in Ag-In-Cd Alloys at 1300 K . .	50
24 Activity of Indium in Ag-In-Cd Alloys at 1300 K . .	51
25 Activity of Silver in Ag-In-Cd Alloys at 1300 K . .	52
26 Activity of Cadmium in Ag-In-Cd Alloys at 1500 K . .	53
27 Activity of Indium in Ag-In-Cd Alloys at 1500 K . .	54

LIST OF ILLUSTRATIONS (Continued)

<u>Figure</u>	<u>Page</u>
28 Activity of Silver in Ag-In-Cd Alloys at 1500 K. . .	55
29 Activity of Cadmium in an 85a/oAg 15a/oIn 5a/oCd Alloy as a Function of Temperature	56
30 Activity of Indium in an 85a/oAg 15a/oIn 5a/oCd Alloy as a Function of Temperature	57
31 Activity of Silver in an 85a/oAg 15a/oIn 5a/oCd Alloy as a Function of Temperature	58
32 Qualitative Molecular Orbital Diagram for Gaseous Dimers	64
33 Sum of the Partial Pressures of Silver-Bearing Species Over Pure Silver	90
34 Sum of the Partial Pressures of Indium-Bearing Species Over Pure Liquid Cadmium	91
35 Sum of the Partial Pressures of Cadmium-Bearing Species Over Pure Liquid Indium.	92
36 Contributions of Various Species to the Vapor Over Pure Silver	93
37 Contributions of Various Species to the Vapor Over Pure Liquid Indium	94
38 Contributions of Various Species to the Vapor Over Pure Liquid Cadmium	95
39 Condensed/Vapor Phase Equilibrium for the System Indium/Silver at One Atmosphere.	98
40 Condensed/Vapor Phase Equilibrium for the Indium/Silver System When Mixed-Metal Vapor Species Are Ignored.	99
41 Effects of Indium and Silver Activity Coefficients on the Azeotrope Location at One Atmosphere Pressure	101
42 Location of the Azeotrope as a Function of Temperature.	102
43 Speciation of the Vapor Along the Azeotropic Line. .	103

LIST OF ILLUSTRATIONS (Continued)

<u>Figure</u>	<u>Page</u>
44 Variations in the Elemental Composition of the Vapor as an Alloy Initially Composed of 15.79 Percent In and 84.21 Percent Ag Vaporizes at 1500 K.	105
45 Condensed/Vapor Phase Equilibrium for Liquid Silver/Cadmium Alloys at One Atmosphere	106
46 Condensed/Vapor Phase Equilibrium for Liquid Indium/Cadmium Alloys at One Atmosphere	107
47 Condensed/Vapor Phase Boundaries at One Atmosphere for Alloys Composed of Cadmium and an Indium/Silver Alloy of the Azeotropic Composition.	109
48 One Atmosphere Isotherms at 1 K Intervals Plotted Against Condensed Phase Compositions in the Vicinity of the Indium/Silver Azeotrope.	110
49 One Atmosphere Isotherms at 100 K Intervals Between 1100 K and 2200 K Plotted Against the Condensed Phase Composition for the Ag-In-Cd System	111
50 One Atmosphere Isotherms at 100 K Intervals Between 2400 K and 1700 K Plotted Against the Vapor Phase Composition for the Ag-In-Cd System	112
51 Total Pressure Over an Alloy of 80 Percent Ag, 15 Percent In, and 5 Percent Cd as a Function of Temperature	113
52 Speciation of the Vapor Over a Nonideal Liquid Alloy of 80 Percent Ag, 15 Percent In, and 5 Percent Cd as a Function of Temperature	115
53 Speciation of the Vapor Over a Liquid Alloy of 80 Percent Ag, 15 Percent In, and 5 Percent Cd Which is Considered to Be an Ideal Mixture as a Function of Temperature	116
54 Variations in the Elemental Composition of the Vapor Phase as an Ideal Mixture Initially Compared of 80 Percent Ag, 15 Percent In, and 5 Percent Cd Vaporizes at 1500 K	117
55 Variations in the Elemental Composition of the Vapor Phase as a Nonideal Alloy With the Initial Composition of 80 Percent Ag, 15 Percent In, and 5 Percent Cd Vaporizes at 1500 K	118

LIST OF ILLUSTRATIONS (Continued)

<u>Figure</u>		<u>Page</u>
56	Variation in the Temperature and Vapor Phase Composition as a Nonideal Alloy Initially of 80 Percent Ag, 15 Percent In, and 5 Percent Cd Evaporates at a Constant Vapor Pressure of One Atmosphere	119
57	Variation in the Temperature and Vapor Phase Composition as an Alloy Initially of 80 Percent Ag, 15 Percent In, and 5 Percent Cd Treated as an Ideal Mixture Evaporates at a Constant Vapor Pressure of One Atmosphere	120
58	Internal Pressure of a Control Rod as a Function of Temperature.	122

LIST OF TABLES

<u>Table</u>		<u>Page</u>
1	Control Rod Geometry for a Westinghouse Four Loop PWR	2
2	Control Rod Initial Composition and the Thermophysical Properties of Its Constituents . .	5
3	Critical Temperatures of Metals	16
4	Critical Properties of the Elements and the Parameters for the Redlich Kwong Equation of State	19
5	Summary of Parametric Values for the Cadmium/Silver System	24
6	Summary of Parametric Values for the Cadmium/Indium System	30
7	Summary of Parametric Values for the Indium/Silver System	38
8	Summary of Spectroscopic Data for $\text{Ag}_2(\text{gas})$	69
9	Summary of Data Used to Calculate the Thermodynamic Properties of $\text{Ag}_2(\text{gas})$	71
10	Summary of Data Used to Calculate the Thermodynamic Properties of $\text{Ag}_3(\text{gas})$	75
11	Summary of Data Used to Calculate the Thermodynamic Properties of $\text{Cd}_2(\text{gas})$	78
12	Summary of Data Used to Calculate the Thermodynamic Properties of $\text{In}_2(\text{gas})$	79
13	Summary of Data Used to Calculate the Thermodynamic Properties of $\text{CdIn}(\text{gas})$	81
14	Summary of Data Used to Calculate the Thermodynamic Properties of $\text{AgIn}(\text{gas})$	83
15	Summary of Free Energy of Formation Data (cal/mole)	84
16	Coefficients for the Function Used to Fit the Free-Energy Functions.	87
17	Total Vapor Pressure and Species Partial Pressures Over Pure Elements at Various Temperatures	89

LIST OF TABLES (Continued)

<u>Table</u>	<u>Page</u>
A-1 Activity Coefficient of Cadmium in Liquid Cadmium/Silver Alloys	A-2
A-2 Activity Coefficient of Cadmium in Liquid Cadmium/Indium Alloys	A-3
A-3 Activity Coefficient of Indium in Liquid Indium/Silver Alloys	A-7
B-1 Data Used to Calculate the Thermodynamic Functions of $\text{Ag}^0(\text{gas})$	B-2
B-2 Data Used to Calculate the Thermodynamic Functions of $\text{In}^0(\text{gas})$	B-3
B-3 Data Used to Calculate the Thermodynamic Functions of $\text{Cd}^0(\text{gas})$	B-4
B-4 Data Used to Calculate the Thermodynamic Functions of $\text{Ag}^+(\text{gas})$	B-5
B-5 Data Used to Calculate the Thermodynamic Functions of $\text{In}^+(\text{gas})$	B-6
B-6 Data Used to Calculate the Thermodynamic Functions of $\text{Cd}^+(\text{gas})$	B-7
B-7 Thermodynamic Properties of $\text{Ag}(\text{gas})$	B-8
B-8 Thermodynamic Properties of $\text{Ag}_2(\text{gas})$	B-9
B-9 Thermodynamic Properties of $\text{Ag}_3(\text{gas})$	B-10
B-10 Thermodynamic Properties of $\text{Ag}^+(\text{gas})$	B-11
B-11 Thermodynamic Properties of $\text{In}(\text{gas})$	B-12
B-12 Thermodynamic Properties of $\text{In}_2(\text{gas})$	B-13
B-13 Thermodynamic Properties of $\text{In}^+(\text{gas})$	B-14
B-14 Thermodynamic Properties of $\text{Cd}(\text{gas})$	B-15
B-15 Thermodynamic Properties of $\text{Cd}_2(\text{gas})$	B-16
B-16 Thermodynamic Properties of $\text{Cd}^+(\text{gas})$	B-17
B-17 Thermodynamic Properties of $\text{AgIn}(\text{gas})$	B-18

LIST OF TABLES (Continued)

<u>Table</u>		<u>Page</u>
B-18	Thermodynamic Properties of CdIn(gas)	B-19
B-19	Silver Reference System	B-20
B-20	Thermodynamic Properties of Silver Liquid . .	B-21
B-21	Indium Reference System	B-22
B-22	Thermodynamic Properties of Indium Liquid . .	B-23
B-23	Cadmium Reference System	B-24
B-24	Thermodynamic Properties of Cadmium Liquid . .	B-25
B-25	e ⁻ Reference System	B-26

I. The Nature of the Problem

Most pressurized water reactors (PWRs) use as a reactor control material an alloy of silver, indium, and cadmium.⁽¹⁾ The alloy is sheathed in type 304 stainless steel. During a severe reactor accident these control rods would be subjected to intense heating that parallels the temperature excursion experienced by the reactor fuel. The constituents of the control rod material are not refractory. As temperatures increase constituents of the control rod vaporize and the rod pressurizes. Eventually, the cladding on the rod would be breached. The rupture of the cladding may be caused by the internal pressure, but will be caused by cladding melting or creep if nothing else. Once the stainless steel sheath is ruptured vapors and liquid control rod alloy can flow out into the reactor core.

There is a significant amount of control rod material in a typical reactor core. Geometric data collected in Table 1 can be used to estimate that there are about 2.9 metric tons of alloy in a four loop PWR. This alloy mass consists of about 2.3 metric tons of silver, 0.44 metric tons of indium, and 0.15 metric tons of cadmium.

Investigators at Oak Ridge National Laboratories appear to have been the first to heat simulated control rods to failure.⁽²⁾ These investigators found that when the control rod was heated in a furnace at normal laboratory pressures, it ruptured violently at a temperature between 1580 and 1700 K. Vaporous cadmium and droplets of silver were expelled. Subsequent investigation at the Atomic Energy Establishment at Winfrith in the United Kingdom have confirmed this behavior and have characterized the aerosols produced by the expelled control rod materials.⁽³⁾

Vapors released from the control rods into the reactor core will be swept into cooler regions of the reactor coolant system along with any radionuclides released from the fuel. In these cooler regions the vapors will condense either as aerosols or on structures within the coolant system. Aerosols formed from vapors of control rod alloys will provide large surface areas for reaction of tellurium or other radionuclides. High aerosol concentrations will accentuate the agglomeration, sedimentation, and deposition of radioactive materials in the reactor coolant system.

Thus, vaporization of control rod materials can affect the efficiency with which radionuclides transport through the reactor coolant system to points where they can be released from the plant. Whether generation of control rod vapors is important for the analysis of radionuclide behavior depends on:

Table 1

Control Rod Geometry for a
Westinghouse Four Loop PWR

I. Control Assemblies

53 full length assemblies
8 partial length assemblies
20 rods per assembly

II. Rod Description

type 304 stainless steel clad
outside diameter = 0.422" = 1.07 cm
wall thickness = 0.019" = 0.048 cm
length of control material in
full length rods = 142" = 361 cm
partial length rods = 36" = 91.4 cm
total rod length = 156.4" = 397 cm

III. Alloy

80% Ag, 15% In, 5% Cd
density = 9.93 g/cm³
total mass of control rod material =
2.94 metric tons
mass of silver = 2.351 metric tons
mass of indium = 0.440 metric tons
mass of cadmium = 0.147 metric tons

1. when, relative to the release of radionuclides from the fuel, extensive vaporization of the control rod material occurs,
2. how much vapor is produced from the control rods, and
3. what is the chemical composition of vapors from the control rods.

Control rod alloys may also affect the course of core degradation in a severe reactor accident. Hagan and co-workers⁽⁴⁾ were the first to note that liquid control rod alloy will interact with zircaloy clad on the fuel. Parker et al.⁽²⁾ have also noted this interaction. A eutectic melting point arises in the Ag/Zr system at 1520 ± 10 K and 90 percent Zr.⁽⁵⁾ Perhaps more important is that exothermic compound formation arises at the nominal stoichiometries of AgZr and AgZr₂. Indium is readily soluble in zirconium⁽⁶⁾ but the consequences of indium dissolution on the melting properties of the mixture have not been reported. Investigators at Winfrith suspect the interaction of In with Zr is quite strong and that the meeting of ternary Ag-In-Zr alloys occur at temperatures lower than the Zr-Ag eutectic.

Formation of alloys between fuel cladding and control rod materials that melt at low temperatures could cause clad to flow off the fuel rods very early in a reactor accident. Collapse of the fuel into a geometry much less easily cooled than an intact core could be a consequence of clad loss. Certainly the facility with which radionuclides could be released into the core atmosphere would increase were the fuel cladding removed.

Liquid control rod material may continue to vaporize whether or not it has interacted with the clad. Some accident analyses have been predicated on this continued vaporization.⁽⁷⁾ These analyses predict that such high aerosol concentrations arise then in the reactor coolant system that only small fractions of radionuclides released from the core escape into the reactor containment building.

Others⁽⁸⁾ have argued that little vaporization other than loss of cadmium will occur. Instead, the control rod alloy will flow out of the hot regions of the core and freeze. The frozen alloy may inhibit steam flow and consequently metal-water reactions in the core.

There are, then, many questions about the behavior of control rods during a severe accident. In this document the vaporization behavior of the silver-indium-cadmium control rod alloy is considered. The objectives of the analyses here are to determine

1. The pressurization of control rods during reactor accidents,
2. The composition of vapors released from molten alloys, and
3. The vaporization potential from control rod alloys after clad rupture.

II. Models of the Thermochemistry of Silver-Indium-Cadmium Liquid Alloys

To estimate the vapor pressures over control rod alloys it is necessary to evaluate expressions of the type:

$$\phi_i P_i = \gamma_i x_i \exp[-\Delta G_i / RT]$$

where ϕ_i = fugacity coefficient of the i^{th} vapor species

P_i = equilibrium partial pressure of the i^{th} vapor species

x_i = mole fraction of the condensed form of the i^{th} vapor species in the alloy

γ_i = activity coefficient of the condensed form of the i^{th} vapor species

ΔG_i = standard-state free-energy change associated with the vaporization process for the i^{th} species

R = gas constant

T = absolute temperature.

An important first step in the evaluation of such expressions is the determination of the concentration and activity of constituents of the liquid alloy.

The initial concentrations of constituents of the control rod alloys are specified, of course. Typical alloy compositions are shown in Table 2 along with thermal and physical properties of the constituents when pure.

Activity coefficients of alloy constituents cannot be calculated a priori with any confidence. In the absence of any significant data for the alloy of interest here, activity coefficients must be derived from models. One such model is the ideal solution model in which all activity coefficients are assumed to have values of unity regardless of composition

Table 2

Control Rod Initial Composition and the
Thermophysical Properties of Its Constituents

Property	Silver	Indium	Cadmium
Initial composition in weight %	80	15	5
Initial composition in atom %	80.9	14.2	4.9
Melting point ^a (K)	1234	429.3	594
Heat of fusion ^a (cal/mole)	2855	780	1460 ± 30
Boiling point ^a (K)	2437	2343	1040
Heat of vaporization ^b (cal/mole)	61106 (±180) -25.066 (±0.079)T(K)	55642 (±70) -23.748 (±0.032)T(K)	57143 (±90) -0.713 (±0.051)T(K)
Molar volume ^c (cm ³)	11.343(1 + $\xi(T-1233)$) $\xi = 0.000111$	(15.5422 ± 0.0307) η (1 + ξT) $\xi = (0.118 \pm 0.004) \times 10^{-3}$	14.015(1 + $\xi(T-593)$) $\xi = 0.000137$
Molecular weight	107.87	114.82	112.40

^aFrom R. Hultgren, P. D. Desai, D. T. Hawkins, M. Gleiser, K. K. Kelley, and D. D. Wagman, Selected Values of Thermodynamic Properties of Elements, American Society for Metals, 1973.

^bLinear least-squares fit of data calculated here.

^cSilver and cadmium data from density equations in the International Critical Tables.

Indium data from linear least square fit using density data from C. Smithells Metals Reference Book, Butterworths.

and temperature. This assumption of ideality for the alloy has a certain attractiveness. It is simple and at sufficiently high temperatures all alloys should behave in accordance with this model.

There are data on binary alloys in the Ag-In-Cd system that do indicate some nonidealities of the system. These data can be used to formulate models that are more complicated and more realistic than the ideal solution model for the ternary alloy. For the analyses here, both the ideal solution model and a more complex model developed from data for binary alloys will be used. This should yield a comparison that might be indicative of the uncertainty in the analyses or the error in results obtained based on the very attractive assumption of ideality.

A. Nonideal Solution Models

The ideal solution model is based, of course, on the assumption that the free energy of a binary mixture is just

$$G_{\text{mix}} = xG_1(T) + (1-x)G_2(T) + RT[x\ln(x) + (1-x)\ln(1-x)]$$

where x = mole fraction of constituent i

$G_i(T)$ = free energy of the pure i^{th} constituent.

To introduce deviations from ideality in the liquid model it is only necessary to add a term, G^{XS} , to the right hand side of the above equation for the free energy of a mixture. G^{XS} can be a function of temperature and composition. The relationship between G^{XS} and activity coefficients for the alloy constituents is just

$$RT\ln\gamma_i = \left. \frac{\partial n_T G^{\text{XS}}}{\partial n_i} \right|_{T, P, n_j (j \neq i)}$$

A model that will be used here to explore the effects of nonideality is the so-called "Wilson equation": (9,10,11)

$$\frac{G^{\text{XS}}}{RT} = - \sum_{i=1}^N x_i \ln \left[\sum_{j=1}^N A[i,j] x_j \right]$$

where x_i = mole fraction of the i^{th} constituent

$A[i,j]$ = molar volume of the i^{th} alloy constituent when a pure liquid

$$V_i^L = \frac{V_j^L}{V_i^L} \exp[-a_{i,j}/RT]$$

R = gas constant

$a_{i,j}$ = parameters such that $a_{ii} = 0$ and $a_{i,j} \neq 0$ when $i \neq j$.

Then, for binary alloys, the Wilson equation yields:

$$\ln \gamma_1 = -\ln[x + A[1,2](1-x)]$$

$$+ (1-x) \left[\frac{A[1,2]}{x + A[1,2](1-x)} - \frac{A[2,1]}{A[2,1]x + 1-x} \right]$$

$$\ln \gamma_2 = -\ln(1-x + A[2,1]x) - x \left[\frac{A[1,2]}{x + A[1,2](1-x)} - \frac{A[2,1]}{A[2,1]x + 1-x} \right]$$

where x is the mole fraction of the first alloy constituent.

The Wilson equation is a two parameter solution model in which the parameters are a_{12} and a_{21} . These parameters are found, of course, by fitting the model to experimental data. When this is done for data covering a very broad temperature range, it is sometimes convenient to make the parameters temperature dependent. Often a linear temperature dependence is assumed:

$$a_{ij} = \alpha_{ij} + \beta_{ij}T$$

Such a temperature dependence implies that the interaction coefficients, $A[i,j]$, do not approach unity as temperatures approach infinity--an implication that is counter to expectations. The consequences of assuming linear temperature dependencies for the parameters are negligible for situations in which there are data spanning the temperature range of interest. Here, however, it is likely the solution model will be used to extrapolate into regimes not explored by

experiment. The only available guidance for such extrapolation is that with increasing temperatures mixtures ought to behave in a more ideal manner.

Two alternate temperature dependencies were investigated:

$$a_{ij} = \alpha_{ij}' + \beta_{ij}' \ln(T)$$

$$a_{ij} = \alpha_{ij} + \beta_{ij}/T$$

Note that the interaction coefficients derived from either of these temperature-dependent parameters will approach unity with increasing temperature. Unfortunately, the data available for the systems of interest do not span such a large range that conclusions could be made concerning the appropriate temperature dependence for the parameters. For analyses with the Wilson equation using temperature dependent parameters, the reciprocal temperature dependence was arbitrarily selected.

The Wilson equation has been used widely for analyses of distillation.⁽¹²⁾ It has a disadvantage that has made it less popular in inorganic fields. It cannot predict condensed phase immiscibility. For the application here, the temperatures of interest are sufficiently far above the alloy liquidus it is unlikely that this failing of the model will be of concern.

An advantage of the Wilson equation is that once parametric values for binary models are known, a ternary or higher order model can immediately be constructed. Thus, for an N constituent alloy,

$$\ln \gamma_i = 1 - \ln \left\{ \sum_{j=1}^N x_j A[i,j] \right\} - \sum_{k=1}^N \left\{ \frac{x_k A[k,i]}{\sum_{j=1}^N x_j A[k,j]} \right\}$$

Notice that ternary and higher order interactions among atoms in the alloy are neglected in the Wilson model. The foundation of the model is on the assumption that all interactive forces in the alloy can be described by sums of pairwise interactions between atoms. The validity of this assumption has been and will continue to be discussed at length in the literature. Neglect of ternary interactions is not alarming for metal alloys of interest here.

Another model that has received attention for metal alloy systems is the subregular solution model.⁽¹³⁾ The excess free energy for a binary subregular model is given by:

$$G^{XS} = x(1-x)[(1-x)h_2 + xh_1]$$

where the parameters, h_2 and h_1 , can be temperature dependent. Activity coefficients derived from the subregular model are:

$$RT\ln(\gamma_2) = x^2[2h_2 - h_1] + x^3[2h_1 - 2h_2]$$

$$RT\ln(\gamma_1) = (1-x)^2[h_2 + 2x(h_1 - h_2)]$$

Again, the subregular model has two parameters and these parameters may be temperature dependent. A linear temperature dependence:

$$h_i = h_i' + h_i''T$$

has nearly always been assumed by authors using the model. Such a linear temperature dependence in the subregular solution model has the same flaw noted above for linearly temperature-dependent parameters in the Wilson equation. Consequently, here the reciprocal temperature dependence is used

$$h_i = h_i' + h_i''/T$$

B. Fitting Procedure

Nonlinear least squares procedures⁽¹³⁾ are used to fit binary data to the solution models. Intercomparisons of models with the same or different numbers of parameters were done based on an F test appropriate for linear models. The F statistic for comparing two models is formulated as

$$F = \left(\frac{\chi_1^2}{\chi_2^2} \right) \frac{(N-P_2)}{(N-P_1)}$$

where $\chi_i^2 = \sum_{j=1}^N \left(y_j^{\text{obs}} - y_j^{\text{calc}} \right)^2$ for the i^{th} model

N = number of data points

P_i = number of parameters in the i^{th} model.

The hypothesis that Model 1 is better than or equal to Model 2 is rejected at a $100(1-\alpha)$ percent confidence if

$$F > F_c(N-P_1, N-P_2, 100(1-\alpha)\%)$$

where F_c is the tabulated critical value of the F statistic with $N-P_1$ and $N-P_2$ degrees of freedom.

The hypothesis that the two models explain the data equally well is rejected when

$$F > F_c(N-P_1, N-P_2, (1-\alpha/2)100\%)$$

or

$$F < F_c(N-P_1, N-P_2, 100\alpha/2\%)$$

The data sets used below are finite. The models that are constructed will be extrapolated beyond the limits of the supporting, finite, data sets. It is important then to have an estimate of the error to ascribe to the predictions of the model. The approximate error estimator used here is appropriate for a model linear in its parameters and is given by:

error in model prediction = $E(X,T)$

$$= \pm t(1-\alpha/2, N-P) \frac{\chi^2}{N-P}^{1/2} \left[1 + \frac{N(x-\bar{x})^2}{\sum_{i=1}^N (x_i - \bar{x})^2} + \frac{N(T-\bar{T})^2}{\sum_{i=1}^N (T_i - \bar{T})^2} \right]$$

where $t(1-\alpha/2, N-P)$ = Student's t statistic for the $(1-\alpha/2)$ 100% confidence level and N-P degrees of freedom

$(1-\alpha)100\%$ = confidence level of estimated range

\hat{x} = average composition in the data set

\hat{T} = average temperature in the data set

x_i = composition of a particular point in the data set

T_i = temperature of a particular point in the data set

x, T = composition and temperature of the estimate.

For the nonlinear models of interest here this estimate of uncertainty is very crude. Some values of the Student t statistic are listed below:

N-P	$t(1-\alpha/2, N-P)$ for			
	$\alpha = 0.2$	0.1	0.05	0.01
23	1.319	1.714	2.069	2.807
35	1.307	1.690	2.031	2.727
81	1.293	1.665	1.990	2.638

An 80 percent confidence level ($\alpha=0.2$) is used routinely in this document. More demanding readers can easily raise this confidence level.

The above definition of the model error yields a minimum error at the midpoint of the data set. The error grows toward the extremities of the data set and expands greatly when the model is used to extrapolate beyond the existing data.

C. Pressure Dependence of Activity Coefficients

All of the data available for alloys of interest here were acquired at normal, laboratory, atmospheric pressure. In application, however, the models will be used for pressures up to at least 170 atmospheres. Though this is not an exceptionally high pressure, it is useful to ascertain if pressures will significantly affect the activity coefficients of the alloy constituents.

The pressure dependence of activity coefficients of condensed phase species is given by:

$$\gamma_i(P) = \gamma_i(P_{\text{ref}}) \exp \left\{ \int_{P_{\text{ref}}}^P \frac{\bar{V}_i^L}{RT} dP \right\}$$

where $\gamma_i(P_{\text{ref}})$ = activity coefficient of the i^{th} constituent at the reference pressure which here is one atmosphere

$\gamma_i(P)$ = activity coefficient of the i^{th} constituent at pressure P

\bar{V}_i^L = partial molar volume of the i^{th} constituent the alloy.

Partial molar volume data for alloys are among the least often measured features of alloys. They are almost never known and certainly have not been reported for the alloy of interest here. In the absence of such data it has become customary to use molar volume data for the pure constituents of the alloy.

O. J. Kleppa⁽¹⁴⁾ has reported data on the excess volume of mixing of several alloys including cadmium/indium alloys. He finds that the excess volume of mixing passes through a maximum at mole fractions of near 0.5. At this maximum the excess volume is about $0.12 \pm 0.01 \text{ cm}^3/\text{g-atom}$. The findings are reminiscent of a regular solution. Thus, to a first approximation

$$V_{\text{mix}} = xV_m^{(1)} + (1-x)V_m^{(2)} + Ax(1-x)$$

where V_{mix} = volume of the mixture

x = mole fraction of constituent 1

$V_m^{(i)}$ = molar volume of the pure i^{th} constituent

A = regular solution interaction constant.

Then, the partial molar volume is given by

$$\bar{V}_1 = V_M^{(1)} + A(1-x)^2$$

$$\bar{V}_2 = V_M^{(2)} + Ax^2$$

From the data for cadmium/indium alloys the value of A is on the order of 0.5 cm³. Thus, the maximum difference between partial molar volumes and molar volumes is on the order of 0.5 cm³ or about 4 percent for species of interest here. This error is not likely to be significant.

For pressures and temperatures well-removed from the critical point, the pressure dependence of molar volume can be neglected. With this assumption, the activity coefficient is:

$$\gamma_i(P) = \gamma_i(P_{ref}) \left[\exp \bar{V}_i^L (P-1)/RT \right]$$

Obviously, the correction term is small. For a molar volume of 20 cm³/g-atom, the activity coefficient at a pressure of 100 atmospheres is greater than the activity coefficient at 1 atmosphere by a factor of 1.024 at 1000 K and a factor of 1.012 at 2000 K. Within the context of this work, errors in the activity coefficients of 1 and 2 percent are not of great concern.

D. Critical Properties of the Elements and Alloys

A proviso on the development above of the pressure dependence of the activity coefficients was that conditions be well-removed from the critical point. In the vicinity of the critical point the compressibility of the liquid and the compressibility of the vapor phase must become similar. The integral

$$\int_{P_{ref}}^P \frac{\bar{V}_i^L}{RT} dP$$

then becomes harder to evaluate.

Critical properties of the alloys of interest here have not been measured. A similar situation exists for nearly all mixtures. It is necessary then to estimate the properties of the mixture from those of the pure constituents. A typical set of "rules" for estimating the critical properties of mixtures is:(12)

$$T_c^{\text{mix}} = \sum_{i=1}^N T_c^i \theta_i ;$$

$$V_c^{\text{mix}} = \sum_{i=1}^N \theta_i V_c^i$$

where
$$\theta_i = \frac{x_i (V_c^i)^{2/3}}{\sum_{i=1}^N x_i (V_c^i)^{2/3}}$$

T_c^i = critical temperature of constituent i

V_c^i = critical volume of constituent i.

Measurements of the critical temperatures of silver and cadmium based on exploding wire techniques have been reported. (15,16) Some average values of the measurements are:

$$T_c(\text{Ag}) = 4210 \pm 210 \text{ K}$$

$$T_c(\text{Cd}) = 2545 \pm 60 \text{ K} .$$

Measurements of the critical temperature of indium have not been reported.

Quite a number of simple, empirical correlations have been proposed for estimating critical temperatures of elements from known properties. (17) Blair (18) advocates the use of the correlation:

$$T_c = 1.3839 T_b^{1.0473}$$

where T_b is the normal boiling point. Based on this correlation, the critical temperatures of the alloy constituents are:

$$T_c(\text{Ag}) = 5756 \text{ K}$$

$$T_c(\text{Cd}) = 1999 \text{ K}$$

$$T_c(\text{In}) = 4883 \text{ K} .$$

These estimates are at substantial odds with experimental data. The estimate for the critical temperature of mercury is 1190 K which is very much different than the well established value, $1753 \pm 20 \text{ K}$.

The above correlation was based on data for a variety of molecules including N_2 , noble gases, and hydrogen. It is difficult to believe that a simple empirical correlation would be so robust that it would successfully treat both metals and noble gases. Some experimental data for critical temperatures of metals are shown in Table 3. These data for metals can be correlated with the normal boiling point of the metal by:

$$\ln(T_c) = (1.6395 \pm 0.336) + (0.8798 \pm 0.0446)\ln(T_b)$$

where the uncertainty in the estimate of $\ln(T_c)$ is given by (80 percent confidence level):

$$\delta \ln(T_c) = \pm 0.2587 \left(1 + \frac{34(\ln(T_b) - 7.56)^2}{1976} \right)^{1/2}$$

and the uncertainty in the estimate of the critical temperature is:

$$\delta(T_c) = \pm T_c \delta(\ln(T_c)) .$$

A plot is shown in Figure 1 of this correlation, the 80 percent confidence bounds and the experimental data. Obviously, this is not an especially useful correlation.

Rather high quality correlations can be developed from data for metal with similar electronic structures. Thus, data for the alkali metals, copper, silver, and gold yield:

$$\ln(T_c) = (2.285 \pm 0.246) + (0.7795 \pm 0.0341)\ln T_b$$

$$\delta[\ln(T_c)] = 0.075 \left(1 + 0.022(\ln(T_b) - 7.185)^2 \right)^{1/2} .$$

Table 3
Critical Temperatures of Metals

Metal	Boiling Point (K)	Critical Temp.* (K)
Li	1603	3223 ⁺
Na	1165	2504
K	1033	2200, 2280
Rb	961	2111, 2106
Cs	963	2056, 1933, 2020, 2053
Nb	3573	9880, 9620
Mo	5833	7990, 11150(c), 14300**
W	6203	11880, 14100**
Cu	2868	5390
Ag	2483	4300
Au	3243	4800
Zn	1179	2500
Cd	1038	2480, 2291, 2665
Hg	630	1733, 1763, 1753
Pt	4803	6983(b)
Pb	1998	3970, 3959
Re	6173	9473(b)
U	4091	12434
Al	2723	3597, 3947

* Most entries from Reference 17.

⁺ J. Dillon et al., J. Chem. Phys. 44 (1966) 4229.

** U. Seydel et al., High Temp-High Pressure 11 (1979) 635.

(b) S. Blairs, J. Inorg. Nucl. Chem. 29 (1977) 905.

(c) U. Seydel and W. Fucke, J. Phys. F 8 (1978) 457.

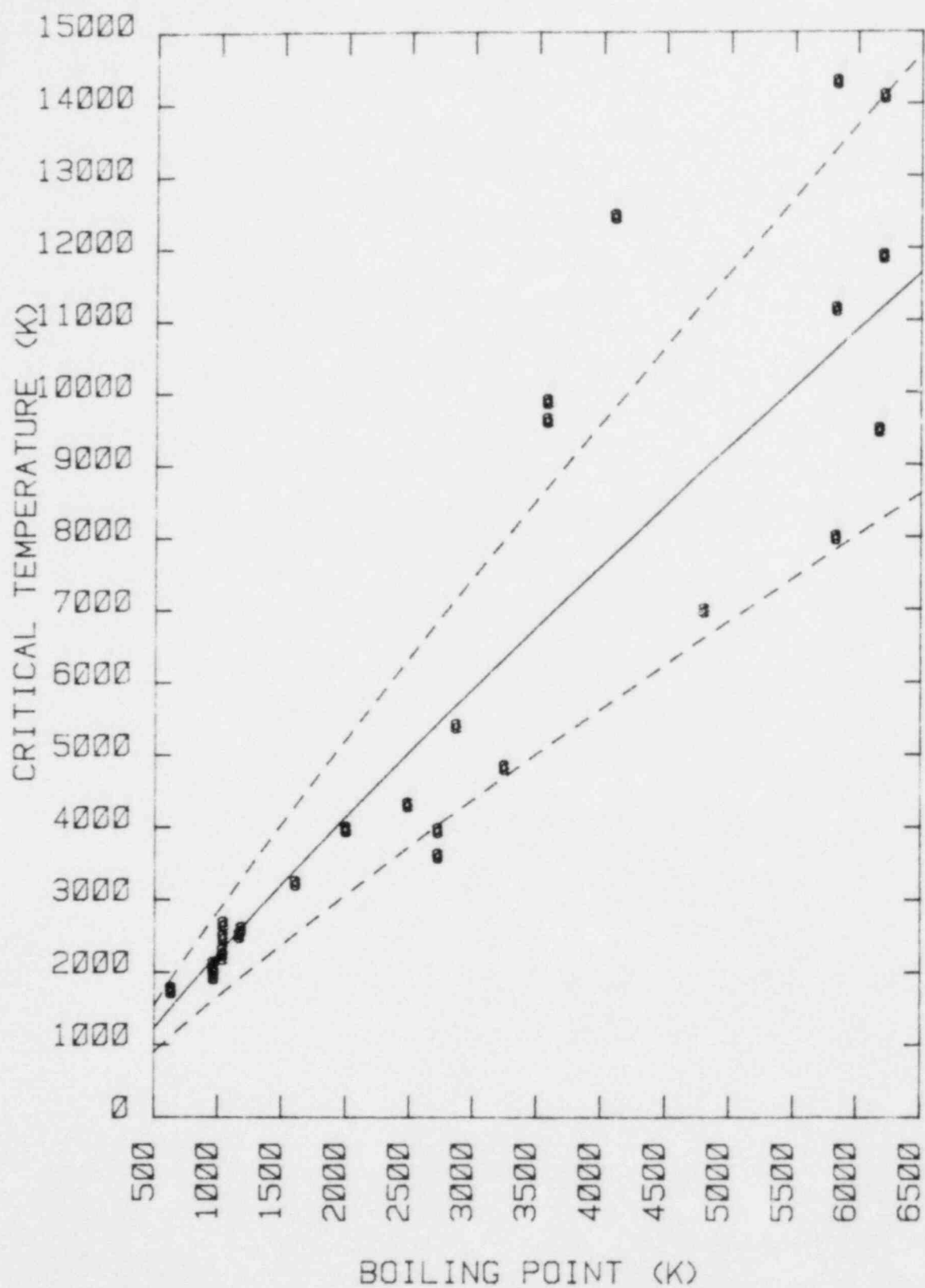


Figure 1. Correlation of Critical Temperatures of Metals With Their Boiling Points

Data for Hg, Cd, and Zn yield:

$$\ln(T_c) = 3.176 + 0.485 + (0.6660 + 0.0718)\ln(T_b)$$

$$\delta[\ln(T_c)] = 0.071 \left(1 + (7/0.495)(\ln(T_b) - 6.749)^2 \right)^{1/2} .$$

Plots of these correlations are shown in Figures 2 and 3. The quality of these correlations add some credence to the experimental data for silver and cadmium.

Unfortunately, there are not enough data available to construct a correlation for elements with electronic structures similar to that of In. The unpaired electron in the 4p orbital of In is similar in some respects to an unpaired s electron. Consequently, the correlation of the data for alkali metals, silver, copper, and gold are used to estimate the critical temperature of indium:

$$T_c(\text{In}) = 4164 \pm 87 \text{ K} .$$

Had the correlation for Hg, Cd, and Zn been used, a value within the above range would have been obtained. Other estimates of the critical temperature of indium⁽¹⁷⁾ based on the law of corresponding states (6000 K), a hard sphere solution model (5823 K), and the entropy of vaporization (6680 K) are all much higher than the estimate here. These other techniques also yield high estimates for the critical temperatures of cadmium and silver.

Critical pressures of the elements Ag, In, and Cd have not been measured. Very crude estimates of the critical pressure can be made by extrapolating low temperature vapor pressure data with the equation:

$$\log P = -A/(T+B)$$

to the critical temperature. Results of the extrapolation are shown in Table 4. Critical molar volumes found from the Redlich-Kwong equation of state:

$$\frac{PV}{RT} = \frac{V}{(V-b)} - \frac{a}{RT^{3/2}(V+b)}$$

Table 4

Critical Properties of the Elements and the
Parameters for the Redlich-Kwong Equation of State

Element	T_c (K)	P_c (atms)	V_c (cm ³)	Z_c
Ag	4200	200	470	0.2739
Cd	2466	905	80	0.3578
In	4174	190	480	0.2772

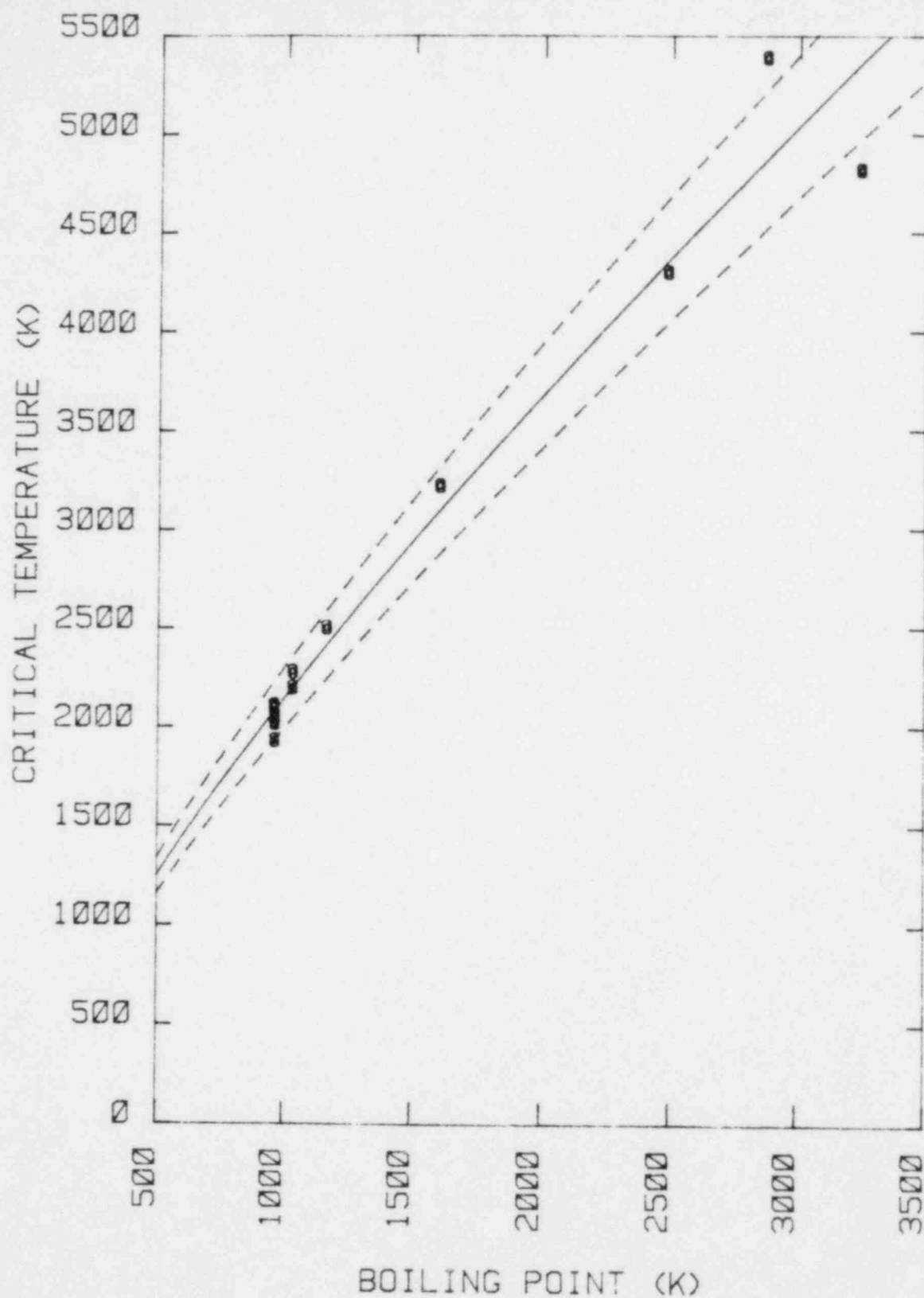


Figure 2. Correlation of Critical Temperatures of Metals Having Unpaired s Electrons With Their Boiling Points

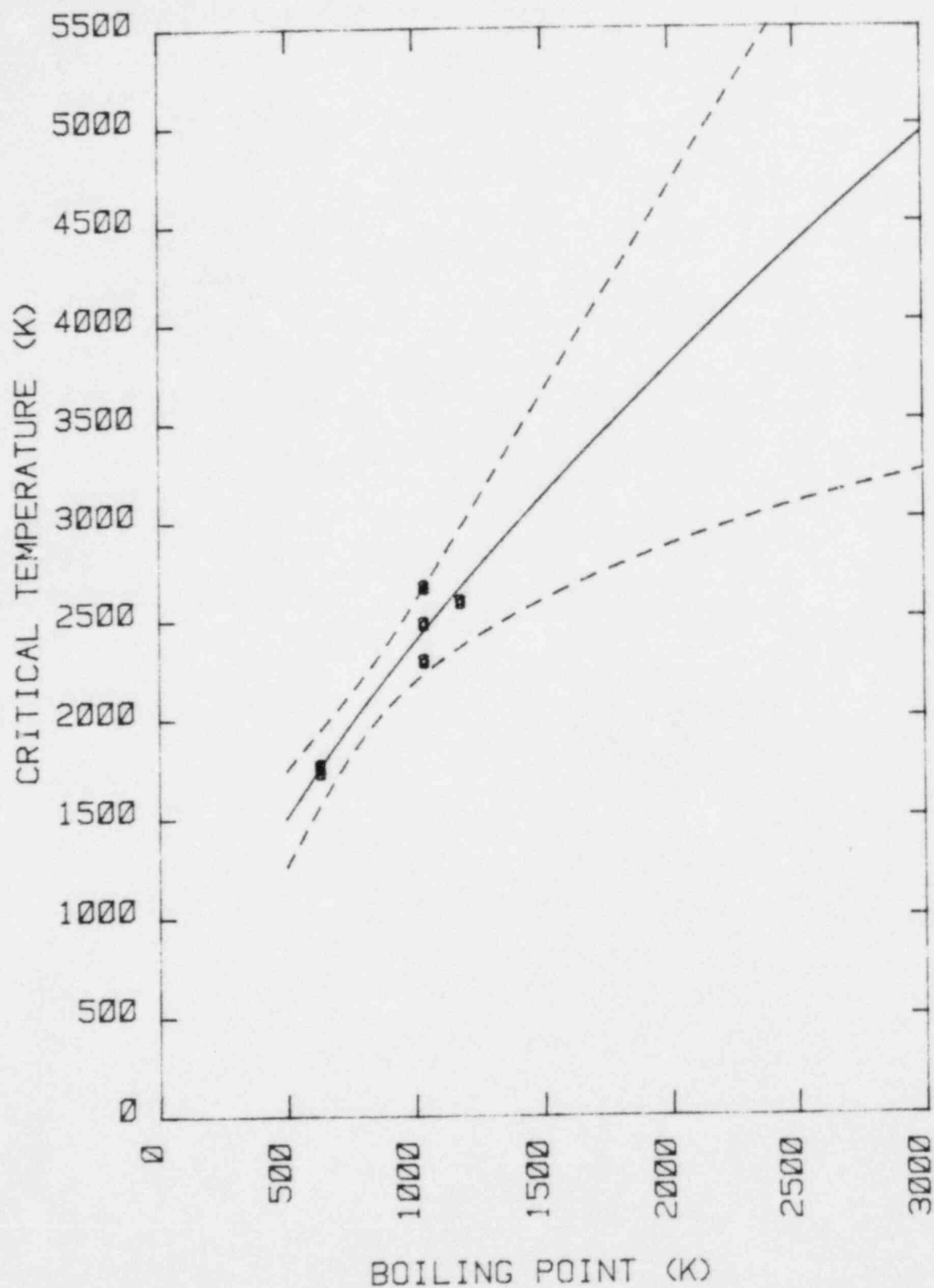


Figure 3. Correlation of Critical Temperatures of Metals Having Paired s Electrons With Their Boiling Points

where $a = 0.4278 R^2 T_C^{5/2} / P_C$

$$b = 0.0867 R T_C / P_C$$

are also shown in Table 4. The parameter $Z_C = P_C V_C / R T_C$ shown in Table 4 is called the critical compressibility. Values of dimensionless parameter Z_C obtained for the elements of interest here can be compared to those derived theoretically. A van der Waals equation of state will yield a compressibility parameter of 0.375 which is remarkably close to that found for cadmium. As will be discussed below, strong bonding interactions would not be expected among cadmium atoms in the gas phase. Weak dimerization of the gaseous atoms would be the result of van der Waals attractive forces.

Compressibility factors for silver and indium are substantially less than that found for cadmium. Both silver and indium have incomplete outer electron shells and enhanced interaction among gaseous atoms would be expected. Values of the compressibility parameter are less than those found for species with filled outer electron shells such as Xe, Ar, CH₄, and N₂ which average 0.292.

From the critical data of the pure constituents, the critical properties of the Ag-In-Cd alloy are found to be

$$T_C^{\text{mix}} = 4170 \text{ K}$$

$$V_C^{\text{mix}} = 460 \text{ cm}^3/\text{mole}$$

$$P_C^{\text{mix}} = 220 \text{ atmospheres}$$

From these results, it is apparent that for reactor safety analyses the pressure dependence of condensed phase activity coefficients can be neglected.

E. Activity Coefficients for Binary Constituent Alloys

The ternary Ag-In-Cd alloy is composed of three binary constituent alloys--Ag/In, Ag/Cd, and Cd/In. Data for the activity coefficients in these binary constituent alloys are collected in Appendix A. In the subsections below, these data are reviewed and are used to find parameters for non-ideal solution models.

1. The Cadmium/Silver System

The various data sets for the activity coefficient of cadmium in liquid cadmium/silver alloys are plotted in Figure 4 against the mole fraction of cadmium. The data sets appear mutually consistent, so all the data were used to estimate parametric values for the models. Results of the nonlinear least squares fitting procedures are shown in Table 5.

The two-parameter version of the Wilson equation fit the data well. A plot of the observed activity coefficients against activity coefficients calculated with the Wilson equation is shown in Figure 5. The "goodness of fit" parameter, $\chi^2/(N-P)$, indicated a standard error in the estimate obtained from the model at the mean values of the temperature and mole fraction cadmium of 0.028. Thus, the error in an estimate obtained from the two-parameter Wilson equation is:

$$\delta(\gamma_{\text{Cd}}) = \pm 0.036 \left(1 + \frac{37(T-1076)^2}{6.85 \times 10^5} + \frac{37(x-0.59)^2}{2.39} \right)^{1/2}.$$

This error is consistent with the uncertainty ascribed to the experimental data.

Rendering temperature dependent the parameters of the Wilson equation did not significantly improve the fit of the model to the data.

Kuo and Lang⁽¹⁵⁾ have apparently been able to fit activity data for the cadmium/silver system with a subregular solution model. Results obtained in their work were not available to the author. Here, too, it was found that the activity data for cadmium in liquid cadmium/silver alloys were well described by a subregular model. A plot of the activities calculated with such a model against observed activities is shown in Figure 6. The subregular model was, however, not significantly better than the Wilson equation. Though rendering parameters in the subregular model temperature dependent did improve the fit of the model to the data, the improvement was not significant.

2. The Cadmium/Indium System

There are four published data sets for the activity of cadmium in liquid cadmium/indium alloys.⁽²⁰⁻²³⁾ These data are plotted in Figure 7 against the mole fraction cadmium in the alloy. All the data sets show the activity of cadmium approaches unity at high concentrations and is much greater than unity in dilute alloys.

Table 5

Summary of Parametric Values for the
Cadmium/Silver System

I. Two-Parameter Wilson Equation:*

$$a_{Cd} = -1133.83$$

$$a_{Ag} = -2516.52$$

$$x^2/(N-P) = 8.254 \times 10^{-4}$$

II. Four-Parameter Wilson Equation:

$$a_{Cd} = -1853.40 + (0.7688 \times 10^6)/T$$

$$a_{Ag} = -2043.09 - (0.5047 \times 10^6)/T$$

$$x^2/(N-P) = 8.70 \times 10^{-4}$$

III. Two-Parameter Subregular Solution Model:

$$h_{Cd} = -3302.8$$

$$h_{Ag} = -5673.9$$

$$x^2/(N-P) = 8.08 \times 10^{-4}$$

IV. Four-Parameter Subregular Solution Model:

$$h_{Cd} = -3590.36 + (0.3202 \times 10^6)/T$$

$$h_{Ag} = -9979.69 + (4.9016 \times 10^6)/T$$

$$x^2/(N-P) = 7.85 \times 10^{-4}$$

* N = 37

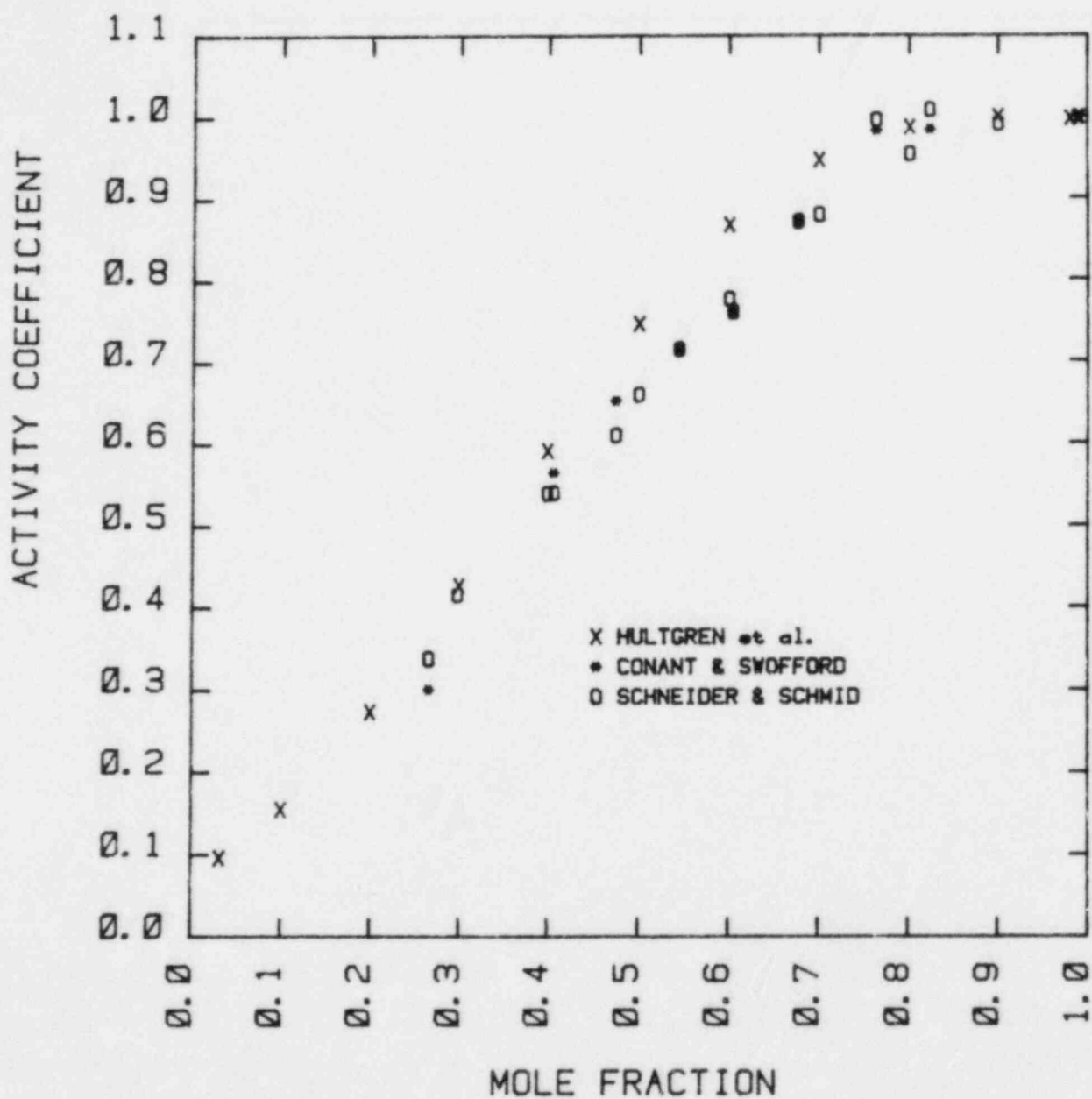


Figure 4. Experimental Data for the Activity Coefficients of Cadmium in Liquid Cadmium/Silver Alloys Plotted Against the Mole Fraction of Cadmium

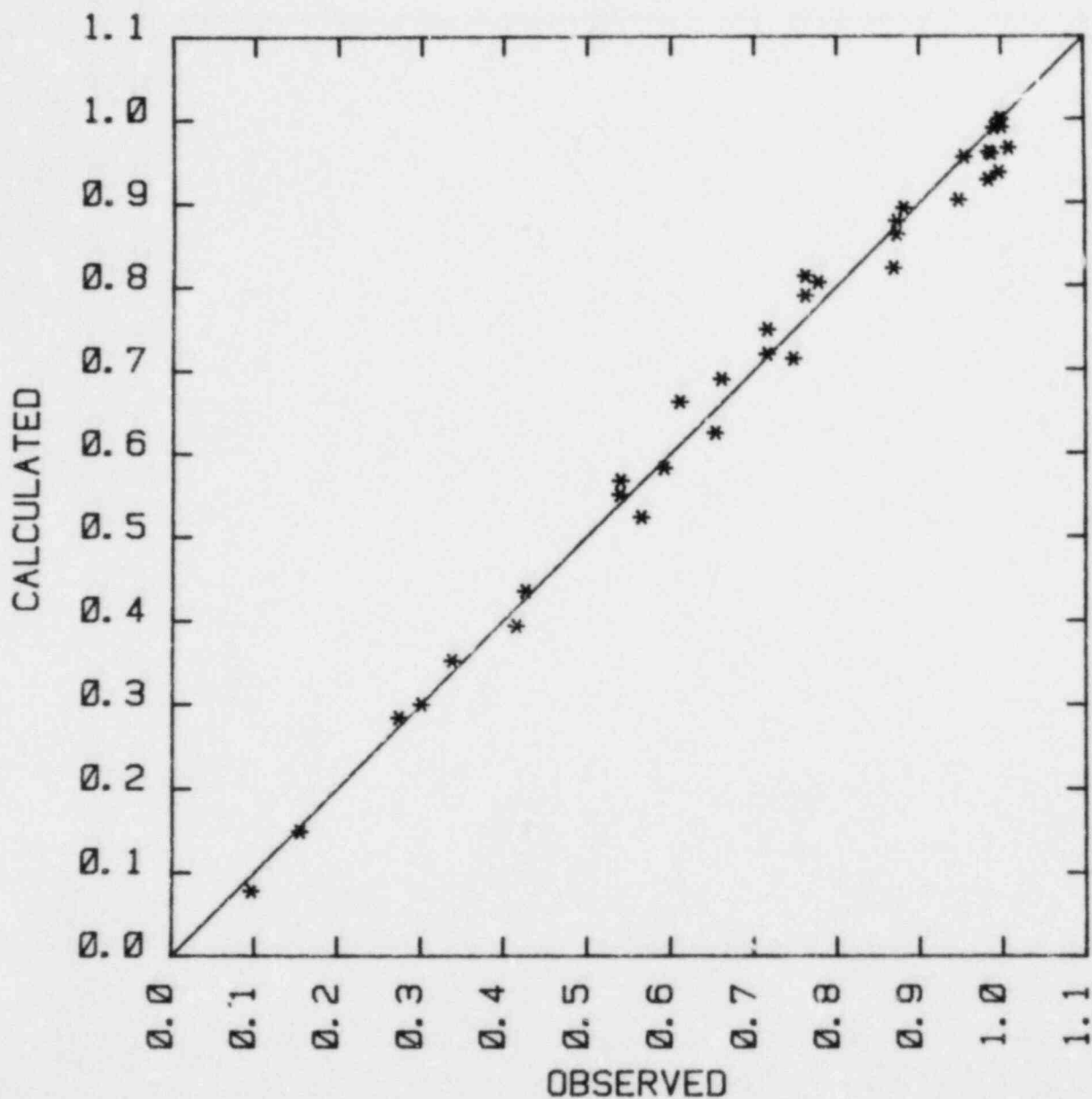


Figure 5. Plot of Cadmium Activity Coefficients Calculated With the Two-Parameter Wilson Equation Against Observed Cadmium Activity Coefficients in Liquid Cadmium/Silver Alloys. (Solid line denotes perfect agreement between predictions and observations.)

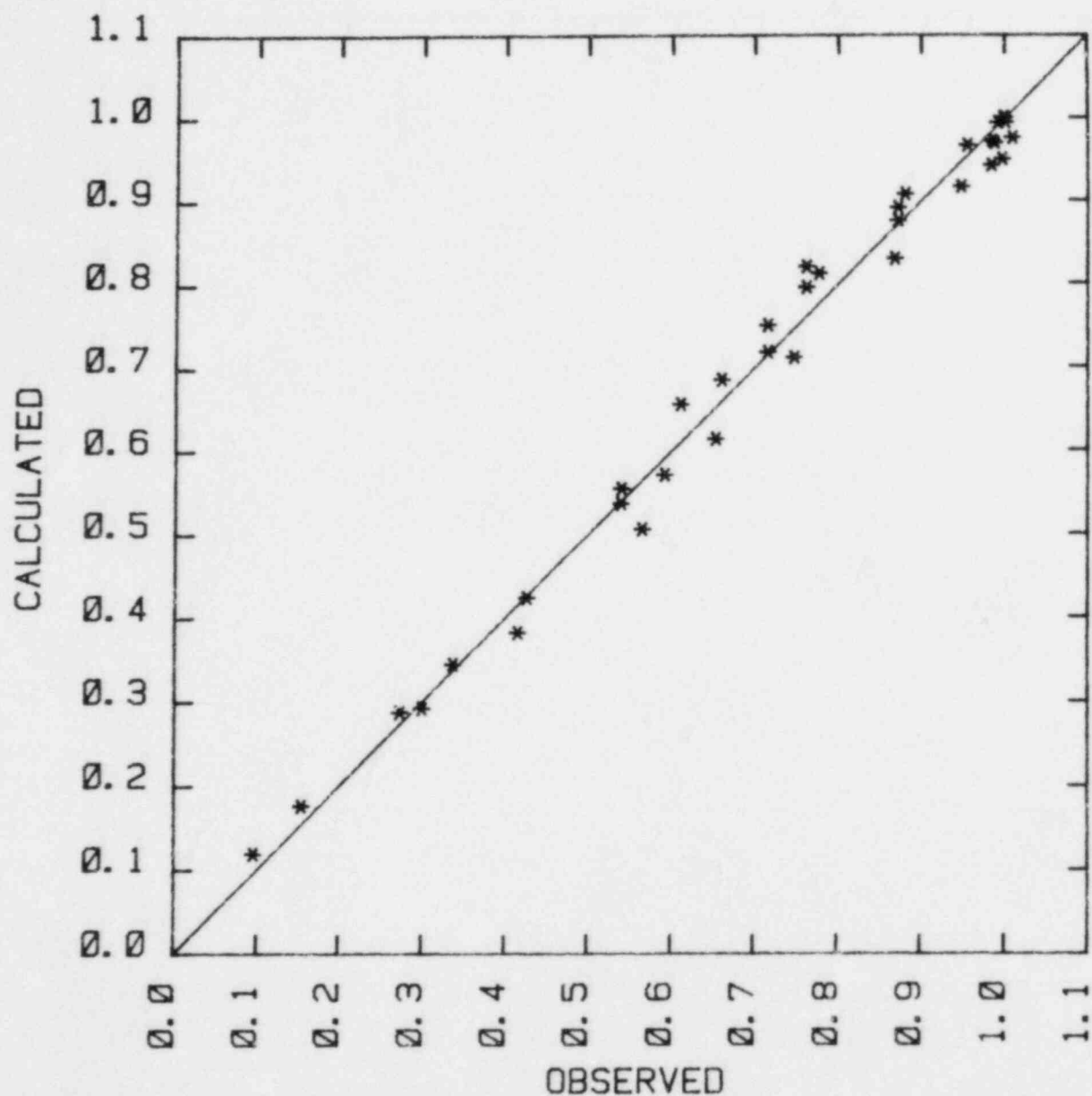


Figure 6. Plot of Cadmium Activity Coefficients Calculated With the Two-Parameter Subregular Solution Model Against Observed Cadmium Activity Coefficients in Liquid Cadmium/Silver Alloys. (Solid line denotes perfect agreement between predictions and observations.)

The data set prepared by Pozharskaya and Evseev(20) is different qualitatively as well as quantitatively than the sets prepared by other authors. In this data set the activity of cadmium passes through a minimum which is less than unity at a composition of about 60 percent cadmium. All the other data sets suggest that cadmium activity coefficients are greater than one throughout the alloy composition range and that the activity coefficients increase with decreasing cadmium concentration.

Servis and Munir(23) have critiqued the data sets obtained by Pozharskaya and Evseev and the data sets obtained by Heumann and Predel.(21) Details of the thermochemistry in the vicinity of 65 mole percent cadmium were their concerns. Perhaps in response to these concerns Predel and Berka(22) reexamined the cadmium/indium system.

The data sets by Pozharskaya and Evseev are discounted here. This work was done at quite low temperatures (<590 K). It is entirely possible that at such low temperatures ordering present in the solid alloy phase is not totally overwhelmed by thermal effects in the liquid phase. There then would be radical variations in liquid properties as temperatures increase. Properties at low temperatures are not of great interest here.

Attainment of equilibrium is also a concern at low temperatures. Pozarskaya and Evseev do not provide in their report persuasive evidence that they were working with an equilibrated alloy.

Results of attempts to reconcile the remaining three data sets by fitting models to the data are summarized in Table 6.

The data set by Predel and Berka can be fitted by a two-parameter Wilson equation. Activities calculated with this model are compared in Figure 8 to those observed by Predel and Berka. The data set by Servis and Munir, too, can be fitted by this model. The combination of these two data sets and the combination with the data sets reported by Heumann and Predel are not well described by the two-parameter Wilson equation. As shown by the comparison of calculated and observed activity coefficients in Figure 9, the discrepancies become large when the cadmium activity coefficient is high. High cadmium activity coefficients occur at low cadmium concentrations and low temperatures.

Making the parameters in the Wilson equation temperature dependent does improve the fit of the model to the combined data sets (see Figure 10). Standard errors for the fit are larger than experimental errors attributed to the data.

Table 6

Summary of Parametric Values for the
Cadmium/Indium System

Data Set	N	$\chi^2/(N-P)$	Parameters	
(Two-Parameter Wilson Equation)				
HP, PB, SM	136	6.351×10^{-3}	$a_{Cd} = 1506.06$	$a_{In} = -230.202$
PB, SM	77	5.916×10^{-3}	$a_{Cd} = 1954.15$	$a_{In} = -480.58$
PB	68	0.447×10^{-3}	$a_{Cd} = 1602.92$	$a_{In} = -182.519$
(Two-Parameter Subregular Solution)				
PB, SM	77	8.216×10^{-3}	$h_{Cd} = 885.476$	$h_{In} = 1279.83$
(Four-Parameter Wilson Equation)				
HP, PB, SM	136	3.591×10^{-3}	$a_{In} = -3044.12 + (2.38121 \times 10^6)/T$	
			$a_{Cd} = 5443.07 - (3.26815 \times 10^6)/T$	
(Four-Parameter Wilson Equation)				
PB, SM	77	0.492×10^{-3}	$a_{Cd} = 6232.68 - (3.83628 \times 10^6)/T$	
			$a_{In} = -3823.49 + (3.02715 \times 10^6)/T$	
(Four-Parameter Subregular Solution)				
PB, SM	77	2.009×10^{-3}	$h_{Cd} = 1004.47 - (0.057266 \times 10^6)/T$	
			$h_{In} = 3002.77 - (1.36955 \times 10^6)/T$	

HP = Heumann and Predel data-reference²¹PB = Predel and Berka data-reference²²SM = Servis and Munir data-reference²³

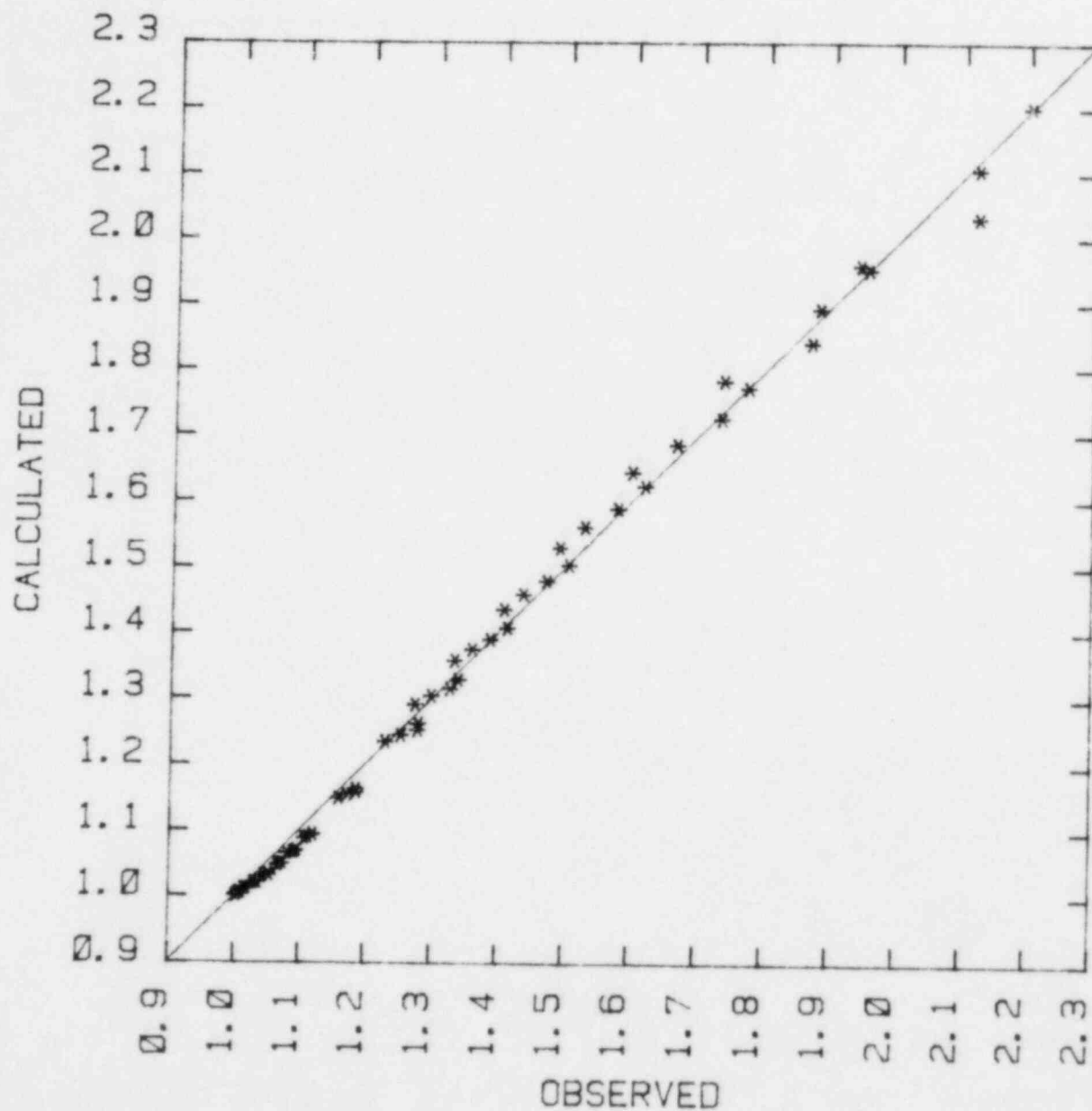


Figure 8. Comparison of Cadmium Activity Coefficients Calculated With the Two-Parameter Wilson Equation Model to Those Observed by Predel and Berka

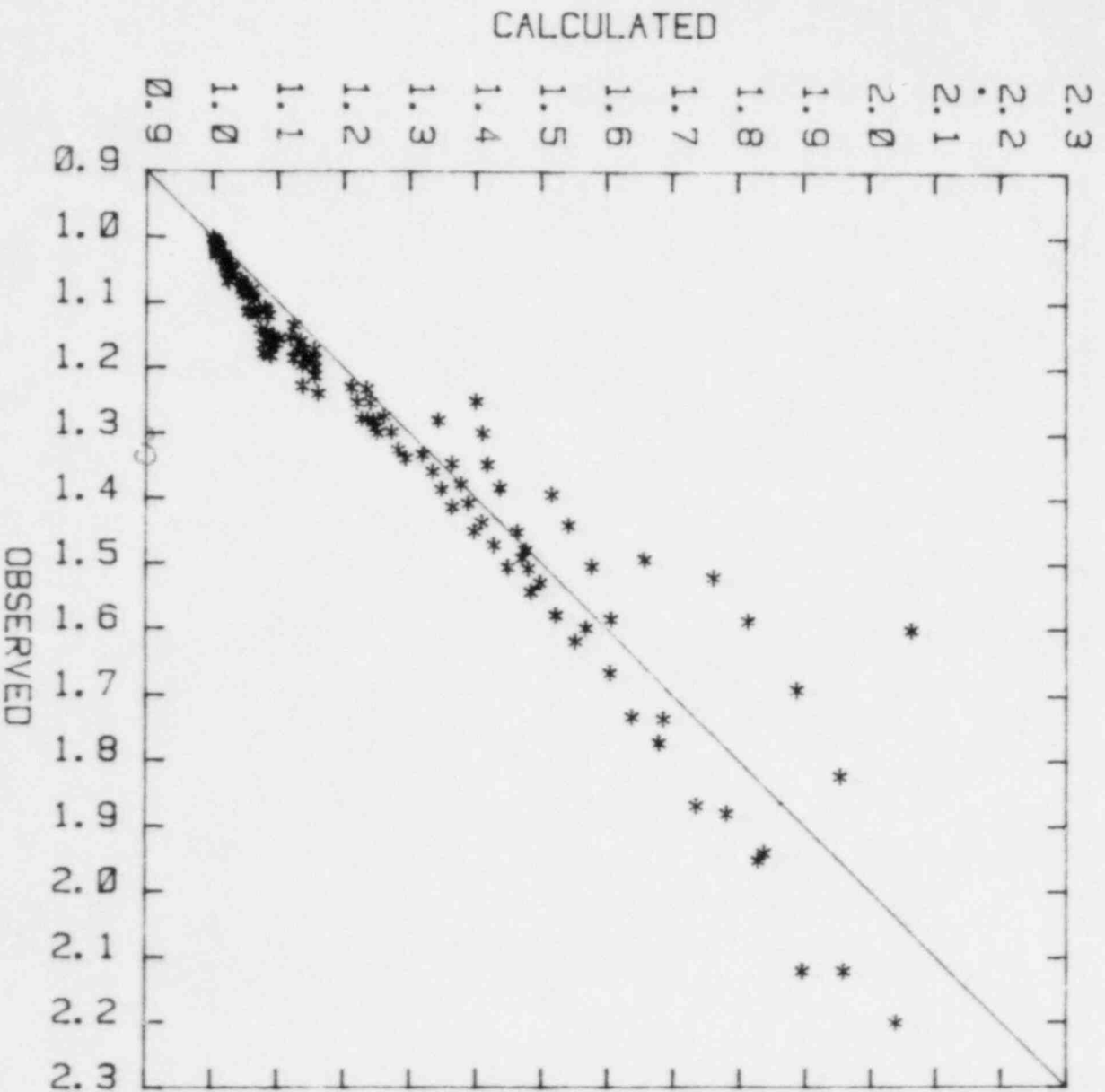


Figure 9. Comparison of Cadmium Activity Coefficients Calculated With the Two-Parameter Wilson Equation to Cadmium Activity Coefficients Measured in Studies by Predel and Berka, Servis and Munitz, and Heumann and Predel

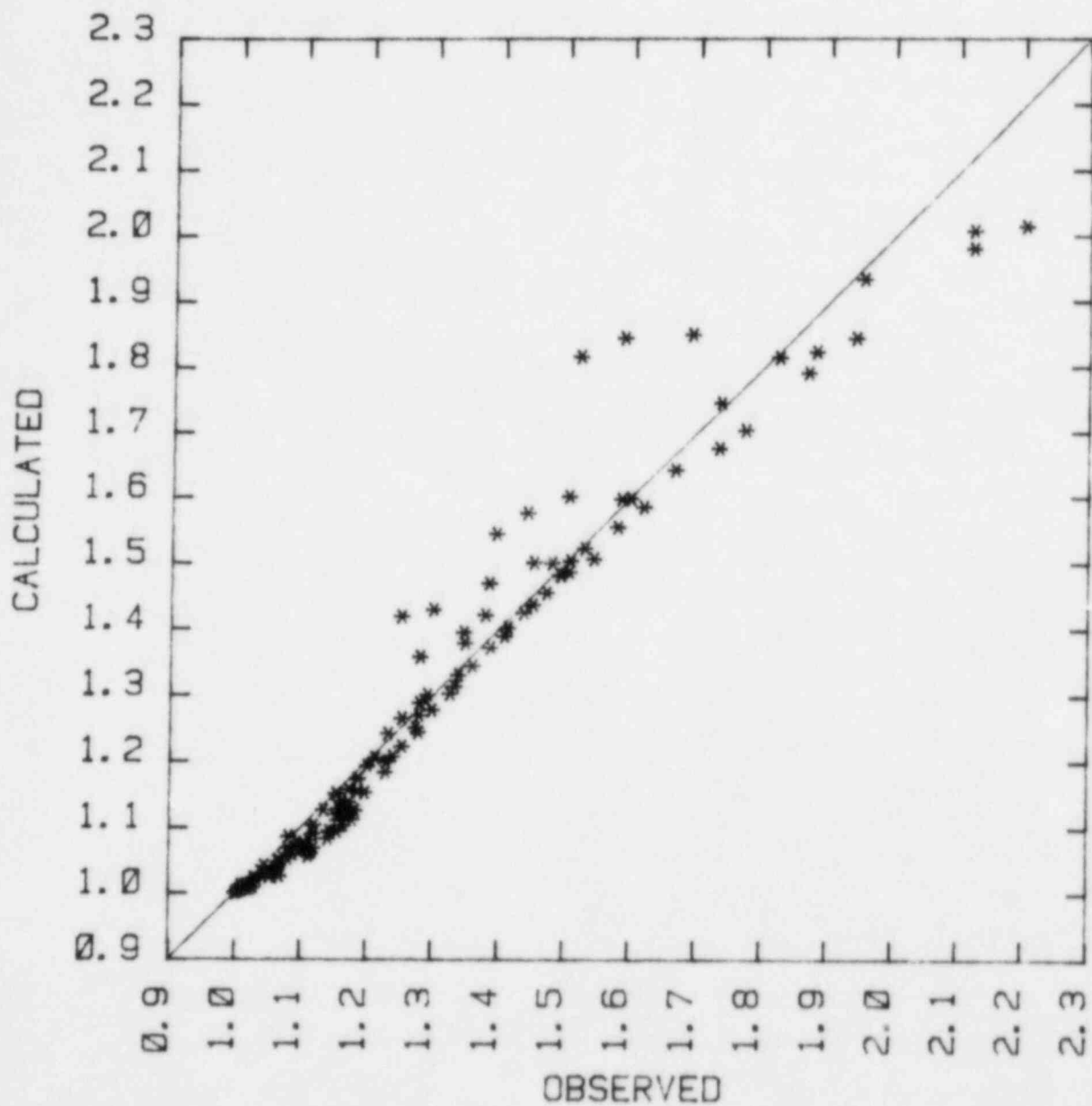


Figure 10. Comparison of Cadmium Activity Coefficients Calculated With the Four-Parameter Wilson Equation to Cadmium Activity Coefficients Measured by Predel and Berka, Servis and Munir, and Heumann and Predel

Predel and Berka seemed to prefer their data set to that produced by Heumann and Predel which had been criticized by Servis and Munir. When the Heumann and Predel data set was eliminated, the four-parameter Wilson equation fit the data very well. The fit was as good as the fits of the two-parameter Wilson equation to the individual data sets (see Figure 11).

Neither the two parameter nor the four-parameter sub-regular solution models showed any capability to fit the data in a way superior to the fits with the Wilson equation.

For further work here, the four-parameter Wilson equation parameterized by fitting to the data sets published by Servis and Munir and by Predel and Berka is used. An estimate of the uncertainty in activity coefficients calculated with this model is given by:

$$\delta(\gamma_{\text{Cd}}) = \pm 0.029 \left(1 + \frac{77(x-0.5)^2}{6.266} + \frac{77(T-821)^2}{5.99 \times 10^5} \right)^{1/2}.$$

3. The Indium/Silver System

The four published data sets for the activity coefficients in the indium/silver system⁽²⁴⁻²⁷⁾ were used to prepare the plot of the indium activity coefficient against the mole fraction indium shown in Figure 12. All four data sets show the same qualitative behavior. The activity coefficient of indium is near one for mole fractions of indium greater than about 0.7. The activity coefficient of indium decreases sharply with decreasing mole fraction of indium for indium mole fractions less than about 0.6.

Data sets by Nozaki et al.,⁽²⁴⁾ Mycielska et al.,⁽²⁷⁾ and by Predel and Schallner⁽²⁶⁾ were obtained using electromotive force measurements. The method employed by Predel and Schallner was to derive activity coefficients for the indium/silver system based on measurements in the ternary indium/silver/zinc system. The data set reported by Alcock et al. was obtained using mass spectroscopic techniques.

The four data sets are not concordant. The data set by Predel and Schallner can be excused because of the indirect nature of the method employed to derive this data set. Alcock et al. have suggested that the method employed by Nozaki et al. is susceptible to errors caused by mass transport. The curious excursion of the activity coefficients through a broad maximum at an indium mole fraction of 0.85-0.55 in the Nozaki et al. data set is at odds with the other data sets.

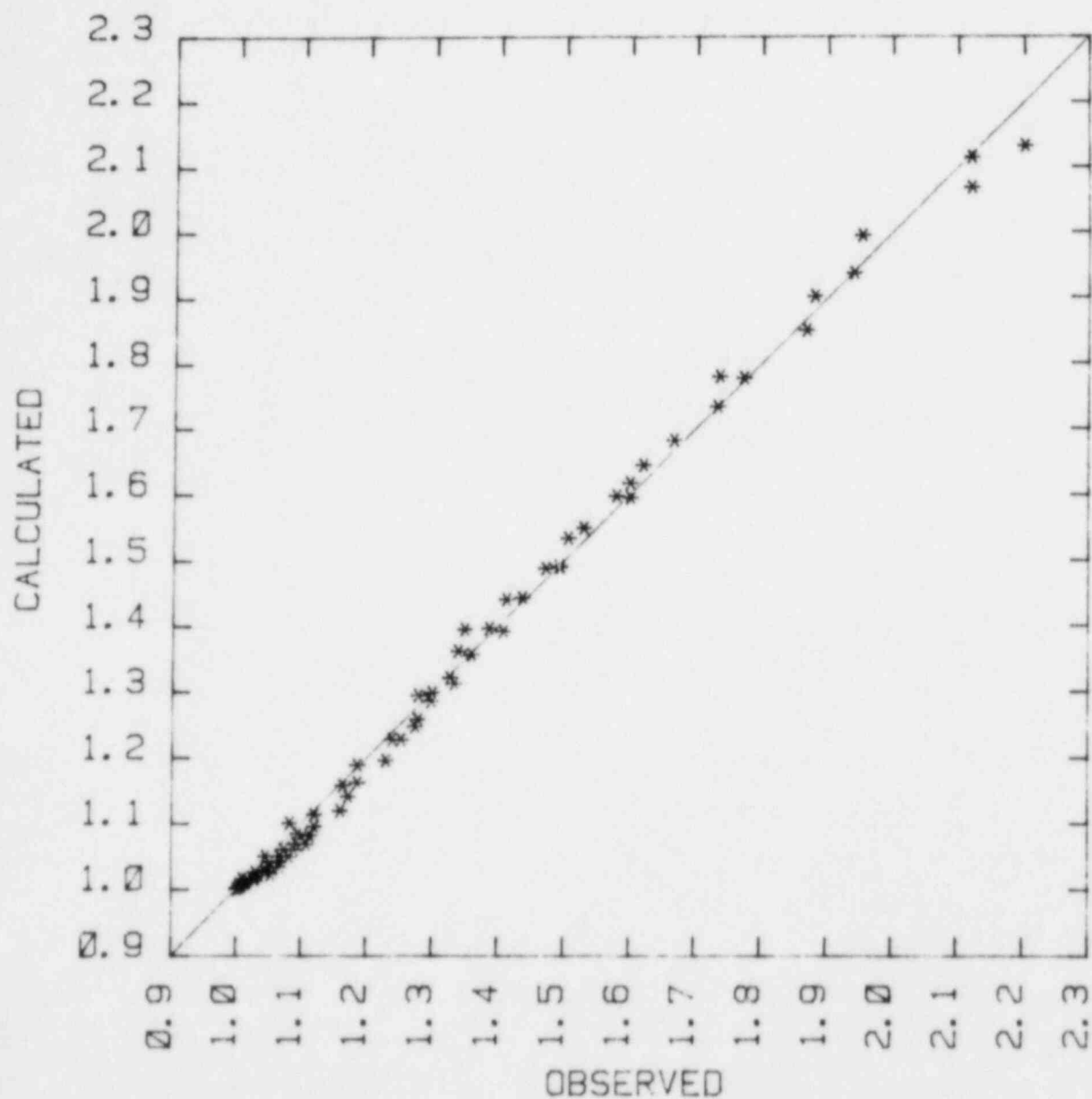


Figure 11. Comparison of Cadmium Activity Coefficients Calculated With the Four-Parameter Wilson Equation to Cadmium Activity Coefficients Measured by Predel and Berka and by Servis and Munir

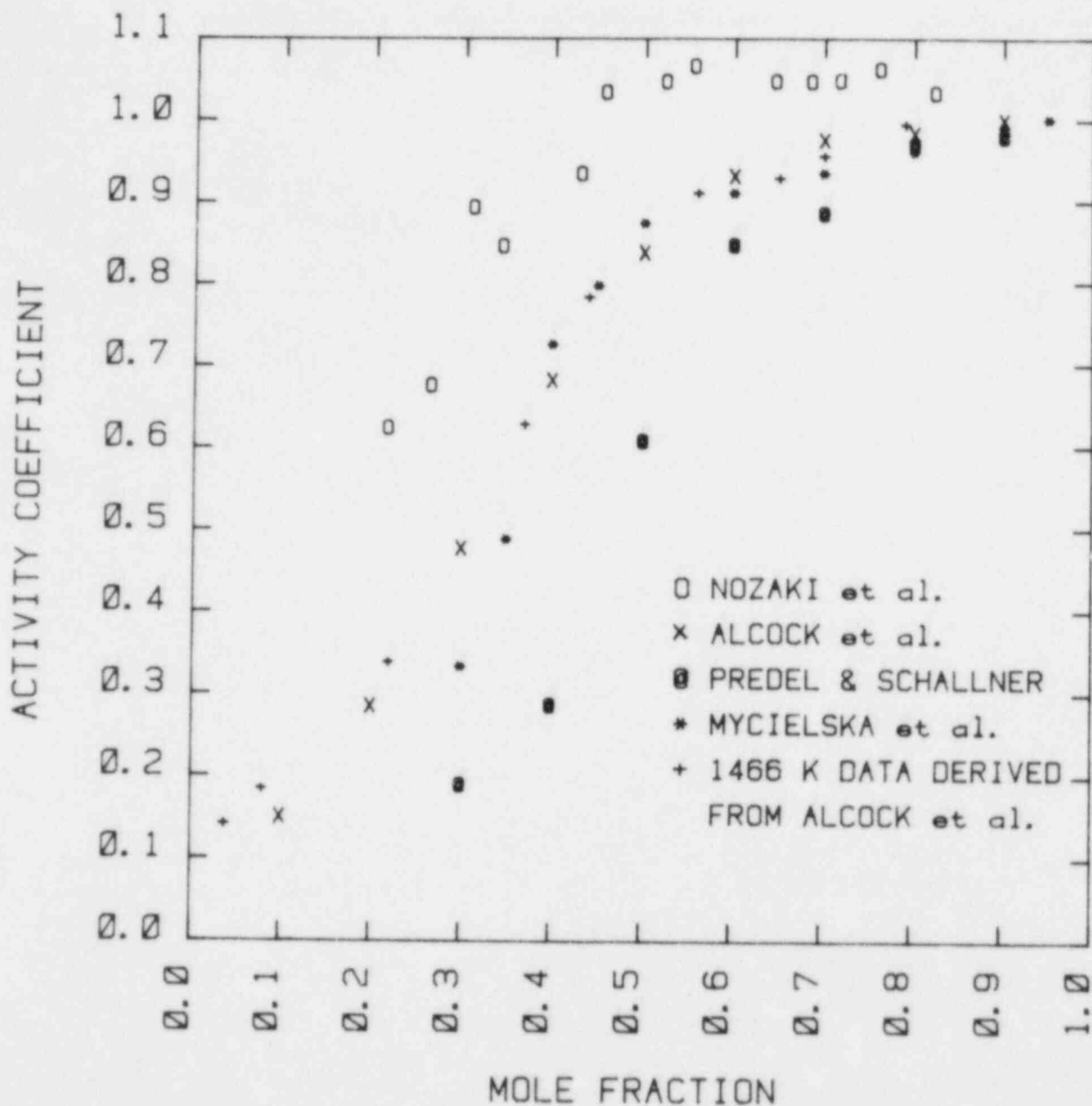


Figure 12. Indium Activity Coefficients Observed in Various Studies of Liquid Indium/Silver Alloys Plotted Against the Mole Fraction of Indium

The data sets obtained by Mycielska et al. and by Alcock et al. are in good agreement at high concentrations of indium. As the concentration of indium falls below 30 percent the data set by Mycielska et al. deviates from that obtained by Alcock et al. This may be a manifestation, again, of the difficulties that arise with mass transport during electromotive force measurements with liquid alloys. The agreement between these two data sets at high indium concentrations suggests that the activity coefficient of indium is relatively insensitive to temperature.

Alcock et al. provide values of the indium activity coefficient at 1300 K only. They also provide raw ion current data in graphical form that can be used to derive activity coefficients at 1466 K. These data, too, show the activity coefficients to be insensitive to temperature.

Results of attempts to fit models to the various data sets are shown in Table 7. Attempts to fit all four data sets or even all data sets less than that obtained by Predel and Schallner yielded impossible parametric values. The combination of the Alcock et al. and Mycielska et al. data sets did yield an adequate parameterization of the two-parameter Wilson equation. The standard error for this fit is ± 0.05 .

Inspection of the fit to the Alcock et al. and Mycielska et al. data sets shows that most of the lack of fit is caused by low concentration data from the Mycielska et al. data sets. When these low concentration data points are excluded a much superior fit is obtained. The standard error for this fit is ± 0.04 which is consistent with the uncertainty in the experimental data.

The two-parameter Wilson equation parameterized with the data from Alcock et al. and data from Mycielska et al. for alloys with more than 40 percent indium is used for further work here. A plot of the activity coefficients calculated with this model against observed activity coefficients is shown in Figure 13. The error of an estimate from this model is given by:

$$\delta(\gamma_{\text{In}}) = \pm 0.037 \left(1 + \frac{25(T-1276)^2}{8.63 \times 10^5} + \frac{25(x-0.53)^2}{1.722} \right)^{1/2}$$

The two-parameter subregular solution model fits the observed data significantly better than does the two-parameter Wilson equation. Improvements also occur by making the models temperature dependent, but these improvements are not significant.

Table 7

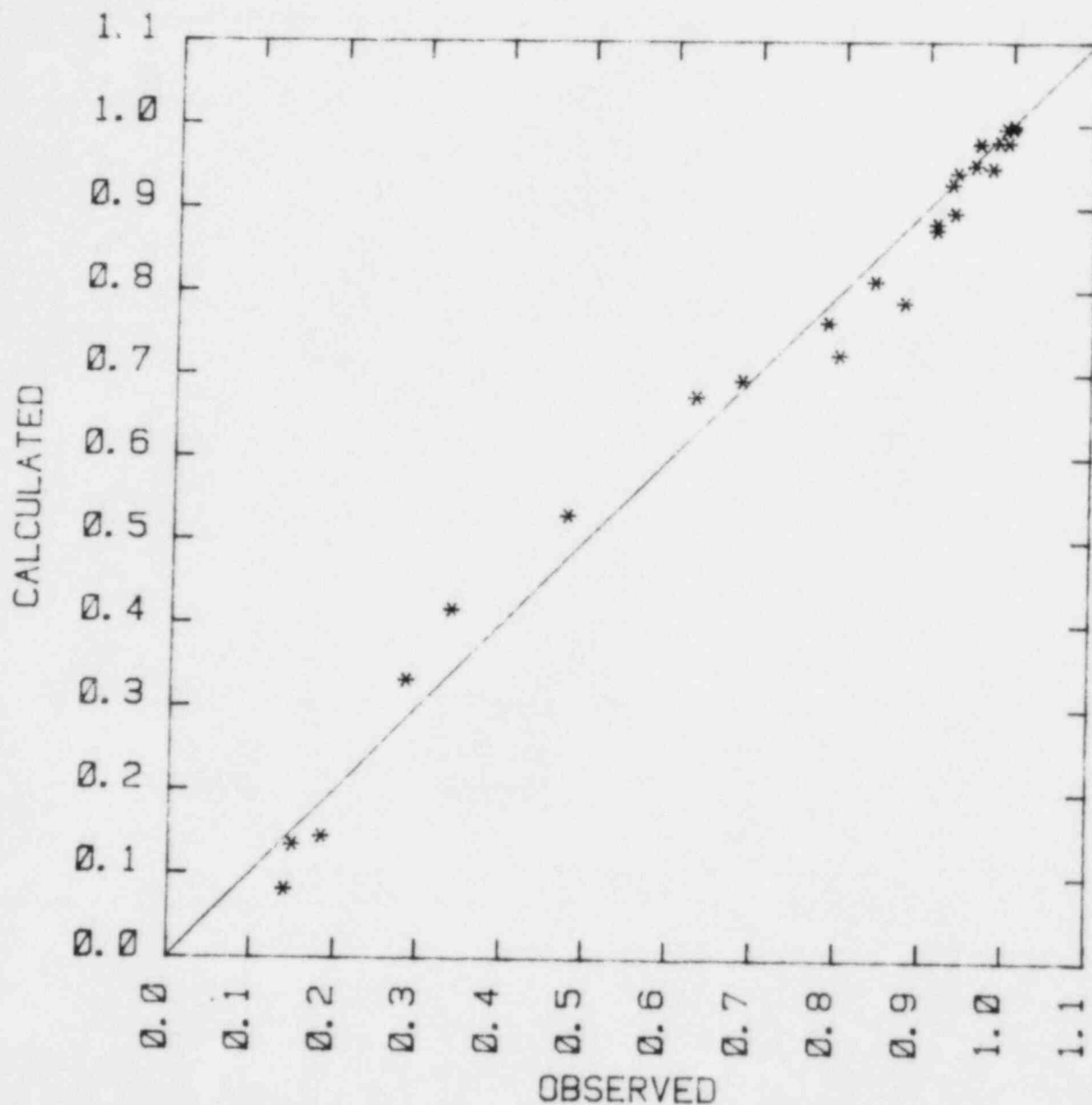
Summary of Parametric Values for the
Indium/Silver System

Data Set	N	$\chi^2/(N-P)$	Parameters	
(Two-Parameter Wilson Equation)				
A	18	1.303×10^{-3}	$a_{In} = 536.286$	$a_{Ag} = -3182.68$
A, M	28	2.450×10^{-3}	$a_{In} = 1267.87$	$a_{Ag} = -3529.46$
A, M*	25	1.644×10^{-3}	$a_{In} = 1466.00$	$a_{Ag} = -3498.28$
(Two-Parameter Subregular Solution)				
A	18	0.526×10^{-3}	$h_{In} = -2127.4$	$h_{Ag} = -6701.47$
A, M	28	2.150×10^{-3}	$h_{In} = -1823.81$	$h_{Ag} = -6605.18$
A, M*	25	1.587×10^{-3}	$h_{In} = -1902.30$	$h_{Ag} = -6561.47$
(Four-Parameter Wilson Equation)				
A, M*	25	1.353×10^{-3}	$a_{In} = -2032.68 + (3.49679 \times 10^6)/T$	
			$a_{Ag} = -4822.01 + (2.3018 \times 10^6)/T$	
(Four-Parameter Subregular Solution)				
A, M*	25	0.772×10^{-3}	$h_{In} = -4189.33 + (2.80368 \times 10^6)/T$	
			$h_{Ag} = -16074.8 + (12.9651 \times 10^6)/T$	

A = Data by Alcock et al. reference²⁵

M = Data by Mycielska et al. reference²⁷

M* = Data for $x_{In} > 0.4$ by Mycielska et al. reference²⁷



4. Summary of Activity Coefficient Models for the Binary Constituent Alloys

The Wilson equation describes activity coefficients in the binary constituent alloys of the Ag-In-Cd system. The parameters for the models of these binary alloys used for continued work here are:

$$a(\text{Cd}, \text{Ag}) = -1133.83$$

$$a(\text{Ag}, \text{Cd}) = -2516.52$$

$$a(\text{Cd}, \text{In}) = 6232.68 - (3.83628 \times 10^6)/T$$

$$a(\text{In}, \text{Cd}) = -3823.49 + (3.02715 \times 10^6)/T$$

$$a(\text{In}, \text{Ag}) = 1466.00$$

$$a(\text{Ag}, \text{In}) = -3498.28$$

Plots of these activity coefficients calculated with these models are shown in Figures 14-16 as functions of the alloy composition. The temperature dependence of the cadmium activity coefficient in a cadmium/silver alloy with a cadmium mole fraction of 0.06 is shown in Figure 17. The activity coefficient of cadmium in a cadmium/indium alloy with a cadmium mole fraction of 0.25 is shown as a function of temperature in Figure 18. The activity coefficient of indium in an indium/silver alloy with an indium mole fraction of 0.19 is shown as a function of temperature in Figure 19. The 80 percent confidence bounds on the estimated activity coefficients are shown as dashed lines in all these figures. Note how the bounds expand as the limits of the data base supporting the model are approached and exceeded.

F. Results for Ternary Alloys

The models of the binary constituent alloys can be used to construct a model of the ternary Ag-In-Cd alloy. This model was used to construct the plots of ternary activities at 1000, 1300, and 1500 K shown in Figures 20-28. The iso-activity curves are plotted on triangular coordinates typically used to describe a ternary system. The iso-activity curves are at intervals of 0.1 activity units. Solid and dashed lines are alternated for the purposes of clarity.

Activity coefficients of cadmium, indium, and silver in a liquid alloy of 80 percent Ag, 15 percent In, and 5 percent Cd are shown as functions of temperature in Figures 29-31, respectively. The activity coefficients of all species are less than one. That is, their activities are significantly

Figure 14. Calculated Activity Coefficient of Cadmium in a Cadmium/Silver Alloy at 1076 K as a Function of the Mole Fraction of Cadmium. The dashed lines are 80 percent confidence bounds on the activity coefficient estimates.

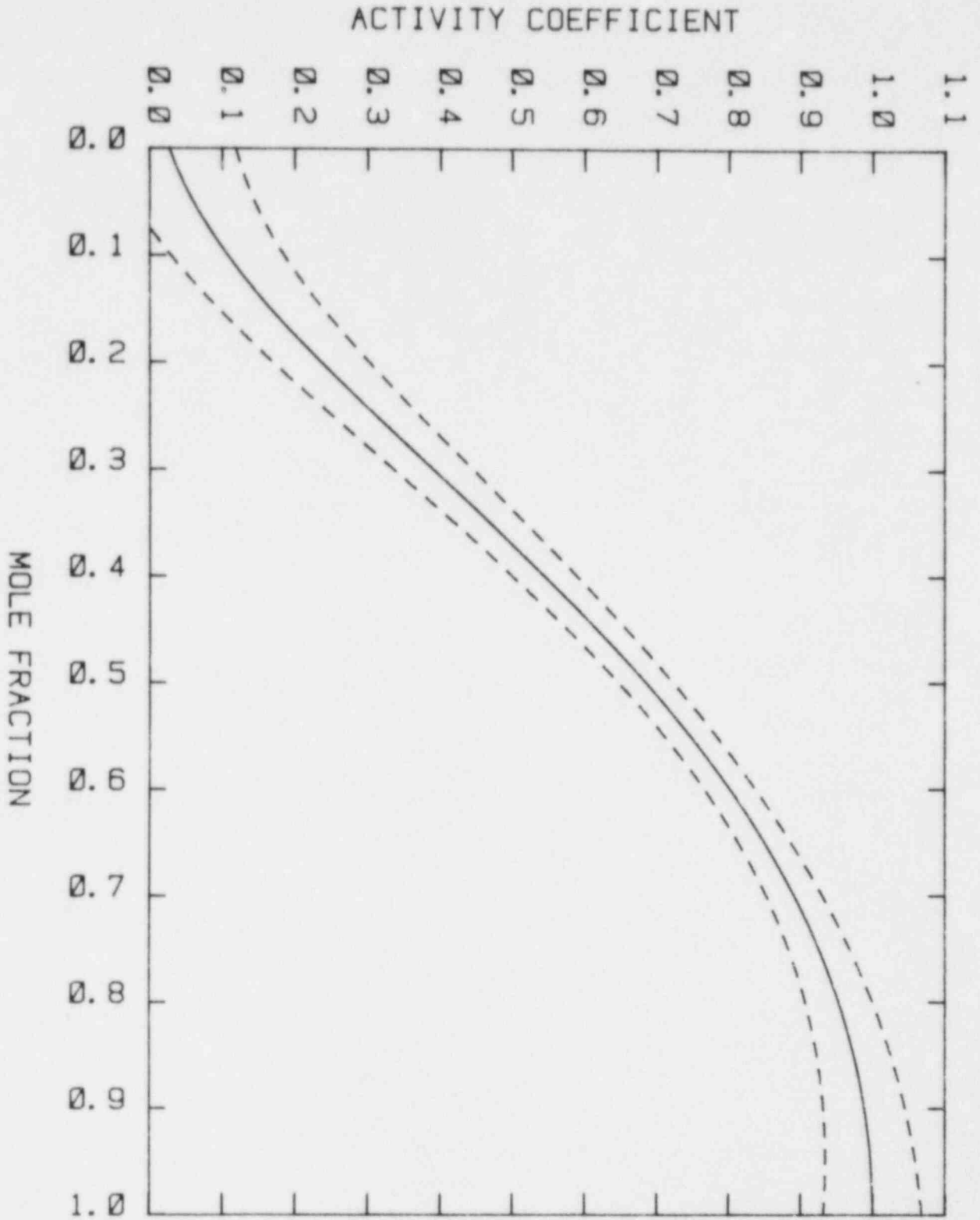
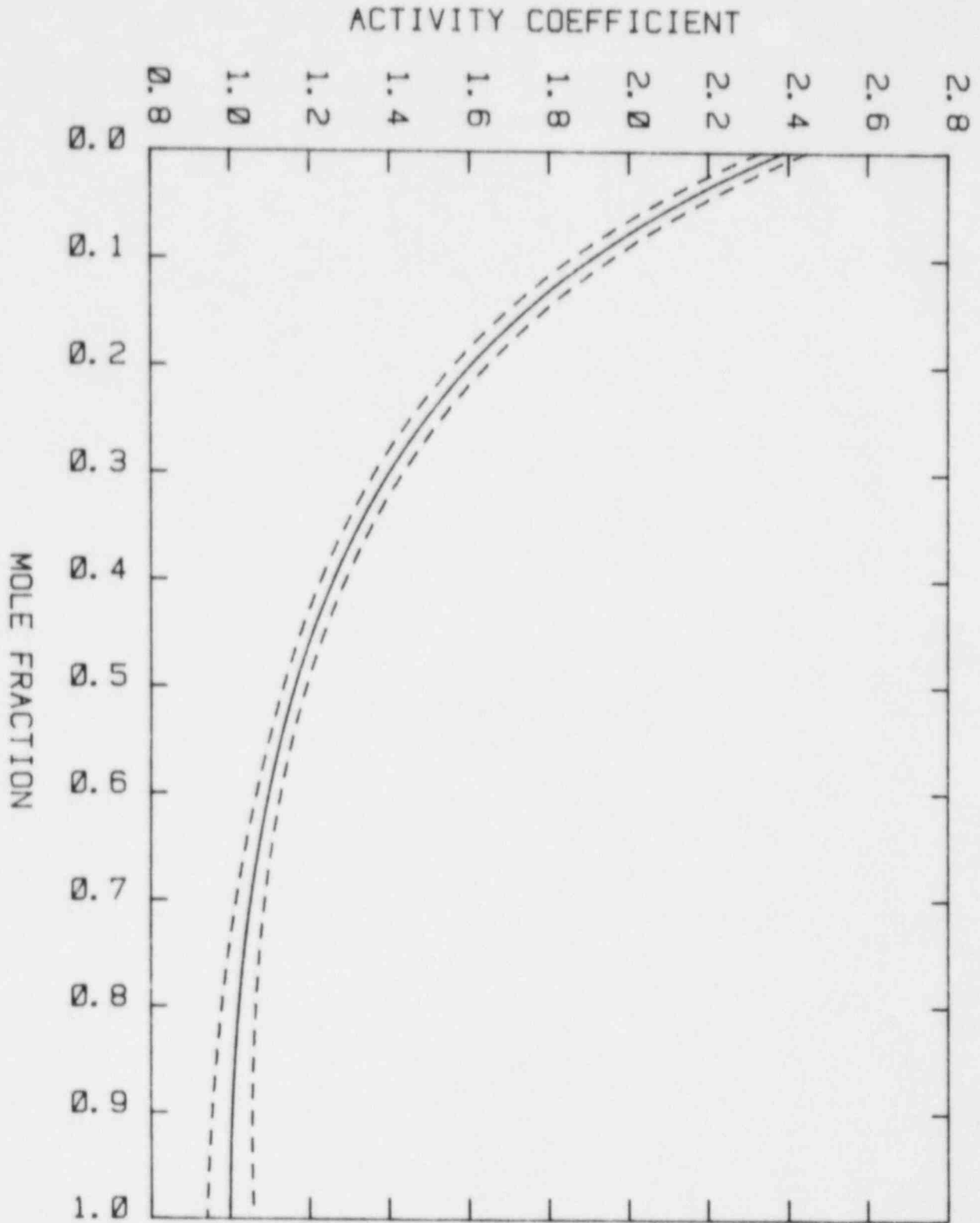


Figure 15. Calculated Activity Coefficient of Cadmium in a Cadmium/Indium Alloy at 821 K as a Function of the Mole Fraction of Cadmium. The dashed lines are the 80 percent confidence limits on the activity coefficient estimates.



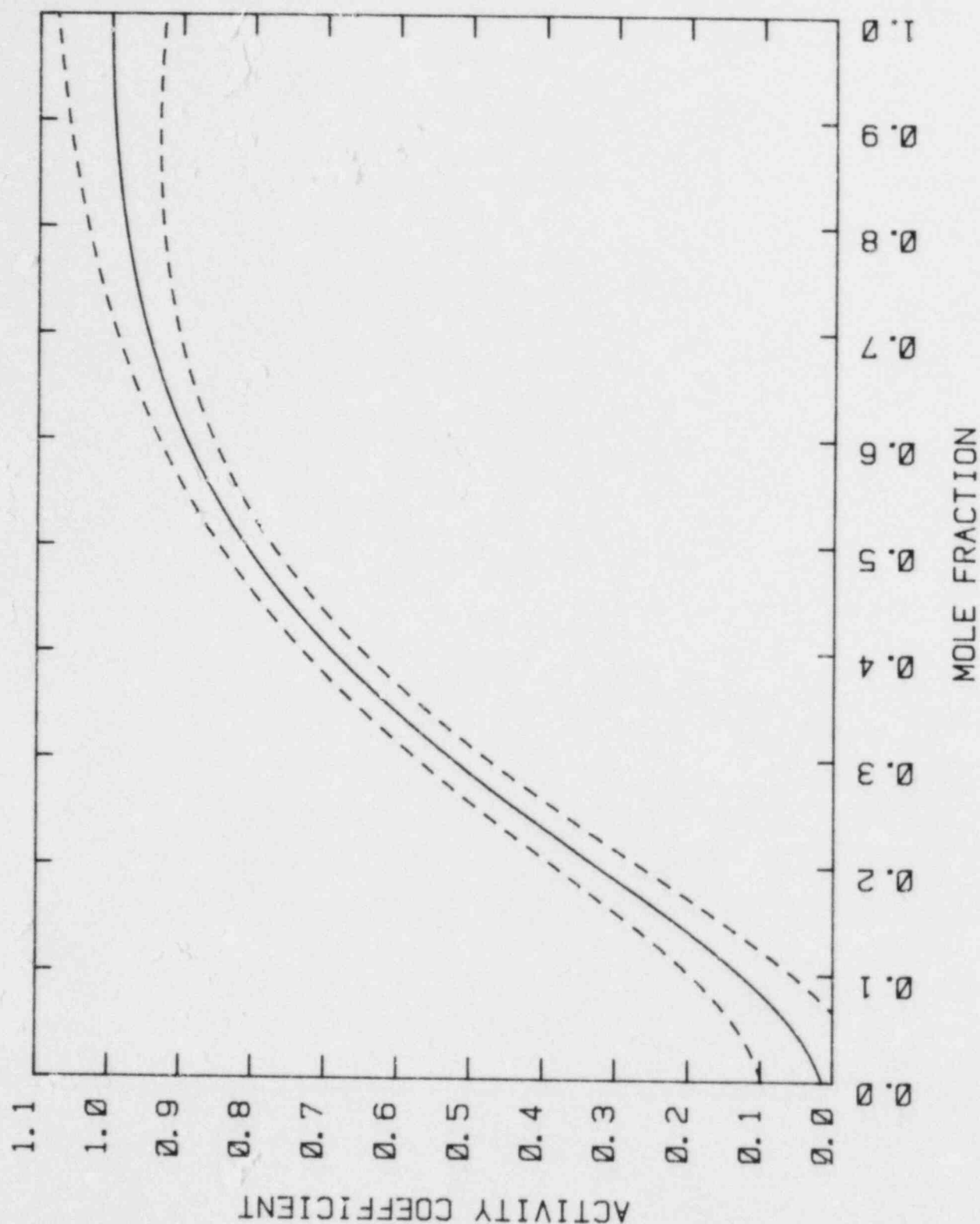


Figure 16. Calculated Activity Coefficient of Indium in an Indium/Silver Alloy at 1300 K as a Function of the Mole Fraction of Indium. The dashed lines are 80 percent confidence limits on the activity coefficient estimates.

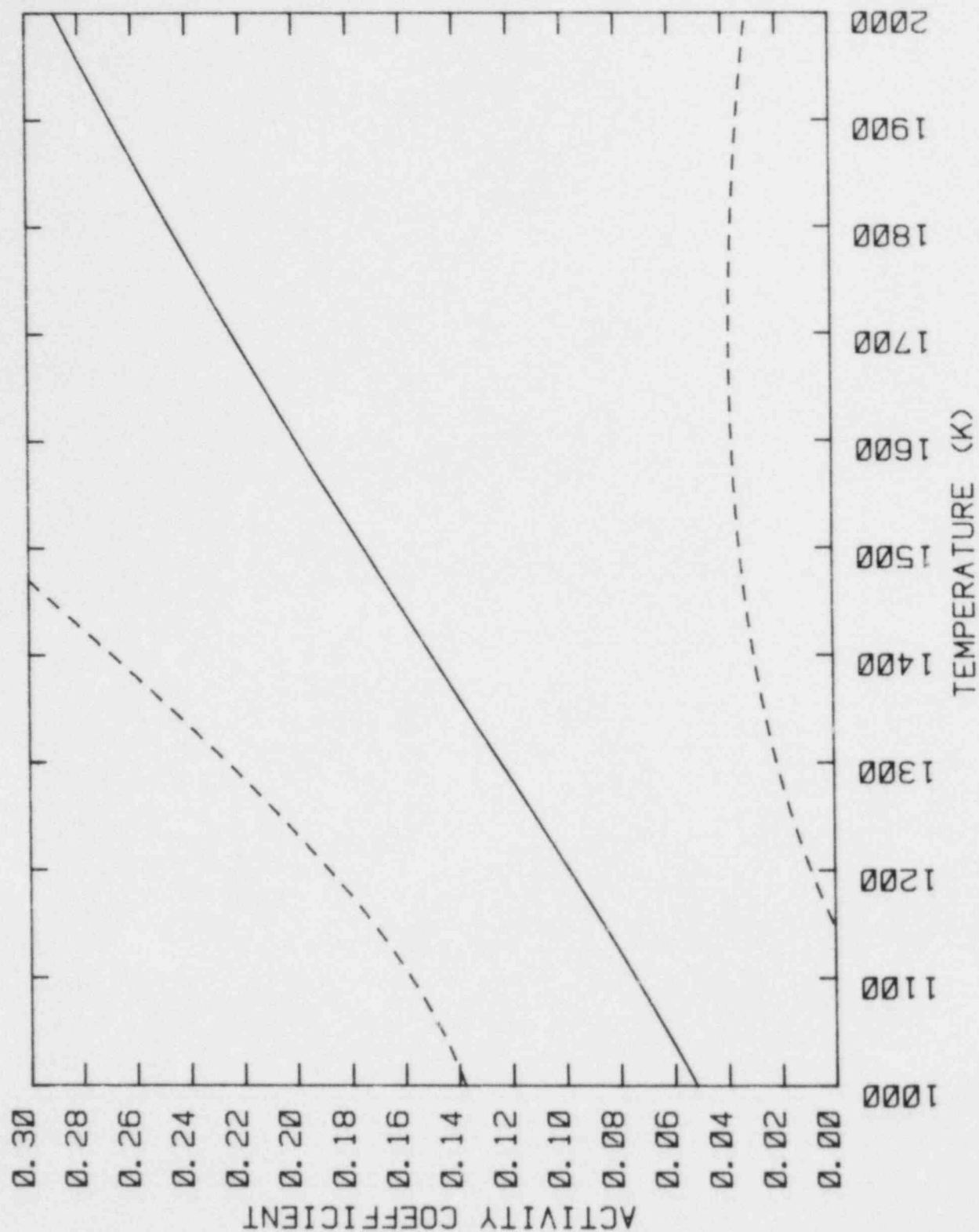


Figure 17. Activity Coefficient of Cadmium in a Cadmium/Silver Alloy With a Cadmium Mole Fraction of 0.06 as a Function of Temperature. The dashed lines are the 80 percent confidence limits on the activity coefficient estimates.

Figure 18. Activity Coefficient of Cadmium in a Cadmium/Indium Alloy With a Cadmium Mole Fraction of 0.25 as a Function of Temperature. The dashed lines are the 80 percent confidence limits on the activity coefficient estimates.

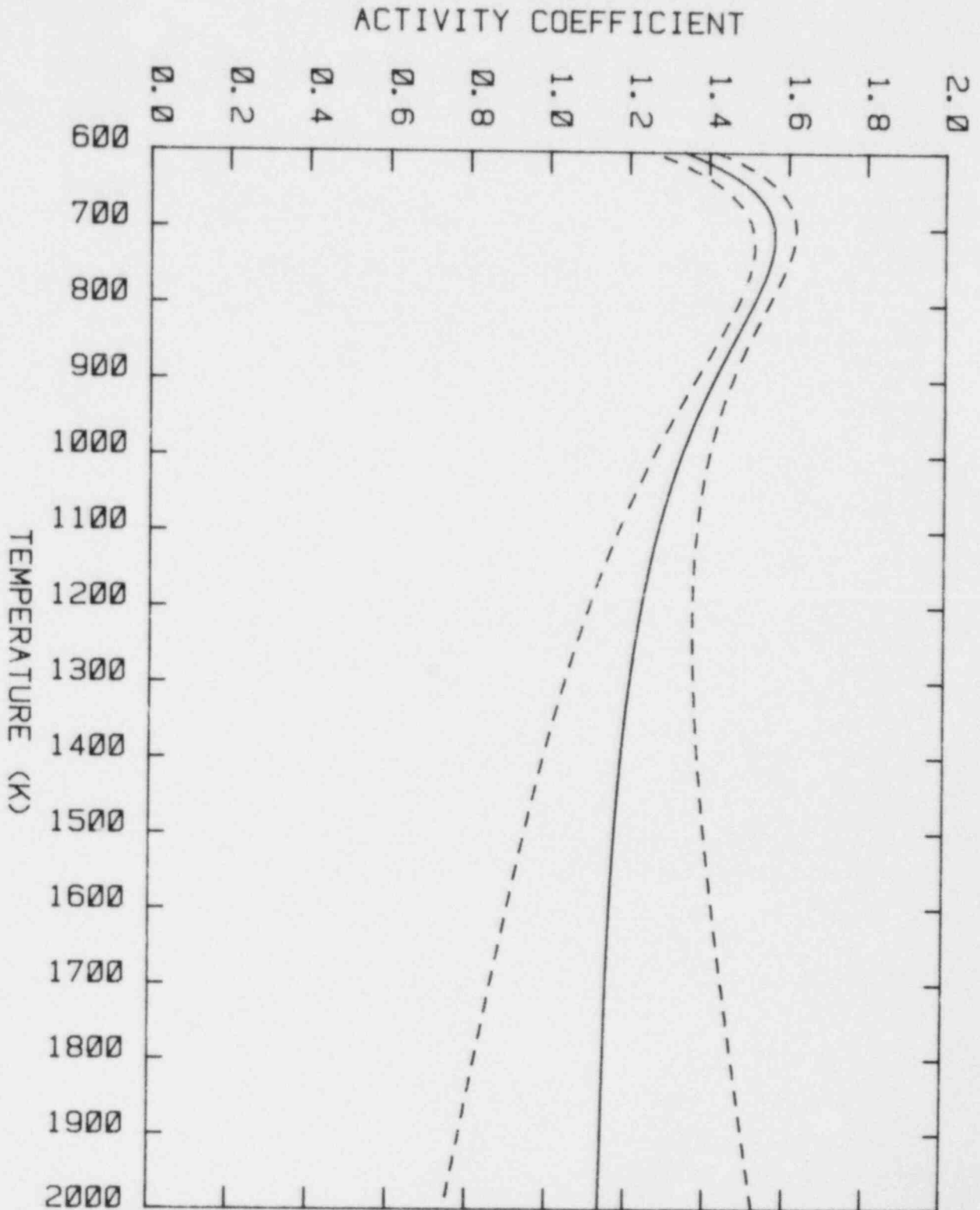
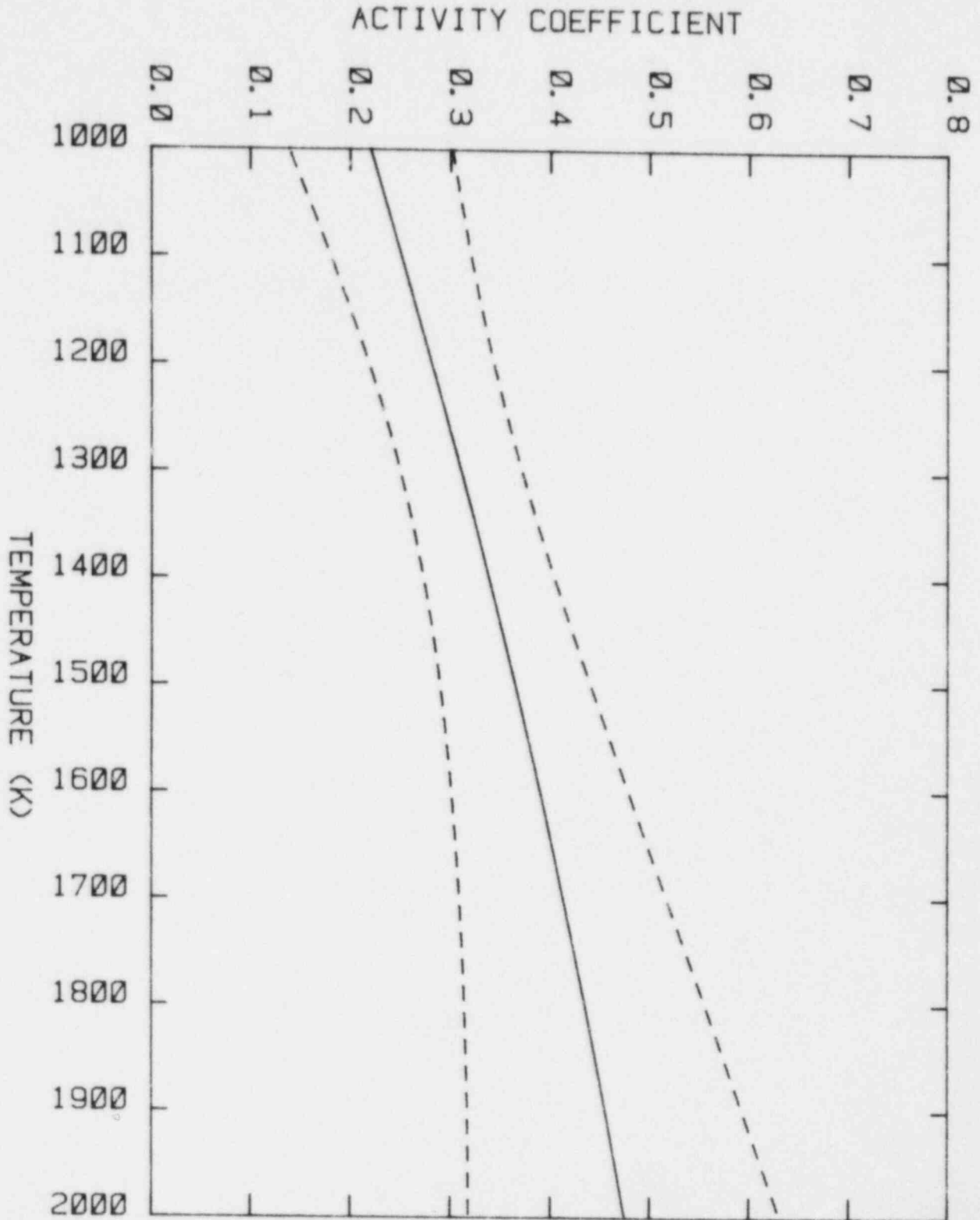


Figure 19. Activity Coefficient of Indium in an Indium/Silver Alloy With an Indium Mole Fraction of 0.19 as a Function of Temperature. The dashed lines are the 80 percent confidence limits on the activity coefficient estimates.



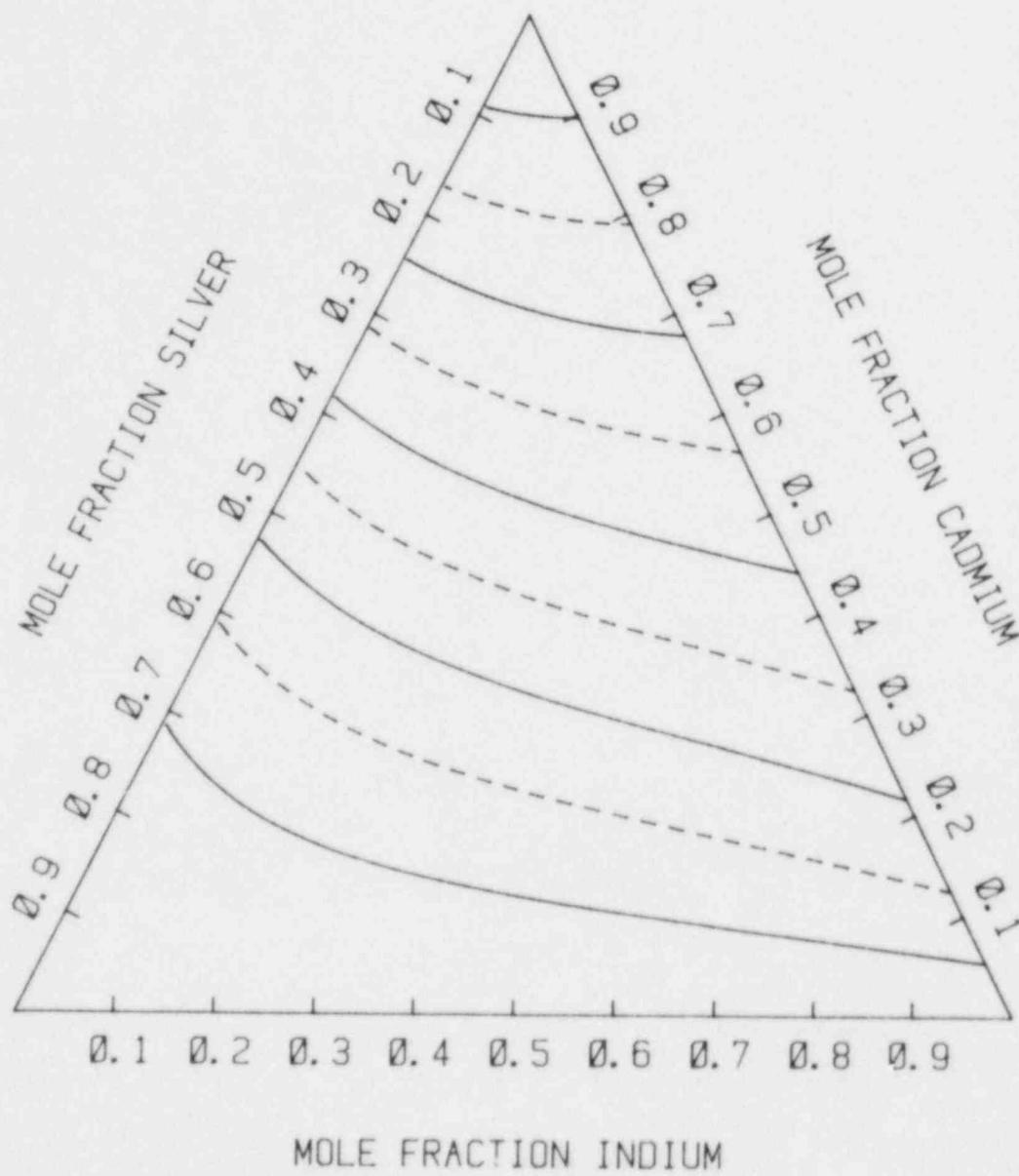


Figure 20. Activity of Cadmium in Ag-In-Cd Alloys at 1000 K

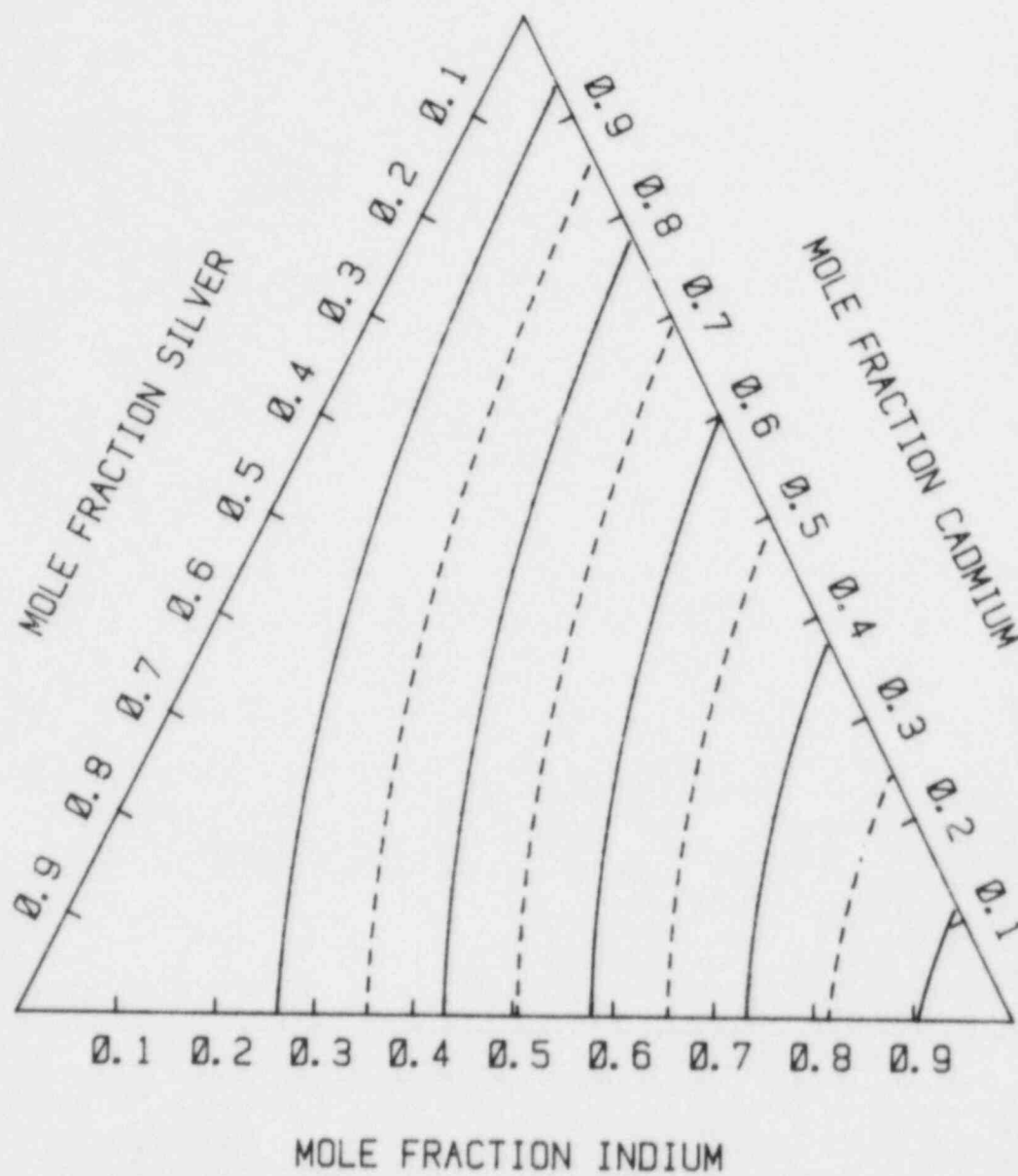


Figure 21. Activity of Indium in Ag-In-Cd Alloys at 1000 K

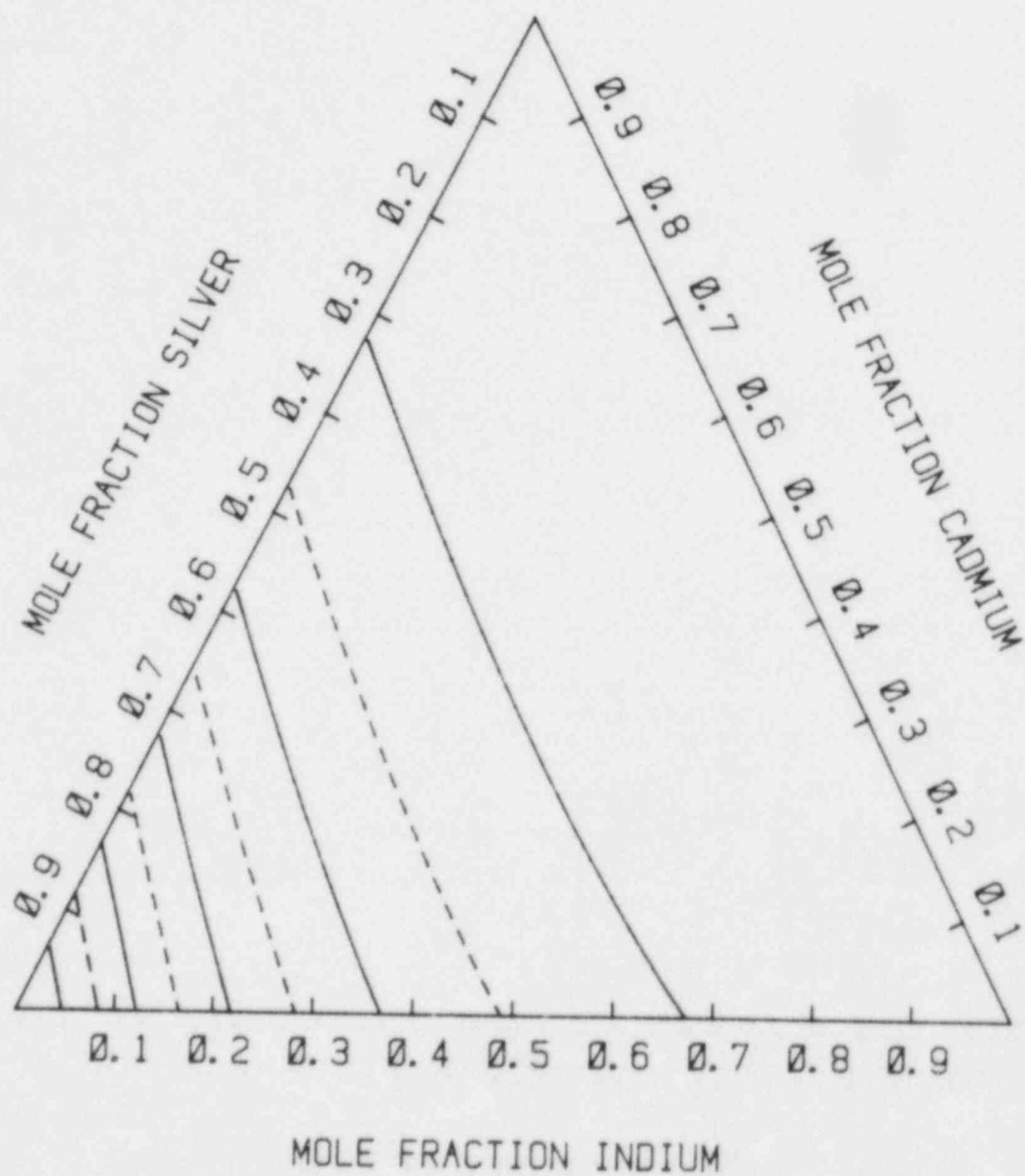


Figure 22. Activity of Silver in Ag-In-Cd Alloys at 1000 K

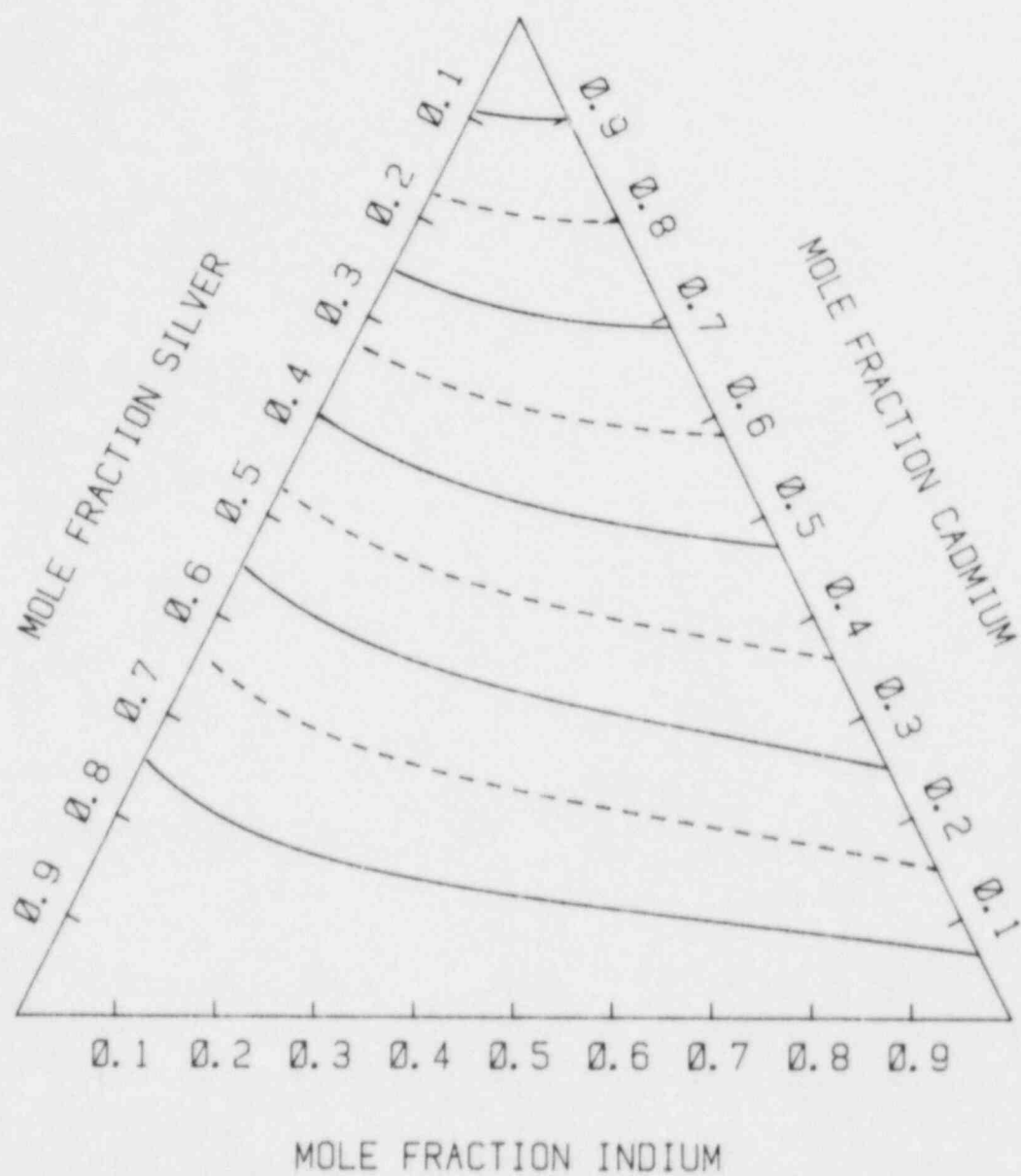


Figure 23. Activity of Cadmium in Ag-In-Cd Alloys at 1300 K

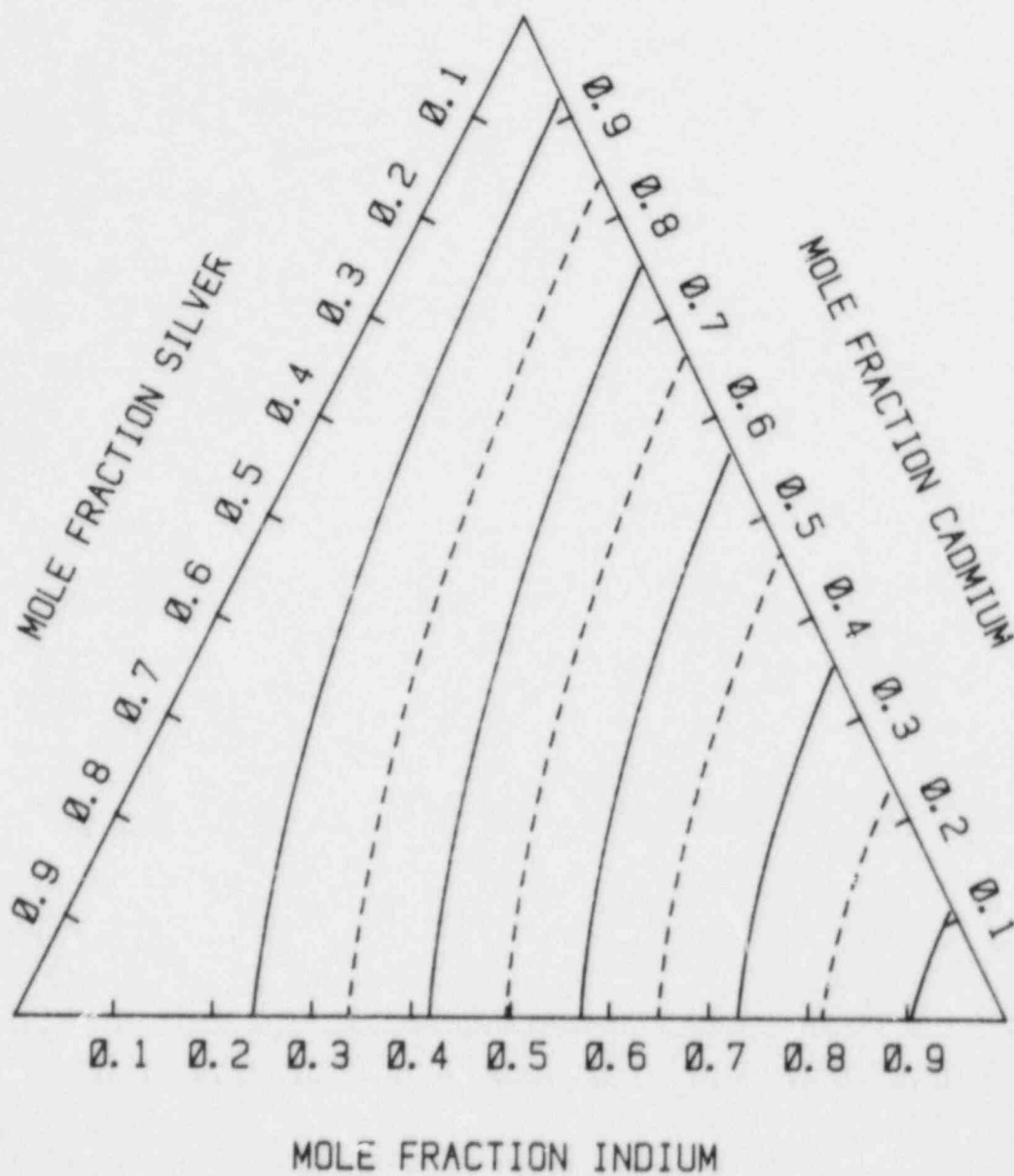


Figure 24. Activity of Indium in Ag-In-Cd Alloys at 1300 K

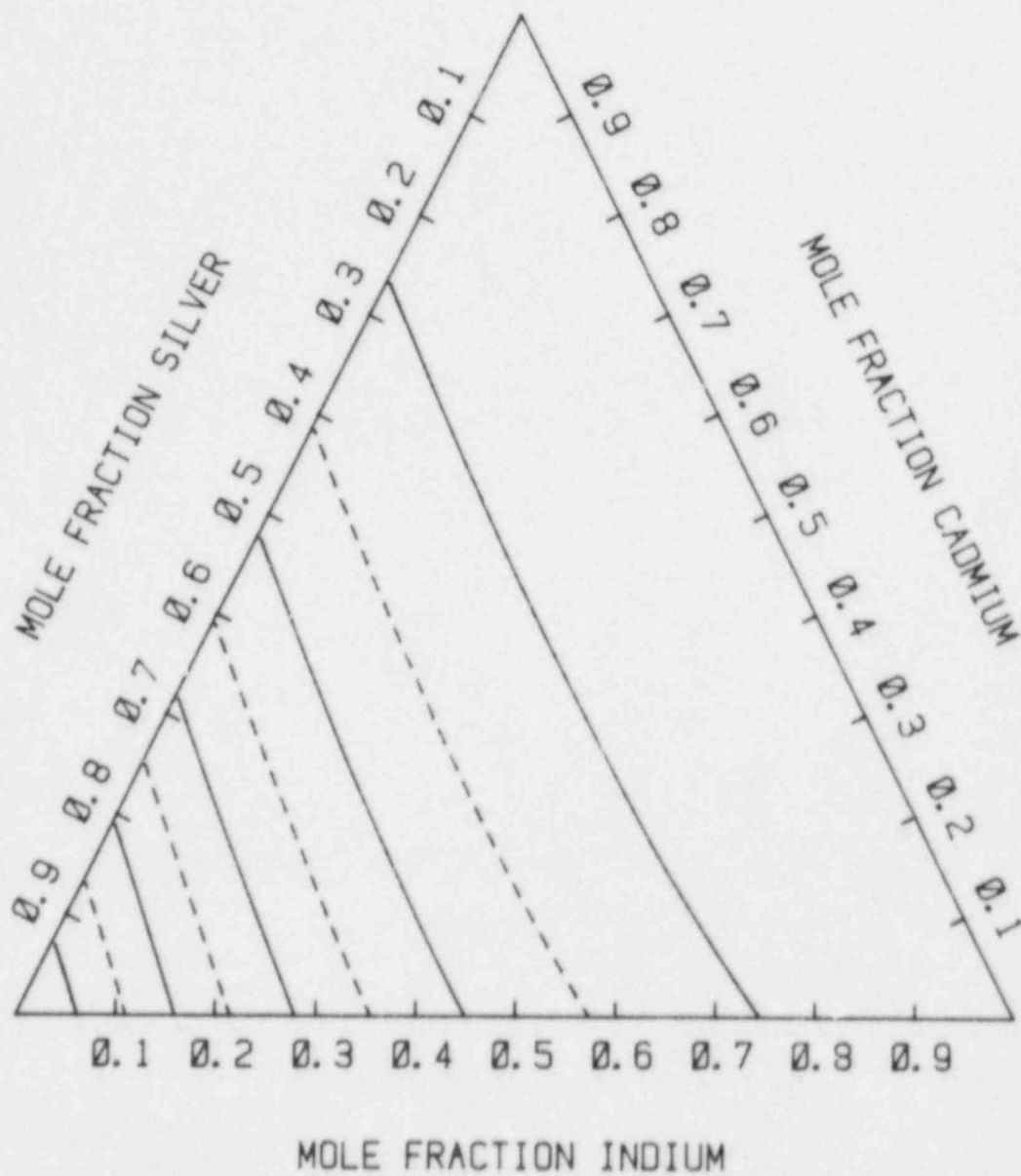


Figure 25. Activity of Silver in Ag-In-Cd Alloys at 1300 K

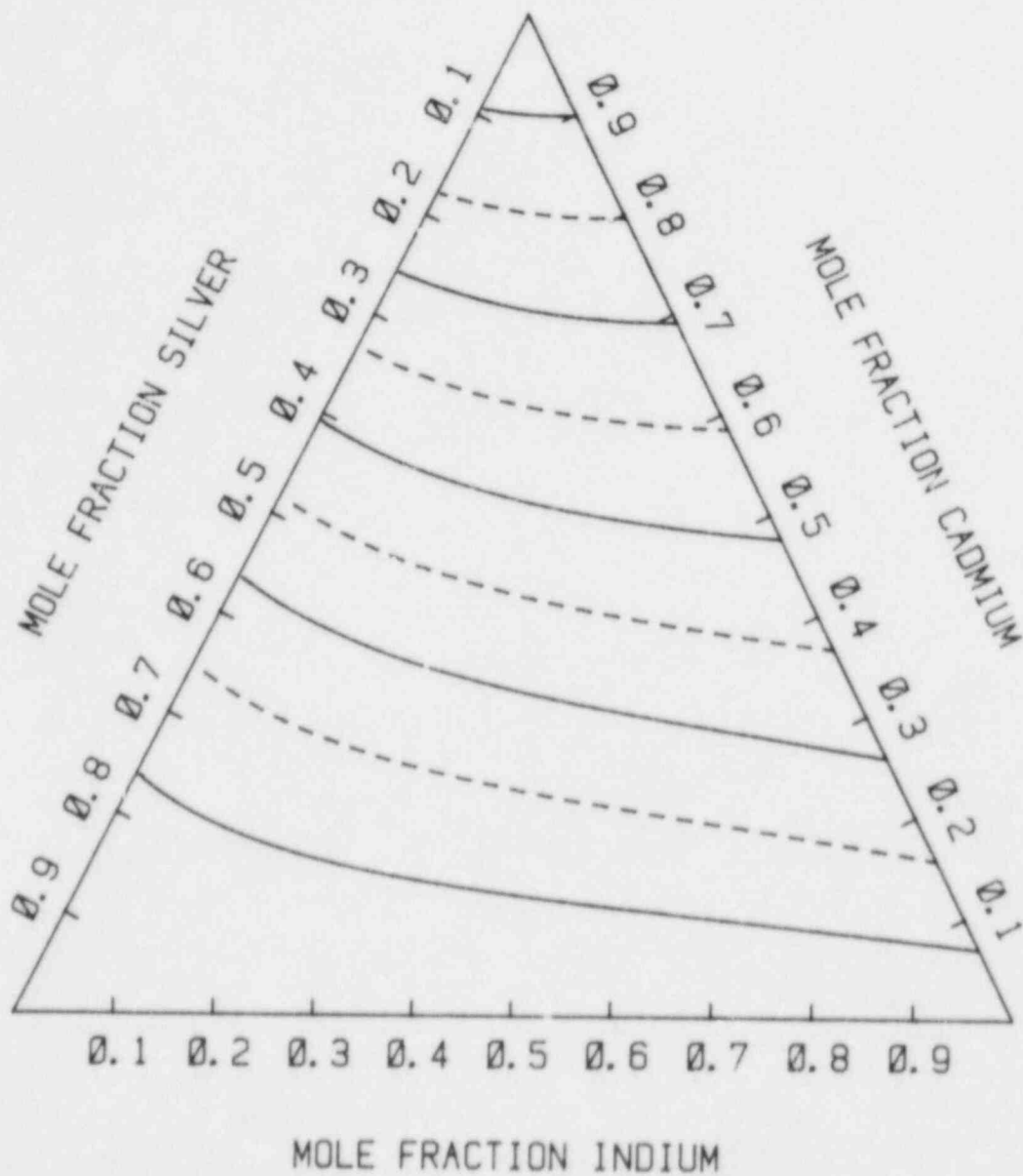


Figure 26. Activity of Cadmium in Ag-In-Cd Alloys at 1500 K

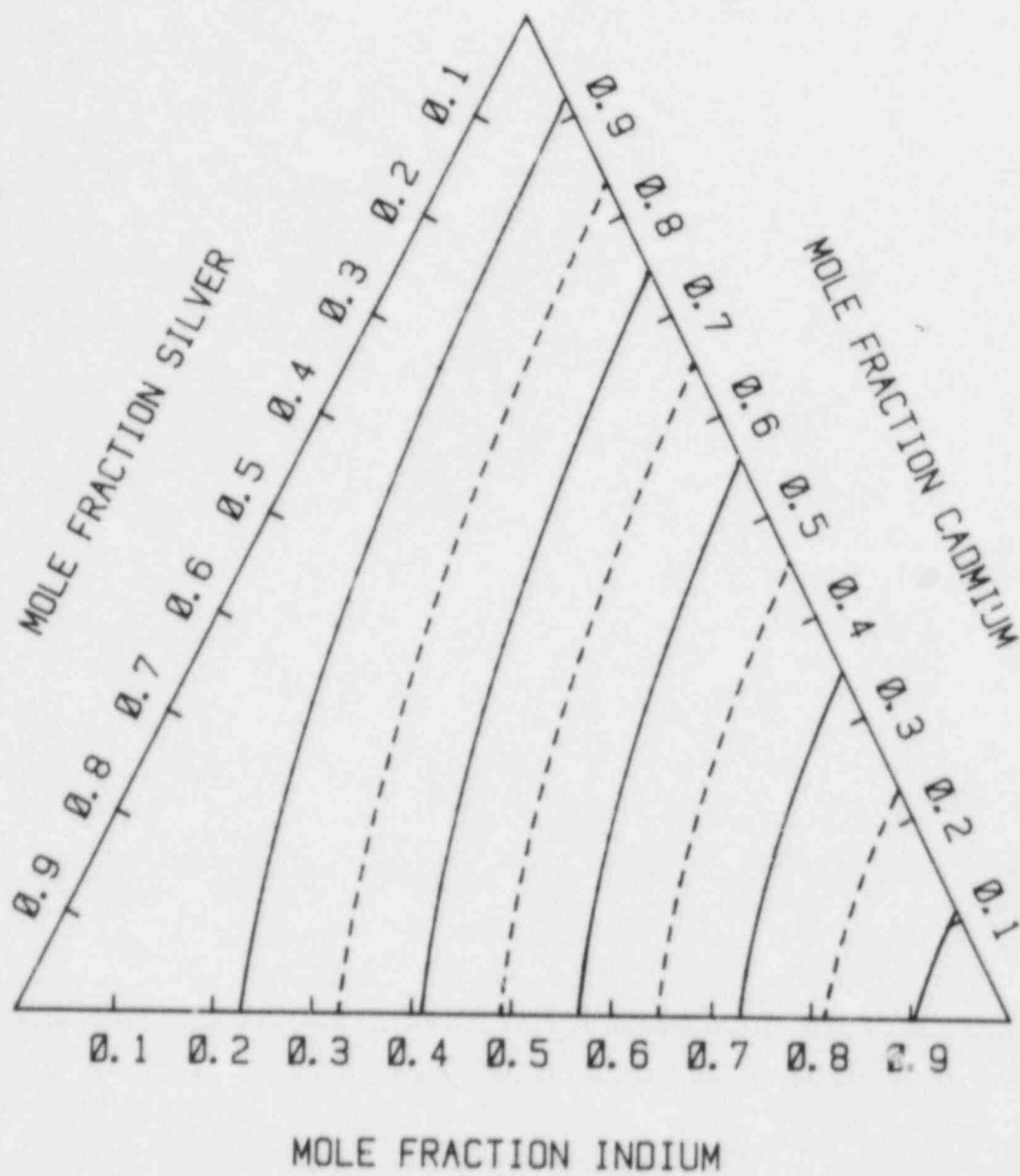


Figure 27. Activity of Indium in Ag-In-Cd Alloys at 1500 K.

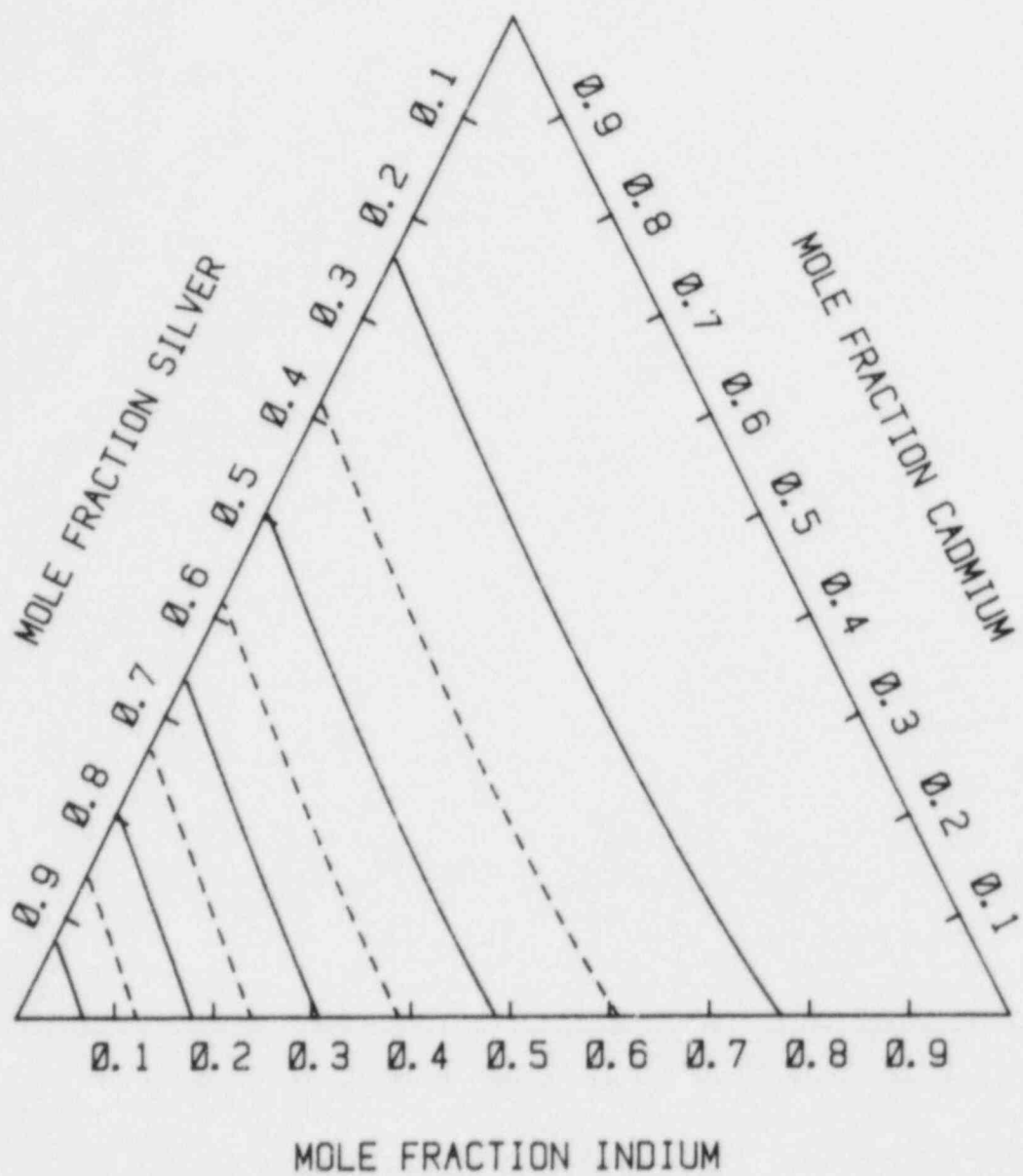


Figure 28. Activity of Silver in Ag-In-Cd Alloys at 1500 K

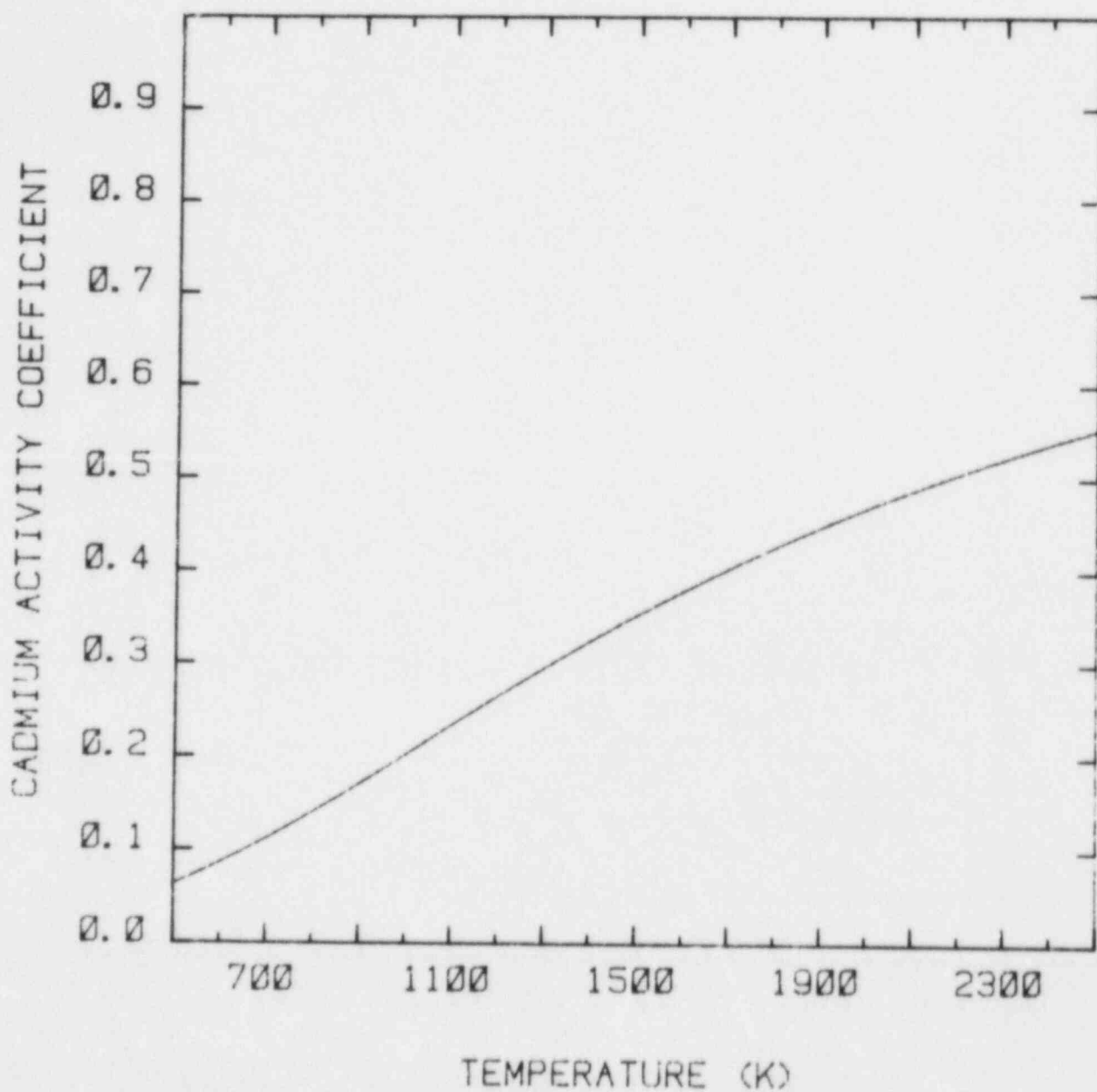


Figure 29. Activity of Cadmium in an 85a/oAg 15a/oIn 5a/oCd Alloy as a Function of Temperature

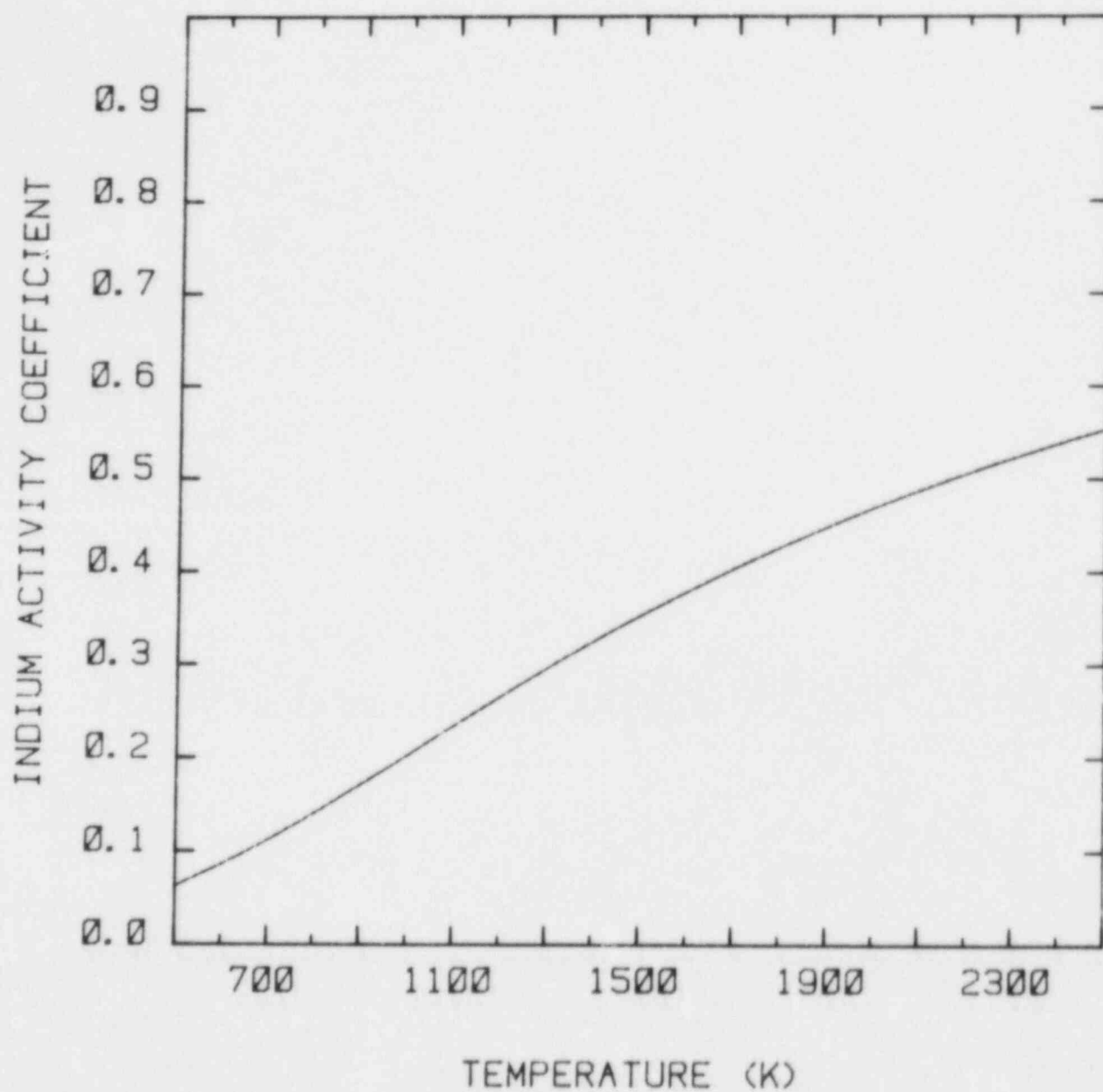


Figure 30. Activity of Indium in an 85a/oAg 15a/oIn 5a/oCd Alloy as a Function of Temperature

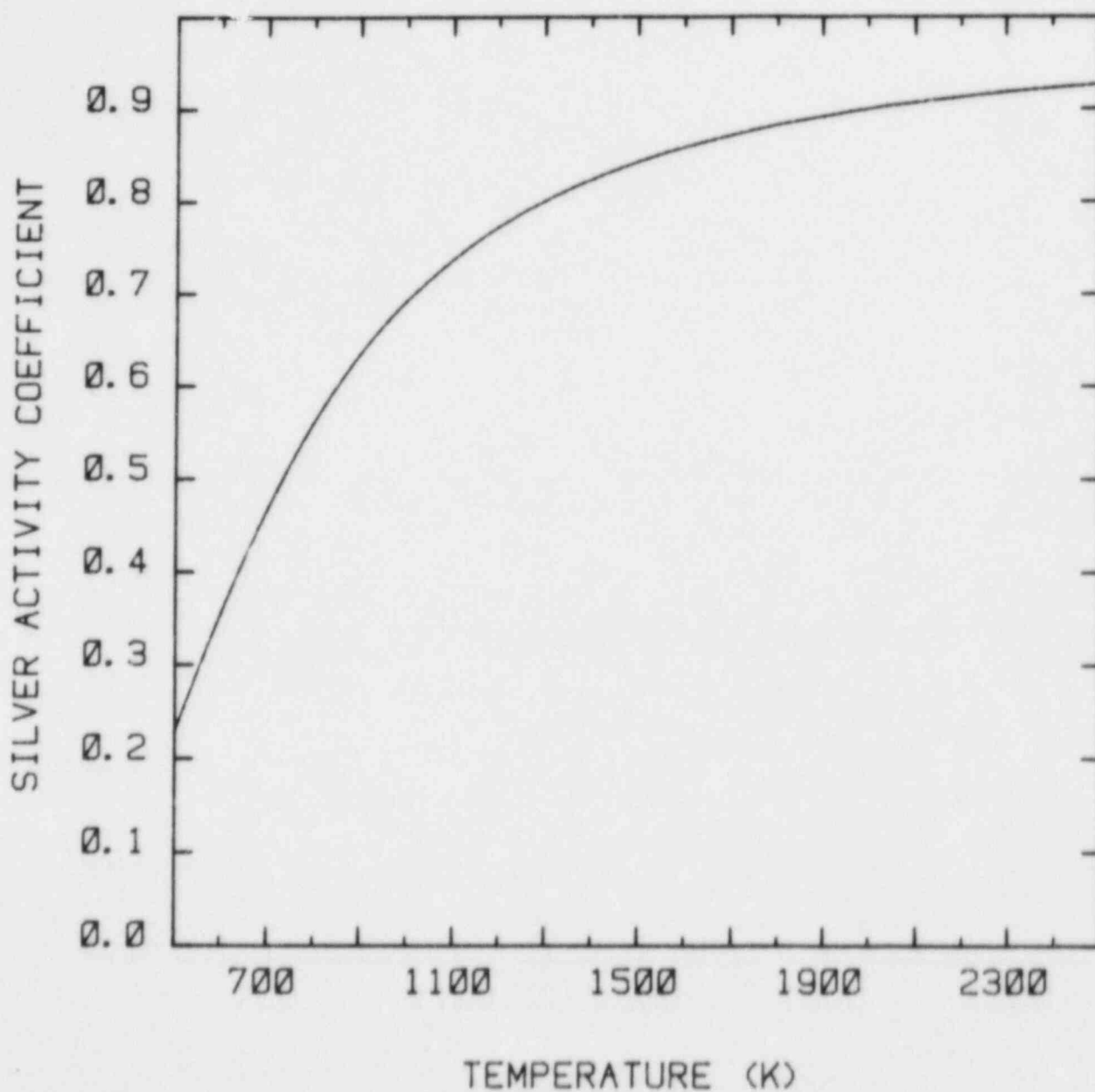


Figure 31. Activity of Silver in an 85a/oAg 15a/oIn 5a/oCd Alloy as a Function of Temperature

less than would be predicted if the condensed alloy were treated as an ideal mixture. The activity coefficients rise with temperature as would be expected. Silver acts, essentially, in an ideal manner at temperatures in excess of 1500 K. Cadmium and indium, however, have depressed activities even at temperatures as high as 2500 K. These species are predicted to behave nonideally at all temperatures that are likely to arise during a reactor accident.

III. Vapor Species in the Ag-In-Cd System

In the subsections below the thermodynamic properties of vapor species that might arise in the Ag-In-Cd system are described. Atomic vapor species are, of course, known. Few investigations have been conducted at pressures approaching those of interest here. Consequently, data for polymeric and mixed metal vapor species are not abundant. Attempts are made to estimate properties for polymeric and mixed metal species whenever suggestions of the existence of such species could be found. There is, however, no reason to believe that the list of species considered here is exhaustive. Results of the calculations of thermodynamic properties described here are collected in Appendix B.

A. Monomeric Species

The pertinent monomeric vapor phase species are the gaseous atoms of Ag, Cd, and In and the ions of these species. Free-energy functions and other thermodynamic quantities for these species were calculated from the statistical mechanical equations listed below:

Heat Capacity: $C_p = C_p^{tr} + C_p^{elec}$

where $C_p^{tr} = 4.967913 \text{ cal/mole} \cdot K$

$$C_p^{elec} = \frac{4.113664}{T^2} \left[\frac{S(3)}{S(1)} - \left(\frac{S(2)}{S(1)} \right)^2 \right] \text{ cal/mole} \cdot K$$

$$S(1) = \sum_{i=1}^N g_i \exp[-1.43879 E_i/T]$$

$$S(2) = \sum_{i=1}^N g_i E_i \exp[-1.43879 E_i/T]$$

$$S(3) = \sum_{i=1}^N g_i E_i^2 \exp[-1.43879 E_i/T]$$

g_i = multiplicity of the i^{th} electronic state

E_i = energy of the i^{th} electronic state

N = number of electronic states.

Enthalpy Function: $[H_o(T) - H_o(0)]/T = h^{\text{tr}} + h^{\text{elec}}$

where $h^{\text{tr}} = 4.967913 \text{ cal/mole} - K$

$$h^{\text{elec}} = \frac{2.859114}{T} \frac{S(2)}{S(1)} \text{ cal/mole} - K$$

Free Energy Function: $-[G^o(T) - H_o(0)]/T = z^{\text{tr}} + z^{\text{elec}}$

where $z^{\text{tr}} = 6.863426 \log_{10}(M) + 11.439043 \log_{10}(T) - 7.282868$

$$z^{\text{elec}} = 4.575617 \log_{10}(S(1)) \text{ cal/mole} - K$$

M = molecular weight.

Entropy: $S_o(T) = x^{\text{tr}} + x^{\text{elec}}$

where $x^{\text{tr}} = 6.863426 \log_{10}(M) + 11.439043 \log_{10}(T) - 2.314954 \text{ cal/mole} - K$

$$x^{\text{elec}} = \frac{2.859114}{T} \left(\frac{S(2)}{S(1)} \right) + 4.575617 \log_{10}(S(1)) \text{ cal/mole} - K$$

Electronic state data necessary for these calculations were taken from the compilation in Reference 28. Because of the relatively high ionization potentials for Ag, In, and Cd, it was thought unnecessary to consider ions with charges greater than +1. No negative ions were considered.

Critically reviewed enthalpies of vaporization were taken from the compilation by Hultgren et al:(29)

<u>Element</u>	<u>$\Delta H_v(298.15 \text{ K})$</u> <u>(cal/mole)</u>
Ag	67,900 \pm 200
Cd	26,720 \pm 150
In	58,000 \pm 250

These enthalpies were used to compute the enthalpies of formations of the gaseous atoms at temperatures up to 3500 K using the equation:

$$\Delta H_f^{M(\text{gas})}(T) = \Delta H_v(298.15 \text{ K}) + [H_o(T) - H_o(298)]_{M(\text{gas})} - [H_o(T) - H_o(298)]_{M(\text{ref})}$$

where $\Delta H_f^{M(\text{gas})}(T)$ = enthalpy of formation of the atomic gas of element M at temperature T

$[H_o(T) - H_o(298.15)]_j$ = enthalpy function for species j

$M_{(\text{ref})}$ = subscript denoting the element M in its reference state.

The reference state used here is that defined in the JANAF Tables.(30)

Free energies of formation were calculated from:

$$\Delta G_f^{M(\text{gas})}(T) = \Delta H_f^{M(\text{gas})}(T) - T[S_o^{M(\text{gas})}(T) - S_o^{M(\text{ref})}(T)]$$

where $\Delta G_f^{M(gas)}$ = free energy of formation of the atomic gas of element M at temperature T

$S_O^{(i)}(T)$ = the absolute entropy of the i^{th} species at temperature T.

The enthalpies of formation of the singly charged ions were calculated from

$$\begin{aligned} IP = & \Delta H_f^{M^+(gas)}(298) + [H_O(0) - H(298)]_{M^+(gas)} \\ & + [H_O(0) - H(298)]_{e^-} - \Delta H_f^{M(gas)} \\ & - [H_O(0) - H(298)]_{M(gas)} \end{aligned}$$

where IP is the ionization potential of the element M. Values of the ionization potential, IP, were taken from Reference 28:

Element	IP (cal/mole)	$M^+(gas)$ $\Delta H_f(298)$ (cal/mole)
Ag	173,935	243,420
Cd	206,637	234,825
In	132,838	192,222

Thermodynamic properties for the electron, e^- , were taken from Reference 30.

Enthalpies and free energies of formation of the ions as functions of temperature were calculated from:

$$\begin{aligned} \Delta H_f^{M^+(gas)}(T) = & \Delta H_f^{M^+(gas)}(298.15) + [H_O(T) - H_O(298)]_{M^+(gas)} \\ & + [H_O(T) - H_O(298)]_{e^-} - [H_O(T) - H(298)]_{M(ref)} \end{aligned}$$

$$\Delta G_f^{M^+}(\text{gas})(T) = \Delta H_f^{M^+}(\text{gas})(T) - T \left[S_o^{M^+}(\text{gas})(T) + S_o^e(T) - S_o^M(\text{ref})(T) \right] .$$

B. Polymeric Gaseous Species

Polymerization of gaseous atoms might be expected at the relatively high pressures of interest in the analyses here. Dimerization of silver, in particular, might be expected. The ground state electronic configuration of atomic silver has an unpaired $5s^1$ electron. This is a configuration similar to that of the atomic alkali metals. A significant stabilization could be achieved in silver by pairing the $5s$ electron by dimerization much as occurs in the alkali metals.

A qualitative molecular orbital diagram for dimers of metals with $5s$ and $5p$ electrons is shown in Figure 32. The $4d$ orbitals of all the elements of interest here are fully occupied. These orbitals are sufficiently separated from the $5p$ and $5s$ orbitals that mixing depicted in the figure is very weak. For silver, Ozin et al.⁽³¹⁾ estimate that the $2\sigma_g$ orbital of the dimer has 89 percent s character, 7 percent p character, and only 4 percent d character. From the diagram it is obvious that substantial stabilization accrues to silver by dimerization because of the lower energy of the highest occupied orbital, $2\sigma_g$, relative to the atomic s orbital.

As the atomic number of the element increases, several changes in the qualitative diagram should occur. First, the addition electrons would have to be placed in orbitals higher than the $2\sigma_g$. This would necessarily destabilize the dimer relative to the silver dimer. This effect should be most important for Cd since its outer shell as an atom is a filled s orbital. The net stabilization brought on by dimerization of cadmium would then be expected to be small. Indium, with an unpaired p electron, would experience some stabilization as a result of dimerization.

A second change in the molecular orbital diagram with increasing atomic number is enhanced mixing among orbitals which would produce greater stabilization of the bonding orbitals. The $2\pi_u$ orbital would be reduced in energy while the $2\sigma_u$ orbital would increase in energy. This would favor, of course, dimerization.

The net effect of the two changes with increasing atomic number is hard to predict without detailed calculations. Qualitative arguments suggest that some net force for dimerization of cadmium might be achieved. Based on these types of arguments it seems likely that dimerization may be most

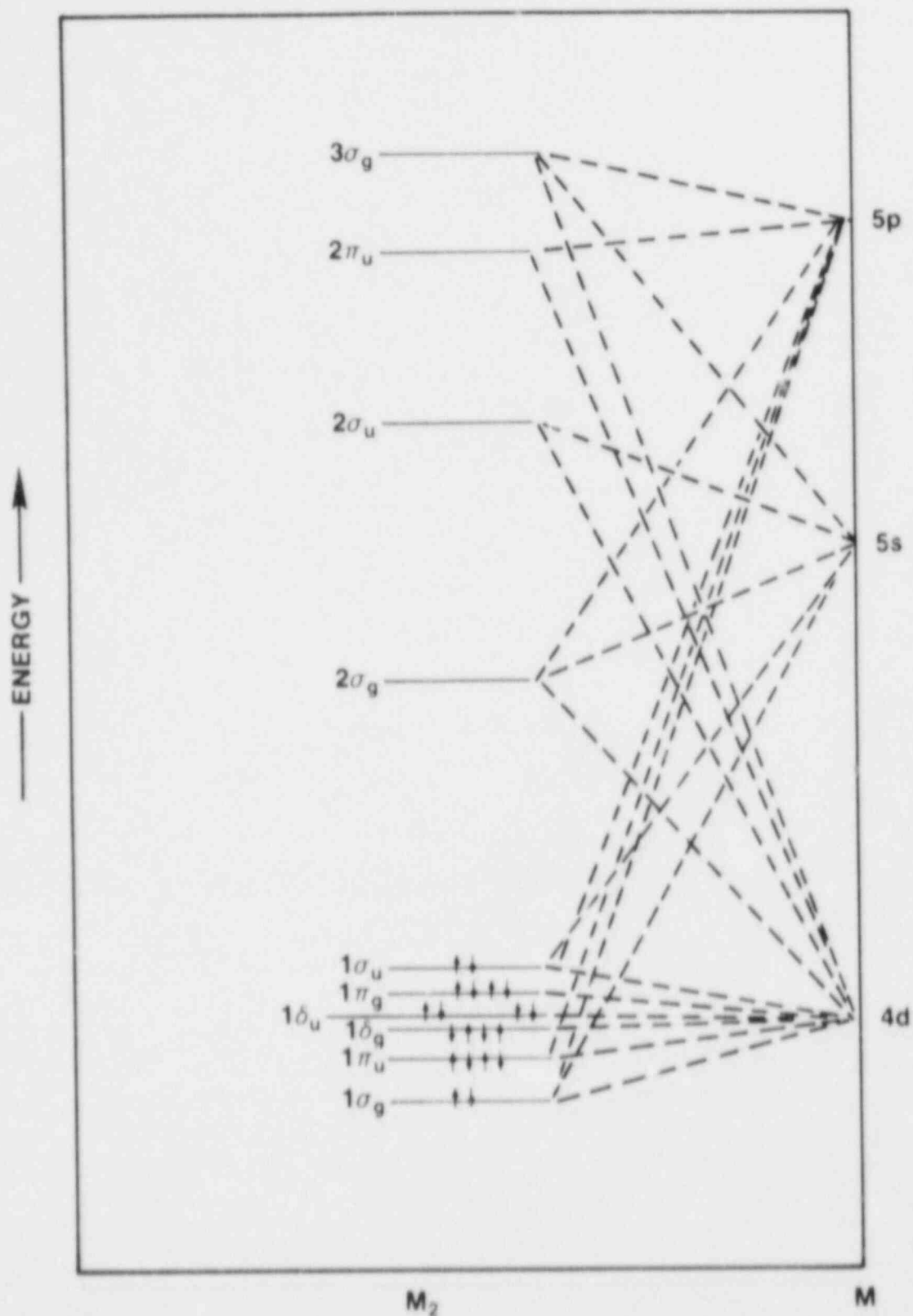


Figure 32. Qualitative Molecular Orbital Diagram for Caseous Dimers

important for silver, somewhat less important for indium, and very unimportant for cadmium. Similar arguments can be formulated to predict the relative importance of higher order polymers of gaseous atoms.

Thermodynamic data for polymers of the atoms have not been published. Here the thermodynamic data for dimers are calculated from the statistical mechanics expressions listed below:

Translation and rotation:

$$C_p^0 = 6.955079 + 0.0914148(B/T)^2$$

$$(H_0(T) - H_0(O))/T = 6.955079 - 0.953038(B/T) - 0.0914148(B/T)^2$$

$$\begin{aligned} -(G^0(T) - H_0(O))/T &= 6.863426 \log_{10} M + 11.439043 \log_{10} T \\ &- 4.575617 \log_{10} (B\sigma/T) + 0.953038(B/T) \\ &+ 0.0457074(B/T)^2 - 8.005804 \end{aligned}$$

$$\begin{aligned} S_0^0(T) &= 6.863426 \log(M) + 11.439043 \log(T) \\ &- 4.575617 \log(B\sigma/T) - 0.0457074(B/T)^2 \\ &- 1.050725 \end{aligned}$$

Vibration:

$$C_p^0 = 1.987165 u^2 \exp(-u)/(1 - \exp(-u))^2$$

$$(H_0(T) - H_0(O))/T = 1.987165 u \exp(-u)/(1 - \exp(-u))$$

$$(G^0(T) - H_0(O))/T = -4.575617 \log(1 - \exp(-u))$$

$$S_{(T)}^0 = 1.987165u \exp(-u)/(1-\exp(-u)) \\ - 4.575617 \log(1-\exp(-u))$$

where $u = \frac{1.438790}{T}(W_e - 2W_e X_e)$.

Electronic:

$$C_p^0 = \frac{4.113664}{T^2} \left\{ \frac{S_3}{S_1} - \left(\frac{S_2}{S_1} \right)^2 \right\}$$

$$(H_O(T) - H_O(O))/T = \frac{2.859114}{T} \frac{S_2}{S_1}$$

$$-(G^O(T) - H_O(O))/T = 4.575617 \log_{10}(S_1)$$

$$S_{(T)}^0 = \frac{2.859114}{T} \frac{S_2}{S_1} + 4.575617 \log_{10}(S_1)$$

where σ = symmetry number

$$S_1 = \sum_{i=1}^N g_i \exp(-1.438790 E_i/T)$$

$$S_2 = \sum_{i=1}^N E_i g_i \exp(-1.438790 E_i/T)$$

$$S_3 = \sum_{i=1}^N E_i^2 g_i \exp(-1.438790 E_i/T) .$$

Anharmonic Correction:

$$C_P^O = 1.987615 \left[\frac{16\gamma}{u} - \frac{\delta u^2 \exp(u)}{(\exp(u)-1)^2} + \frac{u^2 \exp(u)(2\delta \exp(u)-4Xu-8X)}{(\exp(u)-1)^3} + \frac{12Xu^3 \exp(2u)}{(\exp(u)-1)^4} \right] \text{ cal/mole} - K$$

$$[H_O(T) - H_O(0)]/T = 1.987165 \left[\frac{8\gamma}{u} + \frac{u(\delta \exp(u)-2X)}{(\exp(u)-1)^2} + \frac{4Xu^2 \exp(u)}{(\exp(u)-1)^3} \right]$$

$$-[G_O(T) - H_O(0)]/T = 1.987165 \left[\frac{8\gamma}{u} + \frac{\delta}{(\exp(u)-1)} + \frac{2Xu}{(\exp(u)-1)^3} \right]$$

$$S_O(T) = 1.987165 \left[\frac{16\gamma}{u} + \frac{\delta}{(\exp(u)-1)} + \frac{\delta u \exp(u)}{(\exp(u)-1)^2} + \frac{4Xu^2 \exp(u)}{(\exp(u)-1)^3} \right]$$

where $u = (W_e - 2W_e X_e) 1.438790/T$

$$x = \frac{W_e X_e}{W_e}$$

$$\delta = \alpha_e/B_e$$

$$\gamma = B_e/W_e$$

Similar formulae are used for higher order polymers except the anharmonic correction is neglected and additional vibrational terms are included.

In the subsections below, the bases for selecting input to these calculations are reviewed.

1. Silver Dimer--Ag₂

There have been many experimental and theoretical studies of the silver dimer, Ag₂.⁽³¹⁻⁴⁸⁾ Most of the experimental

studies have been of a spectroscopic nature. Matrix isolation techniques have been extensively used. Results of the matrix isolation studies must be viewed with caution. A variety of evidence has been assembled to show that the lattice of dilution gas can trap atoms at abnormal separations.(53,54) The ordering of states in the silver dimer does not appear to be affected significantly by internuclear separation.(40) But, the quantitative natures of the molecular vibrations and electronic transitions are sensitive to separation.

The most useful spectroscopic work is that done in the gas phase. Early work at long wavelengths by Ruamps(33) and by Kleman et al.(34,39) and later work at shorter wavelengths by Brown and Ginter(42) seem the most useful. This spectroscopic work is summarized in Table 8.

Vibrational fine structure on the electronic transitions permit direct determination of the vibrational frequency of the ground state and excited states, W_e . The anharmonic correction, $W_e X_e$, can also be determined directly. The vibrational frequency of the ground state found in the early work, 192 cm^{-1} , is widely accepted, though one review quotes 207 cm^{-1} as a preferred value.(51) The anharmonic correction to the ground state vibration quoted by Brown and Ginter is that of Ruamps.(33) Kleman et al. give a value of 0.643 .(34)

Internuclear separations are not found directly by optical spectroscopy. Brown and Ginter recommended a separation of $2.469 \pm 0.004 \text{ \AA}$ based on correlation of data for the Cu_2 , Ag_2 , and Au_2 dimers with the expression $R_e^3 W_e = \text{constant}$. Rotational constants B_e and α_e were then obtained from the expressions

$$\alpha_e = 6(W_e X_e B_e^3)^{1/2} W_e^{-1} - 6B_e^2 W_e^{-1}$$

$$\alpha_e B_e^{-1} = (W_e X_e) W_e^{-1} .$$

The internuclear separation found by Brown and Ginter is not universally accepted. Drowert recommends 2.68 \AA .(49) A review recommends 2.5 \AA .(51) A separation of 2.515 \AA is suggested by Huber and Herzberg.(50)

The dissociation energy D_0 is recommended by Drowert to be $37.6 \pm 2.2 \text{ kcal/mole}$.(49) The uncertainty range attached to this recommendation spans the range of values suggested by others. Kleman et al. suggest $\sim 42 \text{ kcal/mole}$.(34)

Table 8

Summary of Spectroscopic Data for $\text{Ag}_2(\text{gas})$

State	T_e (cm^{-1})	W_e (cm^{-1})	$W_e X_e$	B_e	α_e	Assignment
X	0	192	0.58	0.0512	0.0002	$^1\Sigma_g^+$
A	22996.4	154.6	0.587			$^1\Sigma_g^+ \rightarrow ^1\Sigma_u^+$
B	35838.6	151.8	0.87			$^3\Pi_u$ (?)
C	37631.6	171.0	0.84	0.05088	0.0003	$^1\Sigma_g^+ \rightarrow ^1\Pi_u$
D	39014.5	168.2	1.20	0.05098	0.00027	$^3\Pi_u$ (?)
E	40159.9	146.1	1.58			$^1\Pi_u$ (?)
H	58273.1	165.9	2.46			

Theoretical investigations of Ag_2 have been attempted using semiempirical techniques such as CNDO (complete neglect of differential overlap) and extended Huckel methods. These techniques seem unable to provide additional insight on the molecule not available directly from the experimental data. More useful have been ab initio work by Ozin et al.⁽⁴⁰⁾ and by Sannigrahi and Dee.⁽⁴⁵⁾ The ground state of Ag_2 is readily assigned to be $1\Sigma_g^+$. The first two excited states are $1\Sigma_u^+$ and $1\Pi_u$ corresponding to promotion of an electron from the $2\sigma_g$ orbital to the $2\sigma_u$ and $2\pi_u$ orbitals, respectively, in the qualitative molecular orbital description presented above. The SCF- X_α -SW methods used by Ozin et al. satisfactorily predict the energies of the excitations observed in experiments if the internuclear separation is taken to be 2.84 \AA . Altering the separation to 2.47 \AA does not radically affect predictions. The methods used by Sannigrahi and Dee closely predict the internuclear separation for Au_2 . When applied to Ag_2 these methods yield a separation of 2.38 \AA . Unfortunately, the predicted vibrational frequency is 517 cm^{-1} which seems at complete odds with the experimentally observed frequency. Ozin et al. predict a vibrational frequency of $187 \pm 2 \text{ cm}^{-1}$. Inclusion of spin-orbit coupling and relativistic effects apparently does not improve the correspondence between experiment and calculations in these areas.⁽⁴⁸⁾

The observed X-B and X-D transitions are thought to be spin-forbidden transitions. Higher order excitations of Ag_2 (the E and H systems) have been assigned only tentatively. These transitions are not observed in matrix isolation studies.

The dimer Ag_2 has been observed by mass spectrometry.^(35,52) Drowart and Honig⁽³⁵⁾ find that between 1260 and 1360 K the partial pressure ratio of dimer to monomer is between 5×10^{-4} and 8×10^{-4} . Hilpert and Gingerrich⁽⁵²⁾ report this ratio to be 23×10^{-4} at 1500 K. The suggestion by Searcy et al.⁽⁷⁰⁾ that silver vapor is highly polymerized between 1310-1420 K is contrary to the mass spectrometer data and a variety of more conventional experiences with silver.

The spectroscopic data used to calculate free-energy functions and thermodynamic data for Ag_2 are summarized in Table 9. Note that the Brown and Ginter internuclear separation of 2.469 \AA has been accepted for the calculations. Distortion of the geometry in the electronically excited states was ignored in these calculations.

2. Silver Trimer-- Ag_3

Spectroscopic^(30-32, 42-45) and mass spectroscopic⁽⁵⁰⁾ data suggest that a silver trimer, Ag_3 , exists. Raman

Table 9

Summary of Data Used to Calculate the
Thermodynamic Properties of $\text{Ag}_2(\text{gas})$

$$\begin{aligned} M &= 215.740 \\ r_e &= 2.469 \text{ \AA}^\circ \\ W_e &= 192 \text{ cm}^{-1} \\ W_e X_e &= 0.580 \text{ cm}^{-1} \\ B_e &= 0.0512 \text{ cm}^{-1} \\ \alpha_e &= 0.0002 \text{ cm}^{-1} \\ D_0 &= 37600 \text{ cal/mole} \end{aligned}$$

g_i

1
1
2

E_i

0
22996.4
37631.6

data using matrix isolation methods(55) suggest the molecule is linear with a stretching vibration at 120.5 cm^{-1} . The linear configuration is supported by CNDO calculations(56) and statistical mechanical calculations.(50) Detailed electronic data are not available. There appear to be excitations at about $41,000 \text{ cm}^{-1}$ and $22,000 \text{ cm}^{-1}$.

Hilpert and Gingerich(50) have found a dissociation energy for Ag_3 :

$$D_0(\text{Ag}_3) = 60500 \pm 3000 \text{ cal/mole} .$$

This indicates a lower bonding strength in Ag_3 than in Ag_2 which is also suggested by CNDO calculations.(56) At 1500 K, the relative abundance of monomer silver and trimer silver is found to be(50)

$$\frac{P_{\text{Ag}}}{P_{\text{Ag}_3}} = 2.9 \times 10^7 .$$

Hilpert and Gingerich have attempted statistical mechanical calculations of the free energy and enthalpy functions of Ag_3 at temperatures between 1400 and 2000 K.(50) A more complete set of thermodynamic properties of Ag_3 is presented here. A difficulty in estimating these thermodynamics is the treatment of the molecular vibrations. Since only a single vibrational absorption is observed in the Raman spectrum, it is likely that the molecule is linear. (A linear configuration would be expected on other grounds as well.) Hilpert and Gingerich used a very simple model to estimate the other two vibrational frequencies that have not been observed.

Here a Urey-Bradley force field is assumed. The vibrational frequencies are then found from:

$$\mu(K+2F) = \lambda_1 = 0.58915 \left(\frac{W_1}{1000} \right)^2$$

$$3\mu(K) = \lambda_2 = 0.58915 \left(\frac{W_2}{1000} \right)^2$$

$$6\mu(H-F^1) = \lambda_3 = 0.58915 \left(\frac{W_3}{1000} \right)^2$$

where

$$\mu = 1/107.87$$

K = stretching force constant (mdyne/A°)

H = bending force constant (mdyne/A°)

F = repulsion force constant (mdyne/A°)

F¹ = internal tension force constant (mdyne/A°)

W_i = ith vibrational constant (cm⁻¹).

F and F¹ are related, and the usual assumption that F¹ = -1/10 F is followed here. The assumption is made here as was done by Hilpert and Gingerich that

$$H = 1/10 K$$

Further, it was assumed that

$$F = K/3$$

The assumptions concerning the relative magnitudes of H, K, and F reflect a wide body of experience with the Urey-Bradley force field. For the Species I₃⁻ the symmetric vibration is at 149 cm⁻¹. Application of the Urey-Bradley force field and the assumed relative magnitudes of the force constants yields 171 and 76 cm⁻¹ for the asymmetric stretch and bending vibrations. Measured values are 149 and 69 cm⁻¹, respectively. (75,76)

The symmetric vibration in Ag₃, after correction for anharmonicity, is taken to be 119.5 cm⁻¹. Then the force constants are found to be:

$$K = 0.553 \text{ mdynes/A}^\circ$$

$$F = 0.184 \text{ mdynes/A}^\circ$$

$$H = 0.055 \text{ mdynes/A}^\circ$$

$$F^1 = -0.018 \text{ mdynes/A}^\circ$$

Hilpert and Gingerich reported a force constant for stretching of 0.916 mdynes/A° based on the simpler force field they used.

The vibrational frequencies of Ag₃ found from the Urey-Bradley force field are

$$W_1 = 119.5 \text{ cm}^{-1} \text{ (symmetric stretch)}$$

$$W_2 = 160 \text{ cm}^{-1} \text{ (asymmetric stretch)}$$

$$W_3 = 83 \text{ cm}^{-1} \text{ (bending-doubly degenerate) .}$$

Vibration frequencies save for that for the symmetric stretch were not reported by Hilpert and Gingerich.

Data used for calculating the thermodynamic properties of Ag₃ are summarized in Table 10. All electronic states for Ag₃ were taken to be doublets. The ground state is undoubtedly ²Σ. Grinter et al.(74) present magnetic circular dichroism data suggesting that the excited state is a ²Π split perhaps by spin-orbit coupling into the ²Π_{3/2} and ²Π_{1/2} components. This would not be inconsistent with assignments made here.

3. Cadmium Dimer--Cd₂

Evidence for a cadmium dimer, Cd₂, comes primarily from matrix isolation experiments.(54,57-61) Ault and Andrews(57) report electronic transitions ascribed to Cd₂ at 36,000-36,600 cm⁻¹ and 47,800-49,000 cm⁻¹. These transitions seem consistent with the limited gas phase spectroscopy for Cd₂. Vibrational fine structure on the electronic transitions had spacings of 90-110 cm⁻¹. Duley(59) found vibrational spacings of 80 ± 20. Given and Lowenschuss(58) report a Raman absorption for Cd₂ at 58 ± 1 cm⁻¹ again using matrix isolation techniques rather different than those used by Ault and Andrews.

Freedhoff(60) and others(54,57,61) have attempted to assign the optical spectrum of Cd₂ to the transitions:

$$1\Sigma_g \leftrightarrow 1\Sigma_u$$

$$1\Sigma_g \leftrightarrow 1\Pi_u \text{ .}$$

This is the assignment that would come about by adding two electrons to the qualitative molecular orbital diagram described above. However, as noted in the description, a dimer formed by two ground state Cd atoms will achieve

Table 10

Summary of Data Used to Calculate the
Thermodynamic Properties of $\text{Ag}_3(\text{gas})$

$$M = 323.61$$

$$D_0 = 60468 \text{ cal/mole}$$

$$\Delta H_f^{\text{Ag}_3}(298) = 263666 \text{ cal/mole}$$

$$W_1 = 119.5 \text{ cm}^{-1}$$

$$W_2 = 160 \text{ cm}^{-1}$$

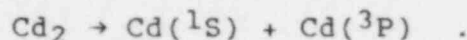
$$W_3 = 83 \text{ cm}^{-1} \text{ (doubly degenerate)}$$

$$B = 0.0114$$

$$\sigma = 2$$

$\underline{g_i}$	$\underline{E_i}$ (cm^{-1})
2	0
2	22000
2	41000

little net bonding. Recent theoretical calculations show that there is no bonding minimum in the potential curve for the Cd_2 state $^1\Sigma_g$. Instead, the $^3\Pi_g$ state formed from a ground state atom, $\text{Cd}(^1\text{S})$, and an excited state atom, $\text{Cd}(^3\text{P})$, is the lowest energy, stable state for Cd_2 . This implies that the dissociation of Cd_2 would be by the process



$$\text{Then, } D_0 = \Delta H_f^{\text{Cd}_2}(0) - \Delta H_f^{\text{Cd}(^1\text{S})}(0) - \Delta H_f^{\text{Cd}(^3\text{P})}(0)$$

The $\text{Cd}(^3\text{P})$ atom is about 22.7 kcal more energetic than a ground state cadmium atom.

To calculate the rotational and vibrational constants, it was assumed the potential function of Cd_2 was well approximated by a Morse potential. Vibrational data by Given and Lowenschuss were obtained using techniques to specifically guard against lattice atom effects. So the value of W_e was taken to be 58 cm^{-1} . Gaydon's value for D_0 was accepted. The remaining parameters were found by solving the equations:

$$D_0 = \frac{(W_e - W_e X_e)^2}{4W_e X_e}$$

$$B = \frac{2.799096 \times 10^{-39}}{I}$$

$$\alpha_e = \frac{W_e X_e B_e}{W_e}$$

$$\alpha_e = 6 \left[\frac{(W_e X_e B_e^3)^{1/2}}{W_e} - \frac{B_e^2}{W_e} \right]$$

$$I = \frac{M}{2} r_e^2$$

where m is the mass of a cadmium atom. Results of the calculations are shown in Table 11.

Theoretical calculations by Bender⁽⁶²⁾ were used to determine the electronic states available to Cd_2 . Absolute energies obtained from the theoretical calculations are not likely to be reliable since they yield dissociation energies of about 18 kcal/mole. But, relative energies, which are of interest here, may be more accurate.

4. Cadmium Trimer-- Cd_3

Some spectroscopic data that are interpreted to be for Cd_3 have appeared.⁽⁶¹⁾ In view of the low stability for Cd_2 and the absence of a defensible basis for preparing estimates of the thermodynamic data, Cd_3 was ignored here.

5. Indium Dimer-- In_2

DeMaria et al.⁽⁶⁵⁾ have reported an indium dimer, In_2 . H. Daidoji⁽⁷¹⁾ has apparently observed In_2 in flames. He reports optical emissions at $36,100\text{--}33,222\text{ cm}^{-1}$, $28,188\text{--}27,397\text{ cm}^{-1}$, and $27,248\text{--}25,773\text{ cm}^{-1}$. Assignment of the bands has not been reported, but it seems likely the ground state would be a $^3\Pi$. The excited states were assumed here to be $^1\Pi$, $^1\Sigma$, and $^1\Sigma$. (DeMaria et al.⁽⁶⁵⁾ assumed the ground state to be $^1\Sigma$ though this would seem to violate some of the empirical rules of electronic configurations.) DeMaria et al. found from their mass spectroscopic data $D_0 = 1.95 \pm 2.5$ kcal/mole. They recommend W_e to 135 cm^{-1} and the equilibrium separation to be 3 \AA . This equilibrium separation seems rather long in view of the stability they attribute to In_2 . If these values are accepted, and the diatomic potential energy curve is assumed to a Morse potential, then the other vibrational and rotation parameters listed in Table 12 are found.

C. Mixed Metal Species

The history of mixed metal vapor species has been somewhat checkered. For instance, a spectrum attributed to CdIn was reported in 1928.⁽⁶⁶⁾ This spectrum was later found to be due to, of all things, Bi_2 !⁽⁶⁷⁾ A study of mixed Hg and In vapors was purported to show the spectrum of HgIn(g) .⁽⁷²⁾ Later investigations suggest the spectrum was actually due to CdIn(g) --the cadmium being an impurity in the indium source for the earlier work.⁽⁶⁸⁾

Data are scant for mixed metal vapor species. Investigations of metal vapors are usually done, deliberately, at low vapor concentrations. Mixed metal species would be expected to make increasingly significant contributions to the vapor with increasing concentrations. But such mixed species may not be significant at low pressures.

Table 11

Summary of Data Used to Calculate the
Thermodynamic Properties of $\text{Cd}_2(\text{gas})$

$$M = 224.8$$

$$r_e = 2.46 \text{ \AA}$$

$$W_e = 58 \text{ cm}^{-1}$$

$$W_e X_e = 1.10 \text{ cm}^{-1}$$

$$B_e = 0.0492 \text{ cm}^{-1}$$

$$\alpha_e = 0.000935 \text{ cm}^{-1}$$

$$D_0 = 2100 \text{ cal/mole}$$

<u>g_i</u>	<u>E_i (cm^{-1})</u>	<u>State</u>
6	0	$^3\Pi_g$
3	888	$^3\Sigma_u^+$
2	1452	$^1\Pi_g$
2	10731	$^1\Pi_u$
1	11215	$^1\Sigma_u^+$
1	13232	$^1\Sigma_g$

Table 12

Summary of Data Used to Calculate the
Thermodynamic Properties of $\text{In}_2(\text{gas})$

$$M = 229.64$$

$$r_e = 3 \text{ \AA}^\circ$$

$$W_e = 135 \text{ cm}^{-1}$$

$$W_e X_e = 0.65 \text{ cm}^{-1}$$

$$B_e = 0.02903 \text{ cm}^{-1}$$

$$\alpha_e = 0.00014 \text{ cm}^{-1}$$

$$D_0 = 19500 \pm 2500 \text{ cal/mole}$$

g_i

3
2
1
1

E_i

0
27248
28188
36100

For the relatively high pressures of interest here, it is prudent to look for mixed metal species. Data have been found for three heteronuclear diatomic species. These data are described in the subsections below.

1. CdIn(g)

Santraw and Winans(68) have reported a spectrum for CdIn(g). CdIn(g) like Cd₂(g) cannot be formed from ground state atoms. Consequently, the lowest lying stable state is formed from an atom of In(2P) and an excited Cd(3P) atom. As would be expected, bonding forms two separate ²Σ states from these atoms. Another pair of states, ²Π and ²Σ, form from the combination of Cd(3S) and In(2P). Observed transitions at 18,008.8 and 17,126.7 cm⁻¹ are interpreted as ²Π ↔ ²Σ(C) and ²Σ(D) ↔ ²Σ(A) transitions. The lowest state vibrational constants are found to be W_e = 167.5 cm⁻¹ and W_eX_e = 0.70 cm⁻¹.

Drowert(49) cites a dissociation energy of 32 Kcal/mole. A value of 28.4 Kcal/mole is found from the formula

$$D_0 = \frac{(W_e - W_e X_e)^2}{4W_e X_e}$$

Rotational constants calculated from

$$\frac{\alpha_e}{B_e} = \frac{W_e X_e}{W_e}$$

$$\alpha_e = \frac{6}{W_e} \left[(W_e X_e B_e^3)^{1/2} - B_e^2 \right]$$

are $\alpha_e = 0.000131$

$B_e = 0.03126$

The value of B_e implies a bond length of 3.08 Å°.

Data used to calculate the thermodynamic properties of CdIn(gas) are summarized in Table 13.

Table 13

Summary of Data Used to Calculate the
Thermodynamic Properties of CdIn(gas)

$$\begin{aligned}
 M &= 227.22 \\
 r_e &= 3.08 \text{ \AA} \\
 W_e &= 167.5 \text{ cm}^{-1} \\
 W_e X_e &= 0.7 \text{ cm}^{-1} \\
 B_e &= 0.03126 \\
 \alpha_e &= 0.000131 \\
 D_0 &= 28400 \text{ cal/mole} \\
 \sigma &= 1
 \end{aligned}$$

$\underline{g_i}$	$\underline{E_i}$ (cm^{-1})
2	0
2	4500
4	18010
2	21830

2. AgIn

Biron(69) has reported a spectrum for AgIn(g) formed at 2000 K in an atmosphere of argon at a pressure of 5 atmospheres. An optical transition is observed at $32,471.4 \text{ cm}^{-1}$. Assignments for this transition have not been made, but it seems likely that the ground state is a $^3\Pi$ and the excited state is $^1\Sigma$.

Vibrational analyses by Biron yield the parameters

$$W_e = 155.22 \text{ cm}^{-1}$$

$$W_e X_e = 0.422 \text{ cm}^{-1}$$

Then, as was done for CdIn the other molecular parameters are found to be:

$$D_0 = 40570 \text{ cal/mole}$$

$$B_e = 0.01885$$

$$\alpha_e = 5.1 \times 10^{-5}$$

The B_e value implies a rather long bond length.

Data used to calculate the thermodynamic properties of AgIn(g) are shown in Table 14.

3. AgCd

An esr spectrum of AgCd has been obtained using matrix isolation techniques.(73) Unfortunately, there does not seem to be sufficient data to calculate thermodynamic properties for the species.

D. Summary of Free Energy of Formation Data

The free energies of formation of species of interest in the Ag-In-Cd system are summarized in Table 15. These free energy of formation data are necessary for the vaporization calculations that are described in the balance of this report. For these calculations tabulated values of the free energy of formation were not directly used. Rather, free energy of formation values were calculated using the enthalpies of formation and the free-energy functions:

Table 14

Summary of Data Used to Calculate the
Thermodynamic Properties of AgIn(gas)

$$\begin{aligned} M &= 222.69 \\ W_e &= 155.2 \\ W_e X_e &= 0.422 \\ B_e &= 0.01885 \\ \alpha_e &= 0.000051 \\ D_0 &= 40600 \text{ cal/mole} \\ \sigma &= 1 \end{aligned}$$

$\underline{g_i}$	$\underline{E_i}$ (cm^{-1})
3	0
1	32471

Table 15

Summary of Free Energy of Formation Data (cal/mole)

Temp (K)	Ag(c)	In(c)	Cd(c)	Ag(g)	Ag ₂	Ag ₃	Ag ⁺	In(g)	In ₂ (g)
298	0	0	0	58,622	85,460	128,526	233,065	49,745	84,731
300	0	0	0	58,564	85,384	128,439	233,000	49,693	84,660
400	0	0	0	55,470	81,337	123,755	229,467	46,948	80,926
500	0	0	0	52,406	77,376	119,165	225,839	44,377	77,570
600	0	0	0	49,369	73,488	114,657	222,137	41,895	74,420
700	0	0	0	46,355	69,666	110,224	218,375	39,438	71,351
800	0	0	0	43,205	65,580	105,379	214,407	36,999	68,354
900	0	0	0	40,397	62,190	101,562	210,718	34,572	65,414
1000	0	0	0	37,454	58,539	97,337	206,837	32,152	62,527
1100	0	0	1,382	34,530	54,935	93,172	202,929	29,738	59,687
1200	0	0	3,650	31,626	51,379	89,069	198,991	27,328	56,887
1300	0	0	5,901	28,891	48,167	85,470	195,184	24,922	54,124
1400	0	0	8,135	26,253	45,155	82,164	191,435	22,521	51,401
1500	0	0	10,354	23,637	42,192	78,922	187,672	20,124	48,709
1600	0	0	12,559	21,040	39,273	75,741	183,893	17,728	46,043
1700	0	0	14,752	18,463	36,396	72,619	180,105	15,338	43,405
1800	0	0	16,930	15,904	33,560	69,550	176,305	12,951	40,794
1900	0	0	19,096	13,361	30,763	66,537	172,497	10,570	38,208
2000	0	0	21,252	10,834	27,999	63,569	168,677	8,192	35,643
2100	0	0	23,396	8,322	25,268	60,648	164,844	5,822	33,105
2200	0	0	25,531	5,825	22,569	57,773	161,003	3,453	30,581
2300	0	0	27,655	3,343	19,904	54,947	157,157	1,090	28,079
2400	0	1,266	29,773	873	17,263	52,157	153,299	0	28,127
2500	1,584	3,620	32,680	0	17,823	54,167	151,019	0	30,363
2600	4,030	5,967	33,978	0	20,131	58,800	149,590	0	32,609
2700	6,464	8,310	36,069	0	22,442	63,438	148,140	0	34,860
2800	8,884	10,646	38,153	0	24,748	68,070	146,680	0	37,112
2900	11,297	12,981	40,227	0	27,063	72,719	145,201	0	39,377
3000	13,697	15,306	42,305	0	29,374	77,362	143,700	0	41,639
3100	16,089	17,625	44,352	0	31,690	81,654	142,182	0	43,904
3200	18,471	19,950	46,407	0	34,009	86,674	140,652	0	46,179
3300	20,840	22,262	48,452	0	36,327	91,338	139,104	0	48,450
3400	23,204	24,574	50,494	0	38,644	96,002	137,542	0	50,728
3500	25,560	26,876	52,528	0	40,969	100,685	135,968	0	53,004

Table 15 (continued)

Summary of Free Energy of Formation Data (cal/mole)

Temp (K)	In ⁺	Cd(g)	Cd ₂	Cd ⁺	CdIn	AgIn	e ⁻
298.15	182,891	18,466	60,804	224,672	66,797	71,877	0
300	182,832	18,414	60,723	224,609	66,724	71,797	0
400	179,648	15,666	56,391	221,146	62,848	67,514	0
500	176,516	12,956	52,117	217,597	59,213	63,462	0
600	173,378	10,301	47,928	214,002	55,745	59,553	0
700	170,190	7,908	44,239	210,585	52,590	55,716	0
800	166,962	5,551	40,593	207,134	49,510	51,786	0
900	163,695	3,222	36,977	203,649	46,494	48,232	0
1000	160,396	917	33,378	200,130	43,531	44,574	0
1100	157,068	0	32,531	197,953	41,984	40,966	0
1200	153,710	0	33,491	196,644	41,375	37,402	0
1300	150,328	0	34,423	195,297	40,788	34,029	0
1400	146,924	0	35,325	193,910	40,218	30,778	0
1500	143,500	0	36,203	192,438	39,667	27,567	0
1600	140,052	0	37,051	191,030	39,126	24,392	0
1700	136,586	0	37,875	189,545	38,601	21,254	0
1800	133,103	0	38,668	188,030	38,086	18,149	0
1900	129,605	0	39,432	186,486	37,581	15,078	0
2000	126,088	0	40,172	184,918	37,085	12,035	0
2100	122,555	0	40,882	183,322	36,602	9,023	0
2200	119,007	0	41,563	181,702	36,123	6,035	0
2300	115,444	0	42,217	180,063	35,653	3,074	0
2400	113,130	0	42,846	178,402	36,458	1,404	0
2500	111,888	0	43,444	176,719	38,353	2,428	0
2600	110,627	0	44,011	175,012	40,249	4,332	0
2700	109,346	0	44,554	173,295	42,147	6,240	0
2800	108,042	0	45,067	171,554	44,045	8,148	0
2900	106,723	0	45,547	169,797	45,944	10,067	0
3000	105,379	0	45,999	168,020	47,839	11,985	0
3100	104,015	0	46,424	166,226	49,737	13,907	0
3200	102,631	0	46,821	164,421	51,637	15,835	0
3300	101,225	0	47,189	162,597	53,532	17,763	0
3400	99,803	0	47,531	160,764	55,431	19,695	0
3500	98,357	0	47,836	158,910	57,325	21,631	0

$$\Phi_i(T) = - \left[G_i^O(T) - H_O^{(i)}(298) \right] / T$$

where $\Phi_i(T)$ is the temperature-dependent free-energy function of the i^{th} species.

Free-energy function values were obtained from polynomial expressions which had been fit to tabulated values of the free-energy functions:

$$\begin{aligned} \Phi_i(T) = & a_0 + a_1x + a_2x^2 + a_3x^3 + a_4\ln(x) \\ & + \frac{a_5}{x} + a_6x\ln(x) \end{aligned}$$

where $x = T/10^4$.

The fitting was done by least-squares procedures. The quality of the fit of the polynomial expression to the tabulated data for a given species was judged with the aid of the reduced chi-squared statistic:

$$\chi^2 = \sum_{j=1}^N \left| \Phi_i(j) \Big|_{\text{tabulated}} - \Phi_i(j) \Big|_{\text{calculated}} \right|^2 / (N-7)$$

where $\Phi_i(j)$ = free-energy function value for the i^{th} species at the j^{th} temperature,

N = number of tabulated points used in the fitting procedure, and

the subscripts "tabulated" and "calculated" denote free-energy function values from the tables in Appendix B and those calculated with the polynomial expression, respectively. The square root of the reduced chi-squared statistic provides an estimate of the magnitude of the difference between the tabulated and the calculated free-energy function for a given species at a given temperature.

Coefficients derived by fitting the polynomial expression to the tabulated free-energy function values are summarized in Table 16. Typically 34 tabulated points were used to obtain the coefficient values. These tabulated points were for temperatures of 298.15 K and at 100 K between 300 K and 3500 K. The typical discrepancy between tabulated and calculated free-energy functions is less than 1×10^{-3} cal/ mole - K.

Table 16

Coefficients for the Function Used to Fit
the Free-Energy Functions

Species	a_0	a_1	a_2	a_3	a_4	a_5	a_6	x^2	$\Delta H_f(298)$
Ag(s)	14.6307	-89.4764	280.220	-322.170	3.67575	0.161345	-52.4857	2.62×10^{-8}	0
Ag(l)	41.3038	109.137	-228.334	138.092	8.95869	0.195529	69.6458	1.12×10^{-5}	2457
Ag(g)	54.0367	0.968621	-2.27304	1.40579	5.02399	0.148747	0.808334	1.04×10^{-7}	67900
Ag ₂ (g)	82.2973	-1.76200	6.64896	-3.04850	8.53773	0.261183	-3.47901	2.2×10^{-9}	97679
Ag ₃ (g)	116.124	9.07643	-18.9140	6.8503	14.9912	0.442341	5.37953	4.5×10^{-8}	142655
Ag _f	52.5319	0.677194	-1.60050	1.12376	4.99089	0.148264	0.466268	6.9×10^{-8}	243420
In(s)									
In(l)	33.3239	-2.76830	5.40492	-3.87448	7.09354	0.211288	-0.881685	3.03×10^{-7}	738
In(g)	47.9766	35.5547	-68.3592	54.2479	3.11990	0.112920	2.84931	2.15×10^{-6}	58000
In ₂ (g)	87.2059	0.317009	3.39847	-1.56370	8.73896	0.265003	-1.76528	1.07×10^{-9}	96047
In _f	51.1102	-2.49924	2.22860	9.53402	4.58929	0.143226	-3.89647	1.03×10^{-7}	192222
Cd(s)									
Cd(l)	30.2508	-3.24552	9.06126	-4.73998	6.49351	0.205325	-4.70013	8.085×10^{-6}	1415
Cd(g)	52.7531	0.0971014	-0.175171	-0.330780	5.02436	0.149096	0.398796	1×10^{-7}	26720
Cd ₂ (g)	80.2550	-16.8988	71.8227	-33.476	6.78084	0.265983	-33.5417	5×10^{-8}	73824
Cd _f	53.1370	-3.12332	7.32125	-4.46580	4.77716	0.145904	-2.67325	7.6×10^{-8}	234825
AgIn(g)	88.8147	-1.03858	4.64998	-2.15377	8.66701	0.263144	-2.40348	1.7×10^{-9}	84817
CdIn(g)	91.1926	9.88834	-12.7622	-0.0655975	9.71463	0.275768	10.0613	1.06×10^{-7}	78528
e-	17.5774	0.340352	-0.703545	0.251687	4.99291	0.148365	0.337700	6.56×10^{-8}	0

An exception to the typical procedure was that used for Ag(s). Only 11 tabulated points at temperatures of 298.15 K and 100 K intervals between 300 K and 1200 K were used.

The highly parameterized form of the polynomial expression was chosen to aid interpolation of the tabulated data. Because of this highly parameterized form, the expression derived for the various species ought not be used to extrapolate beyond the limits of data used to derive the coefficients in the polynomial. That is, no assurance can be given about the adequacy of the polynomial expression for temperatures greater than 3500 K or less than 298 K.

IV. Vapor Pressures

A. Vapor Pressures over Pure Elements

The sums of the partial pressures of metal-bearing gases over silver, indium, and cadmium are plotted against the absolute temperatures in Figures 33, 34, and 35, respectively. In addition, in Table 17, the temperatures at which specified vapor pressures are achieved over the pure elements are listed.

In Figures 36, 37, and 38, the relative contributions of the various gaseous species to the vapor over the elements are plotted against temperature. Partial pressures of these species at various temperatures are shown in Table 17.

Monomeric, neutral species are the dominant contributors to the gas phase for all the elements at temperatures less than 3000 K. The relative contributions of Ag₂ and Ag₃ to the vapor over pure silver are in excellent agreement⁽³⁵⁾ with measurements made by Drowert and Honig at 1260-1360 K and by Hilpert and Gingerrich at 1500 K⁽⁵²⁾.

Though the contributions of the polymeric species are not especially large, they are sufficient to change the normal boiling points of the liquid elements from values estimated based on assuming only monatomic species in the vapor:

<u>Element</u>	<u>Normal Boiling Point (K)</u>
Silver	2429.18
Indium	2345.54
Cadmium	1039.66

The change in the normal boiling point of silver is noticeable. Changes for indium and cadmium are not large enough for concern.

Table 17

Total Vapor Pressure and Species Partial
Pressures Over Pure Elements
at Various Temperatures

Temperature (K)	Total Pressure (atms)	Species			
		Partial M(g)	M ₂ (g)	Pressures M ₃ (g)	(atms) M ⁺ (g)
<u>Silver</u>					
2980	10	9.34	0.66	2x10 ⁻³	2x10 ⁻⁵
2429	1	0.967	0.033	2x10 ⁻⁵	1x10 ⁻⁷
2055	0.1	0.985	2x10 ⁻³	3x10 ⁻⁷	1x10 ⁻⁹
1783	0.01	0.0099	7x10 ⁻⁵	3x10 ⁻⁹	1x10 ⁻¹¹
1576	0.001	1x10 ⁻³	3x10 ⁻⁶	2x10 ⁻¹¹	2x10 ⁻¹³
<u>Indium</u>					
2912	10	9.90	0.104	-	3x10 ⁻⁴
2346	1	0.997	3x10 ⁻³	-	5x10 ⁻⁶
1966	0.1	0.100	9x10 ⁻⁵	-	8x10 ⁻⁸
1693	0.01	0.010	2x10 ⁻⁶	-	2x10 ⁻⁹
1488	0.001	1x10 ⁻³	6x10 ⁻⁸	-	3x10 ⁻¹¹
<u>Cadmium</u>					
1763	100	99.8	0.174	-	2x10 ⁻¹¹
1303	10	10.0	2x10 ⁻⁴	-	1x10 ⁻¹⁶
1040	1	1.0	1x10 ⁻⁷	-	1x10 ⁻²¹
868	0.1	0.1	2x10 ⁻¹⁰	-	2x10 ⁻²⁶
746	0.01	0.01	3x10 ⁻¹³	-	2x10 ⁻³¹
655	0.001	1x10 ⁻³	5x10 ⁻¹⁶	-	4x10 ⁻³⁶

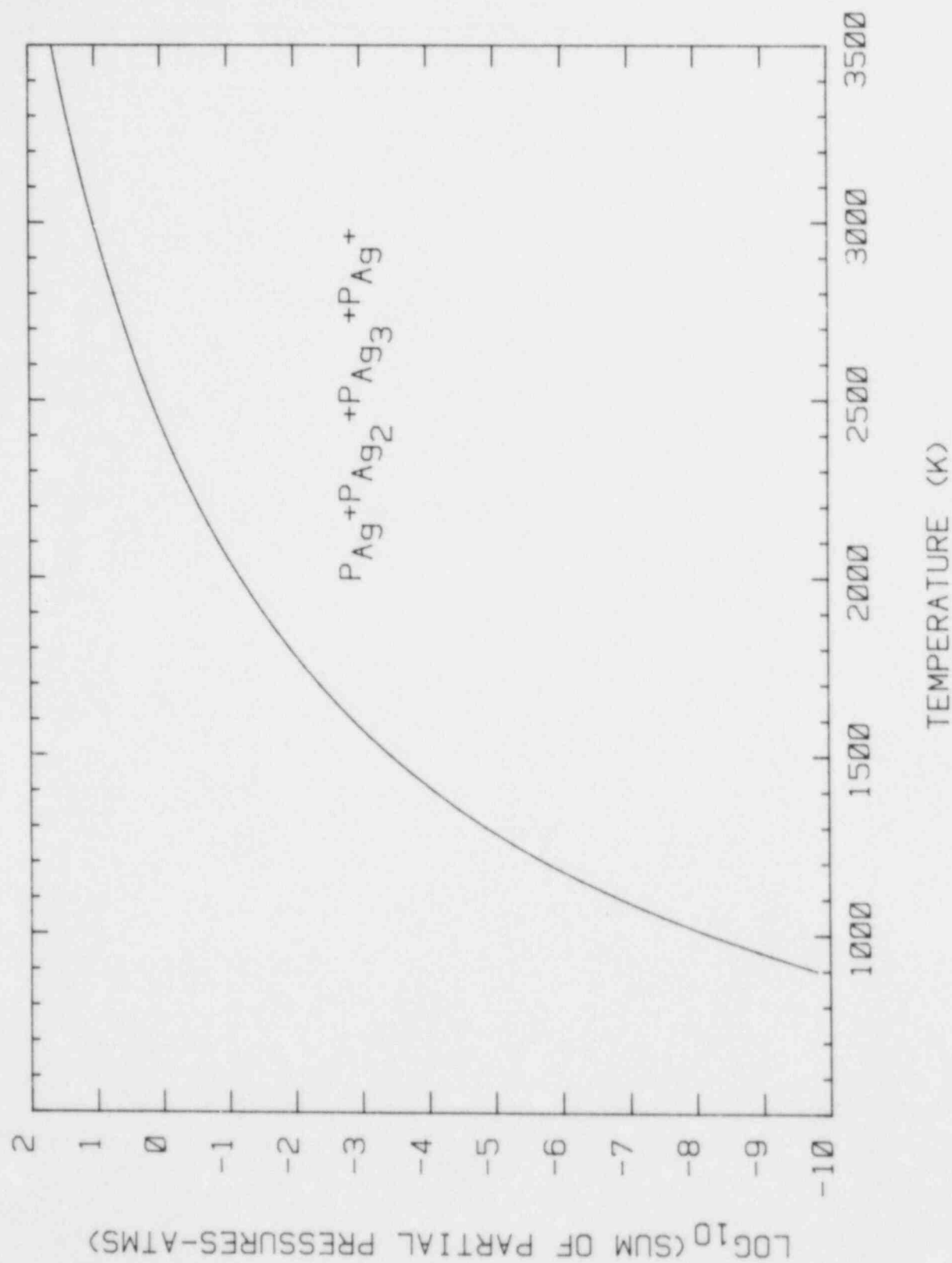


Figure 33. Sum of the Partial Pressures of Silver-Bearing Species Over Pure Silver

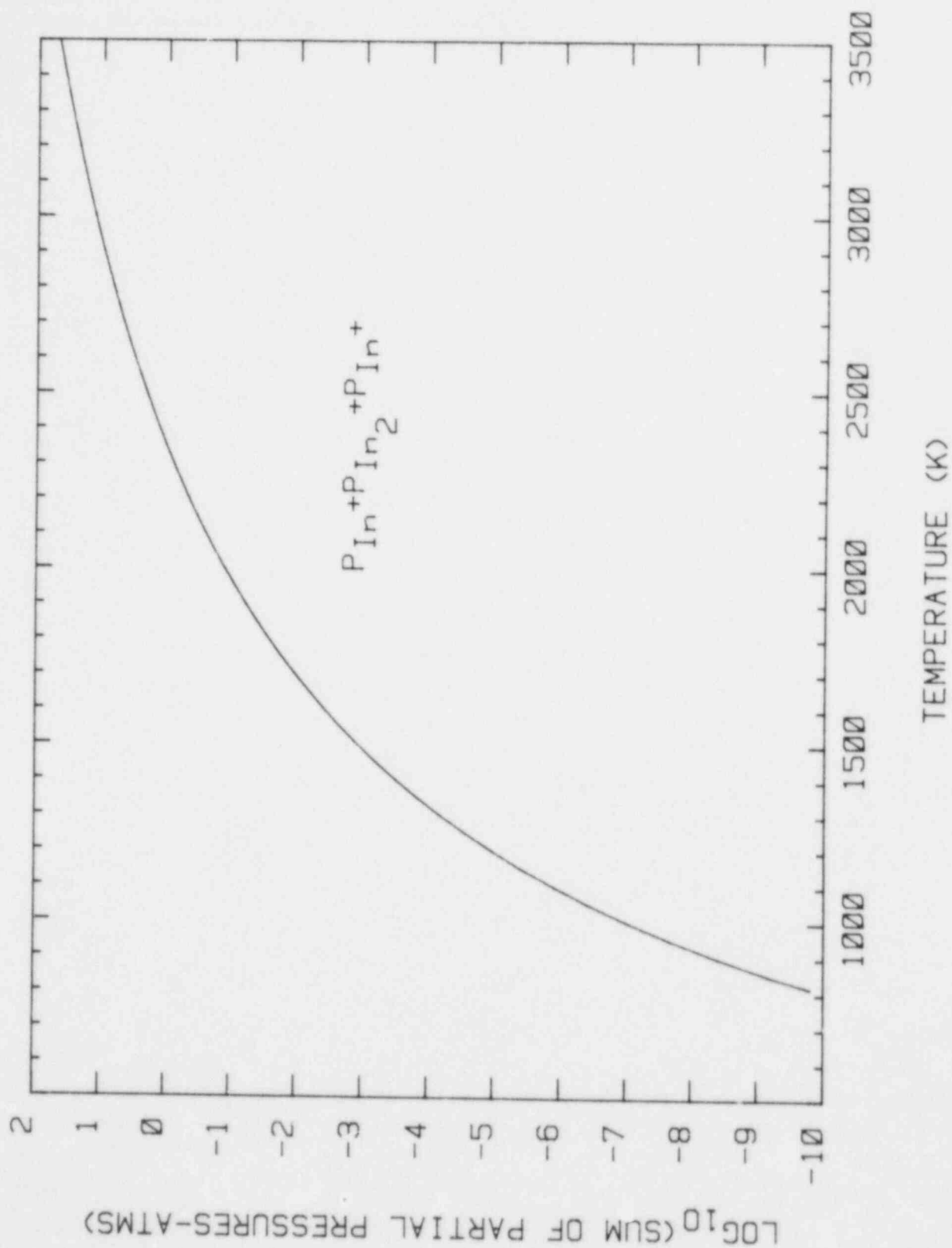


Figure 34. Sum of the Partial Pressures of Indium-Bearing Species Over Pure Liquid Indium

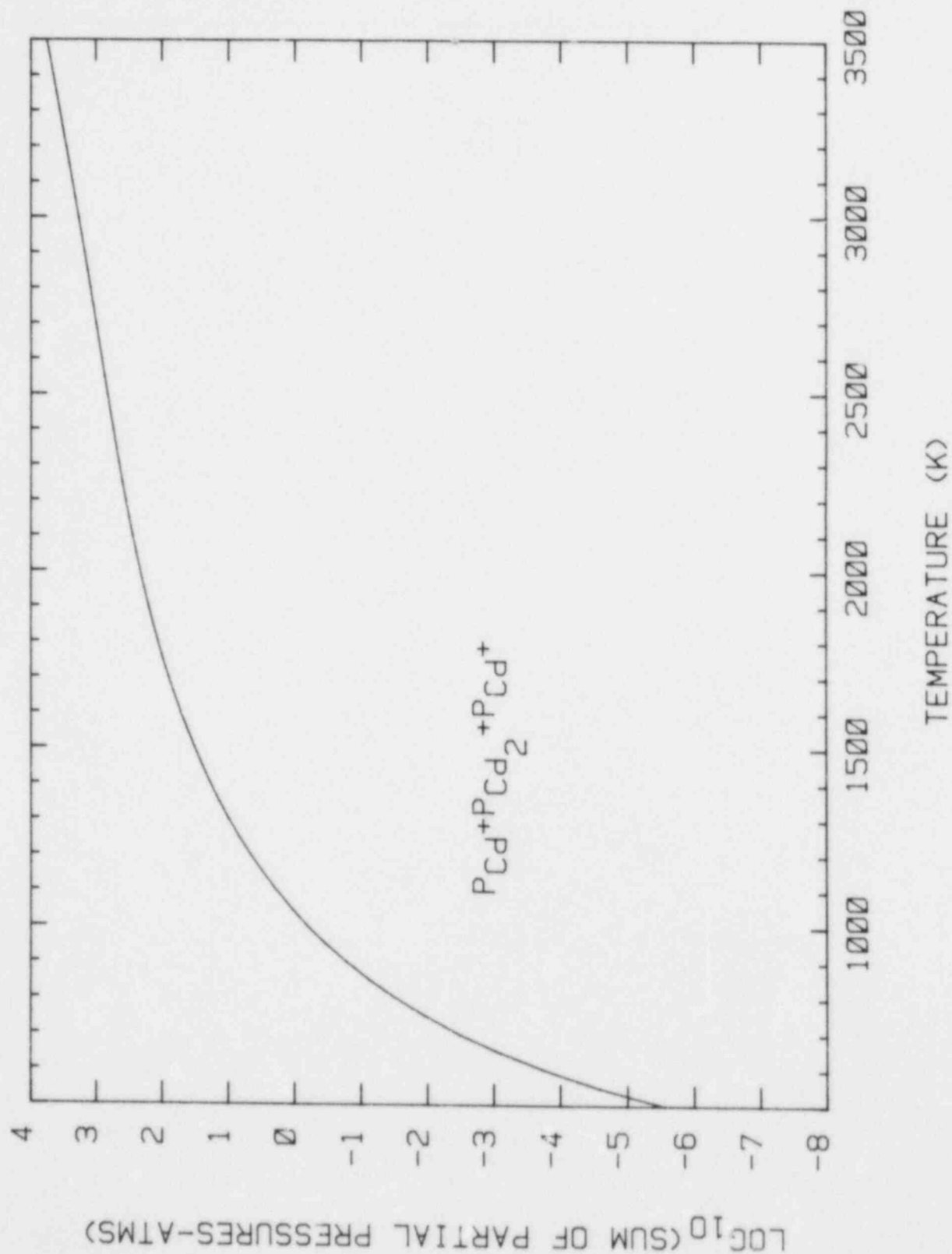


Figure 35. Sum of the Partial Pressures of Cadmium-Bearing Species Over Pure Liquid Cadmium

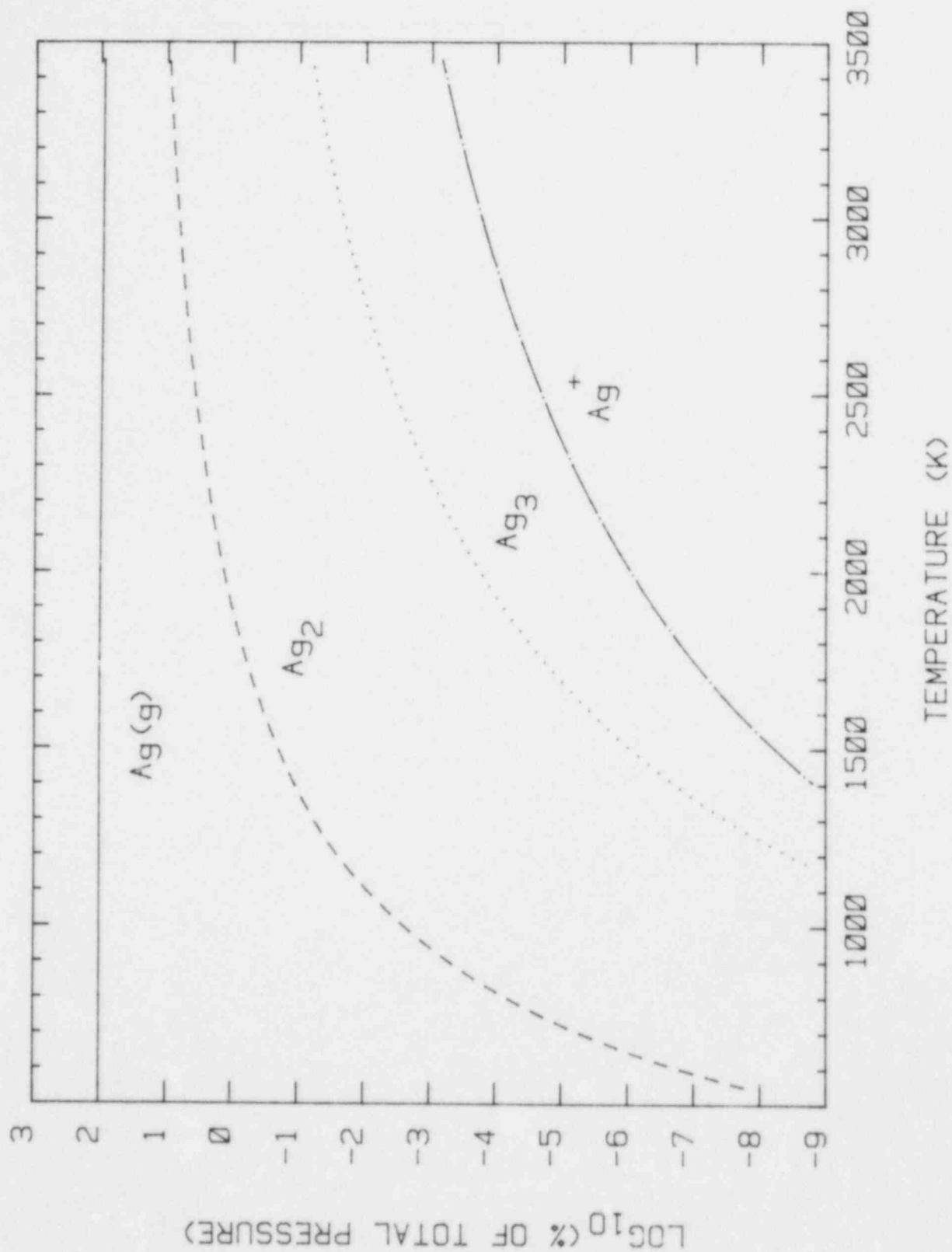


Figure 36. Contributions of Various Species to the Vapor Over Pure Silver

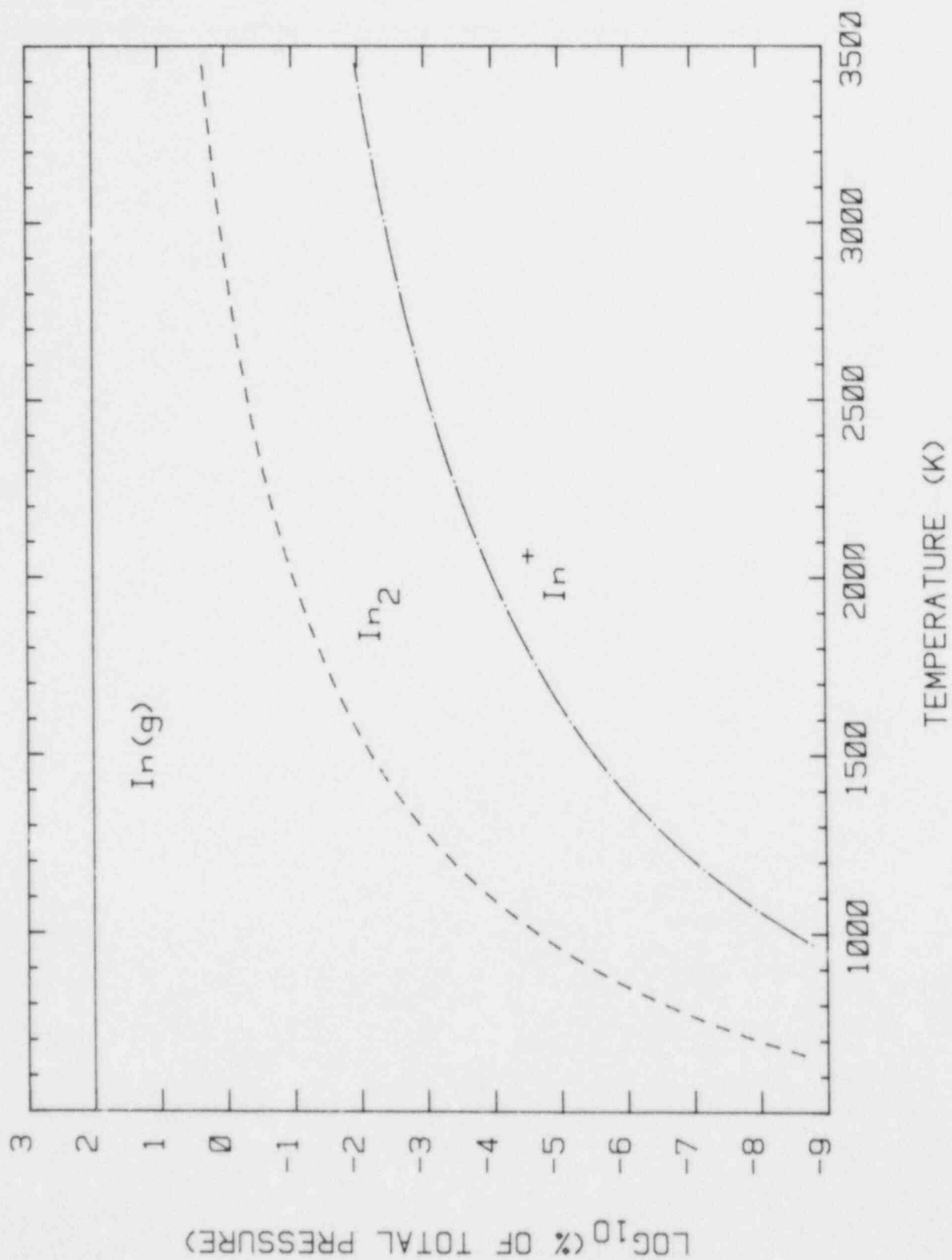


Figure 37. Contributions of Various Species to the Vapor Over Pure Liquid Indium

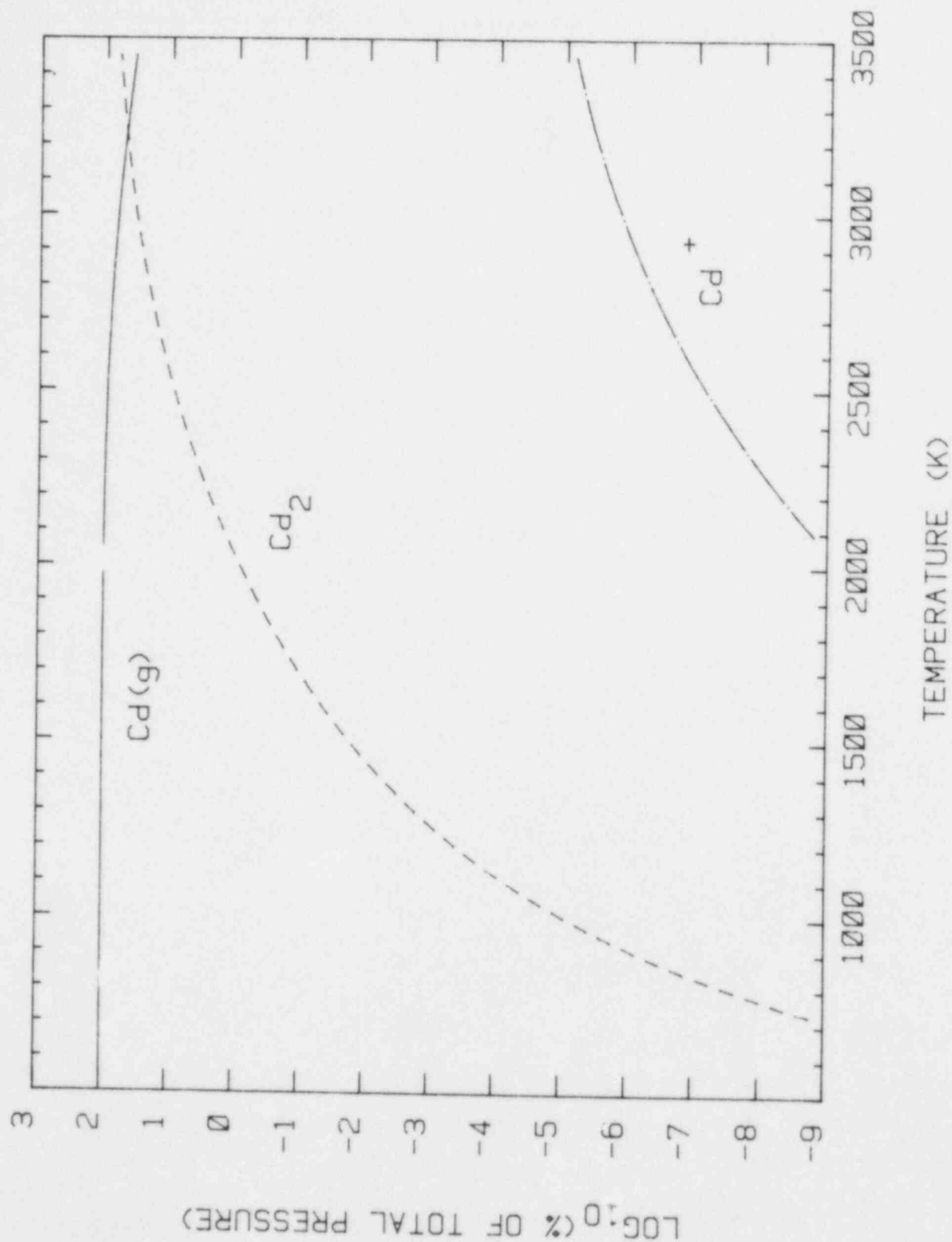


Figure 38. Contributions of Various Species to the Vapor Over Pure Liquid Cadmium

Indium ion is the most stable of the three ions considered here. Even so, its contribution to the vapor over pure indium is less than 10^{-3} percent even at temperatures up to 3400 K.

The cadmium dimer is predicted in these calculations to become the dominant contributor to the vapor phase over liquid cadmium at about 3200 K. This temperature is, however, above the critical point of cadmium. Calculations at such elevated temperatures for cadmium are not reliable since liquid cadmium does not exist at these temperatures.

B. Vapor Pressures Over Binary Alloys

Several additional considerations arise in the treatment of vaporization of binary alloys:

1. Activities of the condensed phase constituents must be recognized;
2. Mixed-metal vapor phase species must be considered;
3. Electroneutrality of the gas phase needs to be included in the equation set; and
4. Azeotropes may arise in the vapor/condensed phase equilibrium.

Here, two models of condensed phase activities are pursued--the ideal solution model and a nonideal solution model based on the Wilson equation. An important objective of the analyses is to ascertain the differences in the predicted vaporization characteristics derived using these two models.

Mixed-metal vapor species such as CdIn(g) and AgIn(g) are readily introduced into the equation sets to be solved for predicting vaporization. To solve for ionic species requires a mass balance equation:

$$n_{\text{Ag}^+} + n_{\text{In}^+} + n_{\text{Cd}^+} = n_{\text{e}^-}$$

where n_i = moles of the species i in the gas phase.

Introduction of this equation makes necessary iterative solution of the equation set. Some care is necessary in programming such an iterative solution. The contribution of ionic species to the gas phase is small. Incautious iterative solution schemes can be oscillatory and nonconvergent. Underrelaxation usually cures this difficulty.

An azeotropic composition is one in which the bulk composition of the vapor and the condensed phases are the same. For this to happen, there must be some nonideality in either the gas or the condensed phases. "Nonideality" in the vapor phase is introduced effectively by the formation of polymeric and mixed-metal vapor species. But, this effective nonideality is of less interest than true nonideal behavior created by interactions in the condensed phase.

A necessary condition for an azeotrope to arise is that there be some combination of temperatures and condensed phase compositions for which the ratio of constituent activity coefficients equals the ratio of pure species vapor pressures. In view of the very high volatility of cadmium relative to either silver or indium, azeotropes are not likely to be important for binary alloys involving cadmium. Silver/indium alloys, on the other hand, are very likely to be susceptible to azeotrope formation.

B-1. Vapor Pressures Over Silver/Indium Alloys

The phase diagram for the silver/indium system at one atmosphere is shown in Figure 39. The solid lines in this figure were calculated considering nonideality of the liquid phase. The dashed lines are the result of calculations in which the condensed phase was considered to be an ideal mixture.

Both the ideal and the nonideal phase diagrams exhibit an azeotrope. The azeotrope is, however, quite different in the two diagrams. The ideal mixture assumption produces a low-boiling azeotrope at high indium concentrations (the azeotrope location at one atmosphere is $x_{\text{In}} = 0.775$, $T = 2339$ K). This azeotrope is strictly the result of considering mixed-metal and polymeric species in the gas phase. Recognizing nonideality of the condensed phase leads to the prediction of a high-boiling azeotrope at low indium concentrations (the azeotrope location at one atmosphere is $x_{\text{In}} = 0.110$, $T = 2434.4$ K). Both the nonideality of the condensed phase and consideration of mixed-metal and polymeric species in the gas phase have produced this azeotrope.

The importance of the mixed-metal vapor species AgIn(g) to phase relations in the silver-indium system is shown by the phase diagrams in Figure 40. These phase diagrams were predicted in calculations which neglected the mixed-metal species. Calculations based on assuming the condensed phase is ideal show no azeotrope. The lenticular miscibility gap is only modestly distorted by other polymeric species. Recognizing nonideality of the condensed phase, but neglecting AgIn(g) , produces an azeotrope shifted to higher temperatures and higher indium concentrations.

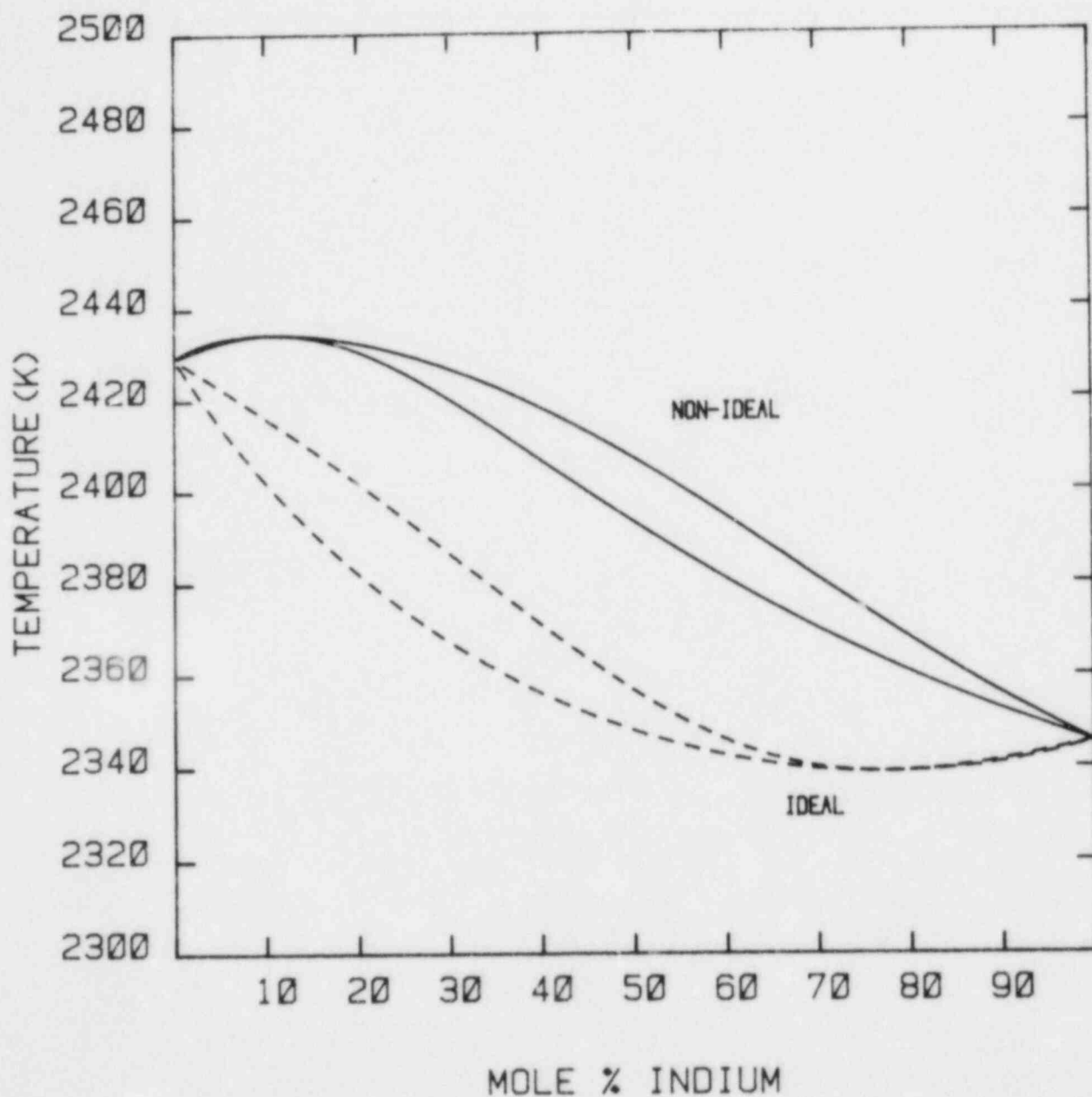


Figure 39. Condensed/Vapor Phase Equilibrium for the System Indium/Silver at One Atmosphere. Solid lines are for a nonideal condensed phase and the dashed lines are for an ideal condensed phase. Both calculations include mixed-metal vapor species.

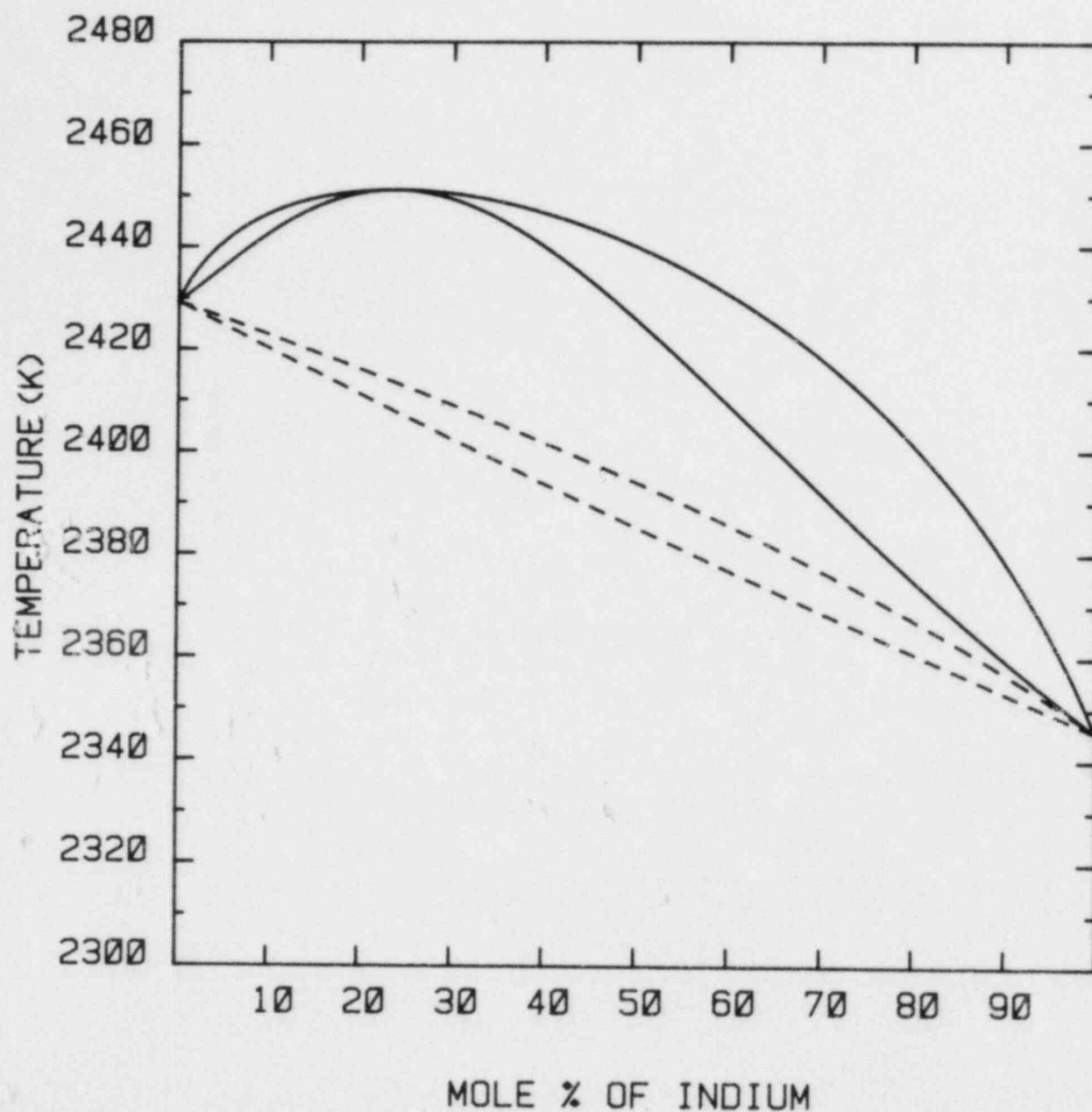


Figure 40. Condensed/Vapor Phase Equilibrium for the Indium/Silver System When Mixed-Metal Vapor Species Are Ignored. Solid lines are for a non-ideal condensed phase and dashed lines are for an ideal condensed phase.

The discussions in Section 3 of this document show that the thermodynamic stability of AgIn(g) is quite uncertain. Variations of the thermodynamic properties of AgIn(g) has some effect on the predicted location of the azeotrope. Such variations do not have as strong an effect as variations in the treatment of the condensed phase.

The calculated phase diagrams of the silver-indium system shown in Figure 41 were obtained by varying the activity coefficients of silver and indium by about 10 percent from their nominal values. The azeotrope location is, obviously, quite sensitive to the activity coefficients of the condensed phase constituents. Significant uncertainties must be ascribed to the activity coefficients developed here. The predictions involve extrapolation of the available data base by almost 1000 K. Consequently, details of the azeotrope location described here must be considered uncertain.

The effects of temperature on the location of the azeotrope in the silver-indium system are shown in Figure 42. The location of the azeotrope as a function of temperature defines the so-called "azeotropic line." Azeotropic pressure varies with temperature as would be predicted by a classic Clausius-Claperon expression:

$$\ln P_A = -H_A/RT + B$$

where P_A = azeotropic pressure (atms)

H_A = enthalpy of azeotropic vaporization

$$= 62,790 \pm 86 \text{ cal/mole}$$

R = gas constant = 1.987 cal/mole

T = absolute temperature (K)

$$B = 13.0024 \pm 0.0267.$$

As might be expected, the enthalpy of vaporization at the azeotropic composition is somewhat larger than the enthalpy of vaporization of either pure silver or pure indium.

The temperature-dependence of the compositional coordinate of the azeotropic line is not so simple as is that of the pressure coordinate. The compositional coordinate is very dependent on the relative contribution of AgIn(g) to the vapor phase. Speciation of the vapor phase along the azeotropic line is shown in Figure 43. The contribution of

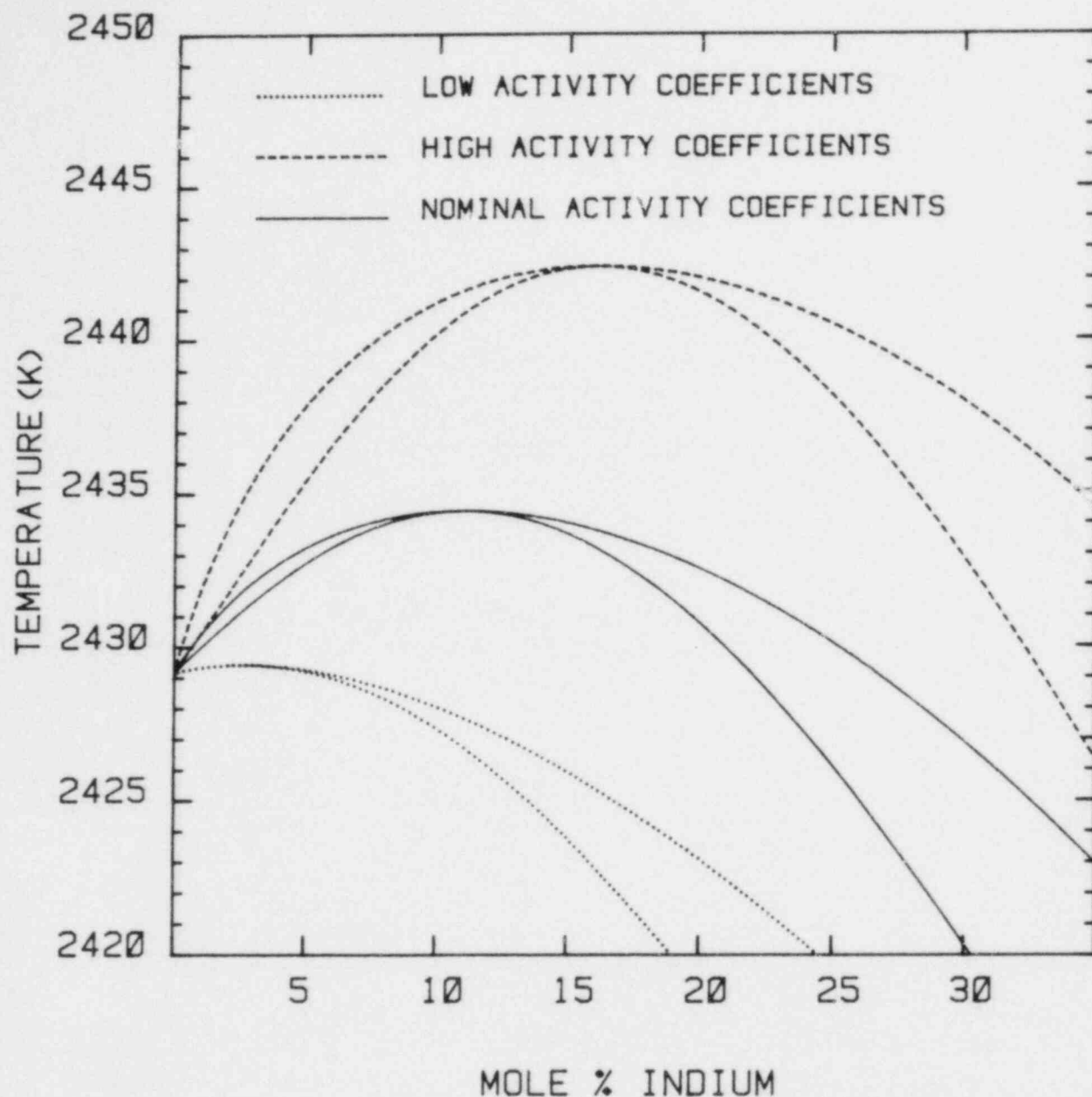
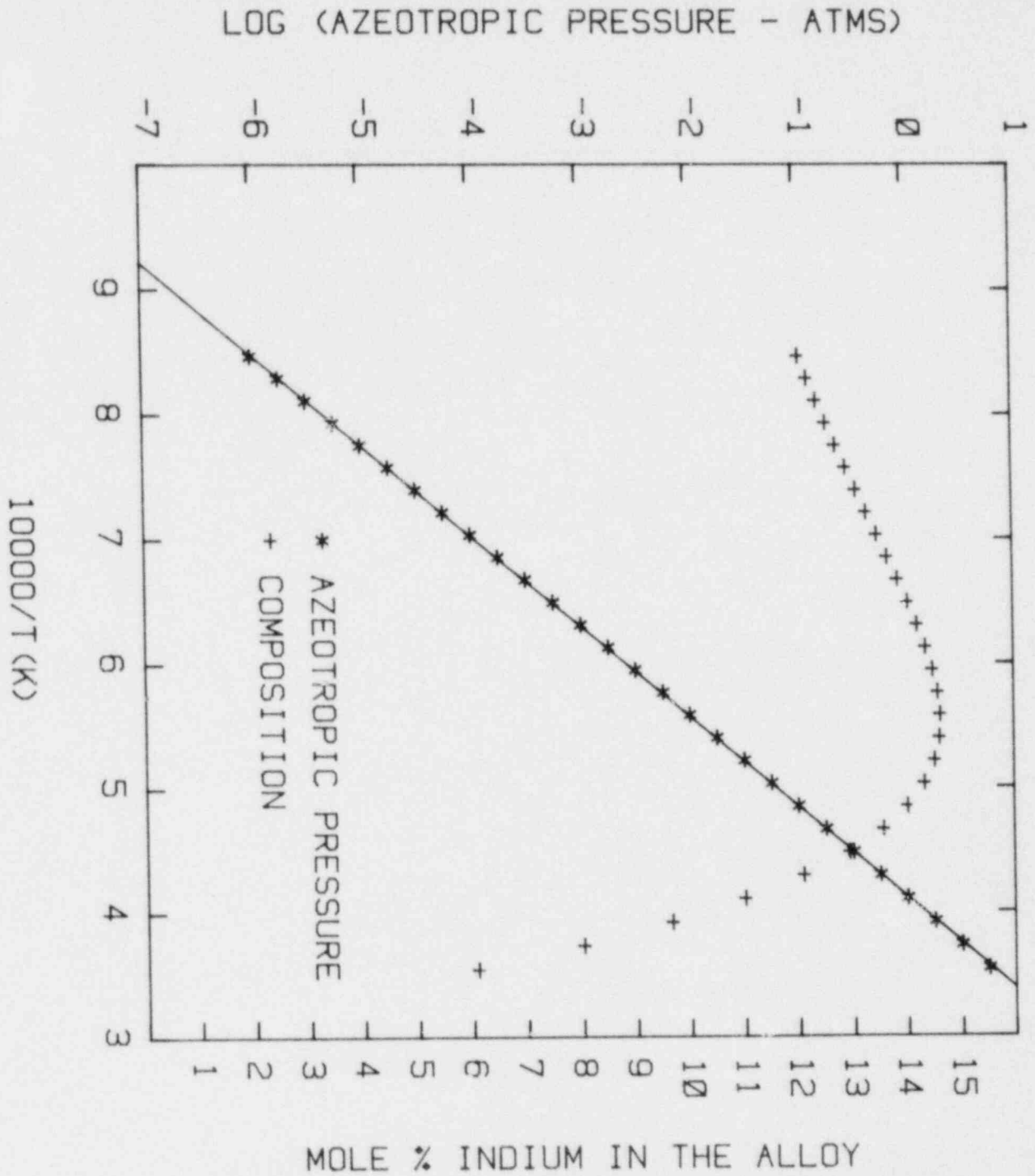


Figure 41. Effects of Indium and Silver Activity Coefficients on the Azeotrope Location at One Atmosphere Pressure. The solid lines were calculated using the nominal activity coefficients of both silver and indium. Dashed lines were computed by incrementing the activity coefficients of both silver and indium to values within the uncertainty ranges of these coefficients. Dotted lines were computed by decreasing the activity coefficients to values with their respective uncertainty ranges.



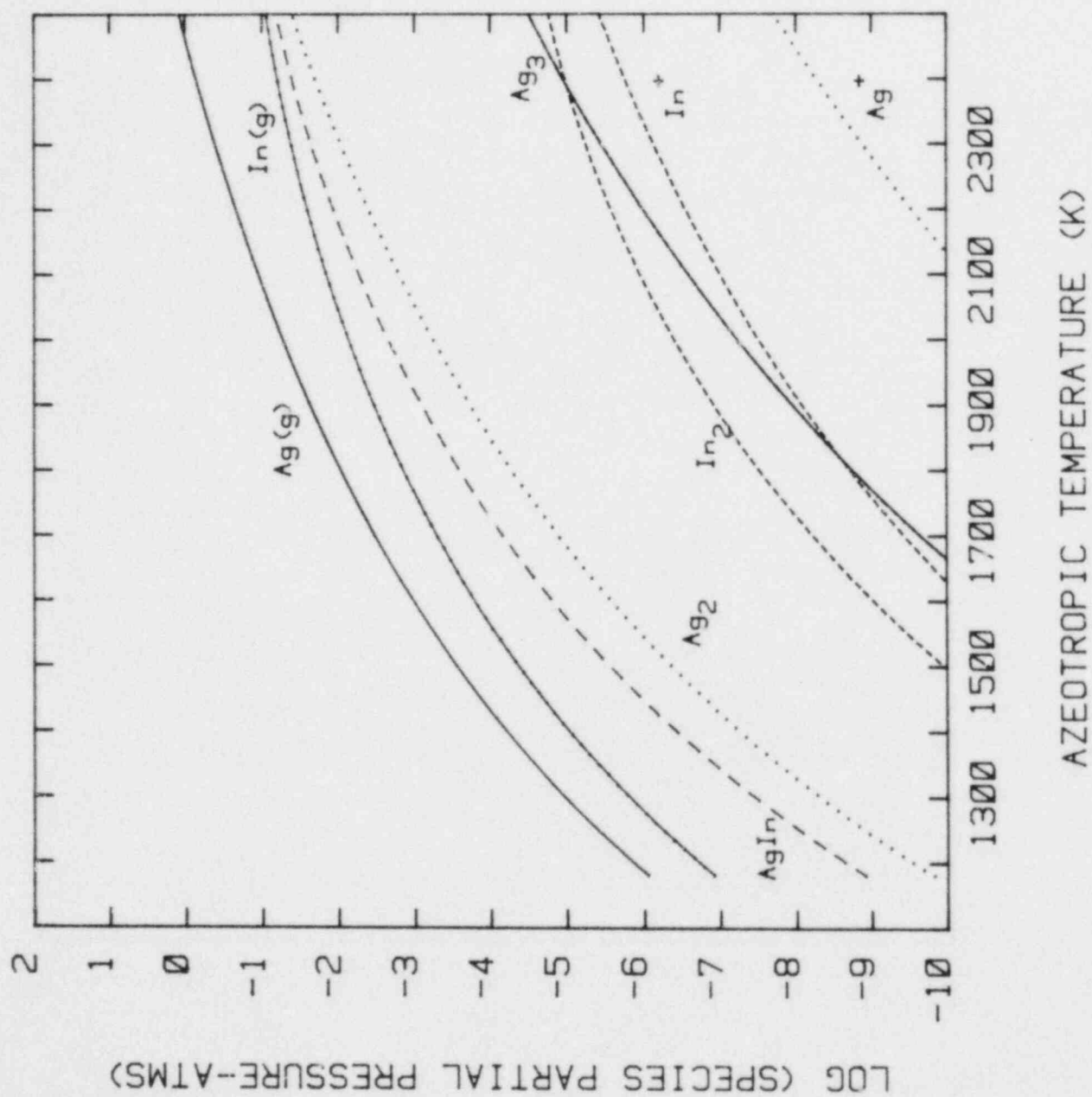


Figure 43. Speciation of the Vapor Along the Azeotropic Line

AgIn(g) to the vapor is shown in this figure to increase significantly as temperatures rise.

The vaporization of indium/silver alloys is influenced by the treatment of the condensed phase. Shown in Figure 44 is the composition of the vapor phase over a vaporizing alloy initially consisting of 84.21 mole percent Ag and 15.79 mole percent In. When the condensed phase is treated as ideal, silver-bearing and indium-bearing vapor species make nearly equivalent contributions to the vapor. Thus, as evaporation progresses, indium is preferentially removed. The relative amount of silver in the vapor then increases continuously as evaporation progresses. Near completion of the evaporation, the vapor phase is composed almost completely of silver-bearing species.

When nonideality of the condensed phase is recognized, the evaporation proceeds in a quite different fashion. The evolution in the vapor and the condensed phase compositions is toward the azeotropic composition which at 1500 K is about 13.9 mole percent In. The relative contributions of indium and silver to the vapor vary little then as the evaporation progresses.

B-2. Vapor Pressures Over Silver/Cadmium Alloys

The phase diagram of the silver/cadmium system at one atmosphere pressure is shown in Figure 45. The solid lines in this figure were calculated recognizing nonideality of the condensed phase. The dashed lines were calculated assuming the condensed phase was an ideal mixture.

The only remarkable feature of the phase diagram is the width of the vapor-liquid gap. Clearly, vaporization of silver/cadmium alloys at one atmosphere takes place by preferential removal of cadmium until the cadmium concentration has fallen to quite small levels (< mole percent Cd). Treatment of the condensed phase as ideal or nonideal affects the phase diagram little. The vapor boundary for ideal and nonideal treatments of the condensed phase coincide in the figure. The liquid boundary shows some small differences depending on the treatment of the condensed phase.

The vapor over most of the alloy composition range is made up of cadmium vapor species in proportions similar to those over pure cadmium.

B-3. Vapor Pressures Over Indium/Cadmium Alloys

The phase diagram of the indium/cadmium system at one atmosphere pressure is shown in Figure 46. The solid lines in this figure were calculated recognizing nonideality of the condensed phase. The dashed lines were calculated assuming the condensed phase was an ideal mixture.

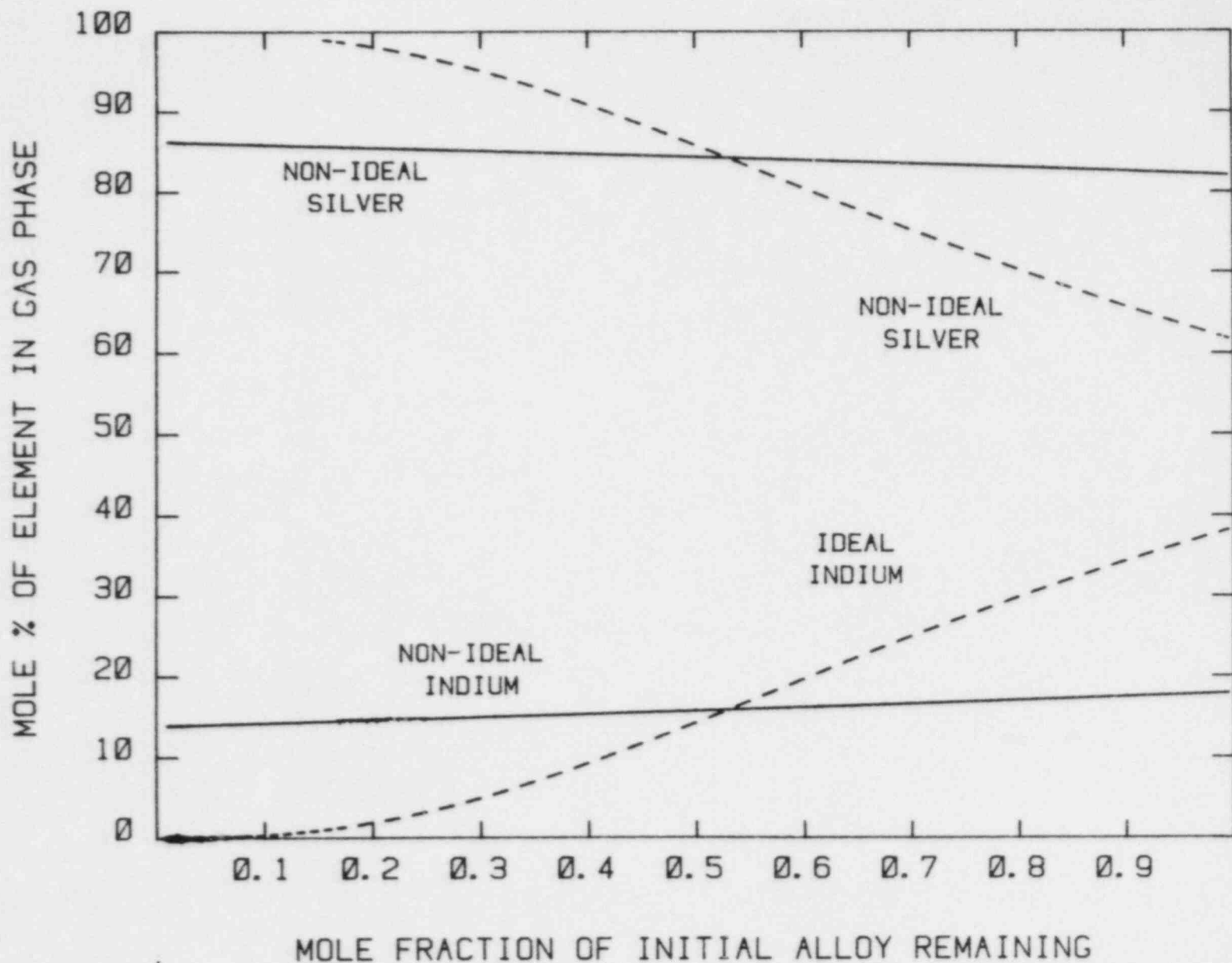


Figure 44. Variations in the Elemental Composition of the Vapor as an Alloy Initially Composed of 15.79 Percent Indium and 84.21 Percent Ag Vaporizes at 1500 K. Solid lines are for calculations recognizing nonideality of the condensed phase. Dashed lines are for calculations in which the condensed phase is treated as an ideal mixture.

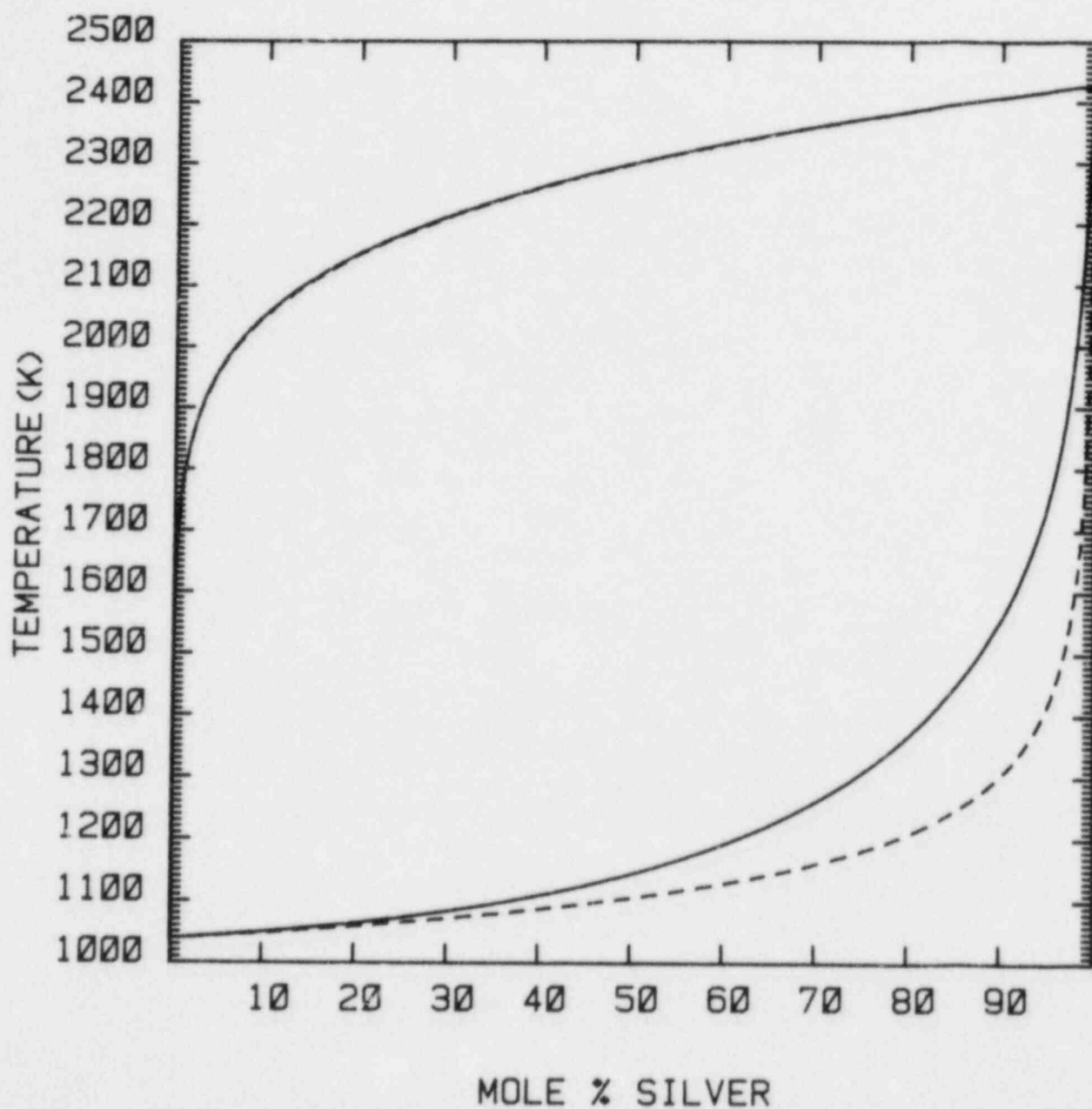


Figure 45. Condensed/Vapor Phase Equilibrium for Liquid Silver/Cadmium Alloys at One Atmosphere

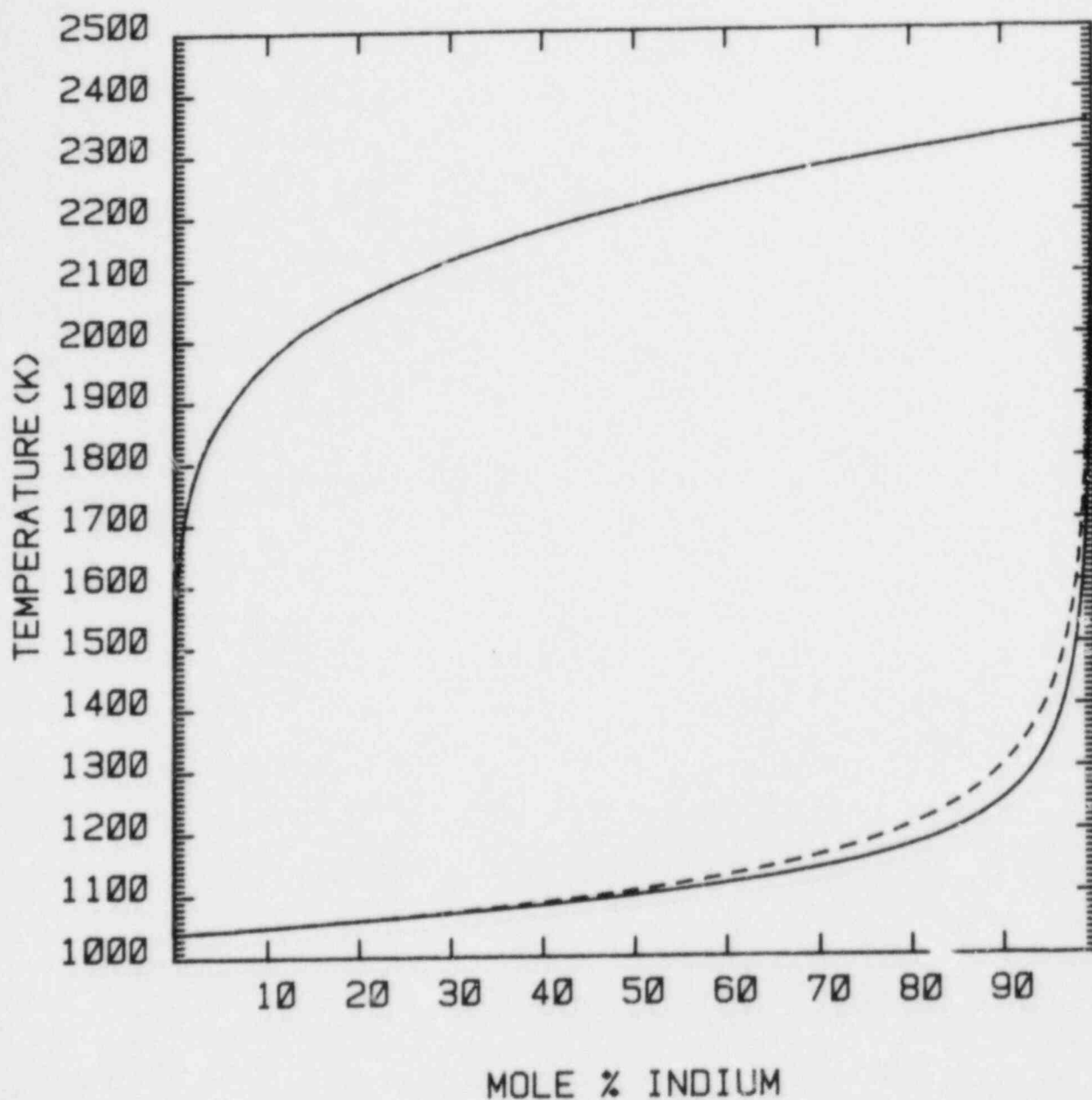


Figure 46. Condensed/Vapor Phase Equilibrium for Liquid Indium/Cadmium Alloys at One Atmosphere. The solid lines in the figure were calculated recognizing nonideality of the condensed phase. The dashed lines are the result of calculations in which the condensed phase was treated as an ideal mixture.

The phase diagram for the indium/cadmium system is similar to that of the silver/cadmium system. The treatment of the condensed phase as ideal or nonideal little affects the phase diagram. The vapor boundary shown in the figure is nearly the same for both treatments. The vapors for most of the composition range are composed primarily of cadmium species. The mixed-metal species, CdIn(g) , makes little contribution to the vapor.

C. Vapor Pressures Over Ternary Alloys

The vaporization of ternary Ag-In-Cd alloys is dominated by the vapor pressure of cadmium for all compositions except those very near the indium/silver binary. A plot of the phase boundaries at one atmosphere for liquid alloys composed of cadmium and an indium/silver mixture of the one atmosphere azeotropic composition (about 11 percent In and 89 percent Ag) is shown in Figure 47. This similarity of these phase boundaries and those for silver/cadmium (Figure 45) and indium/cadmium (Figure 46) should be noted. Cadmium species dominate the vapor until the cadmium content of the condensed phase falls to levels of less than 1 percent.

The azeotropic disturbance in the indium/silver system does not propagate far into the ternary system. A plot of isotherms for one atmosphere total pressure in the vicinity of the azeotrope is shown in Figure 48. As the cadmium content increases beyond about one part in ten thousand, the effects of the azeotropic interactions in the indium/silver system become almost undetectable and temperatures necessary to sustain one atmosphere total vapor pressure fall quite rapidly.

Isotherms at 100 K intervals for the ternary system at one atmosphere pressure are shown in Figures 49 and 50. The classic triangular coordinate systems for ternary systems are used in these figures. In Figure 49 the isotherms are plotted against the compositions of the condensed system. In Figure 50 the isotherms are plotted against the compositions of the vapor phase. The figures show that the temperatures necessary to maintain one atmosphere total vapor pressure rise sharply once cadmium has largely been depleted from the condensed phase. Also, the gas phase is predominantly cadmium until the cadmium content of the condensed phase has been reduced to levels less than 1 mole percent.

The discussion of ternary alloys below reemphasizes alloys having the initial composition of control rods--about 80 percent Ag, 15 percent In, and 5 percent Cd. The total vapor pressures over such an alloy are shown as a function of temperature in Figure 51. The solid lines in this figure were calculated recognizing the nonideality of the condensed

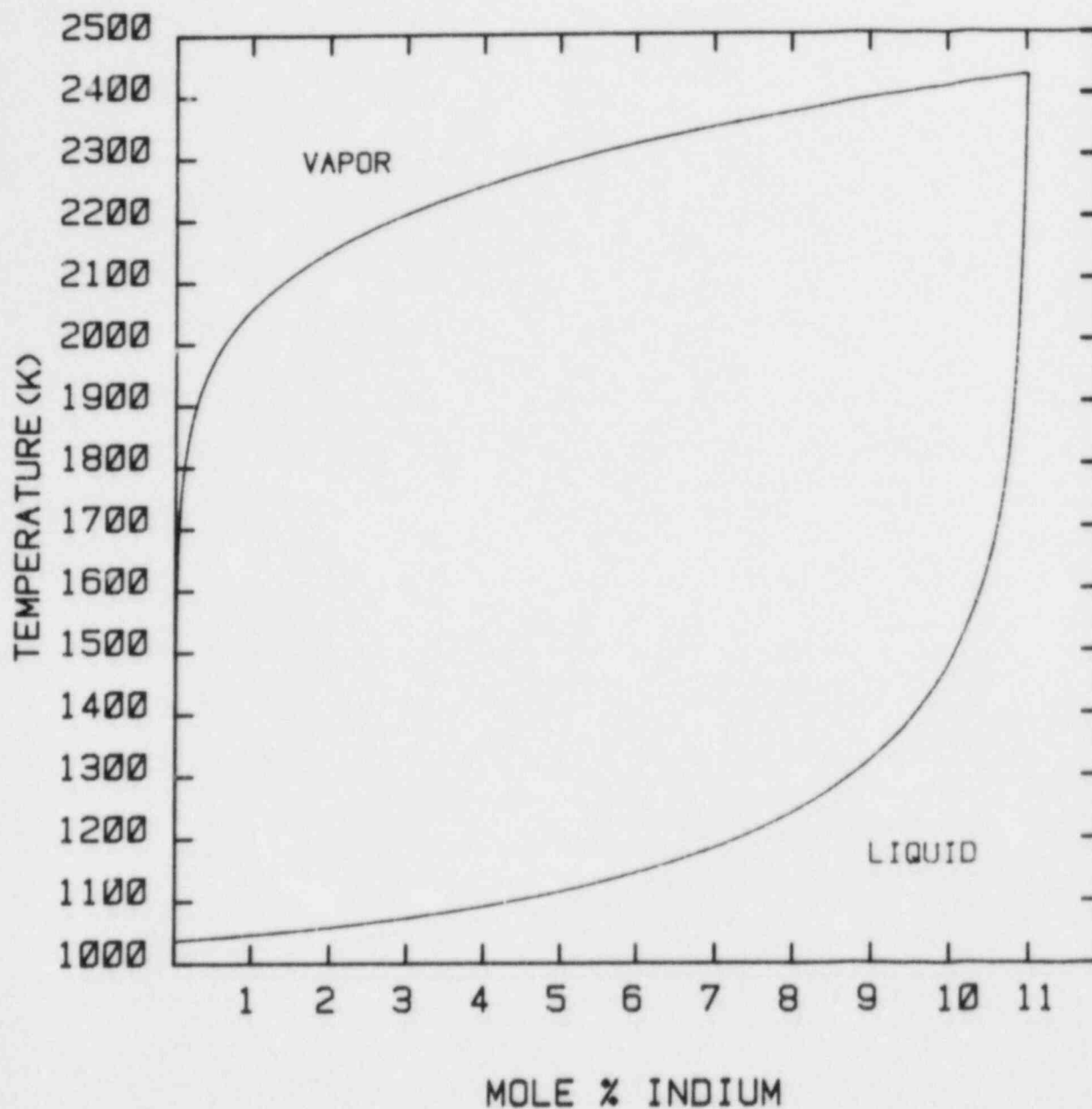


Figure 47. Condensed/Vapor Phase Boundaries at One Atmosphere for Alloys Composed of Cadmium and an Indium/Silver Alloy of the Azeotropic Composition. (The boundaries were calculated recognizing nonideality of the condensed phase.)

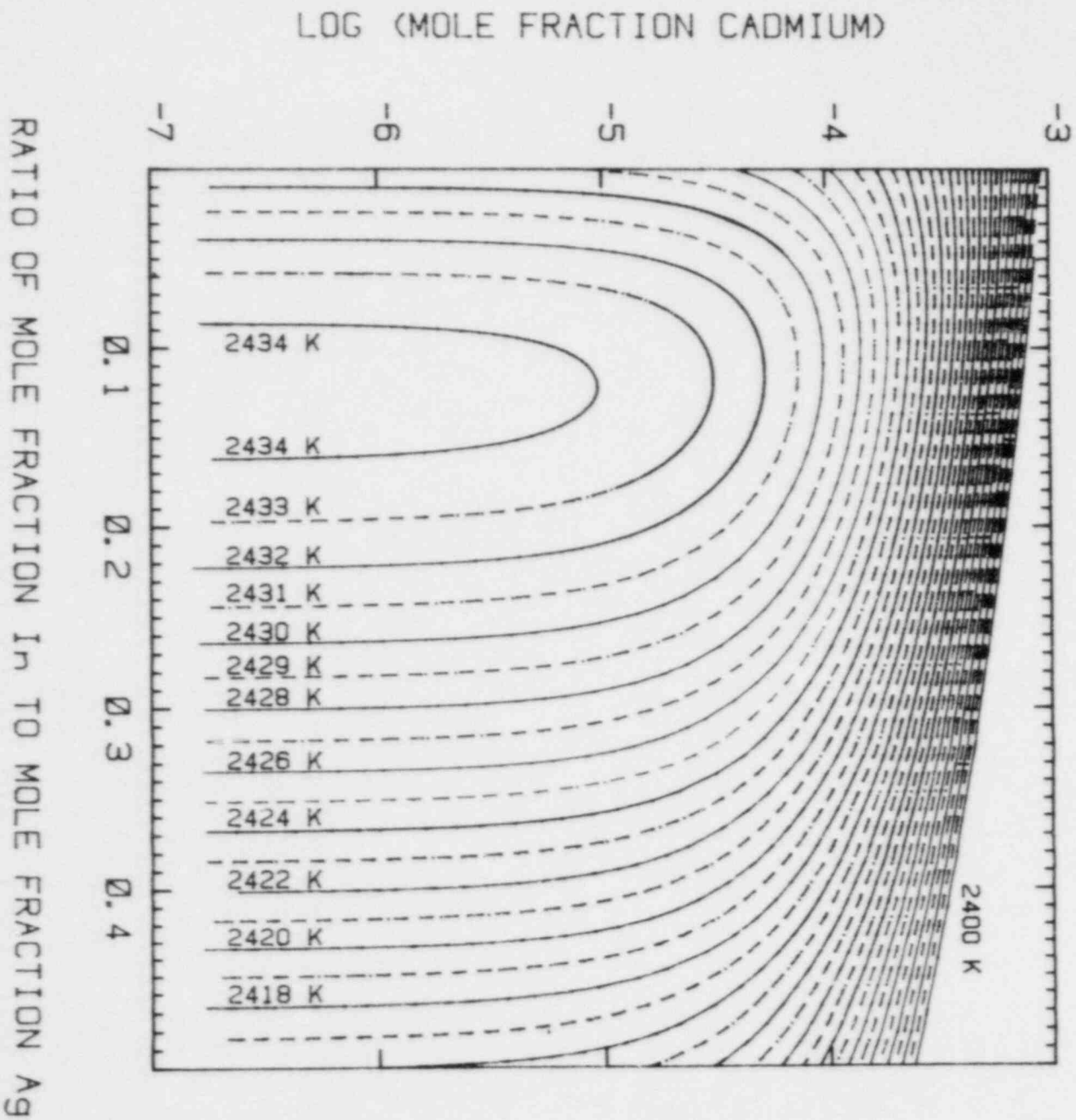


Figure 48. One Atmosphere Isotherms at 1 K Intervals Plotted Against Condensed Phase Compositions in the Vicinity of the Indium/Silver Azotrope

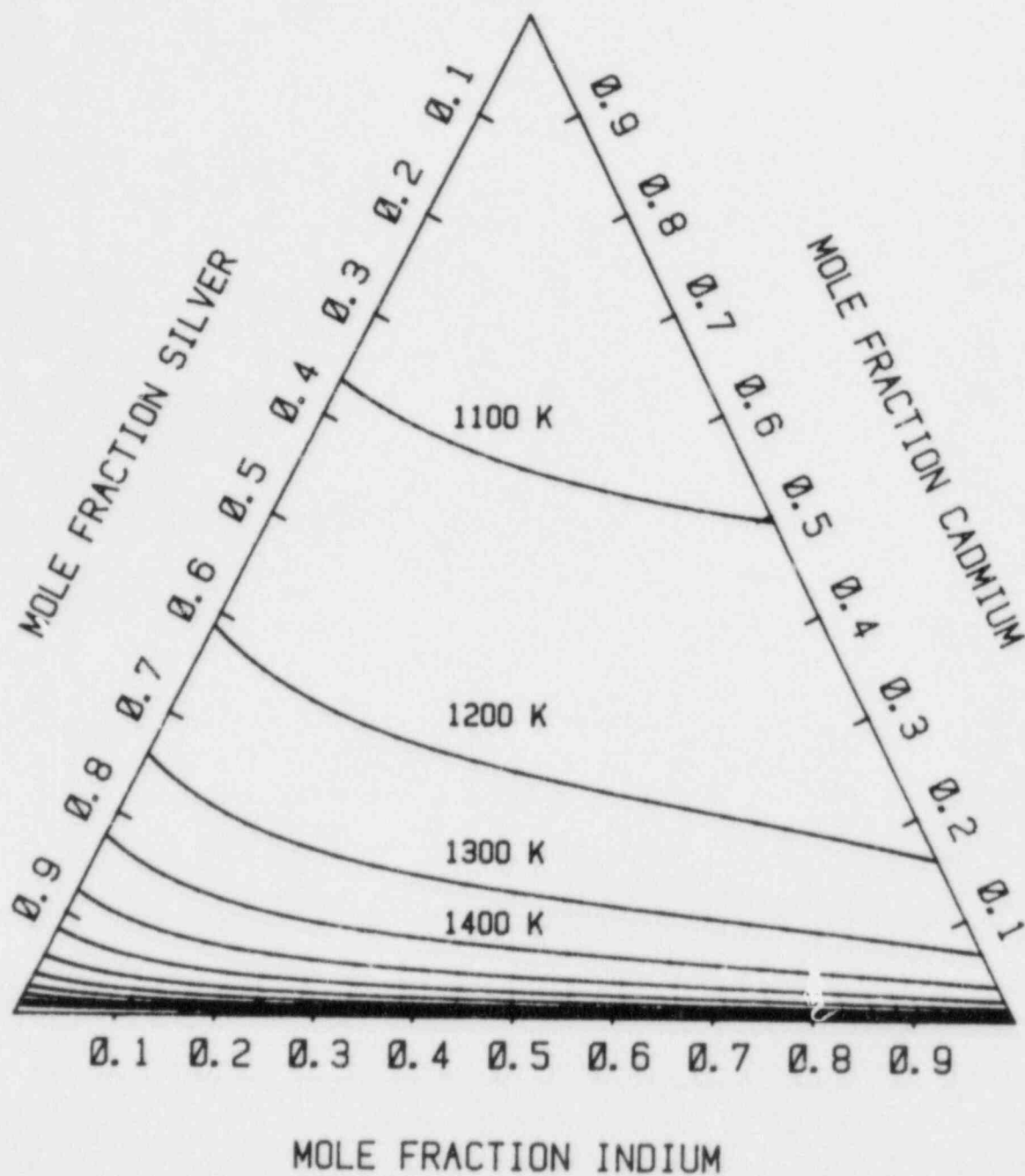


Figure 49. One Atmosphere Isotherms at 100 K Intervals Between 1100 K and 2200 K Plotted Against the Condensed Phase Composition for the Ag-In-Cd System

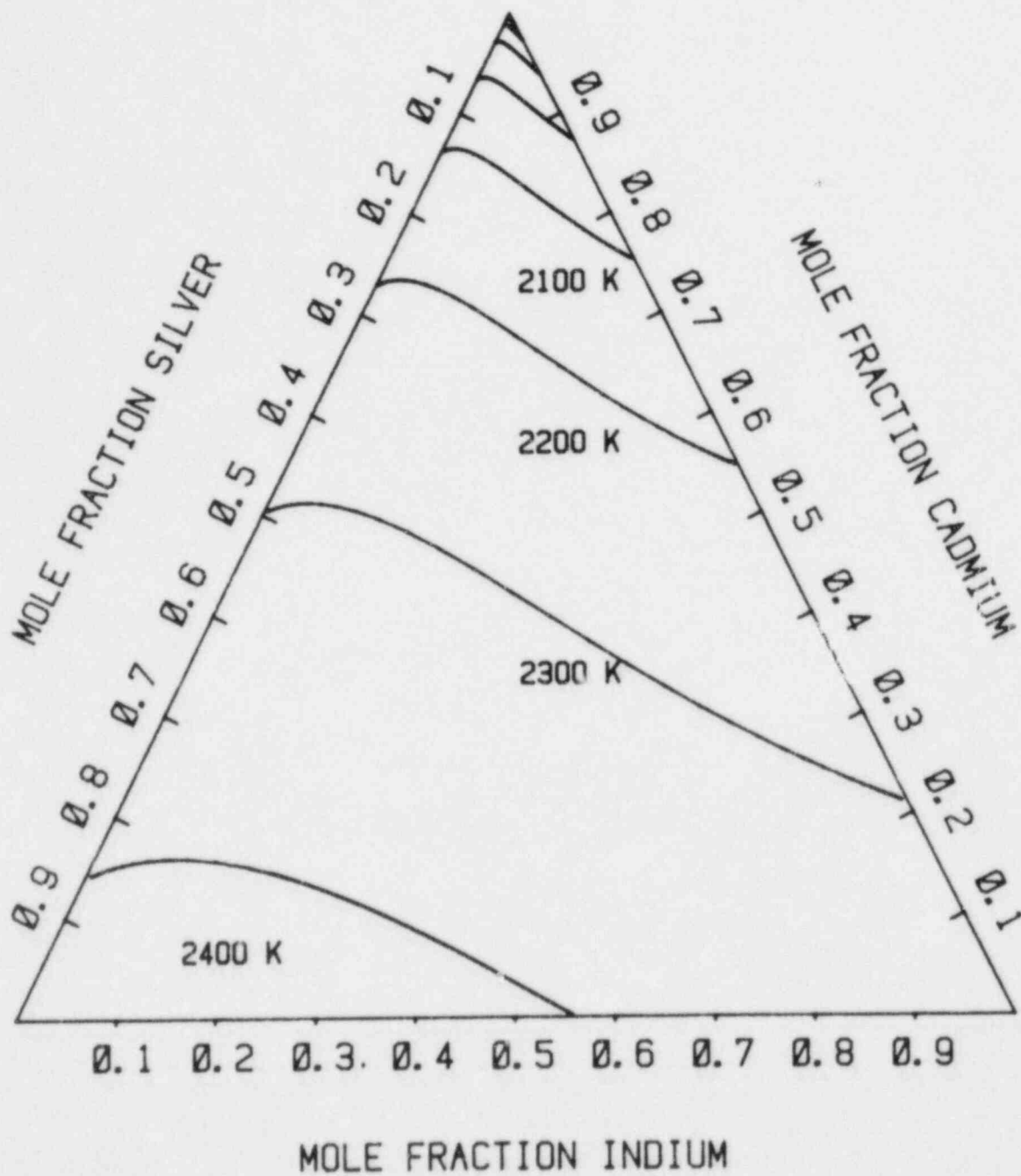


Figure 50. One Atmosphere Isotherms at 100 K Intervals Between 2400 K and 1700 K Plotted Against the Vapor Phase Composition for the Ag-In-Cd System

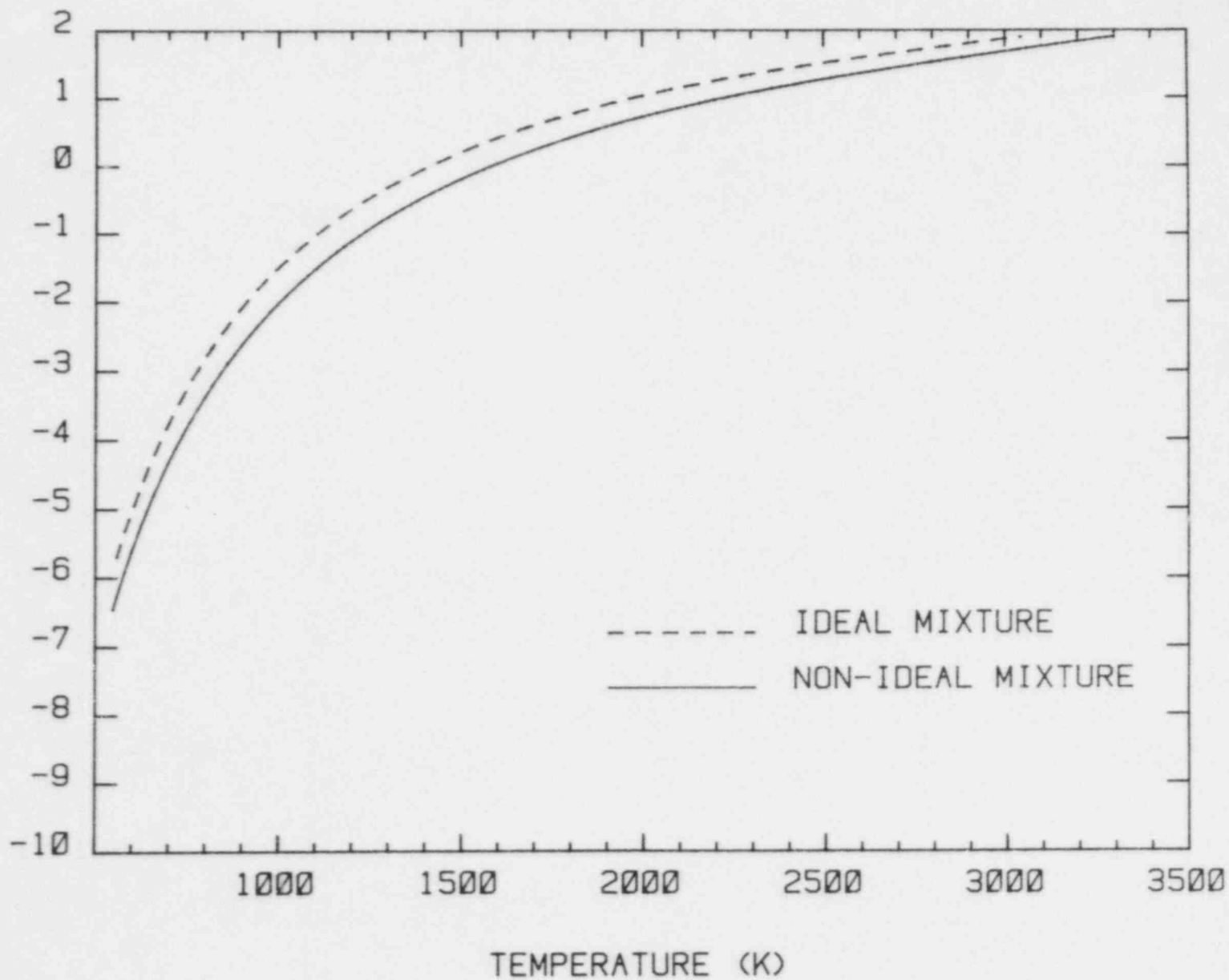


Figure 51. Total Pressure Over an Alloy of 80 Percent Ag, 15 Percent In, and 5 Percent Cd as a Function of Temperature. The solid lines were calculated recognizing nonideality of the condensed phase. The dashed lines were calculated assuming the condensed phase was an ideal mixture.

phase. Vapor pressures found by assuming the condensed phase was an ideal mixture are shown by the dashed line. Nonideality of the condensed phase depresses the calculated vapor pressure.

Speciation of the vapor over an 80 percent Ag, 15 percent In, 5 percent Cd alloy with the nonideal and the ideal condensed phase approximations are shown in Figures 52 and 53, respectively. The relative contributions of the various species are little affected by the assumptions concerning the condensed phase. The vapor for both cases is predominantly cadmium. Monatomic Ag(g) and In(g) are the next most abundant species in the vapor. The dimeric species Cd₂(g) becomes important at very high temperatures. The species CdIn(g) is a relatively unimportant vapor constituent.

The variations in the elemental composition of vapors as an alloy with initially 80 percent Ag, 15 percent In, and 5 percent Cd vaporizes at 1500 K are shown in Figures 54 and 55. The first of these figures was calculated by treating the alloy as an ideal mixture. The second figure shows results of calculations recognizing the nonideality of the condensed phase.

Qualitatively similar behavior is shown in both figures. Initially the vapor is predominantly cadmium. Over a very narrow range the contribution of the cadmium falls. The vapor is then a mixture of silver and indium. Recognizing nonideality of the condensed phase slightly spreads the range over which cadmium content of the vapor falls. Recognizing nonideality of the condensed phase greatly reduces the relative contribution of indium to the vapor after cadmium has been expelled from the alloy. When the condensed phase is treated as ideal, indium constitutes about 38 percent of the vapor over the cadmium-free residue. When nonideality is recognized indium makes up only 18 percent of the vapor.

It is also useful to consider vaporization under conditions in which adequate heat transfer is available to maintain the system at one atmosphere total vapor pressure. The variations of the condensed phase compositions and condensed phase temperature for evaporation of an alloy under these conditions are shown in Figures 56 and 57. Results shown in Figure 56 were calculated recognizing nonideality of the condensed phase. Results in Figure 57 were calculated assuming the condensed phase to be an ideal mixture. Shown in both figures is the alloy temperature necessary to sustain a total vapor pressure of one atmosphere.

Vaporization at constant pressure is qualitatively similar to vaporization at constant temperature. That is, cadmium is preferentially lost. The preference for cadmium

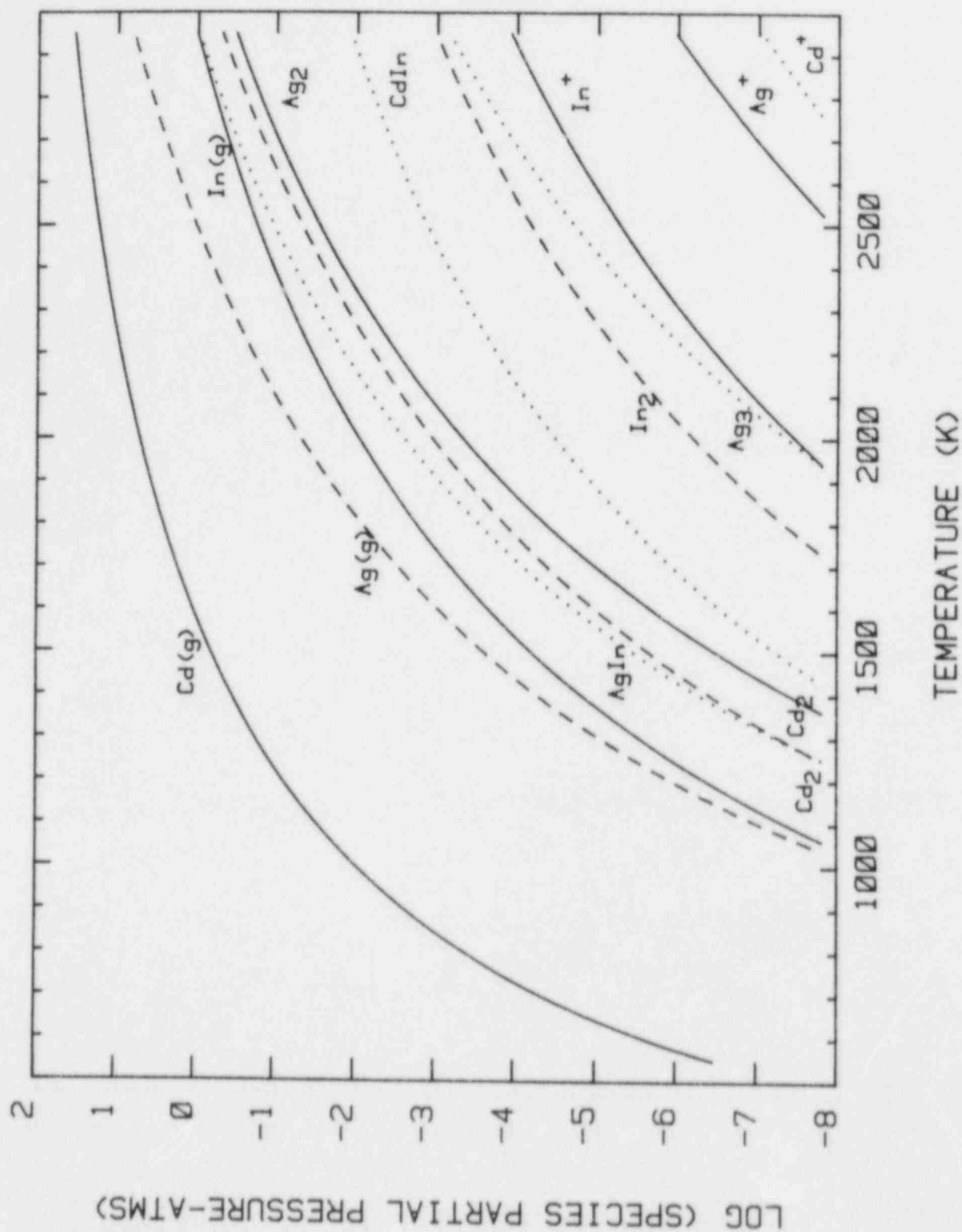


Figure 52. Speciation of the Vapor Over a Nonideal Liquid Alloy of 80 Percent Ag, 15 Percent In, and 5 Percent Cd as a Function of Temperature

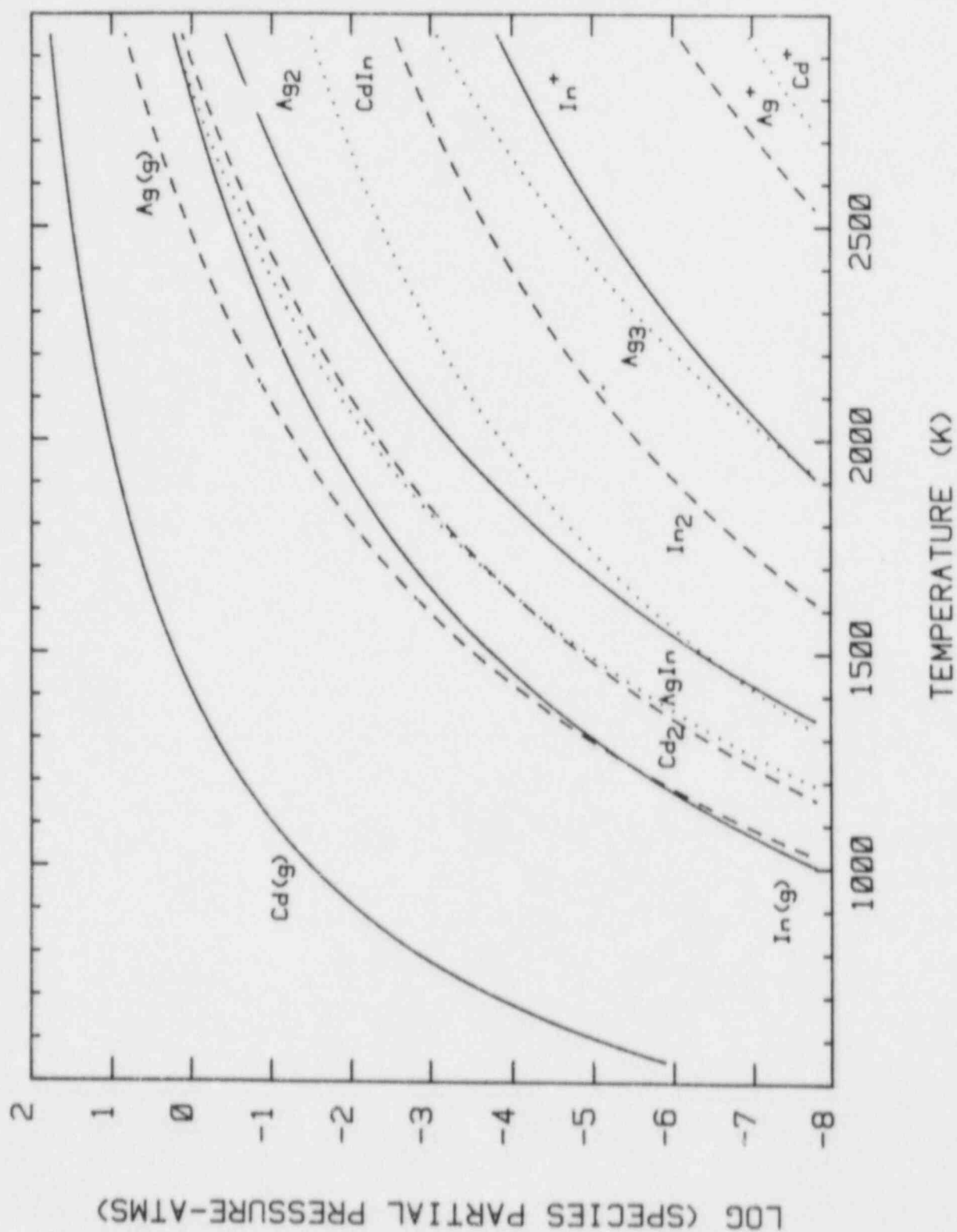


Figure 53. Speciation of the Vapor Over a Liquid Alloy of 80 Percent Ag, 15 Percent In, and 5 Percent Cd Which Is Considered to Be an Ideal Mixture as a Function of Temperature

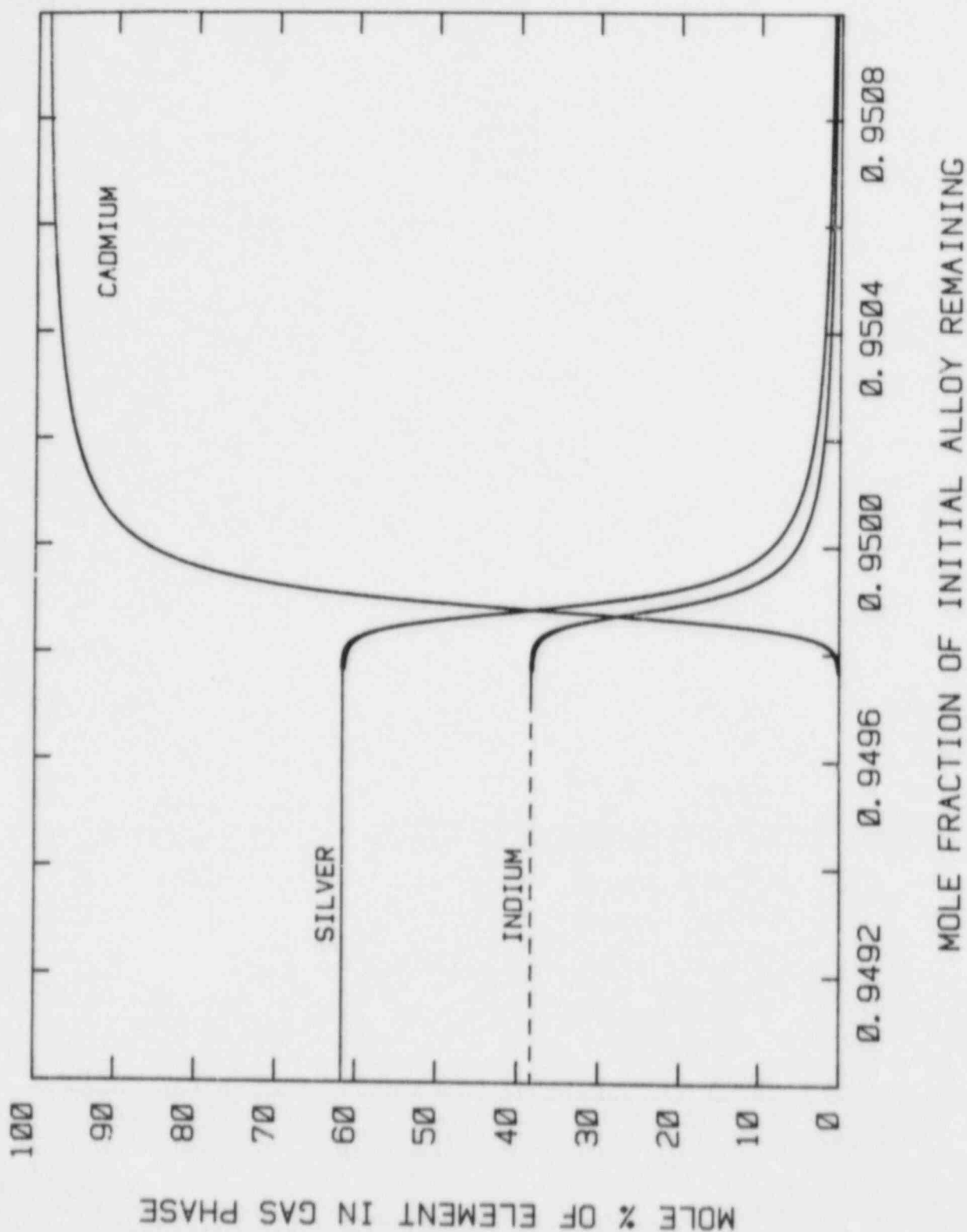


Figure 54. Variations in the Elemental Composition of the Vapor Phase as an Ideal Mixture Initially Composed of 80 Percent Ag, 15 Percent In, and 5 Percent Cd Vaporizes at 1500 K

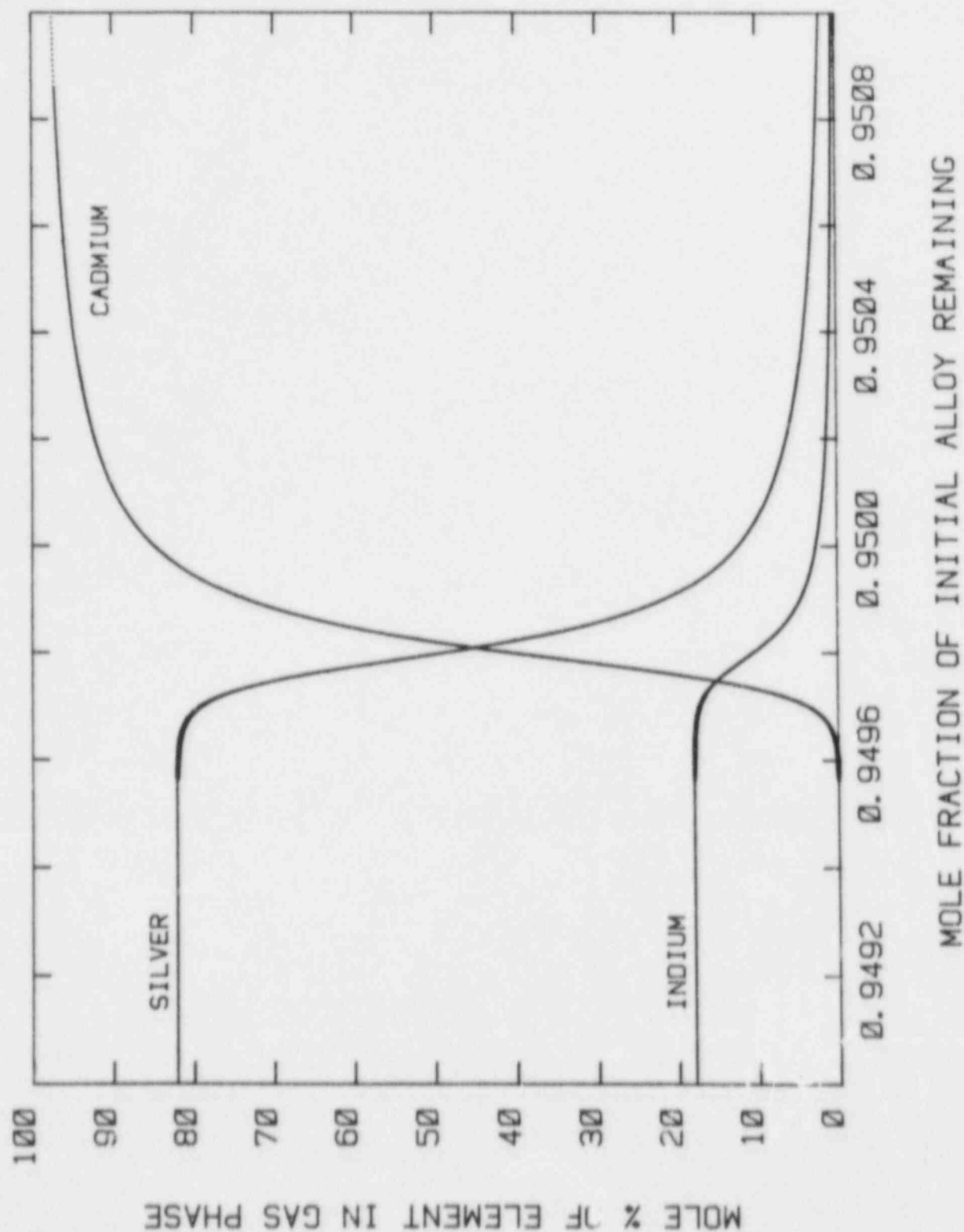


Figure 55. Variations in the Elemental Composition of the Vapor as a Nonideal Alloy With the Initial Composition 80 Percent Ag, 15 Percent In, and 5 Percent Cd Vaporizes at 1500 K

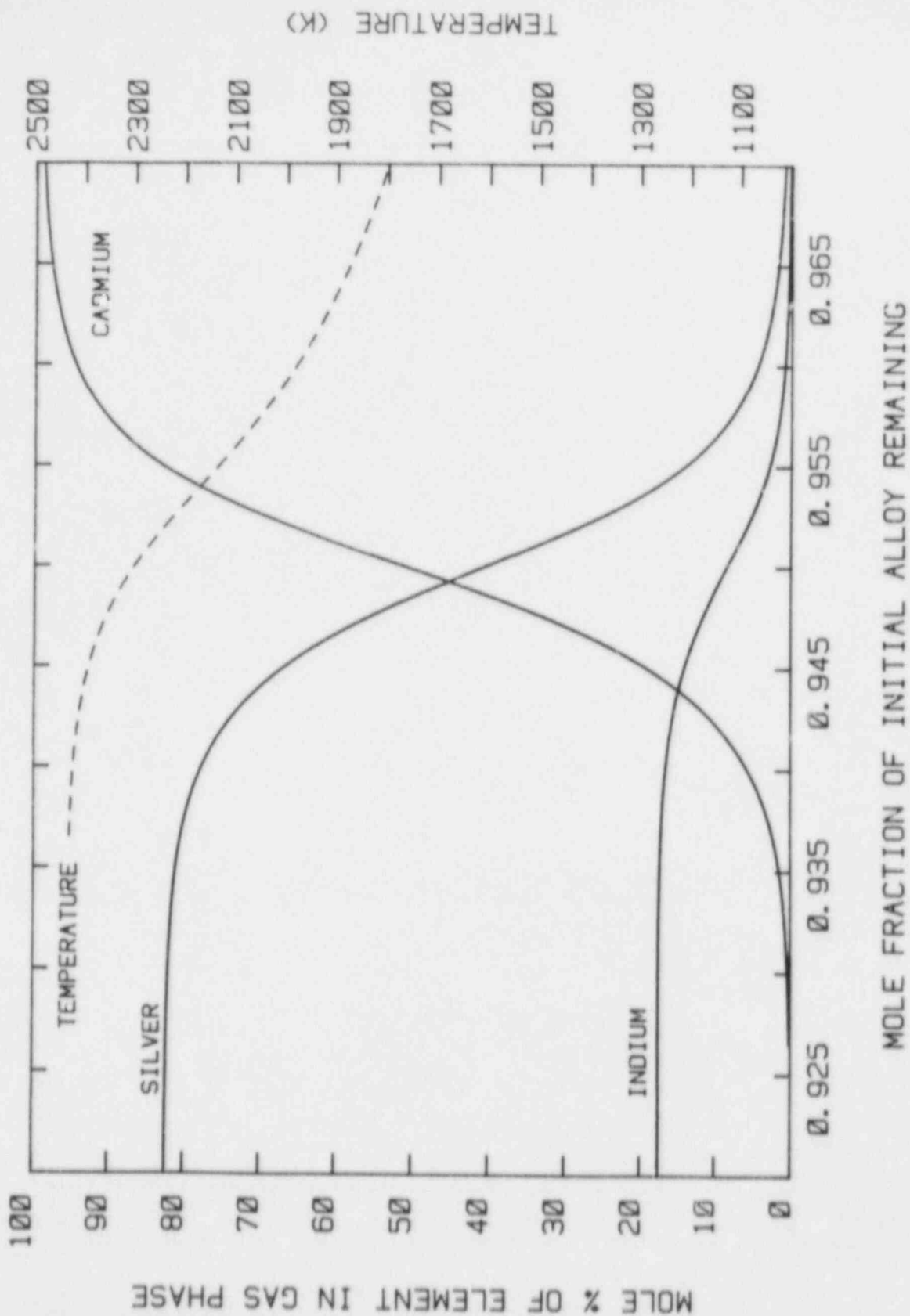


Figure 56. Variation in the Temperature and Vapor Phase Composition as a Nonideal Alloy Initially of 80 Percent Ag, 15 Percent In, and 5 Percent Cd Evaporates at a Constant Vapor Pressure of One Atmosphere

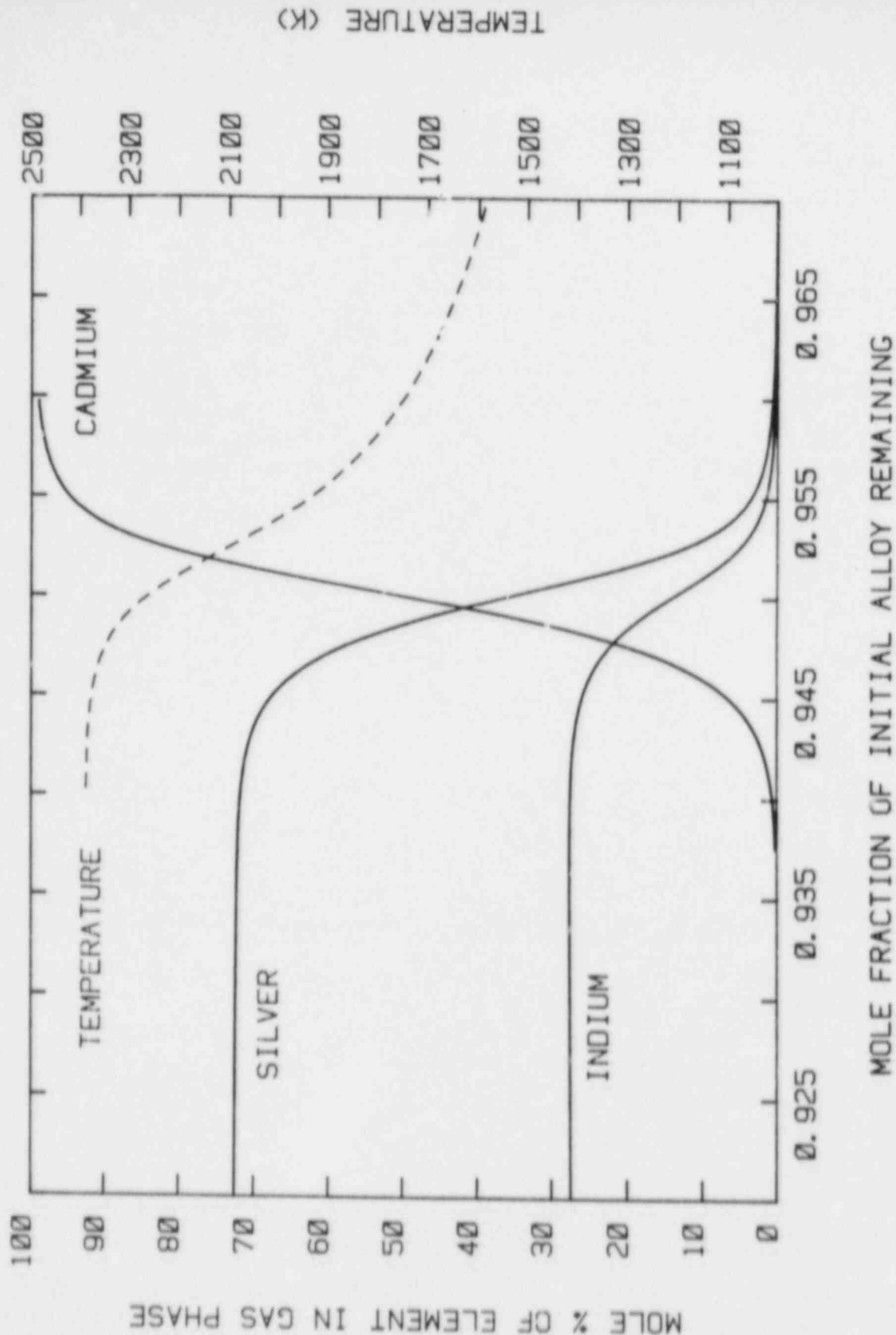


Figure 57. Variation in the Temperature and Vapor Phase Composition as an Alloy Initially of 80 Percent Ag, 15 Percent In, and 5 Percent Cd Treated as an Ideal Mixture Evaporates at a Constant Vapor Pressure of One Atmosphere

release is somewhat less when nonideality of the condensed phase is recognized. Also, the preference for cadmium vaporization is less under constant pressure evaporation than under conditions of constant temperature.

As cadmium is largely lost from the alloy, silver- and indium-bearing species begin to make increasing contributions to the vapor. The relative contributions of silver and indium to the vapor depend critically on the treatment of the condensed phase. When the condensed phase is assumed ideal, the vapor is predicted to be richer in indium than when nonideality of the condensed phase is included in the prediction. The differences in predictions with ideal and nonideal treatments of the condensed phase are not as pronounced in the case of constant pressure evaporation as they are in the case of constant temperature evaporation.

The most notable feature of Figures 56 and 57 is the sharp rise in temperature necessary to maintain a constant vapor pressure. This temperature rise is possible only if there is adequate heat transfer to the vaporizing alloy. Thermal analysis of the vaporization process would have to recognize the sharp variation in the enthalpy of vaporization as the alloy composition changes.

V. Application to Control Rod Behavior in a Reactor Accident

This analysis of the vaporization of silver-indium-cadmium alloys is concluded by considering the behavior of control rod materials in a reactor accident. Two distinct phases of the behavior can be identified. First is the internal pressurization of the control rod as the rod is heated during the thermal excursion of the core. As noted in the introduction, when the ambient pressure is about one atmosphere, internal pressurization of a heated control rod can cause the rod to violently rupture and expel the liquified control rod alloy. The second phase of behavior is the vaporization of control rod materials once the stainless steel sheath is perforated.

A. Internal Pressurization

Control rods are back-filled typically with helium gas. For the estimation of internal pressures, it is assumed here that helium pressure in the rod at room temperature is one atmosphere. Pressurization is calculated assuming that the vapor phase is an ideal gas. Also, changes in the vapor volume caused by thermal expansion of the rod sheath and the alloy have been neglected.

Pressures that develop within the control rod are shown as functions of temperature in Figure 58. Both the total pressure and the contribution of metal-bearing vapors to the

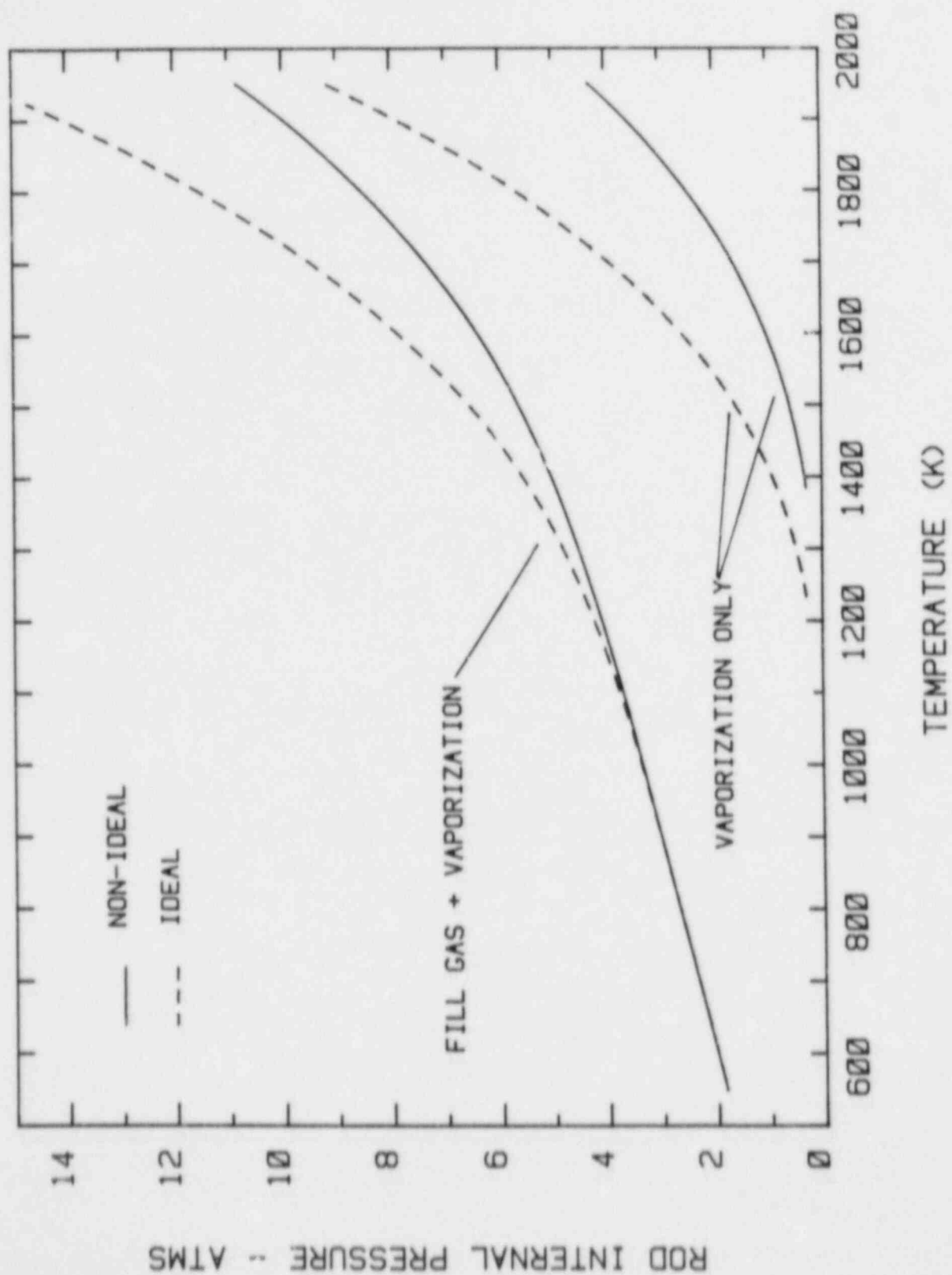


Figure 58. Internal Pressure of a Control Rod as a Function of Temperature. Fill gas was assumed present at a pressure of one atmosphere at room temperature.

total are shown in this figure. Solid lines were calculated recognizing nonideality of the condensed phase. The dashed lines denote results obtained when the condensed phase was considered to be an ideal mixture.

The internal pressure of the rods is shown in Figure 58 to be due predominantly to the fill gas. Significant contributions to the pressure from alloy vaporization occur only after temperatures in excess of about 1300 K are reached. The substantially lower vapor pressures predicted when nonideality of the condensed phase is considered are readily apparent in this figure.

Breaching of the control rod is clearly dependent on the ambient pressure and the pressurization of the fill gas. When the fill gas is initially present at a pressure of one atmosphere as it was considered in preparing Figure 58, ambient pressures in excess of 15 atmospheres will assure sheath breaching is by some mechanism such as sheath melting rather than internal pressurization. That is, the explosive eruption and expulsion of vapor and liquid observed in laboratory experiments are phenomena that occur only at low ambient pressures. In reactor accidents with elevated reactor coolant system pressures such violent control rod failure would not occur. In fact, the sheath may actually collapse onto the liquid alloy at elevated pressure. The vapor volume would be reduced until internal and external pressures were equalized. Again, upon breach of the sheath, no explosive eruption would be expected.

B. Vaporization of the Control Rod Alloy From a Breached Rod

Regardless of how the sheath is breached, the subsequent vaporization of the control rod alloy will depend on the ambient pressure. The ambient atmosphere of the control rod is a mixture of steam and hydrogen. These gases could react with the control rod material and affect its volatility. Such reactive vaporization is not considered here, but will be the subject of a future communication. The focus here is on the vaporization of the alloy in the absence of any significant chemical processes involving the ambient atmosphere.

At low ambient pressures it is possible for cadmium to nucleate bubbles and to "boil" vigorously. Inspection of the vapor pressures calculated in previous sections of this report shows that the alloy temperatures must be in excess of 1400 K at an ambient pressure of one atmosphere for "boiling" to take place. As the ambient pressure increases, so too does the temperature necessary for "boiling." At an ambient pressure of 10 atmospheres, temperatures in excess of the steel liquidus would be necessary. Thus, boiling

will occur only in a few types of reactor accidents. As shown by the variations in compositions and temperatures in Figures 56 and 57, the preferential removal of cadmium means temperatures necessary to sustain "boiling" will increase as alloy evaporates. The temperature rise necessary to sustain boiling is particularly sharp after about 5 percent of the alloy has vaporized.

If boiling is initiated, liquid alloy can be entrained and expelled into the reactor core atmosphere. This entrained material might be present as aerosol-sized particles which would be carried out of the core region by the prevailing flow of gas. Such aerosol produced by entrainment have been observed by Mitchell et. al.³ The entrained material may be macroscopic in size. In this case it would deposit or impact on clad fuel rods. Alloying between the clad and the liquid control rod material has been shown to produce a low melting temperature material. Whether or not this occurs will depend on the extent of oxidation of clad surface contacted by the control rod material.

As ambient pressures increase, vigorous "boiling" of the control rod material will not occur. Instead, more benign vaporization will be the cause of cadmium release. The relatively high vapor pressures of cadmium over liquid control rod alloys assures that there will be an adequate driving force for vaporization. The actual rate of vaporization will be controlled by other factors such as mass transport of the vapors away from the condensed phase surface.

Whether "boiling" occurs or not, cadmium will be quickly depleted from the alloy. The residual condensed phase composed of silver and indium is much less volatile than the original alloy. As the evaporation of this residual material progresses, its composition will evolve toward that of the azeotrope. Temperatures in excess of 2434 K would have to be achieved before the vapor pressure of the azeotrope reached one atmosphere. At such elevated temperatures the stainless steel sheath and perhaps much of the core would have melted. Consequently, there would be many opportunities for the residual alloy of silver and indium to flow into cooler regions of the reactor core.

The high enthalpy of vaporization of silver-indium alloys raises the possibility that the rate of vaporization will be controlled by the rate of heat transfer to the alloy. Since high temperatures are necessary to produce high vaporization rates for silver-indium alloys, heat transfer to the alloy by either radiation or convection would not be very efficient.

It seems probable, then, that during a reactor accident copious release of cadmium is entirely possible. The cadmium vapors could condense once they have escaped the reactor core region to form aerosols or deposits on structures. Any aerosols that are formed would have an effect on the transport of radionuclides through the reactor coolant system.

Extensive aerosol generation by silver and indium constituents of the control rod alloy is less likely. Entrainment of this material by "boiling" of cadmium or the sudden expulsion of gas at the time the control breaches are processes that can take place only when the ambient pressures are low. Evaporation of cadmium does not involve extensive simultaneous evaporation of silver and indium. Once cadmium is exhausted from the alloy, the residue has a much lower volatility. High vapor pressures develop over this residue only at temperatures so high extensive core melting has begun.

VI. Conclusions

Existing data on the thermodynamics of condensed and vapor phase silver, indium, and cadmium have been used to formulate a model of the vaporization of control rod alloys during reactor accidents. From this model, the following conclusions have been reached:

1. Liquid silver-indium-cadmium alloys are not ideal mixtures. The deviations from ideality are described here in terms of a ternary Wilson equation model developed from data for constituent binary systems.
2. Vaporization of cadmium from silver-indium-cadmium alloys is affected by the nonideality of the condensed phase. The effect is, however, not especially large. Vapor pressures of cadmium predicted assuming the condensed phase is ideal will be somewhat larger than vapor pressures calculated when nonideality of the condensed phase is recognized. Qualitative features of the vaporization of the alloy until cadmium is nearly exhausted are not greatly affected by the details of the treatment of the condensed phase.
3. Vaporization of silver-indium alloys is strongly affected by the nonideality of the condensed phase. Also, the vapor pressures are strongly affected by the presence of the mixed-metal vapor species AgIn(g) . An azeotrope is predicted to exist in the silver-indium system. The precise location of the azeotrope is uncertain because of uncertainties in

the activity coefficients of silver and indium in the condensed phase and the stability of AgIn in the gas phase.

4. Neglecting nonideality of the condensed Ag-In alloy will yield excessively high vapor pressures and vapor compositions much too enriched in indium.
5. Explosive rupture of heated control rods observed in laboratory experiments is a phenomenon confined to low ambient pressures. Vapor pressures of the alloy at temperatures less than the liquidus of stainless steel are insufficient to rupture the rods when the ambient pressure exceeds about 15 atmospheres. Fill gas pressures will be more important in determining whether or not a rod overpressurizes and ruptures during an accident.
6. Violent boiling of control rod alloys and entrainment of liquid alloys is also a phenomenon confined to low ambient pressures. At elevated pressures expected to exist in the core region during most reactor accidents, vaporization of the control rod alloy will be a more benign process. The rate of vaporization will be controlled by vapor transport processes. Substantial opportunities for liquid relocation exist.
7. Vapor pressures derived here suggest cadmium will be an important contributor to vapor evolving from a degrading PWR core. The cadmium vapors from a single control rod will make only a transient contribution since only slightly more than 5 percent of the control rod alloy need evaporate to exhaust the cadmium inventory in the condensed phase. If control rods throughout the core fail at different times there could be a more sustained presence of cadmium in a reactor coolant system even though vapors from a single control rod might be dissipated quickly.

References

1. Commonwealth Edison Co., Zion Nuclear Power Plant Final Safety Analysis Report.
2. G. W. Parker, G. E. Creek, and A. L. Sutton, Jr., "Influence of Variable Physical Process Assumptions on Core-Melt Aerosol Release," Proceedings of the International Meeting on Thermal Nuclear Reactor Safety, August 25-September 2, 1982, Chicago, IL, NUREG/CP-0027, Vol. 2, p. 1083.
3. J. P. Mitchell, A. L. Nichols, and J. A. H. Simpson, "The Characterization of Ag-In-Cd Control Rod Aerosols Generated at Temperatures Below 1900 K," CSNI Specialist Meeting on Nuclear Aerosols in Reactor Safety, Karlsruhe, West Germany, September 1984.
4. S. Hagan et al., Projekt Nukleare Sicherheit, KfK-2750, 4300-62, Kernforschungszentrum Karlsruhe, November 1978.
5. M. Hansen and K. Anderko, Constitution of Binary Alloys, 2nd edition, McGraw-Hill Book Co., 1958.
6. R. Hultgren, P. D. Desai, D. T. Hawkins, M. Gleiser, and K. K. Kelly, Selected Values of Thermodynamic Properties of Binary Alloys, American Society for Metals, 1973.
7. J. P. Hosemann, "Wechselwirkungen mit der Containment Struktur und Spalt Produktfreisetzung beim Kernschmelzunfall," Jahrestagung Kerntechnik 1982 der Kerntechnischen Gesellschaft, Mannheim, 2-4 May 1981.
8. Commonwealth Edison Co., Zion Probabilistic Safety Study, 1981.
9. G. M. Wilson, J. Am. Chem. Soc. 86 (1964) 127.
10. R. V. Orye and J. M. Prausnitz, Ind. Eng. Chem. 57 (1965) 18.
11. R. V. Orye, Trans. Faraday Soc. 61 (1965) 1338.
12. J. M. Prausnitz, C. A. Eckert, R. V. Orye, and J. P. O'Connell, Computer Calculations for Multicomponent Vapor-Liquid Equilibria, Prentice-Hall, Inc., 1965.
13. H. K. Hardy, Acta Met. 1 (1953) 202.
14. O. J. Kleppa, J. Phys. Chem. 64 (1960) 1542.

15. M. M. Marynyuk and I. Karmkhodzhaev, Russ. J. of Physical Chemistry 48 (1974) 722.
16. M. M. Marynyuk and O. G. Panteleichuk, Teplofizika Vysokikh Temperatur 14 (1976) 1201.
17. R. W. Ohse and H. V. Tippelskirch, High Temperature--High Pressure 9 (1977) 367.
18. S. Blairs, J. Inorg. Nucl. Chem. 39 (1977) 905.
19. S. Kuo and W. W. Liang, Ts'ai Liao K'o Hsueh 12 (1981) 7, CA:95:121930.
20. G. V. Pozharskaya and A. M. Evseev, Russ. J. Phys. Chem. 36 (1962) 553.
21. T. Heumann and B. Predel, Z. Metallkunde 50 (1959) 396.
22. B. Predel and H. Berka, Z. Metallkunde 67 (1976) 198.
23. H. J. Servis and Z. M. Munir, J. Less Common Metals 34 (1974) 293.
24. T. Nozaki, M. Shimoji, and K. Niwa, Transactions Japanese Institute of Metals 7 (1966) 52.
25. C. B. Alcock, R. Sridhar, and R. C. Svedberg, Acta Met. 17 (1969) 839.
26. B. Predel and U. Schallner, Z. Metallkunde 63 (1972) 341.
27. E. Przezdzlecka-Mycielska, J. Terpilowski, and K. Stozicka, Archiwumhutnictwa 8 (1963) 85.
28. C. E. Moore, Atomic Energy Levels Vol. III, Circular of the National Bureau of Standards 46 (1958).
29. R. Hultgren, P. D. Desai, D. T. Hawkins, M. Gleiser, K. K. Kelley, and D. D. Wagman, Selected Values of the Thermodynamic Properties of the Elements, American Society for Metals, 1973.
30. D. R. Stull and H. Prophet, JANAF Thermochemical Tables, 2nd edition, NSRDS-NBS37, National Bureau of Standards, 1971.
31. G. A. Ozin and H. Huber, Inorg. Chem. 17 (1978) 155.
32. R. Ginter et al., Faraday Symp. R. Soc. Chem. 14 (1980) 94.
33. J. Ruamps, Compt. Rend. 239 (1954) 1200.

34. B. Kleman, S. Lindkvist, and L. E. Selin, Arkiv Fysik 8 (1954) 505.
35. J. Drowart and R. E. Honig, J. Chem. Phys. 25 (1956) 581.
36. J. Drowart and R. E. Honig, J. Phys. Chem. 61 (1957) 980.
37. P. Schissel, J. Chem. Phys. 26 (1957) 1276.
38. M. Ackerman, F. E. Stafford, and J. Drowart, J. Chem. Phys. 33 (1960) 1784.
39. B. Kleman and S. Lindkvist, Arkiv Fysik 9 (1955) 385.
40. G. Ozin et al., J. Amer. Chem. Soc. 101 (1979) 3504.
41. K. A. Gingerich, J. Cryst. Growth 9 (1971) 31.
42. C. M. Brown and M. L. Ginter, J. Mol. Spectroscopy 69 (1978) 25.
43. J. C. Boeyens and R. H. Lemmer, J. Chem. Soc. Faraday Trans. 2 (1977) 321.
44. W. E. Klotzhuecher and G. A. Ozin, Inorg. Chem. 15 (1980) 3776.
45. A. B. Sannigrahi and B. R. Dee, Int'l J. of Quantum Chemistry 17 (1980) 1237.
46. S. A. Mitchell et al., J. Am. Chem. Soc. 103 (1981) 6030.
47. R. C. Baetzold, J. Chem. Phys. 55 (1971) 4355.
48. H. Basch, Faraday Symp. R. Soc. Chem. 14 (1980) 149.
49. J. Drowart, "Gaseous Intermetallic Molecules," in Phase Stability in Metals and Alloys, P. S. Rudman, J. Strings, R. I. Jaffee, editors, McGraw-Hill, 1966.
50. K. P. Huber and G. Herzberg, Molecular Spectra and Structure IV Constants of Diatomic Molecules, Van Nostrand, 1979.
51. S. N. Suchard and J. E. Melzer, Spectroscopic Constants for Selected Homonuclear Diatomic Molecules, Aerospace Corp., 1976.
52. K. Hilpert and K. A. Gingerich, Ber. Bunsenges Phys. Chem. 84 (1980) 739.

53. D. M. Gruen and K. J. Bates, Inorg. Chem. **16** (1977) 2450.
54. R. B. Merrithew, G. V. Marusak, and C. E. Blount, J. Molecular Spectroscopy **29** (1969) 54.
55. W. Schulze et al., Chem. Phys. Letters **55** (1978) 59.
56. R. C. Baetzold, J. Chem. Phys. **55** (1971) 4363.
57. B. S. Ault and L. Andrews, J. Molecular Spectroscopy **65** (1977) 102.
58. A. Given and A. Lowenschuss, Chem. Phys. Letters **62** (1979) 592.
59. W. W. Duley, Proc. Phys. Soc. **92** (1967) 976.
60. H. S. Freedhoff, Proc. Phys. Soc. **92** (1967) 505.
61. H. J. Vreede, R. F. C. Claridge, and L. F. Phillips, Chem. Phys. Letters **27** (1974) 1.
62. C. F. Bender, T. N. Rescigno, H. F. Schaefer III, and A. E. Orgel, J. Chem. Phys. **71** (1979) 1122.
63. W. J. Stevens, Appl. Phys. Letters **35** (1979) 751.
64. A. G. Gaydon, Dissociation Energies, Chapman and Hall Ltd., 1963.
65. G. DeMaria, J. Drowart, and M. G. Ingham, J. Chem. Phys. **31** (1959) 1076.
66. R. K. Waring, Phys. Rev. **32** (1928) 435.
67. S. Barrett and A. R. Bonar, Phil. Mag. **9** (1930) 519.
68. C. Santaram and J. G. Winans, J. Molecular Spectroscopy **16** (1965) 309.
69. M. Biron, Compte. Rend. Ser. A, B, **265b** (1967) 1026.
70. A. W. Searcy, R. D. Freeman, and M. Michel, J. Amer. Chem. Soc. **76** (1954) 4050.
71. H. Daidoji, Nippon Kagaku Kaishi (1980) 1718-22, CA:94: 22371g.
72. R. L. Purbrick, Phys. Rev. **81** (1951) 89.
73. P. H. Kasal and D. McLeod, Jr., J. Phys. Chem. **79** (1975) 2324.

74. R. Ginter et al., Faraday Symp. Royal Society of Chemistry 14 (1980) 94.
75. A. G. Maki and R. Forneris, Spectrochim. Acta 23A (1967) 867.
76. G. C. Haywood and P. J. Hendra, Spectrochim. Acta 23A (1967) 2309.

Appendix A

Activity Coefficient Data for Liquid Binary Alloys

Activity coefficients of cadmium in liquid cadmium/silver alloys are shown in Table A-1. Activity coefficients of cadmium in liquid cadmium/indium alloys are shown in Table A-2. Activity coefficients of indium in liquid indium/silver alloys are shown in Table A-3.

Table A-1
Activity Coefficient of Cadmium in Liquid
Cadmium/Silver Alloys

Temperature (K)	Mole Fraction Cadmium	Cadmium Activity Coefficient	Reference
1223	0.032	0.096	1
1223	0.1	0.155	1
1223	0.2	0.274	1
1223	0.3	0.427	1
1223	0.4	0.592	1
1223	0.5	0.747	1
1223	0.6	0.868	1
1223	0.7	0.947	1
1223	0.8	0.987	1
1223	0.9	0.9999	1
1100	0.298	0.416	2
1100	0.400	0.540	2
1100	0.500	0.660	2
1100	0.600	0.777	2
1100	0.700	0.880	2
1100	0.800	0.954	2
1100	0.900	0.991	2
775	0.9917	0.9987	3
775	0.9911	0.9987	3
775	0.98851	0.9982	3
775	0.98049	0.9971	3
973	0.823	0.9842	4
973	0.763	0.9830	4
973	0.677	0.8715	4
973	0.604	0.7616	4
973	0.545	0.7156	4
973	0.475	0.6526	4
973	0.407	0.5651	4
973	0.266	0.3008	4
1123	0.823	1.0085	4
1123	0.763	0.9961	4
1123	0.677	0.8715	4
1123	0.604	0.7616	4
1123	0.545	0.7156	4
1123	0.475	0.6105	4
1123	0.407	0.5405	4
1123	0.266	0.3383	4

Table A-2

Activity Coefficient of Cadmium in Liquid
Cadmium/Indium Alloys

Temperature (K)	Mole Fraction Cadmium	Cadmium Activity Coefficient	Reference
543	0.1	1.150	5
543	0.2	0.885	5
543	0.3	0.680	5
543	0.4	0.553	5
543	0.5	0.478	5
543	0.6	0.458	5
543	0.7	0.474	5
543	0.8	0.531	5
543	0.9	0.778	5
563	0.1	0.980	5
563	0.2	0.815	5
563	0.3	0.700	5
563	0.4	0.605	5
563	0.5	0.526	5
563	0.6	0.505	5
563	0.7	0.499	5
563	0.8	0.536	5
563	0.9	0.776	5
583	0.1	0.880	5
583	0.2	0.805	5
583	0.3	0.723	5
583	0.4	0.668	5
583	0.5	0.606	5
583	0.6	0.550	5
583	0.7	0.523	5
583	0.8	0.544	5
583	0.9	0.781	5
699	0.890	1.029	6
699	0.797	1.048	6
699	0.703	1.081	6
699	0.622	1.178	6
699	0.600	1.182	6
699	0.596	1.158	6
699	0.522	1.228	6
699	0.497	1.213	6
699	0.401	1.292	6
699	0.295	1.451	6
699	0.254	1.480	6
699	0.252	1.508	6
699	0.250	1.544	6
699	0.198	1.586	6
699	0.096	1.823	6

Table A-2 (continued)

Activity Coefficient of Cadmium in Liquid
Cadmium/Indium Alloys

Temperature (K)	Mole Fraction Cadmium	Cadmium Activity Coefficient	Reference
742	0.892	1.026	6
742	0.789	1.054	6
742	0.694	1.088	6
742	0.618	1.165	6
742	0.594	1.170	6
742	0.590	1.152	6
742	0.544	1.154	6
742	0.537	1.186	6
742	0.492	1.201	6
742	0.397	1.280	6
742	0.298	1.379	6
742	0.250	1.452	6
742	0.198	1.505	6
742	0.097	1.691	6
801	0.894	1.021	6
801	0.777	1.066	6
801	0.673	1.116	6
801	0.625	1.142	6
801	0.604	1.156	6
801	0.603	1.144	6
801	0.575	1.164	6
801	0.512	1.197	6
801	0.485	1.188	6
801	0.391	1.253	6
801	0.294	1.347	6
801	0.250	1.384	6
801	0.197	1.442	6
801	0.097	1.588	6
853	0.900	1.011	6
853	0.767	1.069	6
853	0.663	1.112	6
853	0.644	1.110	6
853	0.632	1.120	6
853	0.580	1.155	6
853	0.566	1.157	6
853	0.525	1.135	6
853	0.518	1.172	6
853	0.480	1.173	6
853	0.388	1.232	6
853	0.297	1.280	6
853	0.259	1.251	6
853	0.253	1.300	6

Table A-2 (continued)

Activity Coefficient of Cadmium in Liquid
Cadmium/Indium Alloys

Temperature (K)	Mole Fraction Cadmium	Cadmium Activity Coefficient	Reference
853	0.195	1.395	6
853	0.096	1.521	6
773	0.95	1.003	7
773	0.90	1.009	7
773	0.85	1.018	7
773	0.80	1.030	7
773	0.75	1.051	7
773	0.70	1.073	7
773	0.65	1.095	7
773	0.60	1.120	7
773	0.50	1.186	7
773	0.40	1.279	7
773	0.35	1.339	7
773	0.30	1.413	7
773	0.25	1.506	7
773	0.20	1.620	7
773	0.15	1.773	7
773	0.10	1.940	7
773	0.05	2.200	7
823	0.95	1.003	7
823	0.90	1.007	7
823	0.85	1.016	7
823	0.80	1.035	7
823	0.75	1.051	7
823	0.70	1.067	7
823	0.65	1.092	7
823	0.60	1.120	7
823	0.50	1.186	7
823	0.40	1.278	7
823	0.35	1.326	7
823	0.30	1.387	7
823	0.25	1.472	7
823	0.20	1.580	7
823	0.15	1.733	7
823	0.10	1.880	7
823	0.05	2.12	7

Table A-2 (continued)
Activity Coefficient of Cadmium in Liquid
Cadmium/Indium Alloys

Temperature (K)	Mole Fraction Cadmium	Cadmium Activity Coefficient	Reference
868	0.95	1.002	7
868	0.90	1.007	7
868	0.85	1.014	7
868	0.80	1.030	7
868	0.75	1.045	7
868	0.70	1.067	7
868	0.65	1.089	7
868	0.60	1.113	7
868	0.50	1.172	7
868	0.40	1.253	7
868	0.35	1.298	7
868	0.30	1.360	7
868	0.25	1.437	7
868	0.20	1.530	7
868	0.15	1.667	7
868	0.10	1.868	7
868	0.05	2.120	7
923	0.95	1.001	7
923	0.90	1.006	7
923	0.85	1.014	7
923	0.80	1.028	7
923	0.75	1.053	7
923	0.70	1.066	7
923	0.65	1.081	7
923	0.60	1.108	7
923	0.50	1.160	7
923	0.40	1.230	7
923	0.35	1.274	7
923	0.30	1.333	7
923	0.25	1.408	7
923	0.20	1.492	7
923	0.15	1.600	7
923	0.10	1.736	7
923	0.05	1.952	7
625	0.099	1.601	8
625	0.200	1.494	8
625	0.299	1.349	8
625	0.409	1.259	8
625	0.498	1.239	8
625	0.598	1.164	8
625	0.692	1.082	8
625	0.794	1.045	8
625	0.892	1.010	8

Table A-3

Activity Coefficient of Indium in Liquid
Indium/Silver Alloys

Temperature (K)	Mole Fraction Indium	Indium Activity Coefficient	Reference
1100	0.218	0.624	9
1100	0.265	0.676	9
1100	0.310	0.894	9
1100	0.343	0.846	9
1100	0.430	0.935	9
1100	0.456	1.035	9
1100	0.523	1.048	9
1100	0.555	1.067	9
1100	0.645	1.048	9
1100	0.685	1.048	9
1100	0.717	1.049	9
1100	0.761	1.063	9
1100	0.823	1.034	9
1000	0.95	1.001	10
1000	0.90	0.992	10
1000	0.80	0.961	10
1000	0.70	0.935	10
1000	0.60	0.911	10
1000	0.50	0.874	10
1000	0.45	0.797	10
1000	0.40	0.725	10
1000	0.35	0.488	10
1000	0.30	0.333	10
1000	0.3	0.189	11
1000	0.4	0.286	11
1000	0.5	0.608	11
1000	0.6	0.847	11
1000	0.7	0.886	11
1000	0.8	0.970	11
1000	0.9	0.980	11
1300	0.1	0.150	12
1300	0.2	0.285	12
1300	0.3	0.477	12
1300	0.4	0.682	12
1300	0.5	0.838	12
1300	0.6	0.932	12
1300	0.7	0.976	12
1300	0.8	0.984	12
1300	0.9	1.000	12

Table A-3 (continued)

Activity Coefficient of Indium in Liquid
Indium/Silver Alloys

Temperature (K)	Mole Fraction Indium	Indium Activity Coefficient	Reference
1466	0.94	0.995	13
1466	0.79	0.956	13
1466	0.70	0.929	13
1466	0.65	0.911	13
1466	0.56	0.783	13
1466	0.44	0.628	13
1466	0.37	0.338	13
1466	0.22	0.184	13
1466	0.08	0.141	13

References

1. R. Hultgren, P. D. Desai, D. T. Hawkins, M. Gleiser, and K. K. Kelley, Selected Values of Thermodynamic Properties of Binary Alloys, American Society for Metals, 1973.
2. R. Hultgren, R. L. Orr, P. D. Anderson, and K. K. Kelley, Selected Values of Thermodynamic Properties of Metals and Alloys, J. Wiley and Sons.
3. D. R. Conant and H. S. Swofford, Jr., J. Chem. Eng. Data **14** (1969) 369.
4. A. Schneider and H. Schmid, Z. für Elektrochem. **48** (1942) 627.
5. G. V. Pozharskaya and A. M. Evseev, Russ. J. Phys. Chem. **36** (1962) 553.
6. T. Heumann and B. Predel, Z. Metallkunde **50** (1959) 396.
7. B. Predel and H. Berka, Z. Metallkunde **67** (1976) 198.
8. H. J. Servis and Z. M. Munir, J. Less Common Metals **34** (1974) 293.
9. T. Nozaki, M. Shimoji, and K. Niwa, Transactions Japanese Institute of Metals **7** (1966) 52.
10. E. Przewdzicka-Mycielska, J. Terpilowski, and K. Strozcka, Archiwum hutnictwa **8** (1963) 85.
11. B. Predel and U. Schallner, Z. Metallkunde **63** (1972) 341.
12. C. B. Alcock, R. Sridhar, and R. C. Svedberg, Acta Met. **17** (1969) 839.
13. Calculated from ion current data presented in Reference 12.

Appendix B

Thermodynamic Data for Species in the Ag-In-Cd System

In Tables B-1 to B-3 are collected the data used to calculate thermodynamic properties of the monatomic species Ag(gas), In(gas), and Cd(gas). Data on the location and degeneracy of the electronic levels were taken from compilations by Moore.⁽¹⁾ Similar data for Ag⁺, In⁺, and Cd⁺ are shown in Tables B-4 and B-5.

The calculated thermodynamic properties of Ag(gas), Ag₂(gas), Ag₃(gas), Ag⁺, In(gas), In₂(gas), In⁺, Cd(gas), Cd₂(gas), Cd⁺, AgIn(gas), and CdIn(gas) are shown in Tables B-7 to B-18. Abbreviations used in these tables include: $e(T) = H_0(T) - H_0(298.15)$, $\phi(T) = -(1/T)(G(T) - H_0(298.15))$. The reference state data for the elements are shown in Tables B-19, B-21, and B-23. These data were obtained from the compilation by Hultgren et al.⁽²⁾ for the condensed states and from the calculations reported here for the gaseous state. Thermodynamic data for the liquid elements are shown in Tables B-20, B-22, and B-24. For temperatures between the melting point and the boiling point of the liquid these data are the same as that tabulated by Hultgren et al.⁽²⁾ To calculate the properties of the superheated liquid, the heat capacity of the element at its boiling point was assumed invariant with increasing temperature. To estimate the thermodynamic properties of the supercooled liquids, glass transition temperatures at 900 K and at 400 K were assumed for silver and cadmium, respectively.

The reference state data for the electron (e⁻) were taken from the JANAF Table⁽³⁾ and are shown in Table B-25.

Table B-1

Data Used to Calculate the
Thermodynamic Functions of $\text{Ag}^0(\text{g})$

Molecular Weight = 107.870

Degeneracy	Energy (cm^{-1})	Degeneracy	Energy (cm^{-1})
2	0.00	2	58,478.13
2	29,552.05	4	58,504.70
6	30,242.26	8	58,789.70
4	30,472.71	2	58,834.25
4	34,714.16	4	58,849.83
2	42,556.15	4	58,862.46
2	48,297.38	6	58,864.66
4	48,500.77	10	58,901.90
4	48,744.00	2	59,135.99
6	48,764.22	6	59,321.10
2	51,886.98	4	59,388.97
2	54,040.99	6	59,390.72
4	54,121.16	2	59,574.56
4	54,203.13	4	59,751.15
14	54,204.73	6	59,751.51
6	54,213.60	10	60,007.60
2	55,581.29	2	60,537.50
6	56,223.30	4	61,241.90
2	56,620.72		
4	56,660.57		
14	56,691.40		
4	56,699.79		
6	56,705.54		
18	56,711.10		
2	57,425.11		
2	58,005.20		
4	58,027.10		
4	58,050.01		
6	58,053.48		
14	58,055.56		

Table B-2

Data Used to Calculate the
Thermodynamic Functions of $\text{In}^0(\text{g})$

Molecular Weight = 114.820

Degeneracy	Energy (cm^{-1})	Degeneracy	Energy (cm^{-1})	Degeneracy	Energy (cm^{-1})
2	0.00	6	44,249.37	14	45,902.92
4	2,212.56	2	44,275.17	2	45,941.90
2	24,372.87	4	44,294.13	4	45,982.20
2	31,816.61	6	44,406.20	6	45,986.69
4	32,114.79	8	44,406.26	2	46,047.40
4	32,892.12	2	44,595.86	10	46,078.60
6	32,915.42	4	44,815.06	2	46,131.60
2	34,977.66	6	44,827.02	10	46,156.10
4	36,020.80	2	44,853.23	2	46,200.00
2	36,301.69	4	44,865.79	10	46,219.90
6	37,451.90	8	44,938.70	2	46,255.60
2	38,861.35	6	44,938.71	10	46,272.30
4	38,972.84	2	45,067.19	2	46,302.10
4	39,048.48	4	45,211.51	10	46,316.00
6	39,098.37	6	45,221.08	2	46,342.20
6	39,707.29	8	45,303.31	10	46,352.70
8	39,707.96	6	45,303.39	2	46,374.90
2	40,636.71	2	45,394.13	10	46,384.30
2	41,827.10	4	45,493.98	2	46,402.60
4	41,836.23	6	45,502.04	10	46,410.60
6	41,861.57	8	45,563.89	10	46,434.50
4	41,881.44	6	45,564.04	10	46,455.20
14	42,220.00	2	45,630.44	10	46,472.50
2	42,718.55	4	45,702.08	10	46,488.10
4	43,335.63	6	45,709.02	10	46,501.70
2	43,369.09	6	45,756.50	10	46,514.20
4	43,399.53	8	45,756.56	10	46,525.50
14	43,584.40	2	45,806.88	6	73,354.62
2	43,880.83	4	45,859.30		
4	44,234.26	6	45,865.32		

Table B-3

Data Used to Calculate the
Thermodynamic Functions of $\text{Cd}^0(\text{g})$

Molecular Weight = 112.400

Degeneracy	Energy (cm^{-1})	Degeneracy	Energy (cm^{-1})	Degeneracy	Energy (cm^{-1})
1	0.00	3	67,842.10	7	70,790.10
1	30,114.02	5	67,875.20	3	70,800.00
3	30,656.13	3	67,990.10	3	70,962.00
5	31,827.00	5	67,992.90	1	70,992.10
3	43,692.47	7	67,997.50	5	71,119.50
3	51,484.01	3	68,055.40	5	71,159.60
1	53,310.16	21	68,093.70	7	71,160.60
1	58,390.90	3	68,682.20	3	71,167.90
3	58,461.80	1	68,799.60	3	71,281.80
5	58,635.70	5	69,292.50	1	71,299.00
5	59,219.82	1	69,314.50	5	71,424.10
3	59,485.79	3	69,321.40	7	71,425.00
5	59,497.90	5	69,340.20	3	71,515.60
7	59,516.02	3	69,400.50	1	71,528.00
3	59,905.60	5	69,402.80	5	71,596.30
3	62,563.46	7	69,405.50	15	71,618.50
1	63,086.70	3	69,435.70	3	71,689.60
1	64,995.90	3	69,805.90	1	71,692.40
3	65,021.30	1	69,873.10	5	71,748.90
5	65,092.80	5	70,175.90	15	71,767.20
5	65,134.87	9	70,207.30	3	71,818.60
3	65,353.50	3	70,244.20	5	71,869.20
5	65,359.30	5	70,245.50	15	71,880.70
7	65,367.26	7	70,247.10	15	71,972.10
3	65,494.20	3	70,262.60	15	72,046.70
21	65,581.70	3	70,501.20	15	72,108.20
3	66,680.92	1	70,543.20	15	72,155.70
1	66,904.70	5	70,741.90		
1	67,829.60	3	70,788.30		
5	67,837.10	5	70,789.00		

Table B-4

Data Used to Calculate the
Thermodynamic Functions of $\text{Ag}^+(\text{g})$

Molecular Weight = 107.870

Degeneracy	Energy (cm^{-1})	Degeneracy	Energy (cm^{-1})	Degeneracy	Energy (cm^{-1})
1	0.00	11	126,660.50	5	136,514.91
7	39,163.90	9	126,673.10	3	136,828.51
5	40,741.00	5	126,760.20	7	137,172.63
3	43,738.70	3	126,763.70	3	137,221.43
5	46,045.70	7	127,205.00	5	137,464.20
5	80,172.20	7	127,484.50	7	138,633.30
7	82,167.56	5	127,517.00	5	139,227.30
3	83,621.36	9	127,601.80	5	140,962.30
9	83,665.41	1	128,528.80	7	144,473.90
5	85,196.61	5	130,721.01	5	144,619.00
1	86,136.02	3	130,756.00	3	149,078.40
7	86,456.54	7	131,246.30	5	149,179.10
5	86,883.95	3	131,500.50	7	155,085.30
7	89,130.64	9	131,510.50	5	155,156.80
3	89,891.40	5	131,783.90	3	159,690.80
3	90,330.74	7	132,013.53	5	159,738.80
5	90,883.70	5	132,148.90		
9	93,928.66	7	132,191.80		
7	97,957.81	9	132,425.50		
5	99,601.90	9	132,684.46		
5	105,258.18	3	132,837.64		
3	108,934.34	5	132,916.29		
1	109,123.59	7	133,017.94		
5	110,769.41	5	133,137.81		
9	113,598.12	5	133,589.40		
7	120,529.45	7	134,339.04		
5	120,907.13	1	134,449.40		
3	125,122.38	3	134,795.04		
5	125,400.89	5	135,411.22		
3	125,568.90	1	136,165.82		

Table B-5

Data Used to Calculate the
Thermodynamic Functions of $\text{In}^+(\text{g})$

Molecular Weight = 114.820

Degeneracy	Energy (cm^{-1})	Degeneracy	Energy (cm^{-1})	Degeneracy	Energy (cm^{-1})
1	0.00	3	127,568.53	9	142,938.34
5	11,388.07	3	133,067.67	7	142,954.91
5	14,008.88	1	133,549.12	16	143,178.79
1	42,275.00	5	133,935.63	20	143,182.34
3	43,349.00	7	133,939.63	3	143,293.63
5	45,827.00	9	133,955.71	5	143,300.48
3	63,033.81	7	133,979.84	7	143,311.02
3	93,919.03	16	134,507.18	5	143,479.10
1	97,025.36	20	134,511.01	4	143,701.70
5	97,623.61	3	134,721.67	5	143,735.80
1	101,603.30	5	134,739.19	3	143,758.23
3	102,083.63	7	134,767.07	3	144,985.21
5	102,169.63	5	135,395.63	1	145,081.50
7	102,303.23	4	135,856.72	5	145,110.98
3	103,244.47	5	135,994.50	7	145,112.70
5	105,560.19	3	136,092.10	9	145,124.50
1	107,657.87	3	139,132.27	7	145,139.62
3	107,837.17	1	139,382.53	16	145,295.24
5	108,425.52	5	139,544.50	20	145,298.81
3	109,775.39	7	139,547.83	20	145,321.51
1	121,284.71	9	139,562.41	24	145,325.60
3	121,437.71	7	139,581.23	3	145,378.26
1	123,368.04	16	139,916.70	5	145,382.99
5	123,637.85	20	139,920.44	7	145,390.20
7	123,643.04	3	140,077.42	5	145,494.76
9	123,659.72	7	140,104.34	10	145,650.93
7	123,694.07	5	140,403.60	3	145,678.91
3	124,737.90	4	140,729.75	3	146,532.37
5	124,771.87	5	140,817.60	1	146,598.23
7	124,825.30	3	140,840.13	7	146,607.43
5	126,666.16	3	142,703.52	5	146,609.33
1	126,928.03	1	142,852.13	9	146,619.81
3	126,990.17	5	142,922.96		
5	127,249.36	7	142,925.37		

Table B-6

Data Used to Calculate the
Thermodynamic Functions of $\text{Cd}^+(\text{g})$

Molecular Weight = 112.400

Degeneracy	Energy (cm^{-1})	Degeneracy	Energy (cm^{-1})	Degeneracy	Energy (cm^{-1})
2	0.00	6	118,545.77	6	129,419.38
2	44,136.08	18	118,769.95	18	129,502.43
4	46,618.55	4	119,056.11	8	129,686.60
6	69,258.91	2	119,293.99	4	129,708.50
4	74,893.66	8	119,373.19	6	129,718.66
2	82,990.66	4	119,522.72	2	129,956.30
4	89,689.25	6	119,561.99	4	130,216.60
6	89,843.78	4	120,135.22	2	130,835.86
2	94,710.40	2	120,618.46	6	130,878.61
4	95,383.63	4	120,711.18	8	130,925.82
6	106,189.20	6	121,281.64	18	130,946.09
2	107,300.88	2	123,751.48	4	131,092.90
6	108,419.47	8	123,972.10	6	131,100.14
8	108,432.43	6	123,988.39	2	131,261.10
4	109,440.86	18	124,151.26	4	131,374.70
18	109,736.82	4	124,613.30	6	131,718.20
6	110,168.11	6	124,636.50	2	131,899.07
4	110,174.10	2	125,223.06	8	131,953.72
6	110,247.60	4	125,254.49	6	131,961.87
2	112,196.50	2	127,152.89	18	131,978.47
2	112,361.06	8	127,249.09	4	132,086.77
4	112,490.39	6	127,283.04	6	132,092.18
4	112,785.19	18	127,396.62	6	132,280.40
8	114,793.91	4	127,697.43	14	132,707.91
6	114,952.30	6	127,712.28	18	132,742.26
4	116,225.71	4	127,996.73	4	132,824.25
6	116,953.70	2	128,076.30	6	132,828.29
2	117,988.79	8	129,189.50	10	133,389.76
2	118,040.65	2	129,343.05		
8	118,444.36	6	129,344.86		

Table B-7

Thermodynamic Properties of Ag(g)

Temp. (K)	C_p $\frac{\text{cal}}{\text{mole}}\text{-K}$	$S_o(T)$ $\frac{\text{cal}}{\text{mole}}\text{-K}$	$e(T)$ $\frac{\text{Kcal}}{\text{mole}}$	$\phi(T)$ $\frac{\text{cal}}{\text{mole}}\text{-K}$	ΔH_f $\frac{\text{cal}}{\text{mole}}$	ΔG_f $\frac{\text{cal}}{\text{mole}}$
298.15	4.968	41.320	0	41.320	67,900	58,622
300	4.968	41.351	0.009	41.320	67,898	58,564
400	4.968	42.780	0.506	41.515	67,783	55,470
500	4.968	43.889	1.003	41.883	67,657	52,406
600	4.968	44.794	1.500	42.295	67,518	49,369
700	4.968	45.560	1.996	42.708	67,363	46,355
800	4.968	46.224	2.493	43.107	67,192	43,205
900	4.968	46.809	2.990	43.487	67,004	40,397
1000	4.968	47.332	3.487	43.846	66,798	37,454
1100	4.968	47.806	3.984	44.184	66,572	34,530
1200	4.968	48.238	4.480	44.504	66,323	31,626
1300	4.968	48.636	4.977	44.807	63,334	28,891
1400	4.968	49.004	5.474	45.094	63,031	26,253
1500	4.968	49.347	5.971	45.366	62,728	23,637
1600	4.968	49.667	6.467	45.625	62,424	21,040
1700	4.968	49.968	6.964	45.872	62,121	18,463
1800	4.968	50.252	7.461	46.107	61,818	15,904
1900	4.968	50.521	7.958	46.333	61,515	13,361
2000	4.968	50.776	8.455	46.548	61,212	10,834
2100	4.968	51.018	8.951	46.756	60,908	8,322
2200	4.968	51.249	9.448	46.955	60,605	5,825
2300	4.968	51.470	9.945	47.146	60,302	3,343
2400	4.968	51.681	10.442	47.331	59,999	873
2500	4.968	51.884	10.939	47.509	0	0
2600	4.968	52.079	11.435	47.681	0	0
2700	4.968	52.267	11.932	47.847	0	0
2800	4.968	52.447	12.429	48.008	0	0
2900	4.969	52.622	12.926	48.164	0	0
3000	4.969	52.790	13.423	48.316	0	0
3100	4.970	52.953	13.920	48.463	0	0
3200	4.971	53.111	14.417	48.606	0	0
3300	4.972	53.264	14.914	48.744	0	0
3400	4.974	53.412	15.411	48.880	0	0
3500	4.976	53.557	15.909	49.011	0	0

Table B-8

Thermodynamic Properties of $\text{Ag}_2(\text{gas})$

Temp. (K)	C_p $\frac{\text{cal}}{\text{mole}}\text{-K}$	$S_o(T)$ $\frac{\text{cal}}{\text{mole}}\text{-K}$	$e(T)$ $\frac{\text{Kcal}}{\text{mole}}$	$\phi(T)$ $\frac{\text{cal}}{\text{mole}}\text{-K}$	ΔH_f $\frac{\text{cal}}{\text{mole}}$	ΔG_f $\frac{\text{cal}}{\text{mole}}$
298.15	8.8583	61.3842	0	61.3842	97,679	85,460
300	8.8602	61.4390	16.4	61.3844	97,673	85,384
400	8.9351	63.9994	906	61.7330	97,339	81,337
500	8.9799	65.9983	1,802	62.3934	96,989	77,376
600	9.0125	67.6386	2,702	63.1350	96,617	73,488
700	9.0391	69.0299	3,605	63.8802	96,218	69,666
800	9.0625	70.2384	4,510	64.6011	95,787	65,580
900	9.0841	71.3071	5,417	65.2880	95,324	62,190
1000	9.1045	72.2653	6,327	65.9387	94,828	58,539
1100	9.1242	73.1340	7,238	66.5539	94,293	54,935
1200	9.1433	73.9287	8,151	67.1358	93,716	51,379
1300	9.1621	74.6613	9,067	67.6869	87,660	48,167
1400	9.1806	75.3410	9,984	68.2096	86,977	45,155
1500	9.1989	75.9750	10,903	68.7064	86,296	42,192
1600	9.2171	76.5693	11,824	69.1795	85,617	39,273
1700	9.2352	77.1286	12,746	69.6308	84,939	36,396
1800	9.2531	77.6570	13,671	70.0621	84,264	33,560
1900	9.2710	78.1577	14,597	70.4752	83,590	30,763
2000	9.2889	78.6337	15,525	70.8713	82,918	27,999
2100	9.3067	79.0874	16,455	71.2518	82,248	25,268
2200	9.3245	79.5207	17,386	71.6179	81,579	22,569
2300	9.3423	79.9356	18,320	71.9706	80,913	19,904
2400	9.3601	80.3336	19,255	72.3108	80,248	17,263
2500	9.3780	80.7160	20,192	72.6394	-39,807	17,823
2600	9.3960	81.0842	21,130	72.9572	-39,861	20,131
2700	9.4141	81.4391	22,071	73.2648	-39,914	22,442
2800	9.4323	81.7818	23,013	73.5629	-39,966	24,748
2900	9.4507	82.1132	23,957	73.8520	-40,016	27,063
3000	9.4694	82.4339	24,903	74.1328	-40,064	29,374
3100	9.4883	82.7447	25,851	74.4056	-40,110	31,690
3200	9.5075	83.0462	26,801	74.6709	-40,154	34,009
3300	9.5271	83.3391	27,753	74.9292	-40,196	36,327
3400	9.5470	83.6238	28,706	75.1807	-40,237	38,644
3500	9.5674	83.9008	29,662	75.4259	-40,277	40,969

Table B-9

Thermodynamic Properties of $\text{Ag}_3(\text{gas})$

Temp. (K)	C_p $\frac{\text{cal}}{\text{mole}}\text{-K}$	$S_o(T)$ $\frac{\text{cal}}{\text{mole}}\text{-K}$	$e(T)$ $\frac{\text{Kcal}}{\text{mole}}$	$\phi(T)$ $\frac{\text{cal}}{\text{mole}}\text{-K}$	ΔH_f $\frac{\text{cal}}{\text{mole}}$	ΔG_f $\frac{\text{cal}}{\text{mole}}$
298.15	14.7010	77.9899	0	77.9899	142,655	128,526
300	14.7035	78.0809	27.2	77.9902	142,649	128,439
400	14.7901	82.3244	1.502	78.5682	142,288	123,755
500	14.8307	85.6296	2,984	79.6621	141,901	119,165
600	14.8529	88.3357	4,468	80.8890	141,477	114,657
700	14.8663	90.6263	5,954	82.1206	141,010	110,224
800	14.8748	92.6121	7,441	83.3107	140,493	105,379
900	14.8799	94.3644	8,929	84.4434	139,926	101,562
1000	14.8817	95.9323	10,417	85.5153	139,305	97,337
1100	14.8794	97.3506	11,905	86.5278	138,624	93,172
1200	14.8720	98.6450	13,393	87.4844	137,877	89,069
1300	14.8579	99.8349	14,879	88.3893	128,905	85,470
1400	14.8358	100.9352	16,364	89.2466	127,990	82,164
1500	14.8048	101.9577	17,846	90.0603	127,072	78,922
1600	14.7643	102.9120	19,325	90.8341	126,151	75,741
1700	14.7139	103.8056	20,799	91.5711	125,225	72,619
1800	14.6538	104.6450	22,267	92.2744	124,293	69,550
1900	14.5843	105.4354	23,729	92.9464	123,355	66,537
2000	14.5060	106.1816	25,184	93.5897	122,410	63,569
2100	14.4197	106.8873	26,630	94.2063	121,456	60,648
2200	14.3262	107.5559	28,067	94.7980	120,493	57,773
2300	14.2263	108.1906	29,495	95.3666	119,521	54,947
2400	14.1209	108.7938	30,912	95.9136	118,538	52,157
2500	14.0110	109.3681	32,319	96.4404	-61,543	54,167
2600	13.8972	109.9154	33,714	96.9482	-61,636	58,800
2700	13.7804	110.4377	35,098	97.4383	-61,743	63,438
2800	13.6613	110.9367	36,470	97.9115	-61,862	68,070
2900	13.5406	111.4140	37,831	98.3689	-61,992	72,719
3000	13.4188	111.8710	39,179	98.8114	-62,135	77,362
3100	13.2966	112.3090	40,514	99.2398	-62,651	81,654
3200	13.1744	112.7292	41,838	99.6548	-62,458	86,674
3300	13.0526	113.1327	43,149	100.057	-62,638	91,338
3400	12.9317	113.5206	44,448	100.448	-62,830	96,002
3500	12.8120	113.8937	45,736	100.826	-63,036	100,685

Table B-10

Thermodynamic Properties of Ag^+

Temp. (K)	C_p $\frac{\text{cal}}{\text{mole}}\text{-K}$	$S_o(T)$ $\frac{\text{cal}}{\text{mole}}\text{-K}$	$e(T)$ $\frac{\text{Kcal}}{\text{mole}}$	$\phi(T)$ $\frac{\text{cal}}{\text{mole}}\text{-K}$	ΔH_f $\frac{\text{cal}}{\text{mole}}$	ΔG_f $\frac{\text{cal}}{\text{mole}}$
298.15	4.968	39.943	0	39.943	243,420	233,065
300	4.968	39.974	0.009	39.943	243,427	233,000
400	4.968	41.403	0.506	40.138	243,809	229,467
500	4.968	42.511	1.003	40.506	244,180	225,839
600	4.968	43.417	1.500	40.918	244,538	222,137
700	4.968	44.183	1.996	41.331	244,879	218,375
800	4.968	44.846	2.493	41.730	245,205	214,407
900	4.968	45.431	2.990	42.109	245,514	210,718
1000	4.968	45.955	3.487	42.468	245,805	206,837
1100	4.968	46.428	3.984	42.807	246,076	202,929
1200	4.968	46.861	4.480	43.127	246,323	198,991
1300	4.968	47.258	4.977	43.430	246,551	195,184
1400	4.968	47.626	5.474	43.716	246,765	191,435
1500	4.968	47.969	5.971	43.989	246,965	187,672
1600	4.968	48.290	6.467	44.248	247,151	183,893
1700	4.968	48.591	6.964	44.494	247,325	180,105
1800	4.968	48.875	7.461	44.730	247,487	176,305
1900	4.968	49.144	7.958	44.955	247,637	172,497
2000	4.968	49.398	8.455	45.171	247,775	168,677
2100	4.968	49.641	8.951	45.378	247,901	164,844
2200	4.968	49.872	9.448	45.577	248,015	161,003
2300	4.968	50.093	9.945	45.769	248,117	157,157
2400	4.968	50.304	10.442	45.953	248,207	153,299
2500	4.968	50.507	10.939	46.131	248,285	151,019
2600	4.968	50.702	11.435	46.304	248,351	149,590
2700	4.968	50.889	11.932	46.470	248,405	148,148
2800	4.968	51.070	12.429	46.631	248,447	146,680
2900	4.968	51.244	12.926	46.787	248,478	145,201
3000	4.968	51.413	13.423	46.938	248,498	143,700
3100	4.968	51.576	13.919	47.085	248,507	142,182
3200	4.968	51.733	14.416	47.228	248,505	140,652
3300	4.968	51.886	14.913	47.367	248,492	139,104
3400	4.968	52.034	15.410	47.502	248,467	137,542
3500	4.968	52.178	15.907	47.634	248,431	135,968

Table B-11

Thermodynamic Properties of In(gas)

Temp. (K)	C_p $\frac{\text{cal}}{\text{mole}}\text{-K}$	$S_o(T)$ $\frac{\text{cal}}{\text{mole}}\text{-K}$	$e(T)$ $\frac{\text{Kcal}}{\text{mole}}$	$\phi(T)$ $\frac{\text{cal}}{\text{mole}}\text{-K}$	ΔH_f $\frac{\text{cal}}{\text{mole}}$	ΔG_f $\frac{\text{cal}}{\text{mole}}$
298.15	4.978	41.507	0	41.507	58,000	49,745
300	4.979	41.538	0.009	41.508	57,997	49,693
400	5.056	42.979	0.510	41.703	57,834	46,948
500	5.243	44.125	1.024	42.077	56,864	44,377
600	5.512	45.104	1.561	42.501	56,699	41,895
700	5.803	45.976	2.127	42.937	56,565	39,438
800	6.061	46.768	2.721	43.367	56,461	36,999
900	6.260	47.494	3.338	43.785	56,382	34,572
1000	6.391	48.161	3.971	44.190	56,320	32,152
1100	6.461	48.774	4.614	44.579	56,268	29,738
1200	6.482	49.337	5.261	44.953	56,220	27,328
1300	6.465	49.855	5.909	45.310	56,173	24,922
1400	6.422	50.333	6.553	45.652	56,122	22,521
1500	6.363	50.774	7.193	45.979	56,067	20,124
1600	6.294	51.183	7.826	46.292	56,005	17,728
1700	6.221	51.562	8.452	46.591	55,936	15,338
1800	6.147	51.916	9.070	46.877	55,859	12,951
1900	6.074	52.246	9.681	47.151	55,775	10,570
2000	6.003	52.556	10.285	47.413	55,684	8,192
2100	5.936	52.847	10.882	47.665	55,586	5,822
2200	5.873	53.122	11.472	47.907	55,481	3,453
2300	5.815	53.382	12.056	48.140	55,370	1,090
2400	5.760	53.628	12.635	48.363	0	0
2500	5.709	53.862	13.209	48.578	0	0
2600	5.663	54.085	13.777	48.786	0	0
2700	5.620	54.298	14.341	48.986	0	0
2800	5.580	54.501	14.901	49.180	0	0
2900	5.544	54.697	15.457	49.366	0	0
3000	5.511	54.884	16.010	49.547	0	0
3100	5.480	55.064	16.560	49.722	0	0
3200	5.452	55.238	17.106	49.892	0	0
3300	5.427	55.405	17.650	50.057	0	0
3400	5.403	55.567	18.192	50.216	0	0
3500	5.383	55.723	18.731	50.371	0	0

Table B-12

Thermodynamic Properties of $\text{In}_2(\text{gas})$

Temp. (K)	C_p $\frac{\text{cal}}{\text{mole}}\text{-K}$	$S_o(T)$ $\frac{\text{cal}}{\text{mole}}\text{-K}$	$e(T)$ $\frac{\text{Kcal}}{\text{mole}}$	$\phi(T)$ $\frac{\text{cal}}{\text{mole}}\text{-K}$	ΔH_f $\frac{\text{cal}}{\text{mole}}$	ΔG_f $\frac{\text{cal}}{\text{mole}}$
298.15	8.9732	65.5937	0	65.5937	96,047	84,731
300	8.9746	65.6492	16.6	65.5939	96,039	84,660
400	9.0374	68.2402	917	65.9467	95,612	80,926
500	9.0845	70.2621	1,824	66.6149	93,551	77,570
600	9.1255	71.9221	2,734	67.3652	93,057	74,420
700	9.1634	73.3316	3,648	68.1194	92,571	71,351
800	9.1998	74.5576	4,567	68.8492	92,094	68,354
900	9.2353	75.6433	5,488	69.5449	91,623	65,414
1000	9.2701	76.6181	6,414	70.2043	91,159	62,527
1100	9.3046	77.5033	7,342	70.8283	90,697	59,687
1200	9.3389	78.3144	8,275	71.4188	90,240	56,887
1300	9.3729	79.0632	9,210	71.9784	89,785	54,124
1400	9.4068	79.7591	10,149	72.5096	89,334	51,401
1500	9.4407	80.4092	11,092	73.0148	88,887	48,709
1600	9.4744	81.0196	12,037	73.4962	88,442	46,043
1700	9.5081	81.5950	12,986	73.9558	88,001	43,405
1800	9.5417	82.1394	13,939	74.3955	87,564	40,794
1900	9.5754	82.6562	14,895	74.8168	87,130	38,208
2000	9.6089	83.1482	15,854	75.2211	86,699	35,643
2100	9.6425	83.6178	16,817	75.6099	86,272	33,105
2200	9.6760	84.0672	17,783	75.9842	85,848	30,581
2300	9.7096	84.4980	18,752	76.3450	85,427	28,079
2400	9.7431	84.9120	19,724	76.6934	-25,499	28,127
2500	9.7766	85.3104	20,700	77.0302	-25,671	30,363
2600	9.8102	85.6945	21,680	77.3561	-25,827	32,609
2700	9.8437	86.0654	22,662	77.6718	-25,973	34,860
2800	9.8773	86.4240	23,649	77.9780	-26,106	37,112
2900	9.9109	86.7711	24,638	78.2753	-26,229	39,377
3000	9.9446	87.1077	25,631	78.5641	-26,342	41,639
3100	9.9783	87.4343	26,627	78.8450	-26,446	43,904
3200	10.0121	87.7517	27,626	79.1184	-26,539	46,179
3300	10.0461	88.0603	28,629	79.3847	-26,624	48,450
3400	10.0801	88.3607	29,636	79.6443	-26,701	50,728
3500	10.1143	88.6534	30,645	79.8976	-26,770	53,004

Table B-13

Thermodynamic Properties of In⁺

Temp. (K)	C _p $\frac{\text{cal}}{\text{mole}}\text{-K}$	S _o (T) $\frac{\text{cal}}{\text{mole}}\text{-K}$	e(T) $\frac{\text{Kcal}}{\text{mole}}$	φ(T) $\frac{\text{cal}}{\text{mole}}\text{-K}$	ΔH _f $\frac{\text{cal}}{\text{mole}}$	ΔG _f $\frac{\text{cal}}{\text{mole}}$
298.15	4.968	40.129	0	40.129	192,222	182,891
300	4.968	40.160	0.009	40.129	192,228	182,832
400	4.968	41.589	0.506	40.324	192,558	179,648
500	4.968	42.697	1.003	40.692	192,068	176,516
600	4.968	43.603	1.500	41.104	192,360	173,378
700	4.968	44.369	1.996	41.517	192,652	170,190
800	4.968	45.032	2.493	41.916	192,948	166,962
900	4.968	45.618	2.990	42.295	193,246	163,695
1000	4.968	46.141	3.487	42.654	193,545	160,396
1100	4.969	46.615	3.984	42.993	193,844	157,068
1200	4.970	47.047	4.481	43.313	194,142	153,710
1300	4.974	47.445	4.978	43.616	194,441	150,328
1400	4.980	47.814	5.475	43.903	194,750	146,924
1500	4.992	48.158	5.974	44.175	195,041	143,500
1600	5.010	48.480	6.474	44.434	195,342	140,052
1700	5.038	48.785	6.976	44.681	195,646	136,586
1800	5.077	49.074	7.482	44.917	195,954	133,103
1900	5.128	49.350	7.992	45.143	196,266	129,605
2000	5.194	49.614	8.508	45.360	196,584	126,088
2100	5.276	49.870	9.031	45.569	196,908	122,555
2200	5.374	50.117	9.564	45.770	197,243	119,007
2300	5.488	50.359	10.107	45.964	197,588	115,444
2400	5.619	50.595	10.662	46.152	142,691	113,130
2500	5.766	50.827	11.231	46.335	143,183	111,888
2600	5.926	51.056	11.816	46.512	143,696	110,627
2700	6.099	51.283	12.417	46.684	144,230	109,346
2800	6.283	51.508	13.036	46.853	144,786	108,042
2900	6.476	51.732	13.674	47.017	145,365	106,723
3000	6.674	51.955	14.331	47.178	145,966	105,379
3100	6.877	52.177	15.009	47.336	146,590	104,015
3200	7.081	52.399	15.707	47.490	147,239	102,631
3300	7.285	52.620	16.425	47.643	147,910	101,225
3400	7.485	52.840	17.163	47.792	148,603	99,803
3500	7.680	53.060	17.922	47.940	149,320	98,357

Table B-14

Thermodynamic Properties of Cd(gas)

Temp. (K)	C_p $\frac{\text{cal}}{\text{mole}}\text{-K}$	$S_o(T)$ $\frac{\text{cal}}{\text{mole}}\text{-K}$	$e(T)$ $\frac{\text{Kcal}}{\text{mole}}$	$\phi(T)$ $\frac{\text{cal}}{\text{mole}}\text{-K}$	ΔH_f $\frac{\text{cal}}{\text{mole}}$	ΔG_f $\frac{\text{cal}}{\text{mole}}$
298.15	4.968	40.065	0	40.065	26,720	18,466
300	4.968	40.096	0.009	40.066	26,718	18,414
400	4.968	41.525	0.506	40.260	26,580	15,666
500	4.968	42.634	1.003	40.628	26,413	12,956
600	4.968	43.540	1.500	41.040	24,737	10,301
700	4.968	44.306	1.996	41.454	24,523	7,908
800	4.968	44.969	2.493	41.852	24,310	5,551
900	4.968	45.554	2.990	42.232	24,097	3,222
1000	4.968	46.077	3.487	42.591	23,884	917
1100	4.968	46.551	3.984	42.930	0	0
1200	4.968	46.983	4.480	43.250	0	0
1300	4.968	47.381	4.977	43.552	0	0
1400	4.968	47.749	5.474	43.839	0	0
1500	4.968	48.092	5.971	44.111	0	0
1600	4.968	48.412	6.467	44.370	0	0
1700	4.968	48.714	6.964	44.617	0	0
1800	4.968	48.998	7.461	44.852	0	0
1900	4.968	49.266	7.958	45.078	0	0
2000	4.968	49.521	8.455	45.294	0	0
2100	4.968	49.763	8.951	45.501	0	0
2200	4.968	49.994	9.448	45.700	0	0
2300	4.968	50.215	9.945	45.891	0	0
2400	4.968	50.427	10.442	46.076	0	0
2500	4.968	50.630	10.939	46.254	0	0
2600	4.968	50.824	11.435	46.426	0	0
2700	4.968	51.012	11.932	46.593	0	0
2800	4.968	51.193	12.429	46.754	0	0
2900	4.969	51.367	12.926	46.910	0	0
3000	4.969	51.535	13.423	47.061	0	0
3100	4.970	51.698	13.920	47.208	0	0
3200	4.971	51.856	14.417	47.351	0	0
3300	4.972	52.009	14.914	47.490	0	0
3400	4.974	52.158	15.411	47.625	0	0
3500	4.976	52.302	15.909	47.756	0	0

Table B-15

Thermodynamic Properties of $\text{Cd}_2(\text{g})$

Temp. (K)	C_p $\frac{\text{cal}}{\text{mole}}\text{-K}$	$S_o(T)$ $\frac{\text{cal}}{\text{mole}}\text{-K}$	$e(T)$ $\frac{\text{Kcal}}{\text{mole}}$	$\phi(T)$ $\frac{\text{cal}}{\text{mole}}\text{-K}$	ΔH_f $\frac{\text{cal}}{\text{mole}}$	ΔG_f $\frac{\text{cal}}{\text{mole}}$
298.15	10.1466	68.4287	0	68.4287	73,824	60,804
300	10.1569	68.4915	18.8	68.4289	73,820	60,723
400	10.6881	71.4877	1,062	68.8338	73,594	56,391
500	11.1408	73.9229	2,154	69.6155	73,358	52,117
600	11.5176	75.9884	3,287	70.5098	70,145	47,928
700	11.8417	77.7887	4,455	71.4237	69,893	44,239
800	12.1347	79.3893	5,654	72.3212	69,672	40,593
900	12.4116	80.8347	6,882	73.1881	69,480	36,977
1000	12.6820	82.1564	8,136	74.0198	69,314	33,378
1100	12.9511	83.3777	9,418	74.8157	21,834	32,531
1200	13.2218	84.5162	10,727	75.5771	22,151	33,491
1300	13.4957	85.5853	12,063	76.3063	22,493	34,423
1400	13.7733	86.5956	13,426	77.0055	22,862	35,325
1500	14.0550	87.5554	14,818	77.6771	23,260	36,203
1600	14.3406	88.4716	16,237	78.3233	23,687	37,051
1700	14.6302	89.3496	17,686	78.9463	24,142	37,875
1800	14.9233	90.1942	19,163	79.5478	24,625	38,668
1900	15.2199	91.0090	20,670	80.1297	25,138	39,432
2000	15.5197	91.7972	22,208	80.6935	25,682	40,172
2100	15.8224	92.5618	23,775	81.2405	26,257	40,882
2200	16.1277	93.3049	25,372	81.7721	26,860	41,563
2300	16.4355	94.0286	27,000	82.2893	27,494	42,217
2400	16.7455	94.7346	28,659	82.7932	28,159	42,846
2500	17.0575	95.4245	30,349	83.2847	28,855	43,444
2600	17.3712	96.0996	32,071	83.7647	29,585	44,011
2700	17.6864	96.7611	33,824	84.2338	30,344	44,554
2800	18.0030	97.4100	35,608	84.6929	31,134	45,067
2900	18.3207	98.0473	37,424	85.1424	31,956	45,547
3000	18.6394	98.6738	39,272	85.5830	32,810	45,999
3100	18.9589	99.2902	41,152	86.0153	33,696	46,424
3200	19.2791	99.8972	43,064	86.4396	34,614	46,821
3300	19.5999	100.4953	45,008	86.8565	35,564	47,189
3400	19.9211	101.0852	46,984	87.2664	36,546	47,531
3500	20.2426	101.6673	48,992	87.6695	37,558	47,836

Table B-16

Thermodynamic Properties of $\text{Cd}^+(\text{g})$

Temp. (K)	C_p $\frac{\text{cal}}{\text{mole}}\text{-K}$	$S_o(T)$ $\frac{\text{cal}}{\text{mole}}\text{-K}$	$e(T)$ $\frac{\text{Kcal}}{\text{mole}}$	$\phi(T)$ $\frac{\text{cal}}{\text{mole}}\text{-K}$	ΔH_f $\frac{\text{cal}}{\text{mole}}$	ΔG_f $\frac{\text{cal}}{\text{mole}}$
298.15	4.968	41.443	0	41.443	234,825	224,672
300	4.968	41.474	0.009	41.443	234,832	224,609
400	4.968	42.903	0.506	41.638	235,191	221,146
500	4.968	44.011	1.003	42.006	235,521	217,597
600	4.968	44.917	1.500	42.418	234,342	214,002
700	4.968	45.683	1.996	42.831	234,624	210,585
800	4.968	46.346	2.493	43.230	234,908	207,134
900	4.968	46.931	2.990	43.609	235,192	203,649
1000	4.968	47.455	3.487	43.968	235,476	200,130
1100	4.968	47.928	3.984	44.307	212,089	197,953
1200	4.968	48.361	4.480	44.627	212,585	196,644
1300	4.968	48.758	4.977	44.930	213,082	195,297
1400	4.968	49.126	5.474	45.216	213,579	193,910
1500	4.968	49.469	5.971	45.489	214,076	192,488
1600	4.968	49.790	6.467	45.748	214,572	191,030
1700	4.968	50.091	6.964	45.994	215,069	189,545
1800	4.968	50.375	7.461	46.230	215,566	188,030
1900	4.968	50.644	7.958	46.455	216,063	186,486
2000	4.968	50.898	8.455	46.671	216,560	184,918
2100	4.968	51.141	8.951	46.878	217,056	183,322
2200	4.968	51.372	9.448	47.077	217,553	181,702
2300	4.968	51.593	9.945	47.269	218,050	180,063
2400	4.968	51.804	10.442	47.453	218,547	178,402
2500	4.968	52.007	10.939	47.631	219,044	176,719
2600	4.968	52.202	11.435	47.804	219,540	175,012
2700	4.968	52.389	11.932	47.970	220,037	173,295
2800	4.968	52.570	12.429	48.131	220,534	171,554
2900	4.968	52.744	12.926	48.287	221,031	169,797
3000	4.968	52.913	13.423	48.439	221,528	168,020
3100	4.968	53.076	13.919	48.586	222,023	166,226
3200	4.968	53.233	14.416	48.728	222,520	164,421
3300	4.968	53.386	14.913	48.867	223,017	162,597
3400	4.968	53.534	15.410	49.002	223,514	160,764
3500	4.968	53.678	15.907	49.133	224,010	158,910

Table B-17

Thermodynamic Properties of AgIn(gas)

Temp. (K)	C_p $\frac{\text{cal}}{\text{mole}}\text{-K}$	$S_o(T)$ $\frac{\text{cal}}{\text{mole}}\text{-K}$	$e(T)$ $\frac{\text{Kcal}}{\text{mole}}$	$\phi(T)$ $\frac{\text{cal}}{\text{mole}}\text{-K}$	ΔH_f $\frac{\text{cal}}{\text{mole}}$	ΔG_f $\frac{\text{cal}}{\text{mole}}$
298.15	8.9006	67.4205	0	67.4205	84,817	71,877
300	8.9020	67.4755	16.5	67.4206	84,810	71,797
400	8.9567	70.0447	910	67.7706	84,428	67,514
500	8.9911	72.0473	1,807	68.4330	83,218	63,462
600	9.0174	73.6890	2,708	69.1762	82,781	59,553
700	9.0397	75.0807	3,610	69.9228	82,332	55,716
800	9.0599	76.2891	4,516	70.6448	81,872	51,786
900	9.0789	77.3573	5,422	71.3324	81,397	48,232
1000	9.0971	78.3148	6,331	71.9836	80,908	44,574
1100	9.1149	79.1827	7,242	72.5992	80,401	40,966
1200	9.1323	79.9766	8,154	73.1814	79,873	37,402
1300	9.1494	80.7082	9,068	73.7326	76,606	34,029
1400	9.1664	81.3869	9,984	74.2554	76,027	30,778
1500	9.1833	82.0199	10,902	74.7522	75,450	27,567
1600	9.2000	82.6131	11,821	75.2251	74,874	24,392
1700	9.2167	83.1713	12,742	75.6763	74,300	21,254
1800	9.2333	83.6986	13,664	76.1075	73,727	18,149
1900	9.2499	84.1983	14,588	76.5203	73,156	15,078
2000	9.2664	84.6732	15,514	76.9161	72,587	12,035
2100	9.2829	85.1257	16,442	77.2964	72,020	9,023
2200	9.2994	85.5579	17,371	77.6521	71,454	6,035
2300	9.3159	85.9716	18,301	78.0145	70,889	3,074
2400	9.3323	86.3685	19,234	78.3544	15,073	1,404
2500	9.3487	86.7498	20,168	78.6826	-45,063	2,428
2600	9.3651	87.1167	21,104	79.0000	-45,191	4,332
2700	9.3816	87.4705	22,041	79.3072	-45,315	6,240
2800	9.3979	87.8120	22,980	79.6049	-45,433	8,148
2900	9.4143	88.1420	23,920	79.8936	-45,546	10,067
3000	9.4307	88.4615	24,863	80.1739	-45,653	11,985
3100	9.4471	88.7710	25,807	80.4463	-45,756	13,907
3200	9.4635	89.0712	26,752	80.7111	-45,854	15,835
3300	9.4799	89.3626	27,699	80.9689	-45,948	17,763
3400	9.4963	89.6459	28,648	81.2200	-46,038	19,695
3500	9.5127	89.9214	29,599	81.4647	-46,124	21,631

Table B-18

Thermodynamic Properties of CdIn(gas)

Temp. (K)	C_p $\frac{\text{cal}}{\text{mole}}\text{-K}$	$S_o(T)$ $\frac{\text{cal}}{\text{mole}}\text{-K}$	$e(T)$ $\frac{\text{Kcal}}{\text{mole}}$	$\phi(T)$ $\frac{\text{cal}}{\text{mole}}\text{-K}$	ΔH_f $\frac{\text{cal}}{\text{mole}}$	ΔG_f $\frac{\text{cal}}{\text{mole}}$
298.15	8.9073	65.5465	0	65.5465	78,528	66,797
300	8.9090	65.6016	16.5	65.5466	78,521	66,724
400	8.9767	68.1747	911	65.8970	78,117	62,848
500	9.0218	70.1829	1,811	66.5607	76,869	59,213
600	9.0606	71.8312	2,715	67.3058	74,898	55,745
700	9.1026	73.2309	3,623	68.0548	74,396	52,590
800	9.1539	74.4496	4,536	68.7796	73,901	49,510
900	9.2177	75.5314	5,454	69.4708	73,413	46,494
1000	9.2943	76.5064	6,380	70.1264	72,934	43,531
1100	9.3814	77.3963	7,314	70.7474	48,792	41,984
1200	9.4759	78.2166	8,256	71.3361	48,543	41,375
1300	9.5742	78.9789	9,209	71.8950	48,304	40,788
1400	9.6730	79.6921	10,171	72.4268	48,074	40,218
1500	9.7696	80.3627	11,144	72.9337	47,855	39,667
1600	9.8617	80.9962	12,125	73.4180	47,645	39,126
1700	9.9480	81.5967	13,116	73.8816	47,444	38,601
1800	10.0276	82.1676	14,115	74.3262	47,251	38,086
1900	10.1002	82.7117	15,121	74.7533	47,065	37,581
2000	10.1656	83.2315	16,134	75.1643	46,886	37,085
2100	10.2243	83.7289	17,154	75.5604	46,715	36,602
2200	10.2767	84.2058	18,179	75.9426	46,548	36,123
2300	10.3235	84.6637	19,209	76.3119	46,386	35,653
2400	10.3653	85.1039	20,244	76.6691	-9,025	36,458
2500	10.4029	85.5278	21,282	77.0151	-9,058	38,353
2600	10.4369	85.9365	22,324	77.3504	-9,080	40,249
2700	10.4681	86.3310	23,369	77.6757	-9,096	42,147
2800	10.4971	86.7122	24,418	77.9917	-9,104	44,045
2900	10.5245	87.0811	25,469	78.2988	-9,106	45,944
3000	10.5508	87.4383	26,522	78.5975	-9,103	47,839
3100	10.5764	87.7847	27,579	78.8883	-9,093	49,737
3200	10.6018	88.1209	28,638	79.1716	-9,077	51,637
3300	10.6273	88.4475	29,699	79.4478	-9,057	53,532
3400	10.6532	88.7652	30,763	79.7172	-9,032	55,431
3500	10.6796	89.0743	31,830	79.9801	-9,002	57,325

Table B-19
Silver Reference System

T(K)	$S_O(T)$ (cal/mole - K)	$H_O(T) - H_O(298)$ (cal/mole)
298.15	10.2	0
300	10.238	11.2
400	11.997	623
500	13.386	1,246
600	14.545	1,882
700	15.549	2,533
800	16.240	3,201
900	17.246	3,886
1000	17.988	4,589
1100	18.677	5,312
1200	19.324	6,057
1300	22.141	9,543
1400	22.734	10,343
1500	23.286	11,143
1600	23.802	11,943
1700	24.287	12,743
1800	24.744	13,543
1900	25.177	14,343
2000	25.587	15,143
2100	25.977	15,943
2200	26.349	16,743
2300	26.705	17,543
2400	27.045	18,343
2500	51.884	78,839
2600	52.079	79,335
2700	52.267	79,832
2800	52.447	80,329
2900	52.622	80,826
3000	52.790	81,323
3100	52.953	81,820
3200	53.111	82,317
3300	53.264	82,814
3400	53.412	83,311
3500	53.557	83,809

Table B-20

Thermodynamic Properties of Silver Liquid

Temp (K)	C_p (cal/mole - K)	S_o (cal/mole - K)	$H^o(T) - H^o(298)$ (cal/mole)	ΔH_f (cal/mole)	ΔG_f (cal/mole)
298.15	6.07	12.153	0	2,457	1,875
300	6.07	12.191	11	2,457	1,871
400	6.17	13.950	623	2,457	1,676
500	6.29	15.339	1,246	2,457	1,480
600	6.44	16.498	1,882	2,457	1,285
700	6.59	17.502	2,533	2,457	1,090
800	6.76	18.393	3,201	2,457	735
900	8	19.199	3,886	2,457	699
1000	8	20.042	4,686	2,554	500
1100	8	20.805	5,486	2,631	290
1200	8	21.501	6,286	2,686	74
1300	8	22.141	7,086	0	0
1400	8	22.734	7,886	0	0
1500	8	23.286	8,686	0	0
1600	8	23.802	9,486	0	0
1700	8	24.287	10,286	0	0
1800	8	24.744	11,086	0	0
1900	8	25.177	11,886	0	0
2000	8	25.587	12,686	0	0
2100	8	25.977	13,486	0	0
2200	8	26.349	14,286	0	0
2300	8	26.705	15,086	0	0
2400	8	27.045	15,886	0	0
2500	8	27.372	16,686	-59,696	1,584
2600	8	27.686	17,486	-59,392	4,030
2700	8	27.988	18,286	-59,089	6,464
2800	8	28.279	19,086	-58,786	8,884
2900	8	28.560	19,886	-58,483	11,297
3000	8	28.831	20,686	-58,180	13,697
3100	8	29.093	21,486	-57,877	16,089
3200	8	29.347	22,286	-57,574	18,471
3300	8	29.594	23,086	-57,271	20,840
3400	8	29.832	23,886	-56,968	23,204
3500	8	30.064	24,686	-56,666	25,560

Table B-21
Indium Reference State

T(K)	$S_o(T)$ (cal/mole - K)	$H_o(T) - H_o(298)$ (cal/mole)
298.15	13.820	0
300	13.860	12.3
400	15.753	676
500	19.150	2,160
600	20.43	2,862
700	21.509	3,562
800	22.441	4,260
900	23.261	4,956
1000	23.993	5,651
1100	24.656	6,346
1200	25.260	7,041
1300	25.816	7,736
1400	26.332	8,431
1500	26.812	9,126
1600	27.260	9,821
1700	27.681	10,516
1800	28.078	11,211
1900	28.454	11,906
2000	28.810	12,601
2100	29.150	13,296
2200	29.473	13,991
2300	29.782	14,686
2400	53.628	70,635
2500	53.862	71,209
2600	54.085	71,777
2700	54.298	72,341
2800	54.501	72,901
2900	54.697	73,457
3000	54.884	74,010
3100	55.064	74,566
3200	55.238	75,106
3300	55.405	75,650
3400	55.567	76,192
3500	55.723	76,731

Table B-22

Thermodynamic Properties of Indium Liquid

Temp (K)	C_p (cal/mole - K)	S_o (cal/mole - K)	$H_o(T) - H_o(298)$ (cal/mole)	ΔH_f (cal/mole)	ΔG_f (cal/mole)
298.15	7.05	15.507	0	738	235
300	7.05	15.551	13	739	232
400	7.05	17.579	718	780	53.6
500	7.03	19.150	1,422	0	0
600	7.01	20.430	2,124	0	0
700	6.99	21.509	2,824	0	0
800	6.97	22.441	3,524	0	0
900	6.95	23.261	4,218	0	0
1000	6.95	23.993	4,913	0	0
1100	6.95	24.656	5,608	0	0
1200	6.95	25.260	6,303	0	0
1300	6.95	25.816	6,998	0	0
1400	6.95	26.332	7,693	0	0
1500	6.95	26.812	8,388	0	0
1600	6.95	27.260	9,083	0	0
1700	6.95	27.681	9,778	0	0
1800	6.95	28.078	10,473	0	0
1900	6.95	28.454	11,168	0	0
2000	6.95	28.810	11,863	0	0
2100	6.95	29.150	12,558	0	0
2200	6.95	29.473	13,253	0	0
2300	6.95	29.782	13,948	0	0
2400	6.95	30.078	14,643	-55,254	1,266
2500	6.95	30.361	15,338	-55,133	3,620
2600	6.95	30.634	16,033	-55,006	5,967
2700	6.95	30.896	16,728	-54,875	8,310
2800	6.95	31.149	17,423	-54,740	10,646
2900	6.95	31.393	18,118	-54,601	12,981
3000	6.95	31.629	18,813	-54,459	15,306
3100	6.95	31.856	19,508	-54,320	17,625
3200	6.95	32.077	20,203	-54,165	19,950
3300	6.95	32.291	20,898	-54,014	22,262
3400	6.95	32.498	21,593	-53,861	24,574
3500	6.95	32.700	22,288	-53,705	26,876

Table B-23
Cadmium Reference System

T(K)	$S_o(T)$ (cal/mole - K)	$H_o(T) - H_o(298)$ (cal/mole)
298.15	12.38	0
300	12.42	11.5
400	14.24	646
500	15.72	1,310
600	19.48	3,483
700	20.57	4,193
800	21.52	4,903
900	22.36	5,613
1000	23.11	6,323
1100	46.551	30,704
1200	46.983	31,200
1300	47.381	31,697
1400	47.749	32,194
1500	48.092	32,691
1600	48.412	33,187
1700	48.714	33,684
1800	48.998	34,181
1900	49.266	34,678
2000	49.521	35,175
2100	49.763	35,671
2200	49.994	36,168
2300	50.215	36,665
2400	50.427	37,162
2500	50.630	37,659
2600	50.824	38,155
2700	51.012	38,652
2800	51.153	39,149
2900	51.367	39,646
3000	51.535	40,130
3100	51.698	40,640
3200	51.856	41,137
3300	52.009	41,634
3400	52.158	42,131
3500	52.302	42,628

Table B-24

Thermodynamic Properties of Cadmium Liquid

Temp (K)	C_p (cal/mole - K)	S_o (cal/mole - K)	$H^o(T) - H^o(298)$ (cal/mole)	ΔH_f (cal/mole)	ΔG_f (cal/mole)
298.15	6.20	14.73	0	1,415	714
300	6.20	14.77	12	1,415	710
400	7.10	16.59	646	1,415	175
500	7.10	18.18	1,356	1,461	233
600	7.10	19.48	2,066	0	0
700	7.10	20.56	2,776	0	0
800	7.10	21.52	3,486	0	0
900	7.10	22.36	4,196	0	0
1000	7.10	23.11	4,906	0	0
1100	7.10	23.774	5,616	-23,673	1,382
1200	7.10	24.392	6,326	-23,459	3,650
1300	7.10	24.960	7,036	-23,246	5,901
1400	7.10	25.486	7,746	-23,033	8,135
1500	7.10	25.976	8,456	-22,820	10,354
1600	7.10	26.434	9,166	-22,606	12,559
1700	7.10	26.864	9,876	-22,393	14,752
1800	7.10	27.270	10,586	-22,180	16,930
1900	7.10	27.654	11,296	-21,967	19,096
2000	7.10	28.018	12,006	-21,754	21,252
2100	7.10	28.365	12,716	-21,540	23,396
2200	7.10	28.695	13,426	-21,327	25,531
2300	7.10	29.011	14,136	-21,114	27,655
2400	7.10	29.313	14,846	-20,901	29,773
2500	7.10	29.603	15,556	-20,688	32,680
2600	7.10	29.881	16,266	-20,474	33,978
2700	7.10	30.149	16,976	-20,261	36,069
2800	7.10	30.407	17,686	-20,048	38,153
2900	7.10	30.656	18,396	-19,835	40,227
3000	7.10	30.897	19,106	-19,609	42,305
3100	7.10	31.130	19,816	-19,406	44,352
3200	7.10	31.355	20,526	-19,196	46,407
3300	7.10	31.574	21,236	-18,983	48,452
3400	7.10	31.786	21,946	-18,770	50,494
3500	7.10	31.992	22,656	-18,557	52,528

Table B-25
e⁻ Reference State

T(K)	S _O (T) (cal/mole - K)	H _O (T) - H _O (298) (cal/mole)
298.15	4.989	0
300	5.019	9
400	6.449	506
500	7.557	1,003
600	8.463	1,500
700	9.229	1,996
800	9.892	2,493
900	10.477	2,990
1000	11.001	3,487
1100	11.474	3,984
1200	11.906	4,480
1300	12.304	4,977
1400	12.672	5,474
1500	13.015	5,971
1600	13.336	6,467
1700	13.637	6,964
1800	13.921	7,461
1900	14.189	7,958
2000	14.444	8,455
2100	14.686	8,951
2200	14.918	9,448
2300	15.138	9,945
2400	15.350	10,442
2500	15.553	10,939
2600	15.748	11,435
2700	15.935	11,932
2800	16.116	12,429
2900	16.290	12,926
3000	16.458	13,423
3100	16.621	13,919
3200	16.779	14,416
3300	16.932	14,913
3400	17.080	15,410
3500	17.224	15,907

References

1. C. E. Moore, Atomic Energy Levels, National Bureau of Standards Circular 467, Volumes II and III.
2. R. Hultgren, P. D. Desai, D. T. Hawkins, M. Gleiser, K. K. Kelley, and D. D. Wagman, Selected Values of the Thermodynamic Properties of the Elements, American Society for Metals, 1973.
3. D. R. Stull and H. Prophet, JANAF Thermochemical Tables, Second Edition, NSRDS-NBS-37, National Bureau of Standards, 1971.

Distribution:

U.S. Government Printing Office
Receiving Branch (Attn: NRC Stock)
8610 Cherry Lane
Laurel, MD 20707
250 copies for R7

U.S. Nuclear Regulatory Commission (16)
Office of Nuclear Regulatory Research
Washington, DC 20555
Attn: O. E. Bassett
B. S. Burson
R. T. Curtis
C. N. Kelber
J. Larkins
T. Lee (5)
M. Silberberg
R. W. Wright
T. Walker
M. Jankowski

U.S. Nuclear Regulatory Commission (4)
Office of Nuclear Regulatory Regulation
Washington, DC 20555
Attn: L. G. Hulman
P. Easky
J. Rosenthal
J. Mitchell

U.S. Department of Energy (2)
Albuquerque Operations Office
P.O. Box 5400
Albuquerque, NM 87185
Attn: J. R. Roeder, Director
Operational Safety Division
D. K. Nowlin, Director
Special Programs Division
For: C. B. Quinn
D. Plymale

U.S. Department of Energy
Office of Nuclear Safety Coordination
Washington, DC 20545
Attn: R. W. Barber

Electric Power Research Institute (2)
3412 Hillview Avenue
Palo Alto, CA 94303
Attn: R. Vogel
R. Sehgal

Professor T. Theofanous
Purdue University
School of Engineering
West Lafayette, IN 47907

Dr. R. Henry
Fauske & Associates
16W070 West 83rd Street
Burr-Ridge, IL 60521

M. L. Corradini
Nuclear Engineering Department
University of Wisconsin
Madison, WI 53706

I. Catton
UCLA
Nuclear Energy Laboratory
405 Hilgard Avenue
Los Angeles, CA 90024

Brookhaven National Laboratory (4)
Department of Nuclear Energy
Building 820
Upton, NY 11973
Attn: R. A. Bari
T. Pratt
G. Greene
T. Ginsberg

Professor R. Seale
Department of Nuclear Engineering
University of Arizona
Tucson, AZ 85721

Oak Ridge National Laboratory (2)
P.O. Box Y
Oak Ridge, TN 37830
Attn: T. Kress
S. Hodge

K. Holtzclaw
General Electric - San Jose
Mail Code 682
175 Kurtner Avenue
San Jose, CA 95125

Argonne National Laboratory
9700 S. Cass Avenue
Argonne, IL 60439
Attn: D. Pedersen

Cathy Anderson
Nuclear Safety Oversight Commission
1133 15th St., NW
Room 307
Washington, DC 20005

Battelle Columbus Laboratory (3)
505 King Avenue
Columbus, OH 43201
Attn: P. Cybulskis
R. Denning
J. Gieseke

J. E. Antill
Berkeley Nuclear Laboratory
Berkeley GL 139 PB
Gloucestershire
United Kingdom

W. G. Cunliffe
Bldg. 396
British Nuclear Fuels, Ltd.
Springfields Works
Salwick, Preston
Lancs
United Kingdom

Reactor Development Division (4)
UKAEA - Atomic Energy Establishment
Winfrith, Dorchester
Dorset
United Kingdom
Attn: R. G. Tyror, Head
T. Briggs
R. Potter
A. Nichols

Projekt Nucleare Sicherheit (3)
Kerforschungszentrum Karlsruhe
Postfach 3640
75 Karlsruhe
Federal Republic of Germany
Attn: J. P. Hoseman
Albrecht
H. H. Rininsland

Mr. G. Petrangeli
Direzione Centrale della Sicurezza
Nucleare e della Protezione Sanitaria (DISP)
Ente Nazionale Energie Alternative (ENEA)
Viale Regina Margherita, 125
Casella Postale N. 2358
I-00100 Roma A.D., ITALY

Dr. K. J. Brinkman
Reactor Centrum Nederland
P.O. Box 1
1755 ZG Petten
THE NETHERLANDS

Mr. H. Bairiot, Chief
Department LWR Fuel
Belgonucleaire
Rue de Champde Mars. 25
B-1050 BRUSSELS, BELGIUM

Dr. S. Saito
Japan Atomic Energy Research Institute
Takai Research Establishment
Tokai-Mura, Naku-Gun
Ibaraki-ken
JAPAN

Wang Lu
TVA
400 Commerce, W9C157-CK
Knoxville, TN 37902

M. Fontana
Director, IDCOR Program
Technology for Energy, Inc.
P.O. Box 22996
10770 Dutchtown Rd.
Knoxville, TN 37922

H. J. Teague (3)
UKAEA
Safety and Reliability Directorate
Wigshaw Lane
Culcheth
Warrington, WA3 4NE
United Kingdom

Dr. Fran Reusenbach
Gesellschaft fur Reaktorsicherheit (GRS mbH)
Postfach 101650
Glockengasse 2
5000 Koeln 1
Federal Republic of Germany

S. J. Niemczyk
Union of Concerned Scientists
1346 Connecticut Avenue, NW
S. 1101
Washington, DC 20036

M. Jankowski
IAEA
Division of Nuclear Reactor Safety
Wagranerstrasse 5
P.O. Box 100
A/1400 Vienna, Austria

3141 C. M. Ostrander (5)
3151 W. L. Garner (1)
6000 E. H. Beckner
6400 A. W. Snyder
6410 J. W. Hickman
6420 J. V. Walker
6421 T. R. Schmidt
6422 D. A. Powers (5)
6422 F. E. Arellano
6422 J. E. Brockmann (5)
6422 R. M. Elrick
6422 E. R. Copus
6422 J. E. Gronager
6422 T. M. Kerley
6422 D. A. Lucero
6422 A. L. Ouellette, Jr.
6422 W. W. Tarbell (5)
6423 P. S. Pickard
6425 D. R. Bradley
6425 W. J. Camp
6425 M. Pilch (5)
6425 A. Suo Anttila
6425 W. Frid
6427 M. Berman
6430 N. R. Ortiz
6440 D. A. Dahlgren
6442 W. A. Von Rieseemann
6449 K. D. Bergeron
6450 J. A. Reuscher
6454 G. L. Cano
7530 T. B. Lane
7537 N. R. Keltner
7537 T. Y. Chu
7537 R. U. Acton
7537 B. F. Blackwell
8024 P. W. Dean

NRC FORM 335 (2-84) NRCM 1102 3201, 3202		U.S. NUCLEAR REGULATORY COMMISSION		REPORT NUMBER (Assigned by NRC add Vol. No. if any) NUREG/CR-4401 SAND85-0469	
BIBLIOGRAPHIC DATA SHEET					
SEE INSTRUCTIONS ON THE REVERSE					
2. TITLE AND SUBTITLE BEHAVIOR OF CONTROL RODS DURING CORE DEGRADATION: PRESSURIZATION OF SILVER- INDIUM-CADMIUM CONTROL RODS				3. LEAVE BLANK	
5. AUTHOR(S) D. A. Powers				4. DATE REPORT COMPLETED MONTH YEAR September 1985 6. DATE REPRINT ISSUED MONTH YEAR November 1985	
7. PERFORMING ORGANIZATION NAME AND MAILING ADDRESS (Include Zip Code) Severe Accident Source Terms Division 6422 Sandia National Laboratories Albuquerque, NM 87185				8. PROJECT TASK WORK UNIT NUMBER A1227	
10. SPONSORING ORGANIZATION NAME AND MAILING ADDRESS (Include Zip Code) Division of Accident Evaluation Office of Nuclear Regulatory Research U.S. Nuclear Regulatory Commission Washington, DC 20555				11a. TYPE OF REPORT Final Report b. PERIOD COVERED (Indicate date)	
12. SUPPLEMENTARY NOTES					
13. ABSTRACT (200 words or less) Activity data for the liquid binary systems Ag-Cd, Ag-In, and In-Cd are correlated in terms of the Wilson equation. These correlations are used to construct a model of the ternary system Ag-In-Cd. Spectroscopic data for the vapor species Ag(g), Ag ₂ (g), Ag ₃ (g), Ag ⁺ (g), In(g), In ₂ (g), In ⁺ (g), Cd(g), Cd ₂ (g), Cd ⁺ (g), AgIn(g), and CdIn(g) are reviewed and are used to define thermodynamic functions for these species for temperatures between 298 and 3500 K. Vapor pressures for the liquid phase pure elements, liquid binary alloys, and the liquid ternary alloy are calculated using the Wilson equation model and using the assumption that the condensed phase is an ideal mixture. An azeotrope is predicted for the Ag-In system. Predictions are made of the vaporization of alloys of 80 percent Ag, 15 percent In, and 5 percent Cd used as control materials in some pressurized water reactors.					
14. DOCUMENT ANALYSIS - a. KEYWORDS-DESCRIPTORS Control Rods, Core Degradation, Silver-Indium-Cadmium, Binary Liquid Activity, Ternary Ag-In-Cd, Vapor Pressure				15. AVAILABILITY STATEMENT Unlimited	
b. IDENTIFIERS/OPEN-ENDED TERMS				16. SECURITY CLASSIFICATION (This page) Unclassified (The report) Unclassified	
				17. NUMBER OF PAGES	
				18. PRICE	